Metabolic Analysis of Neural Tube Defects

Katie Ann Burren

Neural Development
Institute of Child Health
University College London

May 2007

ProQuest LLC
789 East Eisenhower Parkway
P.O. Box 1346
Ann Arbor, MI 48106-1346

I, Katie Ann Burren, confirm that the work presented in this thesis is my own. Where information has been derived from other sources, I confirm that this has been indicated in the thesis.

Signature_____

Date_____

Abstract

Neural tube defects (NTDs), such as exencephaly and spina bifida, occur when the neural tube fails to close properly during embryonic development. Folic acid supplementation has been shown to effectively reduce the occurrence of NTDs and low folate is a known risk factor for human NTDs. However despite extensive research, the mechanism explaining how the folate status affects the incidence of NTDs remains unknown.

One effect of sub-optimal folate could be suppression of the methylation cycle, which is interlinked with the folate cycle. To explore this hypothesis, a method has been developed to quantitatively measure the substrate, S-Adenosylmethionine (SAM), and the product, S-Adenosylhomocysteine (SAH), of methylation reactions in neurulation-stage mouse embryos by Liquid Chromatography Tandem Mass Spectrometry (LC-MS/MS). To investigate the link between methylation perturbation and neural tube defects, the abundance of SAM and SAH has been quantified in a series of experimental models and human NTD cell lines.

Using a folate-deficient diet, this study also investigates folate deficiency using mouse models (*splotch* and *curly tail*) for NTDs. Results illustrate that folate deficiency, in both mouse models, caused an increase in the incidence of neural tube defects and, embryos were growth retarded. To examine the effect the folate deficient diet was having on endogenous folate metabolism, embryonic folate levels were analysed, in addition to maternal folate. Furthermore, using the established lc-ms/ms method, the effect of folate deficiency on the abundance of SAM and SAH was determined.

Increasing evidence suggests that *myo*-inositol may prove effective in preventing NTDs, in conjunction with folic acid. Thus, a double-blind, randomised clinical trial has been designed to investigate this and, in order to monitor patient compliance an LC-MS/MS method has been developed to quantify *myo*-inositol in urine.

Table of Contents

List of Figures:

Chapter 1

Chapter 2

Chapter 3

Chapter 4

Chapter 5

Chapter 6

Chapter 7

Chapter 8

List of Tables:

Chapter 1

Chapter 2

Chapter 3

Chapter 4

Chapter 5

Chapter 6

Chapter 7

Chapter 8

CHAPTER 1

Introduction

1.1 Neurulation

Neurulation is a major developmental event of embryogenesis, that results in the formation of the neural tube; the embryonic precursor of the brain and spinal cord. Neural tube defects (NTDs), which occur due to failure of neurulation, result in life threatening and debilitating conditions which affect approximately 1 per 1000 births worldwide (Borman et al., 1986;Carter, 1974). Dietary supplementation with folic acid (FA) offers a major breakthrough in the prevention of NTDs, however the mechanism of prevention remains to be identified (Blom et al., 2006).

1.1.1 Primary and Secondary Neurulation

The process of neurulation is classically sub-divided into two parts; primary and secondary neurulation. Primary neurulation is the transformation of the flat ectodermal neural plate into the closed cylindrical neural tube (Figure 1.1). During gastrulation, cells that do not migrate through the node form the ectoderm layer, from which the neural plate is derived. Following induction of the neural plate, it elongates by cell division (Sausedo et al., 1997) and a process known as convergent extension whereby cells move towards the midline and extend along the body axis (Wallingford and Harland, 2002) (Figure 1.1).

The lateral borders of the ectodermal neural plate thicken and elevate to form neural folds (Figure 1.1), that subsequently bend towards the midline through the formation of median and/or dorsal-lateral hinge points (Carroll et al., 2003;Copp et al., 2003;Sadler, 2005). Fusion of the apposed neural folds then completes neural tube closure (Sadler, 1978). During secondary neurulation, the mesenchymal tail bud cells coalesce and become epithelial reorganising around a lumen to form a neural tube continuous with the remainder of the neural tube formed by primary neurulation (Schoenwolf, 1979).

In mouse embryogenesis, primary neurulation initiates at embryonic day 8, when the embryo is at the 6 to 7 somite stage. The process begins at the boundary between the hindbrain and the cervical region, an initiation event known as closure 1 (Copp et al., 2003;Greene and Copp, 2006). Closure spreads both rostrally into the hindbrain to initiate cranial neural tube closure and caudally into the spinal region to initiate spinal neural tube closure (Figure 1.2). The second point of *de novo* neural tube closure (closure 2) occurs at the forebrain-midbrain barrier around the 10-somite stage and a third closure site (closure 3) follows rapidly at the rostral extremity of the forebrain (Figure 1.2). Although the location of closure 1 and 3 is uniform, the exact location of closure 2 does vary between mouse strains (Fleming and Copp, 2000). Thus, strains

with a more caudal location of closure 2 are relatively resistant to NTDs, whereas strains with a rostrally positioned closure 2 exhibit increased susceptibility to NTDs.

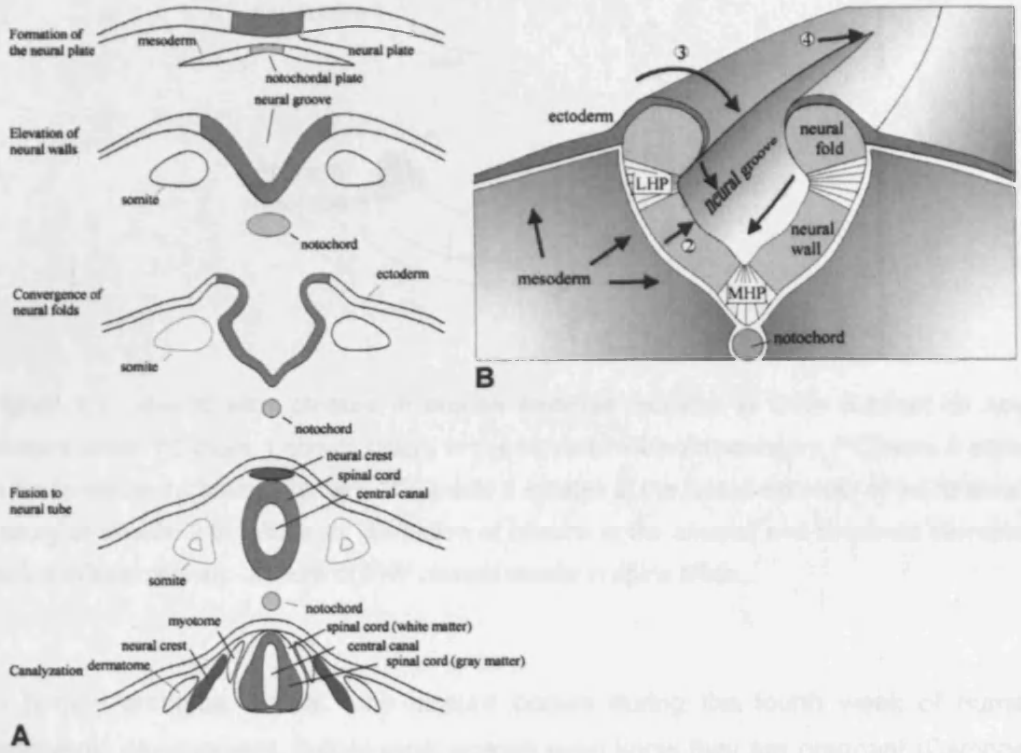

Figure 1.1. Primary neurulation. (A) A transverse view of neural tube closure. (B) Processes during primary neurulation. 1, the arrows in the neural groove indicate the narrowing and elongation, resulting in convergent extension; 2, elevation of the neural wall; 3, convergence of the neural fold; 4, fusion. MHP, medial hinge point; LHP, dorsolateral hinge point. Taken from (Van der Put et al., 2001).

Neural tube closure spreads from the initiation sites into neighbouring regions. Open regions are termed neuropores and these gradually shorten as closure proceeds. The completion of cranial neural tube closure occurs at the anterior neuropore and the hindbrain neuropore (Figure 1.2), around the 15 somite stage (embryonic day 9.5). As cranial neurulation is occurring, neural tube closure also progresses from closure 1 in a caudal direction, through the spinal region (Figure 1.2). Primary neurulation is completed by closure of the posterior neuropore (PNP) at embryonic day 10, at the 31 to 33 somite stage. Secondary neurulation forms the remainder of the spinal cord, caudal to the lowest sacral level of primary neurulation.

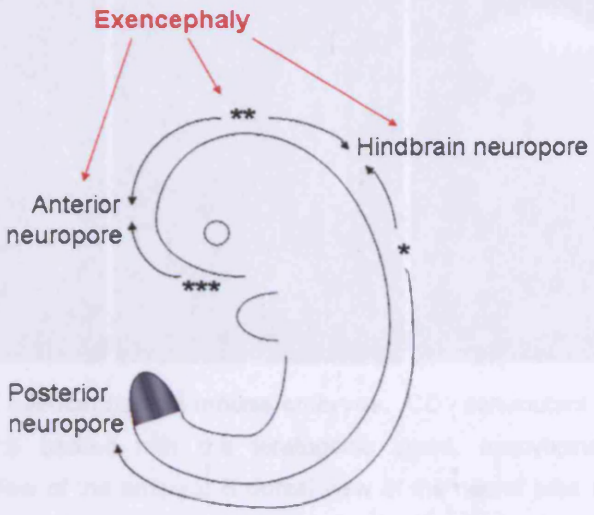

Figure 1.2. Neural tube closure in mouse embryos initiates at three distinct *de novo* closure sites. *Closure 1 occurs initially at the cervical/hindbrain boundary, **Closure 2 occurs at the forebrain/midbrain boundary, ***Closure 3 initiates at the rostral extremity of the forebrain. Failure of closure 2 to initiate, or disruption of closure at the anterior and hindbrain neuropore results in exencephaly. Failure of PNP closure results in spina bifida.

In human embryos, neural tube closure occurs during the fourth week of human embryonic development, before most women even know they are pregnant (Campbell et al., 1986). Like mouse embryos, primary neurulation in human embryos appears to occur by a multi-site closure process. Although the exact location of the closure sites in human embryos remains to be definitively identified, the positions of the closure sites do appear to be different to mice (De Marco et al., 2006).

1.1.2 Neural Tube Defects (NTDs)

Neural tube defects (NTDs) occur when the neural tube fails to close. The most common type of NTD, and the focus of this study, occurs in the cranial region due to defective primary neurulation (De Marco et al., 2006). Cranial neural tube defects, referred to as exencephaly (EX; Figure 1.3), arise when the cranial neural tube fails to close in the developing brain, often as a result of failure of closure 2 (Copp, 2005). Exposure of cranial tissue to the amniotic fluid leads to neural degeneration, resulting in the condition anencephaly (Matsumoto et al., 2002). Unless terminated or miscarried, the pregnancy may be still born or the baby will die shortly after birth.

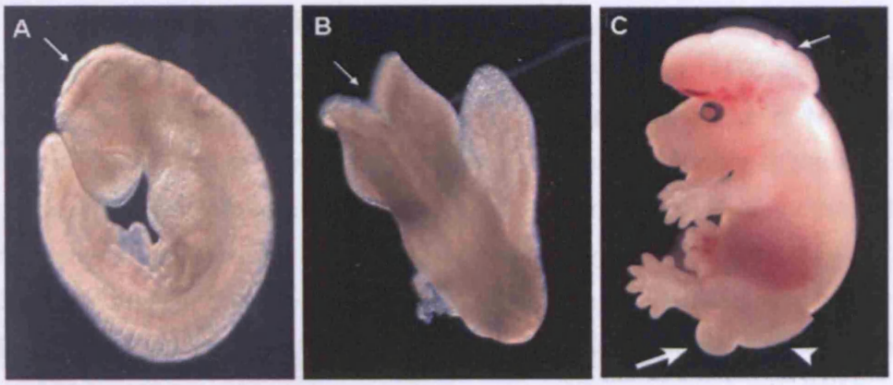

Figure 1.3. Images of exencephaly in mouse embryos. CD1 non-mutant mouse embryo at embryonic day (E) 9.5 treated with the teratogenic agent, azacytidine, which causes exencephaly (A, side view of the embryo; B dorsal view of the neural tube at the cranial and upper sacral level). *Curly tail* mutant embryo at embryonic day (E) 15.5 with exencephaly and open spina bifida (Taken from (Copp et al., 2003)). Thin arrow in a, b and c, midbrain exencephaly; arrowhead in c, open spina bifida; thick arrow in c, curled tail.

Failure of primary neurulation in the spinal neural tube is known as myelomeningocele or, more commonly, spina bifida (Copp et al., 2003;Seller, 1981;Seller, 1994a). This arises when the caudal progression of neural tube closure fails to complete and the posterior neuropore remains open (Figure 1.3). Human fetuses with spina bifida are often viable. However, the individual will suffer from physical and developmental disabilities of varying severities, due to abnormal neural innervation below the lesion. Other types of NTDs include spina bifida occulta and craniorachischisis (Copp et al., 2003).

1.2 Causes of NTDs in humans

NTDs have been the focus of much research but a common mechanism explaining how NTDs arise has yet to be described. In most cases, the underlying genetic predisposition is unknown and very few cases of multiple NTDs in large families have been described. When studied, they display complex inheritance patterns (Copp, 1994). The cause of NTDs may involve a combination of various polymorphisms which can then be influenced by external environmental factors. Thus, some cases of NTD may occur by the summation and/or interaction of several predisposing factors which individually are insufficient to cause NTDs. Furthermore, the causes of NTDs which occur in association with other malformations or as part of a syndrome are likely to differ from the causes of NTDs that occur as isolated defects (Rasmussen and Frias, 2006).

1.2.1 Genetic predisposition

Genetic studies of human NTDs have revealed but a few human NTD risk genes, while no single gene has been identified as a major independent cause of NTDs (Harris, 2001). Nonetheless, there is evidence to support a genetic influence in the aetiology of NTDs. Investigations into familial cases have shown that there is an increased risk of an NTD pregnancy following a previous affected pregnancy, termed the recurrence risk. Studies conducted in several countries report recurrence risks ranging from 2.3 – 4 % (Elwood et al., 1992; Czeizel and Metneki, 1984; Cowchock, S., 1980; Elwood and Elwood, 1980). Whilst, a study in the UK reported a 3% recurrence rate among women who were given dietary counselling before the pregnancy, compared to a 7% recurrence rate among uncounselled women (Laurence et al., 1980). After two or more affected pregnancies, the recurrence risk has been reported to be as high as 10% (Elwood et al., 1992;Elwood and Elwood, 1980). Thus analysis of recurrence risk provides evidence of a genetic influence, but factors such as geographical location and diet are also associated with variations in the incidence of NTDs. Further evidence to support a genetic predisposition comes from studies which have shown that the risks are higher for first-degree relatives (Toriello and Higgins, 1983) and monozygotic twins (Janerich and Piper, 1978). The prevalence of NTDs is also higher among females compared to males (Seller, 1987), yet the reason for this sex difference is unknown (Brook et al., 1994).

1.2.2 Environmental influences

In addition to genetic susceptibility, epidemiological studies have conclusively shown that environmental factors affect the prevalence rates of NTDs (Borman et al., 1986;Carter, 1974). Many of the environmental factors that are believed to play a role in the aetiology of NTDs in humans could be related to maternal nutrition. These include seasonal trends, variations in geographic area, social class and the consumption of toxin-contaminated food products. The continued decline in NTD prevalence observed during the last five decades in both US and British populations may be due to improvements in maternal nutrition (Yen et al., 1992). Particular nutrients, such as folic acid (see section 1.4) and vitamin B_{12} have been shown to play a major role in the prevention of NTDs and consequently, much research has focused on elucidating the preventative mechanisms involved (Copp and Greene, 2000;Scott, 1999;Van der Put et al., 2001).

1.3 The mouse as an experimental model for NTDs

The benefits of the mouse for understanding the development of NTDs are, first, that neural folding and fusion to create a closed neural tube only occurs in higher vertebrates; second, the wealth of available mouse strains which exhibit NTDs; third, the ease of use as a laboratory animal for experimental studies and fourth, the genetics of the mouse are well-understood. Experimental studies are not permitted in humans for ethical reasons whilst epidemiology studies and clinical trials are often hampered by low numbers of NTD cases. Thus, mouse research is critical to address issues of molecular and cellular pathologies in NTDs, and to conduct experimental studies on the action of agents in preventing NTDs.

1.3.1 Range of NTDs exhibited by the mouse mutants

There are a large number of mutant mouse models with NTD phenotypes (Harris and Juriloff, 2006;Juriloff and Harris, 2000), including models that arose spontaneously and models that were generated experimentally. The majority of NTD mouse models develop exencephaly either alone, as seen in *Cited-2* null mutants (Martinez-Barbera et al., 2002) or in combination with spina bifida as observed in the well-studied *splotch* and *curly tail* mutants (Auerbach, 1954;Van Straaten and Copp, 2001). Relatively few mouse mutants exhibit spina bifida alone, as seen in *Vacuolated lens* (*vl*) mice (Wilson and Wyatt, 1988). Delay of spinal closure can be seen as an enlarged posterior neuropore in embryos with 28-30 somites. Severe delay prevents neural tube closure, as in spina bifida, but a minor delay is compatible with posterior neuropore closure yet tail flexion defects are frequent, as seen in *curly tail* mutants (Van Straaten and Copp, 2001).

1.3.2 Mechanisms underlying cranial neural tube closure as revealed by mouse mutants

1.3.2.1 Cytoskeleton

It is believed that 'purse string' contractions of actin microfilaments, located in the bending neural plate, are required for neural tube closure (Karfunkel, 1974;Sadler et al., 1982). Indeed, the application of cytochalasins that disassemble actin microfilaments disturbs cranial neural tube closure (Morriss-Kay and Tuckett, 1985;Smedley and Stanisstreet, 1986). Gene targeting of cytoskeleton-related proteins has been shown to cause exencephaly in several mouse mutants, including the F-

actin-associated protein shroom (Hildebrand and Soriano, 1999), the actin-binding protein vinculin (Xu et al., 1998), the protein kinase C target MARCKS, which cross-links actin filaments (Stumpo et al., 1995) and the RhoGAP p190 regulator of the actin cytoskeleton (Brouns et al., 2000). Embryos doubly mutant for other cytoskeleton-related genes also develop exencephaly (Koleske et al., 1998;Lanier et al., 1999;Menzies et al., 2004). Of interest, spinal neural tube closure occurs normally in all these mutants, with the exception of *shroom* where a proportion of embryos have spina bifida. Hence, a microfilament-based mechanism is crucial for cranial neural tube closure, but plays a less certain role in spinal neurulation.

1.3.2.2 Apoptosis

Studies of several knockout mouse strains have demonstrated that both increased and decreased apoptosis in the cranial neural tube disrupts cranial neurulation (Copp, 2005), whilst inhibition of apoptosis using the peptide Zvad-fmk produces NTDs in the chick embryo (Weil et al., 1997). In the majority of cases, only cranial neurulation is affected whilst spinal neurulation occurs normally. In the cranial neural tube, apoptotic cells observed at the sites of dorsolateral bending of the neural plate are thought to enhance the conversion of neural fold morphology from convex to concave, whilst apoptosis at the tips of the neural folds is believed to play a role in tissue remodelling required for fusion of the apposed neural tips (Copp, 2005).

1.3.2.3 Cell Proliferation and differentiation

During neural tube closure, cells continue to proliferate and will only begin to exit the cell cycle and differentiate following completion of neurulation. Premature onset of neuronal differentiation in the neural plate appears to prevent cranial neural tube closure in mouse knockouts affecting the Notch and related signalling pathways (Ishibashi et al., 1995;Oka et al., 1995;Zhong et al., 2000). However, the exact mechanism underlying neural tube defects caused by premature differentiation through the disruption of the Notch pathway is unknown. Exencephaly has also been associated with excessive cell proliferation in some mouse mutants, for example over-expression of *Notch3* (Lardelli et al., 1996).

1.3.2.4 Convergent Extension

The most severe type of NTD is craniorachischisis, in which the neural tube is open throughout part of the cranial region as well as the whole of the spine. A small number

of mutants exhibit craniorachischisis, including *loop-tail, circletail,* and *crash* (Curtin et al., 2003;Hamblet et al., 2002;Murdoch et al., 2001b;Murdoch et al., 2001a). In these mutants the initial closure event, closure 1, fails thereby preventing further closure events in the midbrain, hindbrain and spinal neural tube (Greene et al., 1998). Analysis of the craniorachischisis mutants revealed that the neural folds at the cervical-hindbrain region are spaced widely apart and cannot appose at the midline to enable closure 1 to occur. Recent studies have implicated defects in non-canonical Wnt / planar cell pathway signalling in causation of craniorachischisis. Shaping of the neural plate occurs by a process termed convergent extension whereby mesodermal cells move medially and intercalate in the midline lengthening the body axis (Keller et al., 2000). Disruption of cellular polarity via the planar cell polarity (PCP) genes in *Xenopus* disrupts convergent extension yielding short, broad neural plates that fail to complete neural tube closure (Wallingford and Harland, 2002). Significantly, the genes mutated in *loop-tail, circletail, crash* and *dishevelled-1/2* are homologues of the *Drosophila* PCP genes (Curtin et al., 2003;Murdoch et al., 2001a;Murdoch et al., 2003). Similarly, cell labelling studies reveal that convergent extension movements are defective in *loop-tail* mutant embryos (Ybot-Gonzalez et al., 2007). Hence, the use of mouse mutants has demonstrated that the PCP signalling pathway is required for shaping of the neural plate, a process vital for the initiation of neural tube closure.

1.3.3 Gene-gene, gene-background and gene-environment interactions identified in mouse mutants

Many of the mouse mutants only exhibit NTDs when the mutant allele is present in homozygous state, such that NTD phenotypes are rare amongst heterozygotes. In humans, abnormal gene dosage is a common cause of spontaneous abortion and birth defects, for example those caused by chromosomal trisomy such as Down syndrome (Fisher and Scambler, 1994). Thus, abnormal gene dosage may be common among human NTD cases. Furthermore, it may be gene-gene interactions that result in the development of NTDs as is known to occur in mouse mutants. For example, while *ct/ct* and Sp^{2H}/Sp^{2H} mutants develop spina bifida, a proportion of double heterozygotes (*ct/+* ; $Sp^{2H}/+$) also have NTDs whilst *ct/ct* ; $Sp^{2H}/+$ embryos exhibit severe spina bifida (Estibeiro et al., 1993).

The severity and frequency of NTDs is also affected by *modifier* genes that are present in the genetic background. Mouse inbred strains, which have identical genetic backgrounds, can be used to demonstrate the role of genetic background. The *curly tail* mutant gene, for example, when crossed onto different inbred mouse genetic

backgrounds gives rise to widely differing frequencies of spina bifida (Embury et al., 1979;Neumann et al., 1994). Similarly, the frequency of exencephaly in *splotch* (Sp^{2H}) is governed by genetic background whereby variations in the position of closure 2 between inbred strains can enhance or hinder midbrain closure (Fleming and Copp, 2000). The role of genetic background in humans has yet to be demonstrated but with its continuously varying genetic background, it provides enormous scope for background effects on NTD occurrence (Copp et al., 2006).

The gene-gene and gene-background interactions are further influenced by the environment in which the embryo develops. Many agents delivered to the developing embryo exhibit teratogenic effects which include neural tube defects. Mouse embryos are particularly useful to study the effects of exogenous agents on neural tube development as they can be maintained *in vitro* throughout the stages of neurulation using the method of whole embryo culture (Copp et al., 1993). Examples of agents which cause NTDs include drugs, (for example, valproic acid used to treat epilepsy (Trotz et al., 1987)), chemicals, (for example, methanol (Bolon et al., 1994)), molecules that may be present at abnormal levels, particularly in maternal disease conditions (for example, elevated glucose and ketone body concentrations, as found in diabetes (Sadler, 1980)) and heavy metals (for example, arsenic, cadmium, lead and mercury (Brender et al., 2006). These teratogenic agents can also interact directly with genetic mutant effects to affect the frequency of NTDs. For example, mitomycin C (an inhibitor of DNA synthesis) increases the incidence of exencephaly in *curly tail* mutants when administered on embryonic day 8, but decreases the incidence of spina bifida when administered on embryonic day 9 (Seller and Perkins, 1986).

1.3.4 Prevention of NTDs by vitamins

Amelioration of NTDs by exogenous agents highlights potential therapeutic agents for the prevention of NTDs. Folic acid has proved to be a very successful preventative agent for human NTDs, particularly since there are no teratogenic side effects, making it suitable for clinical use. Although the initial research highlighting folic acid as a preventative agent was established in human studies, folic acid is also capable of preventing NTDs in several mouse mutants (see section 1.4.5). Thus, folate prevention of NTDs in mouse mutants provides a means to study the underlying mechanisms of prevention which are as yet unknown.

There are however some mouse mutants which do not respond to folic acid, including *curly tail*, *Axial defects*, and the *EphA7* (Essien and Wannberg, 1993;Holmberg et al.,

2000;Seller, 1994b). This mirrors the situation in humans in which there appears to be a sub-set of cases which do not respond to folic acid as highlighted by the existence of NTD cases which occurred despite high folic acid intake in the MRC clinical trial (see section 1.4.4). Evidence from mouse studies is now accumulating to suggest that inositol may be a potentially useful therapeutic agent to be used in combination with folic acid to prevent more cases of NTDs (Greene et al., 1997; Cogram et al., 2002).

1.4 Folate-Sensitive Neural Tube Defects

1.4.1 Folates and Folic Acid

Folate is the generic term used to describe a group of molecules derived from tetrahydrofolate (THF), which consists of a pteridine ring, p-aminobenzoic acid and one to six glutamic acids (Lucock, 2000). THF can be reduced or oxidised, by the removal or addition of one-carbon units at the N-5 and/or N-10 position, to give the remaining folate species (Figure 1.4). A folate molecule conjugated to a single glutamate residue is referred to as a "monoglutamate" or "monoglutamylfolate" whilst a folate molecule conjugated to multiple glutamate residues is a "polyglutamate" or "polyglutamylfolate". The addition of a polyglutamyl chain to folates, catalysed by folylpolyglutamate synthetase (FPGS) (EC 6.3.2.12), is important for cellular retention and polyglutamates are generally the preferred substrates for folate-utilising enzymes rather than monoglutamates (Shane, 1989).

Humans are not able to synthesise folate and therefore rely entirely on exogenous sources to provide it. The principal dietary sources of folate are Marmite, leafy green vegetables, legumes (beans, peas), citrus fruits and juices, liver and whole wheat bread (Locksmith and Duff, 1998;Lucock, 2000). Most naturally occurring folates, including those found in food, are present as polyglutamates which must be converted to the absorbable monoglutamate, 5-methyltetrahydrofolate, in the small intestine (Erbe and Wang, 1984).

Folic acid (pteroylmonoglutamate, FA) is a synthetic, stable monoglutamylfolate found in vitamin tablets and fortified foods. At low levels it can be efficiently metabolised to 5-MeTHF, yet the absorption and conversion to 5-MeTHF is saturable at doses between 266-400 µg (Lucock et al., 1989). The recommended daily intake of folic acid for woman planning a pregnancy is 400 µg per day (Whitehead and Bates, 1997), thus it is not uncommon to find unmetabolised folic acid in the circulation. Upon entry into the cell, unmetabolised folic acid becomes incorporated in the folate cycle following

reduction to DHF and subsequently forms THF, whilst 5-MeTHF is converted to THF by methionine synthase (MS) (Figure 1.5).

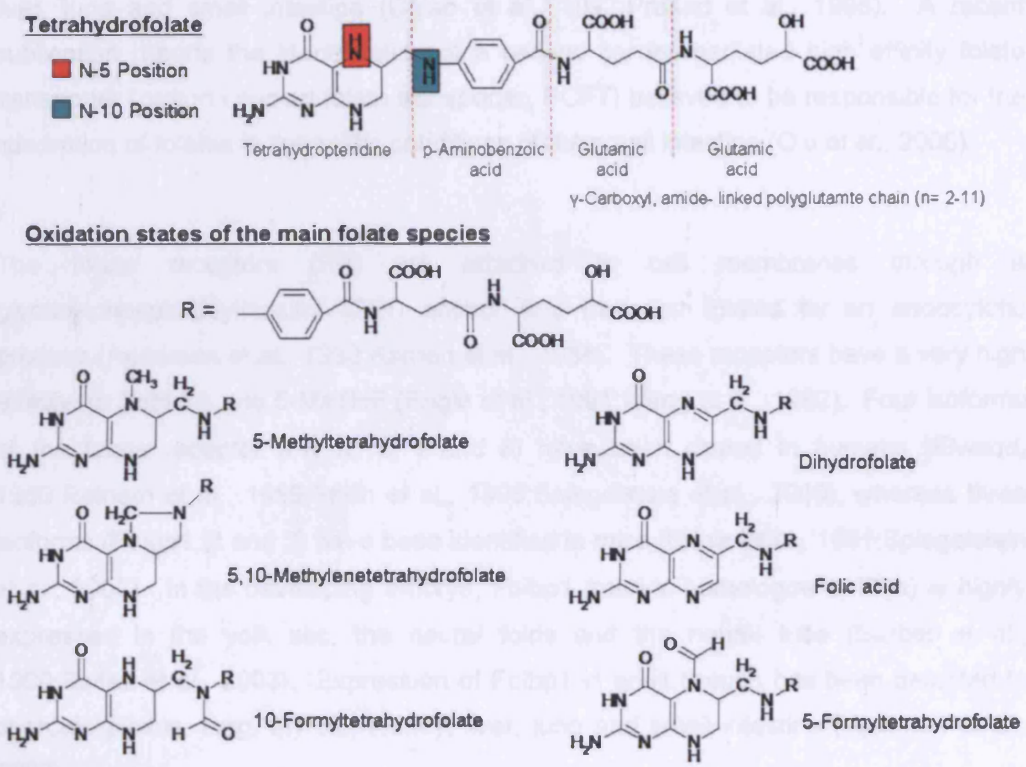

Figure 1.4. The chemical structure of Tetrahydrofolate, highlighting the N-5 and N-10 positions and the oxidation states of the main folate species. The figure displays the diglutamate derivative with two glutamate residues attached. The major folate species are Tetrahydrofolate (THF), 5-Methyltetrahydrofolate (5-MeTHF), 5,10-Methylenetetrahydrofolate (5,10-MethyleneTHF), 10-Formyltetrahydrofolate (10-FormylTHF), Dihydrofolate (DHF), Folic Acid (FA) and 5-Formyltetrahydrofolate (5-FormylTHF).

1.4.2 Folate Receptors

There are two different categories of transporters which facilitate cellular uptake of folate: a) membrane channels or carriers, such as the reduced folate carrier (RFC), and b) cell surface molecules that facilitate uptake by vesicle endocytosis, collectively termed the folate receptors (FR). The reduced folate carrier (RFC1) is a facilitative anion-exchanger that mediates folate delivery into a variety of cell types (Sierra and Goldman, 1999;Sirotnak and Tolner, 1999). RFC1 has a high affinity for reduced folates, including the physiological substrate 5-MeTHF, and a low affinity for FA

(Goldman, 1971). RFC1 is expressed during neurulation (E9.5-E11.5) in the placenta, yolk sac and throughout the embryo, with intense expression localised in the neural tube, forebrain, hindbrain, craniofacial regions, eye, limb buds, somites, tail bud and the heart (Maddox et al., 2003). RFC1 expression in adult tissues is localised to the liver, lung and small intestine (Chiao et al., 1997;Prasad et al., 1995). A recent publication reports the identification of a second carrier-mediated high affinity folate transporter (proton coupled folate transporter, PCFT) believed to be responsible for the absorption of folates in the acidic conditions of the small intestine (Qiu et al., 2006).

The folate receptors (FR) are attached to cell membranes through a glycosylphosphatidylinositol (GPI) anchor and transport folates by an endocytotic process (Anderson et al., 1992;Kamen et al., 1988). These receptors have a very high affinity for both FA and 5-MeTHF (Brigle et al., 1991;Wang et al., 1992). Four isoforms of the folate receptor (FR α, β, γ and δ) have been cloned in humans (Elwood, 1989;Ratnam et al., 1989;Shen et al., 1995;Spiegelstein et al., 2000), whereas three isoforms (Folbp1, 2 and 3) have been identified in mice (Brigle et al., 1991;Spiegelstein et al., 2000). In the developing embryo, Folbp1 (murine homologue of FRα) is highly expressed in the yolk sac, the neural folds and the neural tube (Barber et al., 1999;Saitsu et al., 2003). Expression of Folbp1 in adult tissues has been detected in choroids plexus, lung, thyroid, kidney, liver, lung and small intestine (Weitman et al., 1992).

1.4.3 Folate Cycle

Once taken up into the cell, the role of folates is to act as acceptors and donors of one-carbon units in a series of cyclic reactions involving nucleotide and amino acid metabolism, collectively known as one-carbon metabolism (Figure 1.5). The principle origin of the one-carbon units is serine, provided by the action of serine hydroxylmethyltransferase (SHMT) which converts serine and tetrahydrofolate (THF) to 5,10-methylene THF and glycine. Other sources of one-carbon units include formiminoglutamic acid, the mitochondrial glycine cleavage pathway, choline metabolism and formate. Folates have two important direct biological effects. First, via the folate cycle, they provide single carbon units for the synthesis of nucleotide bases required for DNA and RNA synthesis. Secondly, folates are the methyl-donors for the recycling of homocysteine to methionine, an essential step in the methylation cycle.

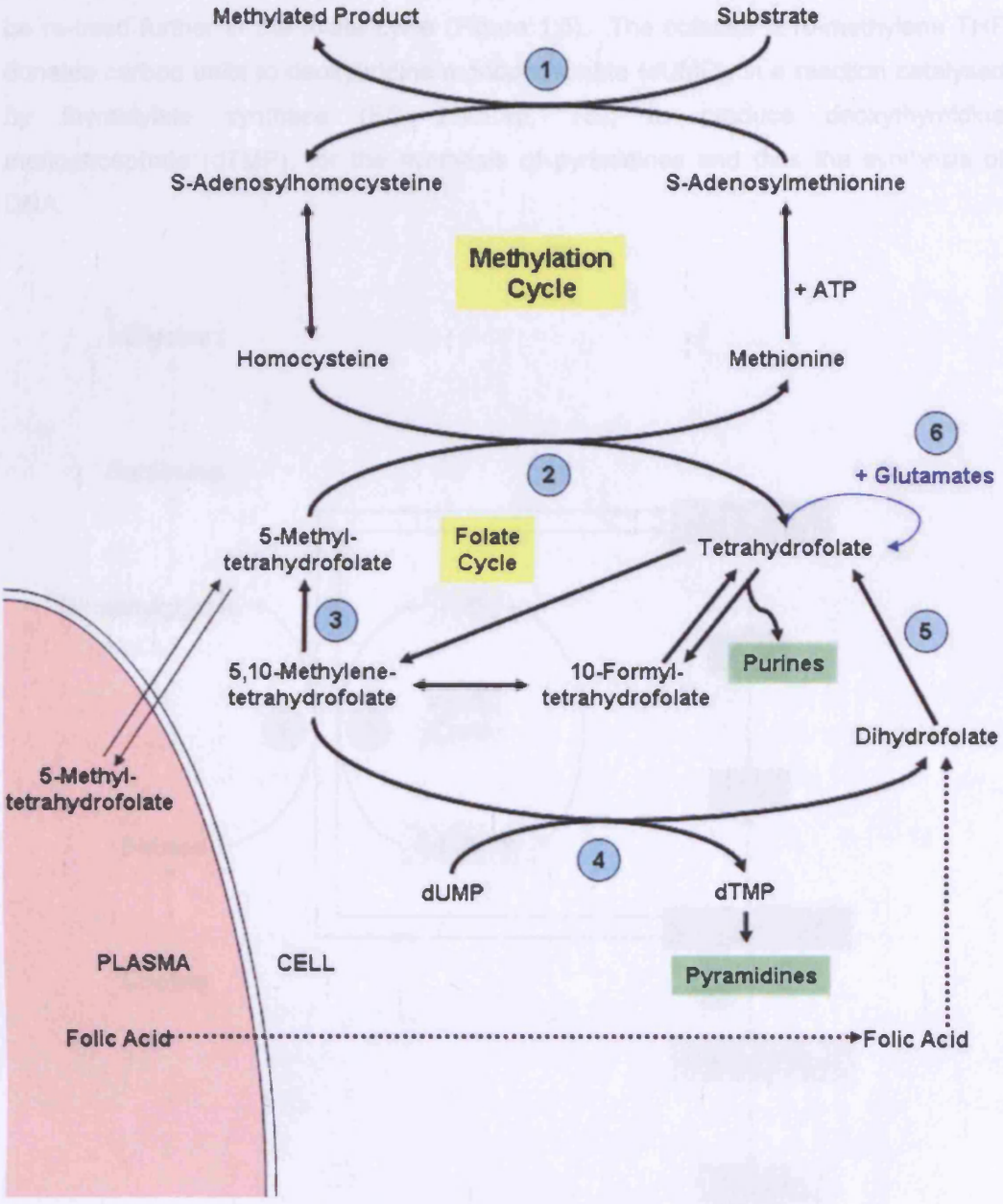

Figure 1.5. A diagram of One-Carbon Metabolism. Blue numbered circles represent the following enzymes: (1) Methyltransferases (MT), (2) Methionine Synthase (MS), (3) 5,10-Methylenetetrahydrofolate Reductase (MTHFR), (4) Thymidylate Synthase (TS), (5) Dihydrofolate Reductase and (6) Folylpolyglutamate Synthetase (FPGS). For chemical structures of folate species refer to Fig. 1.4, and of S-Adenosylmethionine and S-Adenosylhomocysteine refer to Fig. 3.2.

For the synthesis of DNA and RNA, folates are required for the *de novo* synthesis of both purines and pyrimidines. The cofactor 10-formyl THF donates its formyl groups to two enzymes involved in purine biosynthesis, both of which generate THF which can be re-used further in the folate cycle (Figure 1.5). The cofactor 5,10-methylene THF donates carbon units to deoxyuridine monophosphate (dUMP), in a reaction catalysed by thymidylate synthase (EC 2.1.1.45, TS), to produce deoxythymidine monophosphate (dTMP), for the synthesis of pyrimidines and thus the synthesis of DNA.

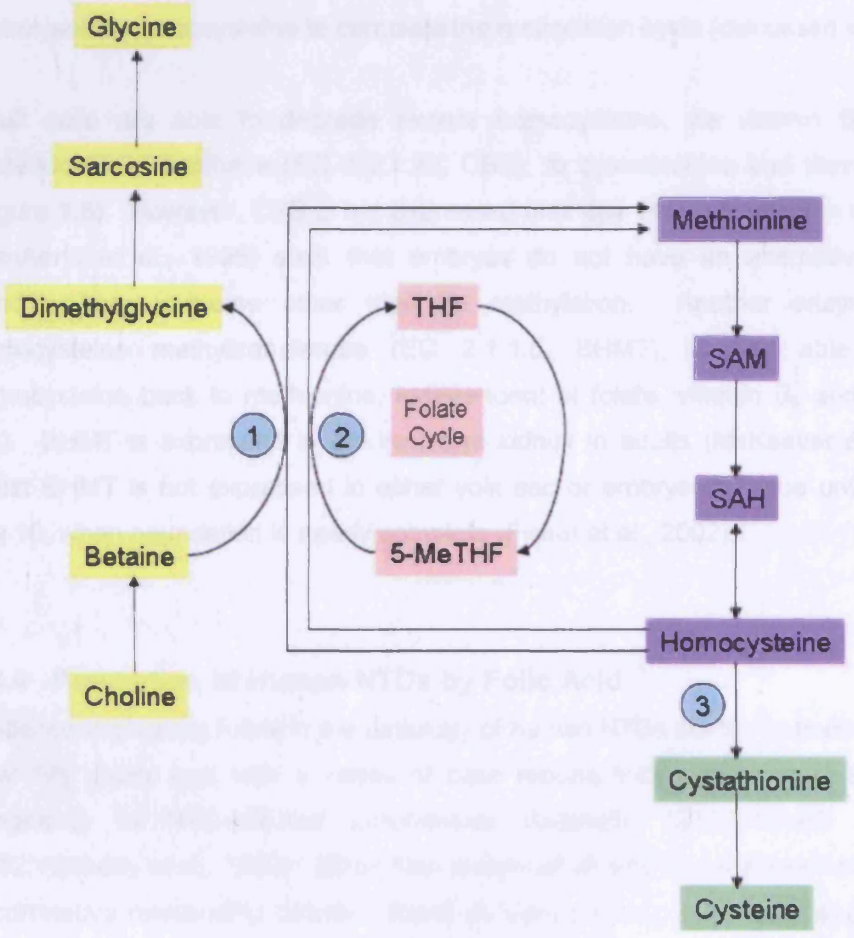

Figure 1.6. Pathways of Homocysteine Metabolism. 1, Betaine-homocysteine methyltransferase (BHMT); 2, Methionine Synthase (MS); 3, Cystathionine β Synthase (CBS). For chemical structures of folate species refer to Fig. 1.4, and of S-Adenosylmethionine and S-Adenosylhomocysteine refer to Fig. 3.2.

The enzyme, 5,10-methylenetetrahydrofolate reductase (EC 1.7.99.5, MTHFR) converts 5,10-methyleneTHF to 5-MeTHF in an irreversible reaction (Figure 1.5). This step provides a means to channel single carbon units derived from amino acids such as serine, histidine, glycine and also formate, to participate in the methylation cycle. The methyl group of 5-MeTHF is used by methionine synthase (MS) to methylate homocysteine to methionine, which is subsequently converted to S-adenosylmethionine (SAM), the universal methyl donor in methylation reactions catalysed by methyltransferases (MT). There are 115 different MT enzymes that transfer the methyl group of SAM to a wide variety of compounds including DNA, RNA, proteins and lipids. The product of this reaction, S-Adenosylhomocysteine (SAH), is hydrolysed to homocysteine to complete the methylation cycle (discussed in chapter 3).

Adult cells are able to degrade excess homocysteine, via vitamin B_6-dependent cystathionine β synthase (EC 4.2.1.22, CBS), to cystathionine and then to cysteine (Figure 1.6). However, CBS is not expressed until day 14 of gestation in the fetal liver (VanAerts et al., 1995) such that embryos do not have an alternative means of removing homocysteine other than by methylation. Another enzyme betaine-homocysteine methyltransferase (EC 2.1.1.5, BHMT) is also able to recycle homocysteine back to methionine, independent of folate, vitamin B_6 and B_{12} (Figure 1.6). BHMT is expressed in the liver and kidney in adults (McKeever et al., 1991), whilst BHMT is not expressed in either yolk sac or embryonic tissue until embryonic day 10, when neurulation is nearly complete (Fisher et al., 2002).

1.4.4 Prevention of Human NTDs by Folic Acid

Evidence implicating folate in the aetiology of human NTDs started to become apparent over fifty years ago, with a series of case reports linking the use of antifolates in pregnancy to NTD-affected pregnancies (Goetsch, 1962;Thiersch and Wash, 1952;Warkany et al., 1959). Since then a number of other publications have described a correlative relationship between folate deficiency during pregnancy and NTDs (see section 1.3.1) (Kirke et al., 1993;Smithells et al., 1976). Thus it became apparent with time that folate appeared to play a distinct role in the pathogenesis of human NTDs. These findings ultimately prompted various study groups to begin trials involving the administration of folic acid to women planning a pregnancy (Czeizel and Dudás, 1992;Kirke et al., 1992;Laurence et al., 1981;Smithells et al., 1981a;Smithells et al., 1981b;Smithells et al., 1983;Smithells and Sheppard, 1980;Wald et al., 1991).

The strongest evidence for the prevention of recurrent NTDs by folic acid came from the United Kingdom Medical Research Council Trial, a randomised, double-blind trial involving 1817 women with a history of a previous pregnancy affected by an NTD (Wald et al., 1991). Women were randomised into four groups: folic acid (4 mg/day) alone, folic acid (4 mg /day) plus multivitamins, multivitamins without folic acid, and placebo. Among 1195 completed pregnancies, there were six NTD recurrences among the 593 (1.0%) women who took folic acid compared with 21 among the 602 women (3.5%) who did not receive folic acid which represents a 72% protective effect. The multivitamin preparation without folic acid was found to have no protective effect. Around the same time, Czeizal and Dudas carried out a randomised double blind trial comparing multivitamin preparations to test the effects of NTD prevention (Czeizel and Dudás, 1992). Importantly, this trial studied the prevention of occurrence, rather than recurrence, of NTDs (women with no previous history of an NTD affected pregnancy) and the amount of folic acid used in this trial was at the lower level of 800 µg/day. Among the 2104 women receiving multivitamins including folic acid there were no NTD affected pregnancies compared to 6 NTD-affected pregnancies among 2052 women not receiving folic acid. While the numbers of affected pregnancies were lower than in the MRC trial, the results were significant ($p = 0.029$).

Critics of the MRC clinical trial, the only trial to conclusively demonstrate the effectiveness of folic acid alone, argue that there was no pure placebo group since the placebo capsules contained iron and calcium, both of which can affect zinc status which has been linked to neural tube defects (Turner et al., 2001). Additionally, serum folate levels were exceptionally high among women randomised to receive folic acid alone or multi-vitamins containing folic acid which might suggest that some women took several previously missed capsules at the same time to "catch up" just before their blood test (Turner et al., 2001). Thus, women taking multiple doses in the multivitamin alone and multivitamins plus folic acid groups would have been exposed to very high doses of vitamin A which is known to cause NTDs. Critics point out that this could explain why the incidences were higher in the multivitamins alone and the multivitamins plus folic acid groups, compared to the low incidences reported in the folic acid alone group.

Despite the criticism, in the early 1990s, publication of the two clinical trials convinced many that if women take folic acid beginning before conception they will lower their risk of having a baby with a NTD. This was followed by a large public health campaign undertaken in China whereby women who reported having taken folic acid alone (0.4 mg) during the periconceptual period had a lower prevalence of NTD affected

pregnancies (Berry et al., 1999). However, critics believe that the evidence was weakened by the fact that women were required to purchase the tablets themselves. Thus women who could not afford to purchase the folic acid, such as farmers and factory workers, may have been exposed to different risk factors or diet (Turner et al., 2001).

Recommendations are now in place in several countries to advise women planning their first pregnancy to supplement their diet with 0.4 mg/day of folic acid, whilst to prevent recurrence of NTDs women should take 4 mg/day of folic acid (Whitehead and Bates, 1997). Any risks associated with the use of high dose folic acid to treat recurrence are thought to be outweighed by the benefit, as such women have a recurrence risk of 4% (Scott et al., 1995). In the USA, millers have been required by law to fortify their flour with folic acid since 1998 to ensure women have an intake of 100 µg/day (Food and Drug Administration, 1996). Fortification led to a threefold increase in the median serum folate concentration and a twofold increase in the median red blood cell folate concentration in women of child bearing age (Centers for Disease Control and Prevention., 2002). This coincided with an estimated decline in the number of NTD-affected pregnancies in the US from 4,000 in 1995-1996 to 3,000 in 1999-2000 (Centers for Disease Control and Prevention., 2004;Centers for Disease Control and Prevention., 1999)). The main risk associated with folic acid fortification in a general population is that it may complicate the diagnosis of vitamin B_{12} deficiency which is common in the elderly, and can, if undetected, lead to pernicious anemia and neuropathy.

1.4.5 Folate prevents NTDs in mouse models

Among the numerous genetically manipulated mutant mouse strains which display a NTD mutant phenotype (Copp et al., 2003;Greene and Copp, 2005;Juriloff and Harris, 2000), the preventative action of folic acid has been observed in several mouse models including *splotch* (*Sp*^{2H}) and *Crooked tail* and the *Cart1* and *Cited2* knockouts (Carter et al., 1999;Fleming and Copp, 1998;Martinez-Barbera et al., 2002;Zhao et al., 1996). These mouse models provide an experimental system to study the unknown mechanisms underlying the prevention of human NTDs by folic acid.

Homozygous mice for *Cart1* develop cranial NTDs believed to result from excessive cell death of the forebrain mesenchyme, which causes a reduction in cell number that is assumed to prevent the closure of the cranial neural folds (Zhao et al., 1996). Folic acid reduces the incidence of exencephaly by 60%, although it is not clear whether this

is through the prevention of apoptosis or a compensatory increase in cell number, perhaps by stimulation of proliferation. The development of exencephaly in *Cited2* homozygous null mice is also associated with excessive apoptosis at the forebrain-midbrain boundary (Martinez-Barbera et al., 2002). Treatment with folic acid significantly reduces the incidence of exencephaly, but there is no obvious amelioration of the excessive apoptosis. Cell proliferation in the neuroepithelium of *Cited2* null embryos was comparable to that in wild-type litter mates but, unfortunately, it was not established whether folic acid treatment caused an up-regulation of cell proliferation to overcome the excessive apoptosis. The cellular mechanism of NTD in *splotch* has yet to be clarified (discussed further in chapter 5) but it has been suggested that failure of neural tube closure also occurs as a result of increased cell death (Pani et al., 2002).

In contrast to the previously mentioned studies in which FA was administered by maternal i.p. injections, the effect of maternal folate supplementation on the incidence of exencephaly in the *Crooked tail* mouse model was investigated using diets differing only in the concentration of folic acid. Embryonic lethality was prevalent among *Cd/Cd* embryos receiving a folate deficient diet (0 mg/kg), while on the 4 mg/kg diet, exencephaly became a more common outcome. On diets containing a higher FA content, most *Cd/Cd* embryos were viable and closed their neural tubes. Thus, low dose FA rescues lethality and high dose FA rescues NTDs. A recent report identified the *Crooked tail* gene as low density lipoprotein receptor 6 (Lrp6), a co-receptor required for Wnt signalling (Carter et al., 2005), but it remains to be investigated if folate affects this pathway.

Mouse Model	Reference	NTD	Suggested mechanism	Prevention by other agents?
Cart1-/-	(Zhao et al., 1996)	EX	Excess apoptosis	-
Cited2-/-	(Martinez-Barbera et al., 2002)	EX	Excess apoptosis	-
Crooked tail	(Carter et al., 1999)	EX	Canonical Wnt signalling	-
Splotch^{2H}	(Fleming and Copp, 1998)	SB and EX	Excess apoptosis	Thymidine

Table 1.1. Summary of Mouse Models in which NTDs are preventable by folic acid. EX, exencephaly, SB, Spina bifida.

Using the dU suppression test (for details see Chapter 4) *Cited2* null embryos have been shown to have apparently normal folate cycling whilst homozygous *splotch* mutant embryos do not. Moreover, a recent publication demonstrated that *Crooked tail* mutants appear to have an underlying defect in the utilisation of intracellular folate (Ernest et al., 2006). Thus, it appears that among the mutants in which folic acid is known to prevent NTDs, only the *Cart1* and *Cited2* mutants do not have a folate-related defect, but further work may question this.

1.5 Mechanisms of prevention of NTDs by folic acid

Despite extensive research the mechanism explaining the preventative effect of folic acid on NTDs remains unclear. Several areas of research are described below.

1.5.1 Maternal folate deficiency

The original mechanism proposed that folic acid supplementation rescues maternal folate deficiency, arising from insufficient folate in the diet (Smithells et al., 1976). Thus, there have been numerous studies to date, using a variety of methods which attempted to definitively establish whether maternal folate status is linked to NTD risk (Table 1.2).

The main criticism of studies that determine folate status late in pregnancy or following delivery is that they would only be predictive of folate status at the critical time of neural tube closure if the mother kept to the same diet after pregnancy (Scott et al., 1995). However, retrospective analysis of this type may identify genetic disturbances which have long term effects. Analysis of maternal folate status in serum taken at the first antenatal clinic visit (two months after the neural tube has closed) attempted to overcome this potential drawback (Kirke et al., 1993;Mills et al., 1995;Molloy et al., 1985). However, the results failed to conclusively demonstrate a correlation between maternal folate deficiency and the incidence of NTD (Table 1.2).

Ref.	Maternal Sample Type	Time of study	Difference in folate status between cases and controls?	Other findings
1	Serum	Retrospective	No difference	-
2	Serum	Retrospective	No difference	-
3	RCF & serum	Early pregnancy	Cases had lower RCF	-
4	RCF & serum	Retrospective	More cases had a lower RCF	-
5	Serum	1st antenatal clinic visit	No difference	No difference in vit. B_{12}
6	RCF & serum	Retrospective	Cases had lower RCF	-
7	Whole blood	Mid-gestation	No difference	Amniotic fluid vit. B_{12} was lower in cases
8	Serum	8 weeks after neurulation	No difference	No difference in vit. B_{12} or retinol
9	RCF & plasma	1st antenatal clinic visit	Cases had lower RCF & plasma folate	Cases had lower vit. B_{12}
10	RCF & serum	Retrospective	Relationship between RCF & serum folate differs between cases and controls	No difference in vit. B_{12} or vit. C
11	RCF & plasma	1st antenatal clinic visit	No difference	Cases had higher homocysteine
12	RCF & serum	Before & during pregnancy	Cases had lower RCF and serum folate	Cases had lower vit. B_{12}
13	RCF & plasma	Retrospective	Cases had lower plasma folate. SB patients also had lower plasma folate.	SB patients & parents had higher homocysteine & subset had lower vit. B_{12}

Table 1.2. Studies investigating differences in maternal folate status between cases and controls. Cases, mothers with an NTD-affected pregnancy; controls, mothers with a normal pregnancy. 1, (Emery et al., 1969); 2, (Hall, 1972); 3, (Smithells et al., 1976); 4, (Schorah et al., 1983); 5, (Molloy et al., 1985); 6, (Yates et al., 1987); 7, (Economides et al., 1992); 8, (Mills et al., 1992); 9, (Kirke et al., 1993); 10, (Wild et al., 1993); 11, (Mills et al., 1995); 12, (Wald et al., 1996); 13, (Van der Put et al., 1997b).

Sample type also has an effect on the outcome of studies in which folate is quantified. Red blood cell folate (RCF) estimations are believed to be a reliable method of assessing long-term folate status, due to the stable nature of red cell folate (Hoffbrand et al., 1966). Serum folate is dramatically altered by food intake, whereas red cell folate is only affected by long-term changes in dietary folate. Thus, sample type needs to be chosen depending on whether interest is in retrospective examination of the effects of genetic variations which cause long-term changes in folate status. Alternatively, the aim may be to quantify folate level at the time of neural tube closure, to determine if there is a transient folate deficiency (e.g. due to dietary folate deficiency) which leads to a NTD. Significantly lower maternal RCF levels were detected in NTD affected pregnancies, supporting the view that an inherited disorder of folate metabolism is involved in the etiology of NTDs (Smithells et al., 1976;Yates et al., 1987). In addition, changes in serum and plasma folate during pregnancy also support the idea that transient folate deficiency may be related to NTD risk (Economides et al., 1992;Kirke et al., 1993). However, low maternal folate levels associated with NTDs are not considered clinically folate deficient, thus maternal status appears to be sub-optimal but within the 'normal range' (Kalter, 2000).

Two studies using folate deficient diets concluded that folate deficiency does not produce NTDs in wild-type mice (discussed in section 5.1.1) (Burgoon et al., 2002;Heid et al., 1992). The level of dietary folate in a genetically predisposed mutant can affect the incidence of NTDs (Carter et al., 1999) such that a higher rate of exencephaly is observed with lower dietary content of folic acid (see section 1.4.5). Overall, sub-optimal folate status does appear to be involved in the pathogenesis of NTD but the findings to date are inconclusive and further work is needed for clarification.

1.5.2. Insufficient uptake of folate due to defective intracellular transport

Folic acid supplementation may act to overcome defective intracellular uptake of folate. For example, insufficient maternal uptake could lead to embryonic folate deficiency or affect the uterine environment. Isolated embryonic folate deficiency could also arise from defective maternal-to-fetal folate transport or insufficient uptake of folate by embryonic cells. Thus, it has been proposed by several groups that defective intracellular transport of folate, as a result of a genetic variation in genes encoding the folate receptors, could increase susceptibility to NTDs. Folic acid supplementation could be envisaged to promote intracellular uptake either by the defective receptor, due to an increase in folate availability, or the presence of a different folate species could perhaps promote uptake by an alternative receptor. To investigate this mechanism, the

role of the folate receptors has been examined using transgenic mice and studies of genetic variants of the human folate receptors.

Targeted inactivation of *RFC1* causes early embryonic death at E9.5 with very severe growth retardation. However, the development of *RFC-/-* embryos could be sustained until E18.5 with supplemental folic acid, but the authors did not find any evidence of a NTD phenotype in these supplemented embryos (Zhao et al., 2001). The impact of a known A80G polymorphic variant in the human *RFC1* gene on NTD risk was evaluated in 174 Italian probands. The data supported the hypothesis that the *RFC1* A80G variant may contribute to NTD susceptibility in the Italian population (De Marco et al., 2003b). However this finding was not supported by a second study in a different population (Shaw et al., 2002) (Table 1.2.). A recent study reported that mothers with the homozygous mutant GG genotype, with a low red blood cell folate, were at increased risk for having a child with a NTD (Morin et al., 2003), suggesting an interaction between genotype and nutritional status.

Loss of function of the recently identified PCFT intestinal folate receptor has been associated with hereditary folate malabsorption. However, patients with this disease have no evidence of NTDs and symptoms appear months after birth, implying that this gene is not absolutely required for neural tube closure (Qiu et al., 2006). Rather, owing to its role in intestinal folate absorption, polymorphisms in this gene might contribute to maternal folate deficiency and thereby increase the chances of NTDs associated with dietary folate deficiency. Thus, if polymorphisms which affect function of PCFT are identified it would be of interest to investigate the frequency of NTDs in offspring of mothers who carry those polymorphisms.

Inactivation of *Folbp1* (murine homologue of FRα) causes early embryonic death although when embryos are sustained until later in development, following supplementation of dams with exogenous folate, embryos do develop NTDs (Piedrahita et al., 1999). In the same study, embryos were reported to be unaffected following the loss of Folbp2 (murine homologue of FRβ). An antisense oligonucleotide against Folbp1 mRNA was found to cause NTDs in a dose-dependent manner when injected into the amniotic sac of mouse embryos (Hansen et al., 2003). Thus, overall, cellular uptake of folate by Folbp1 appears to be essential for murine neural tube closure. However, candidate gene analysis has failed to demonstrate evidence for an association between genetic variations in FRα and the incidence of NTDs (Table 1.2).

Human Gene	Reference	Sample	Conclusion
FRα	(Trembath et al., 1999)	172 US families	No evidence for an association
FRβ	(Trembath et al., 1999)	172 US families	No evidence for an association
RFC1	(De Marco et al., 2002)	203 cases, 98 mothers and 67 fathers (Italian)	Higher frequency of the RFC1 A80G and MTHFR A1298C polymorphisms in cases, mothers and fathers
RFC1	(Shaw et al., 2002)	133 case infants and 188 control infants (California)	Non-significant increase in risk associated with A80G in newborns whose mothers had not used vitamins.
RFC1	(De Marco et al., 2003a)	174 cases, 43 mothers, 53 fathers and 156 controls (Italian)	Evidence for increased risk to cases and mothers (A80G), but not in combination with MTHFR
PCFT	-	-	No studies undertaken to date

Table 1.3. Genetic variants in genes coding for folate transporters and their association with NTDs.

A pilot study in humans has shown that serum from women with a pregnancy complicated by a NTD contains auto-antibodies that bind to folate receptors (FR) and may block the cellular uptake of folate (Rothenberg et al., 2004). It could be envisaged that the blockage of cellular folate uptake by the auto-antibody could be bypassed by folic acid because it is transported into cells by the reduced folate carrier (RFC1). Alternatively, folic acid which has a high affinity for the folate receptors (FR) may displace an autoantibody with a lower affinity for the folate receptors (FR). This study highlights a possible role for FR in NTD affected pregnancies, independent of a mutation in folate receptor genes.

1.5.3 Disorders in folate metabolism

Disorders in folate metabolism in either the fetus or the mother may contribute to NTD risk, such that supplemental folate could act to overcome this metabolic disturbance. Thus, following the recognition of folate as an important environmental contributor to the risk of NTD, numerous studies have attempted to identify polymorphic variants in genes related to folate metabolism that alter NTD risk. This led to the emergence of the first genetic risk factor for NTDs, at bp 677 in the folate enzyme methylenetetrahydrofolate reductase (MTHFR).

A thermolabile variant of MTHFR was first reported in a group of coronary artery disease patients, in which reduced residual enzyme activity was observed after heating lymphocyte extracts at 46 °C for 5 minutes (Kang et al., 1988). Following the isolation of the cDNA for MTHFR (Goyette et al., 1994), a C → T base substitution at bp 677 was identified, which converted an alanine residue to a valine residue (Frosst et al., 1995). Biochemical analysis showed that this was the previously described thermolabile variant and, furthermore, reduced specific activity was recorded at 37 °C. Later reports demonstrated that individuals with the 677TT genotype were predisposed to hyperhomocysteinemia, when associated with low folate status (Jacques et al., 1996). Folate has been shown to stabilise the wild-type and mutant enzyme, by preventing the loss of flavin adenine dinucleotide. Thus with higher folate levels the mutant enzyme is able to function relatively normally, providing adequate amounts of 5-MeTHF to prevent hyperhomocysteinemia (Guenther et al., 1999;Malinow et al., 1997;Yamada et al., 2001).

Two groups demonstrated that mothers of NTD infants have higher than normal homocysteine concentrations (Mills et al., 1995;Steegers-Theunissen et al., 1994). Since plasma homocysteine is a sensitive marker of folate status, researchers turned

their attention to investigating whether folate metabolism was abnormal in these mothers. This ultimately led to the identification of MTHFR 677C → T variant as the first genetic risk factor for NTD in patients and parents (Van der Put et al., 1995). Following the initial report, many studies worldwide reported similar findings, although in other cases its association with NTDs was not detected (Boyles et al., 2005). The MTHFR C677T variant is extremely common occurring in approximately 5-15% of the population (Botto and Yang, 2000), although this varies widely between different populations. It is believed that in areas where the frequency of homozygosity is low, the relationship between the C677T and the incidence of NTDs may not be apparent, thus explaining why some studies were inconclusive. To clarify the relationship between MTHFR and NTD risk, various meta-analyses have been performed taking into account all studies (Blom et al., 2006;Botto and Yang, 2000;Van der Put et al., 1997a). The most up-to-date estimate calculated that mothers who were homozygous for the 677TT variant have a 60% increased risk of having an NTD-affected pregnancy, whereas homozygous offspring themselves have a 90% increased risk of being born with an NTD (Blom et al., 2006). Additionally, there is a 10% and 30% increased risk for mothers and offspring who are heterozygous (677CT) (Blom et al., 2006).

Despite the identification of the *MTHFR* C677T variant, the search to find other genetic variants involved in folate metabolism has been relatively unsuccessful (Boyles et al., 2005;Rozen, 2006). A second common variant in MTHFR, A1298C, by itself does not appear to affect NTD risk (Botto and Yang, 2000;Van der Put et al., 1998). However, compound heterozygosity for 1298C and 677T has been suggested to increase risk, although the results are conflicting (Richter et al., 2001;Trembath et al., 1999;Van der Put et al., 1998).

Mouse models in which enzymes involved in folate metabolism are disrupted may be very useful in studying the relationship between abnormal folate metabolism and risk of NTD. Examples of folate metabolising enzymes that have been knocked out in mice by gene targeting include CBS, MTHFR and MS (Figure 1.5 and 1.6), all of which are associated with hyperhomocysteinenia. Mice with a disruption of CBS, the first enzyme in the transsulfation pathway for homocysteine metabolism, do not develop NTDs (Watanabe et al., 1995). The significance of this model for the study of NTDs may be limited as it appears that this enzyme, which is found primarily in the adult liver, is not expressed in embryonic tissues at neurulation stages (VanAerts et al., 1995). However, an effect via maternal metabolism may be plausible.

In order to further investigate the possible association between MTHFR deficiency and increased risk for NTD, a MTHFR null mutant mouse was generated by gene targeting (Chen et al., 2001a). Heterozygous mutant mice appeared normal, whilst homozygous mice were smaller and developmentally retarded with a cerebellar pathology. Pre-natal survival of homozygous mice was reduced and surviving pups died within the first two weeks of their lives. The homozygous mutant animals that died before weaning had the appearance of a kinked tail, but there was no evidence of exencephaly or spina bifida.

Methionine Synthase (MS) would be an interesting candidate to influence NTD risk since it requires vitamin B_{12} as a co-factor and lies at the intersection between the folate and methylation cycle. A knockout model of MS was generated to gain further insight into the physiological roles of MS and the effects of impaired MS activity (Swanson et al., 2001). Heterozgous MS knockout mice were found to be indistinguishable from wild-type littermates despite having slightly elevated homocysteine and methionine, whilst homozygous MS knockout mice die soon after implantation, demonstrating the importance of this enzyme for early embryonic development (Swanson et al., 2001). Since MS null mice die prior to neurulation, the role of MS in neurulation has yet to be clarified in mouse embryos. A large study of plasma vitamin B_{12} levels collected at the first antenatal clinic conclusively showed that women affected by NTD pregnancies had lower plasma B_{12}, in addition to lower plasma folate and RCF, compared to controls (Kirke et al., 1993). Moreover, candidate gene analysis of the MS A2756G polymorphism has been associated with reduced risk for NTDs (Christensen et al., 1999), although this finding has not been supported by other groups (Boyles et al., 2005).

Overall, knockouts of MTHFR, CBS and MS have not provided immediately obvious animal models of NTDs. However, it is possible that heterozygotes may prove useful since it is possible that heterozygotes would be more susceptible to dietary deficiencies than wild-types and thus, would enable interactions between genetic and nutritional status to be studied. In addition, it is possible that crosses between heterozygous mice deficient in different enzymes involved in folate metabolism may uncover genetic interactions which increase NTD risk. Further work is required to study the roles of the other enzymes in the folate and methylation cycle. However, other techniques may need to be employed since many folate enzymes are essential for embryonic development such that genetic knockouts of folate enzymes may result in homozygotes which do not survive to neurulation stages.

1.5.4 Disorders in one-carbon metabolism

Recent findings have prompted the "methylation hypothesis" which proposes that folic acid prevents NTDs by stimulating cellular methylation reactions (Blom et al., 2006). The strongest genetic variant identified to date which increases risk of an NTD-affected pregnancy is the *MTHFR* C677T polymorphism (Van der Put et al., 1995). The *MTHFR* enzyme directs one-carbon units, away from DNA synthesis, towards the methylation cycle. Thus, an association between the *MTHFR* C677T polymorphism and NTDs supports a role for the methylation cycle in the etiology of NTDs. Moreover, *MTHFR* polymorphisms which affect the efficiency of this enzyme have been associated with DNA hypomethylation (Castro et al., 2004;Friso et al., 2002b). However, MTHFR null mice do not develop NTDs (Chen et al., 2001a) therefore compensatory mechanisms may operate to overcome this disruption in one-carbon metabolism.

Cancer research has clearly demonstrated that variation in dietary levels of methyl-donors and folate can alter DNA methylation and subsequently, gene transcription (Poirier, 2002). For example, alterations in hepatic p53 gene methylation patterns were observed during tumour progression with folate/methyl deficiency in the rat (Pogribny et al., 1997). Increases in levels of plasma homocysteine, such as those associated with nutritional deficiencies or genetic polymorphisms in the folate pathway, have also been associated with parallel increases in plasma SAH and lymphocyte DNA hypomethylation (Yi et al., 2000). Similarly, diet induced folate-depletion in post-menopausal women was found to increase homocysteine levels and decrease lymphocyte DNA methylation (Jacob et al., 1998). A study in pregnant women and newborns has also linked vitamin deficiency with low SAM/SAH ratios (Guerra-Shinohara et al., 2004).

A direct link between dietary folate, DNA methylation and gene transcription has been demonstrated in animal models. For example, epigenetic regulation of transcription was demonstrated in the viable yellow agouti (Avy/a) mouse model using a methyl-rich diet which caused increased DNA methylation. This methylation silenced transcription of a retro-viral transposon within the *agouti* gene and normalised expression of the *agouti* gene, resulting in a change of coat colour from yellow to brown (Waterland and Jirtle, 2003;Wolff et al., 1998). Thus, it is evident that folate nutrition may play a key role in the regulation of the methylation cycle and DNA methylation. However, it remains to be definitively established how the diet, particularly the folate content, might affect methylation in NTD models.

Microarray analysis following folic acid supplementation to rescue NTDs in *Folbp-/-* embryos demonstrated an increase in the expression of the *PCMT1* gene (which encodes the protein repair enzyme L-isoaspartate *O*-methyltransferase, PIMT), thus implicating a possible role for protein methylation in the prevention of NTD (Spiegelstein et al., 2004). Additionally, a known functional polymorphism of the *PCMT1* protein (Ile120Val) in the SAM binding motif has been found to be associated with a reduced risk for spina bifida when patients are of the Val120Val genotype (Zhu et al., 2006).

Other pathways involved in one-carbon metabolism, besides the folate and methylation cycles, may also play a role in the pathogenesis of NTDs. These include the pathways for polyamine synthesis and the catabolism of choline and betaine. Decarboxylated SAM, formed from the methylation cycle metabolite SAM, is required for the synthesis of the polyamines, spermidine and spermine. Polyamines are positively charged molecules which interact with DNA, RNA and phospholipids, and play essential roles in the growth and function of normal cells (Wallace et al., 2003). Their role during neurulation has yet to be investigated but the recent development of polyamine inhibitors may prove useful agents in the future. Choline can be metabolised to betaine, which serves as an alternative methyl donor for the remethylation of homocysteine to methionine by the enzyme BHMT (Figure 1.6). Dietary intake of choline and betaine has been associated with reduced risk of NTDs (Shaw et al., 2004), whilst perturbation of choline metabolism in mouse embryo culture causes NTDs (Fisher et al., 2001;Fisher et al., 2002). However, to date, there is no evidence implicating abnormalities in the *BHMT* gene as NTD risk factors (Boyles et al., 2005).

1.5.5 NTD causing teratogens and folates

Embryonic exposure to environmental agents and conditions plays a key role in the aetiology of NTDs (see section 1.2.2). Described below are three examples whereby folate has been shown to prevent NTDs induced by teratogenic or environmental agents.

1.5.5.1 Valproic Acid

Maternal use of the anti-convulsant drug, valproic acid (VPA), is associated with a 1-2% risk of spina bifida in infants, compared with a risk of 0.06% in the general population (Robert and Guidbaud, 1982). In contrast, VPA treatment in mice induces

mainly exencephaly, whilst spina bifida is rarely reported (Ehlers et al., 1992;Nau et al., 1991). The reason why VPA induces exencephaly in mice and spina bifida in humans is not understood but it may be that there are some common events in cranial and spinal closure which are susceptible to VPA. Published reports of the effects of folic acid on the frequency and severity of VPA-induced NTDs have described differing results claiming both ameliorative and augmentative effects, whilst some studies report no effects at all (Hansen et al., 1995;Hansen and Grafton, 1991;Nau et al., 1991;Padmanabhan, 1997;Padmanabhan and Shafiullah, 2003;Seller, 1994b;Trotz et al., 1987). These differences may have arisen due to species and strain variations, and differences in dose and timing of folic acid treatment.

Epileptic patients with malformed infants have a particularly low plasma folate concentration (Dansky and Finnell, 1991;Ogawa et al., 1991). The link between VPA therapy and alterations in folate metabolism comes from the fact that anti-epileptic agents, including VPA, were shown to interfere with folate metabolism in the embryo (Hansen and Billings, 1985;Netzloff et al., 1979). Folate levels are known to be lowered during pregnancy and anti-epileptic drugs including VPA, intensify this effect (Handel et al., 1984;Lewis et al., 1998). VPA may also reduce folic acid and B12 levels in pregnant mice (Padmanabhan, 1997). One study, investigating maternal metabolic effects after treating pregnant mice with VPA reported methioinine deficiency. This was associated with elevated homocysteine in plasma, whilst hepatic concentrations of SAM and SAH were both increased (Hishida and Nau, 1998). Thus, VPA-induced NTDs may be associated with impaired folate or methylation cycle metabolism which can be ameliorated by supplemental folate metabolites.

1.5.5.2 Fumonisins

Fumonisins are a family of toxic and carcinogenic mycotoxins produced by a common fungal contaminant of maize (Gelderblom et al., 1988). Fumonisins cause accumulation of bioactive sphingolipid intermediates as well as the depletion of complex sphingolipids, through inhibition of ceramide synthase. Disruption of sphingolipids can affect cell membrane lipid microdomains which are required for the function of membrane proteins. High incidences of NTDs occur in some regions of the world where substantial consumption of fumonisins has been documented or suggested, suggesting that fumonisin intake is a risk factor for human NTDs.

In mouse embryos, exposure to a prevalent fumonisin isoform, FB_1, affects overall growth and causes cranial NTDs both *in vivo* and in embryos maintained in culture

(Marasas et al., 2004;Sadler et al., 2002). Significantly, administration of supplemental folate or complex sphingolipids protected embryos from the teratogenic effects of FB_1. A potential link between fumonisins, folates and NTD risk originates from studies by Stevens and Tang who demonstrated that receptor-mediated folate uptake was halved in cells pretreated with fumonisin (Stevens and Tang, 1997). The folate transporter (Folbp1/FRα) is a glycosylphophatidylinositol-anchored protein associated with lipid microdomains. Since fumonisins act via the inhibition of ceramide synthase, it has been proposed that this teratogen interferes with the function of the folate receptor, and thereby affects growth and neural tube closure. Thus, fumonisin may cause embryonic folate deficiency due to impaired function of the placental folate receptor.

1.5.5.3 Hyperthermia-induced NTDs

Both in humans and laboratory animals, brief maternal exposure to high temperatures (>2.5 °C above normal) early in pregnancy has been associated with the occurrence of NTDs (Edwards et al., 1995). Experimental exposure to hyperthermia in mouse embryos causes exencephaly, the frequency of which can be modified by other exogenous agents such as alcohol (Shiota, 1988;Shiota et al., 1988). Supplemental folic acid is capable of preventing hyperthermia-induced NTDs (Shin and Shiota, 1999), thus, demonstrating that FA can protect against environmentally induced NTDs. It is not clear how FA can prevent heat-induced NTDs but it has been proposed that FA may ameliorate the transient arrest of cell proliferation, which has been reported following brief maternal hyperthermia (Shin and Shiota, 1999).

1.6 Summary

In summary, there has been a vast array of studies investigating the role of folate in the prevention of NTDs and several mechanisms have been described. Overall, studies of folate-preventable NTDs implicate a role for multiple interacting genes and environmental influences. Further work is needed to study the role of gene-gene and gene-environment interactions that alter NTD risk. Nonetheless, despite worldwide recommendations on folate supplementation and folate fortification in the USA, women are still having NTD-affected pregnancies. This fact demonstrates the need for adequate education about the benefit of folic acid and highlights the need for approaches for prevention of folate-resistant NTD.

1.7 Aims of this study

The main aims behind this study are to gain a greater understanding of the protective effect exerted by folic acid against neural tube defects, to study how low folate status increases NTD risk and to investigate other agents capable of preventing NTDs, which can be used in conjunction with folic acid. The study attempts to answer the following questions;

1) What is the abundance of methylation cycle intermediates in neurulation-stage embryos?

To explore the role of embryonic one-carbon metabolism in the pathogenesis of NTDs, a novel method was developed using Liquid Chromatography Tandem Mass Spectrometry (LC-MS/MS) to quantify the concentration of two one-carbon metabolites, S-Adenosylmethionine (SAM) and S-Adenosylhomocysteine (SAH) in neurulation-stage mouse embryos.

2) Are NTDs associated with perturbations of the methylation cycle?

The method developed to quantify SAM and SAH provided the means to analyse mouse embryos in which NTDs occurred following perturbation of the methylation cycle or DNA methylation. The method was further adapted to quantify SAM and SAH in cells derived from two populations of NTD patients, to test whether the methylation cycle was disturbed.

3) Does dietary folate deficiency influence the incidence of NTDs in a folate-preventable mouse model?

A folate-deficient diet was used to test whether dietary folate deficiency increases the incidence of NTDs in a folate-preventable (*splotch*) mutant mouse strain. Using this system, I explored the interaction between an environmental and a genetic factor in the etiology of folate-preventable NTDs.

4) Does dietary folate deficiency influence the incidence of NTDs in a mouse model which does not respond to folic acid supplementation?

A folate-deficient diet was used to test the effect of dietary folate deficiency on the incidence of NTDs in the *curly tail* mutant mouse strain, in which spinal NTDs are not preventable by folic acid. Folate deficiency caused an increased rate of exencephaly both in *curly tail* and a genetically matched wild-type strain. Maternal and embryonic one-carbon metabolism was then studied in these mice.

CHAPTER 2

General Methods

2.1 Materials

Unless stated, all compounds were purchased from Sigma-Aldrich. Solvents and water used for LC-MS/MS were of HPLC grade (Fisher Scientific). For the *L.casei* micobiological assay and the protein determination assay, samples were analysed in sterile microwell (96 well) plates (Nunc). The folic acid *L. casei* media provided by Prof. John Scott was purchased from Difco in large batches to ensure consistency for clinical assays. Prof. John Scott also kindly donated the prepared *Lactobaccillius casei* (*L.casei*) bacteria inoculums. Samples were analysed by LC-MS/MS using vials with 200 µl inserts sealed with standard PTFE caps (Chromocol). Sterile phosphate buffered saline (PBS) solutions, prepared by adding 1 PBS tablet (Oxoid) to 100 ml of dH_2O, were sterilised by autoclaving at 115 °C for 10 min.

2.2 Mouse Colonies

Non-mutant CD1 mice (Charles River Laboratories Inc.) and wild-type mice on a partially congenic *curly tail* background ($+/+^{ct}$) were maintained as random bred colonies. *Curly tail* mice (*ct/ct*) were maintained as a homozygous, random-bred stock to ensure that all mice/embryos were homozygous for the unknown *ct* mutation. *Splotch* (Sp^{2H}) mice were maintained as a closed colony by matings of $Sp^{2H}/+$ males with wild-type females. Heterozygous offspring, which are identified by the presence of a belly spot, were used for generation of experimental litters. Female $Sp^{2H}/+$ were mated with $Sp^{2H}/+$ males to produce embryos of +/+, $Sp^{2H}/+$ and Sp^{2H}/Sp^{2H} genotype (section 2.5). All mice were housed in plastic-bottomed cages with shavings and were exposed to a 12 hour light/dark cycle in a temperature-controlled room.

2.3 Dietary Studies

A normal diet (ND; Harlan, Ref. No. 2018), the recommended diet intended for laboratory animals (Harlan), contained adequate quantities of all nutrients (Table 2.1). For the dietary studies in chapters 5 and 6, mice received synthetic diets which, apart from the folic acid, succinylsulfathiazole and myo-inositol content, contained identical levels of all other nutrients (Table 2.1). Mice had free access to the assigned diets for a minimum of three weeks prior to mating. Injections (I.P. injections) of folic acid, thymidine, and myo-inositol, dissolved in PBS, into the peritoneal cavity were given at E7.5, E8.5, E9.5 and E10.5 (for further details see section 5.2 and 6.2).

Minerals		
Calcium	%	1.01
Phosphorus	%	0.65
Sodium	%	0.23
Potassium	%	0.68
Chloride	%	0.40
Magnesium	%	0.20
Zinc	mg/kg	77.00
Manganese	mg/kg	118.00
Copper	mg/kg	15.21
Iodine (added)	mg/kg	11.55
Iron	mg/kg	226.00
Selenium	mg/kg	0.20
Cobalt	mg/kg	0.63
Chromium	mg/kg	0.53

Amino Acids		
Aspartic Acid	%	1.42
Glutamic Acid	%	3.70
Alanine	%	1.08
Glycine	%	0.79
Threonine	%	0.67
Proline	%	1.55
Serine	%	0.97
Leucine	%	1.94
Isoleucine	%	0.85
Valine	%	0.95
Phenylalanine	%	0.99
Tyrosine	%	0.61
Phe + Tyr	%	1.60
Methionine	%	0.35
Cysteine	%	0.33
Met + Cyst	%	0.69
Lysine	%	0.92
Histidine	%	0.47
Arginine	%	1.06
Tryptophan	%	0.20
Available Lysine	%	0.83

Vitamins		
Vitamin A	iu/g	15.40
Retinol	mg/kg	4.65
Vitamin D_3	iu/g	1.54
Cholecalciferol	µg/kg	38.39
Vitamin E	mg/kg	101.00
Vitamin K_3	mg/kg	51.00
Vitamin B_1	mg/kg	16.50
Vitamin B_2	mg/kg	14.90
Available Niacin	mg/kg	41.20
Vitamin B_6	mg/kg	18.50
Pantothenic Acid	mg/kg	33.00
Vitamin B_{12}	mg/kg	0.08
Available Biotin	mg/kg	0.30
Folate	*mg/kg*	*3.34*
Vitamin C	mg/kg	0.00
Choline	mg/kg	1120.00
B Carotene	mg/kg	2.47
Inositol	*mg/kg*	*1455.00*

Fatty Acids		
C12:O Lauric	g/kg	0.26
C14:O Myristic	g/kg	0.06
C16:O Palmitic	g/kg	7.64
C18:O Stearic	g/kg	1.50
C20:O Arachidic	g/kg	0.10
C22:O Behenic	g/kg	0.03
C16:1ω7 Palmitoleic	g/kg	0.07
C18:1ω9 Oleic	g/kg	12.59
C20:1ω9 Gadoleic	g/kg	0.17
C22:1ω9 Erucic	g/kg	0.01
C18:2ω6 Linoleic	g/kg	31.35
C18:3ω3 Linolenic	g/kg	2.76

Proximate Analysis		
Crude Protein	%	18.90
Crude Oil	%	6.00
Crude Fiber	%	3.80
Ash	%	5.90
NFE	%	55.40
Carbohydrate	%	57.33
Starch	%	41.24
Sugar	%	4.93
Digestible Energy	Kcal/g	3.4
Metabolizable Energy	Kcal/g	3.4

Table 2.1. Nutritional content of mouse diets. *Italics* indicate nutrients that were removed to give rise to the various research diets (FD, FID, BFD, DFD). Succinylsulfathiazole (10 g/Kg) was added to the FD, FID and BFD diets to eliminate folate produced by the gut bacteria.

2.4 Maternal whole blood and plasma collection

After a minimum of three weeks on the designated diet, blood was collected from the dams immediately after anaesthesia with halothane. A 1 ml syringe with a 21 gauge needle was inserted directly into the contracting heart and the blood slowly withdrawn. The blood was then transferred to a lithium-heparin coated tube (Microtainer^{TM}, BD) to stop the blood from clotting. For whole blood folate analysis, 50 µl of blood was diluted into a fresh eppendorf with 50 µl of 1 % ascorbic acid to prevent oxidation of folates during storage, and stored at -80 ^{o}C until required (maternal folate analysis; section 2.9.1). For homocysteine analysis, the whole blood sample was centrifuged at 12,000g for 15 min to collect plasma. Plasma was stored briefly at -20 ^{o}C prior to shipment overnight on dry ice.

The measurement of total homocysteine in the collected plasma samples was undertaken by Ms. R. Dempsey at the Vitamin Research Laboratory (Trinity College, Dublin, Ireland) using the Abbott IMx instrument set-up for the FPIA (Fluorescent Polarisation Immunoassay) method.

2.5 Embryo collection and dissection

Experimental litters were generated by timed matings in which females were paired with males overnight and checked for a copulation plug the following morning, this being designated embryonic day 0.5 (E0.5). To study neurulation-stage embryos, litters were collected at embryonic day (E) 9.5, 10.5 and 11.5.

On the required embryonic day, each female mouse was killed by cervical dislocation and the uterus was explanted into Dulbecco's Modified Eagle's medium (DMEM) containing 10% fetal calf serum. The total number of implantations (classified as viable embryos/fetuses) or resorptions, was recorded. For embryos not undergoing whole embryo culture, embryos were explanted from the maternal decidua and separated from the visceral yolk sac and Reichert's membrane.

2.6 Embryo Culture

At E8.5, mice were killed by cervical dislocation and the uterus was explanted into Dulbecco's Modified Eagle's medium (DMEM) containing 10% fetal calf serum. Embryos, contained within the visceral yolk sac, were explanted from the maternal deciduas and cultured in immediately centrifuged, heat inactivated rat serum at 37 °C

(section 2.7). At E8.5, serum was equilibrated with 5% O_2, 5% CO_2, 90% N_2, and then at E9.5, with 20% O_2, 5% CO_2, and 75% N_2. Embryos from within litters were randomly selected for different treatment groups to minimise any effect of litter to litter variation.

Stock solutions of 400 mM methionine (ICN Biomedicals Inc.), 200 mM ethionine, 375 mM cycloleucine and 410 mM azacytidine in phosphate-buffered saline (PBS) were prepared and added as 0.2 - 4.0 % additions to the culture medium (2 - 40 µl/ml) giving final concentrations of 5 mM methionine, 5 mM ethionine, 15 mM cycloleucine and, 0.8 and 2 mM azacytidine. PBS alone was added to control groups at the same volume as reagent being tested. At the end of the culture period, the yolk sac circulation was observed as an indication of viability and quantified on a scale of 0 (no circulation) to 3 (vigourous circulation throughout the entire yolk sac). For further details on embryo culture refer to (Copp et al., 1999).

2.7 Preparation of rat serum for culture of mouse embryos

Wistar rats were anaesthetised using diethyl ether and then dissected to reveal the dorsal aorta. A 21 gauge needle attached to a 20 ml syringe was inserted into the dorsal aorta and blood was extracted. The diaphragm was punctured to ensure the rat could not survive post-operation. The extracted blood was immediately centrifuged for 5 minutes at 4000 rpm. The blood which had by then separated into plasma and red blood cells was left at room temperature to allow clotting. The resulting fibrin clot was then squeezed to allow a maximal amount of serum to be collected. Serum was removed and centrifuged again for 5 minutes at 4000 rpm to remove any residual blood cells. Serum was then heat inactivated at 56°C for 30 minutes, and allowed to cool to room temperature before aliquoting into bijoux tubes for storage at -20°C.

2.8 Processing of Embryos

After dissection or whole embryo culture, the embryos were inspected for the presence of cranial defects, consistent with the appearance of exposed and open neural folds or cranial tissue or, openings in the cranial neural tube. The number of somites was counted as a measure of developmental progression. The crown-rump length and posterior neuropore length were recorded using an eyepiece graticule, to give an indication of embryonic growth and progression of spinal neural tube closure, respectively. The position of each embryo with respect to the uterine horn and neighbouring embryos was also noted in some experiments. For biochemical assays, embryos were briefly washed with PBS and immediately frozen on dry-ice prior to storage at -80 °C. The yolk sacs were retained for genotyping by PCR.

2.9 Genotyping of embryos by Polymerase Chain Reaction (PCR)

2.9.1 Extraction of DNA from yolk sac samples

Yolk sacs, previously dissected from the embryos, were digested with 50 µl of 10 µg/ml proteinase K (Invitrogen) at 50 °C overnight. The solution was subsequently incubated at 100 °C for 10 minutes to denature the proteinase K followed by centrifugation at 14,000 rpm for 5 min to pellet the cell debris. A 2 µl sample of the supernatant was used for the PCR reaction.

2.9.2 PCR Protocol

A reaction mixture was prepared containing 1X NH_4-PCR buffer (Bioline), 1.5 mM $MgCl_2$ (Bioline), 0.25 mM of each deoxynucleoside triphosphate (dNTP) (Bioline), and 0.8 mM of both reverse and forward primers (Table 2.2). The reaction mixture was kept on ice and immediately prior to use 1 unit of Taq polymerase (Bioline) per reaction was added followed by distilled deionised water (ddH_2O) to give a final volume of 23 µl for each reaction. The resulting solution was mixed and 23 µl was added to 2 µl of yolk sac DNA solution. Controls were run with each PCR reaction; the negative control did not contain any DNA to ensure the reaction mixture was not contaminated and the positive control used previously genotyped DNA to check the components of the reaction mixture (Table 2.2). The amplification reaction was carried out on a PTC-200 DNA Engine (MJ Research) and involved an initial denaturation step followed by amplification cycles of denaturation, annealing and extension (Table 2.2). Each amplification cycle was repeated a number of times (Table 2.2) before a final extension step was carried out (Table 2.2).

The primers used to genotype Sp^{2H} mice were designed to span the 32 bp deletion in the paired box region of the *Pax3* gene, as described by Epstein and colleagues (Epstein et al., 1991), resulting in different sized bands for wild type and mutant alleles (Table 2.2, Figure 2.1 and 2.2). The sex of the embryo was determined by PCR using sex-specific primers to amplify the *Smcx* and *Smcy* genes (Agulnik et al., 1999). In each case, the PCR products were resolved by horizontal agarose gel electrophoresis (section 2.9.3).

2.9.3 Agarose gel electrophoresis

A 2% (w/v) agarose in 1X TAE (0.04 M Tris-acetate, 0.001 M EDTA) gel was made by melting the mixture in a microwave with occasional stirring. The gel was then left to

cool, approximately 0.5 mg/ml ethidium bromide was added and the mixture was poured into a casting tray with combs and allowed to set at room temperature. Once the gel was solid, it was placed in a horizon gel tank (Gibco BRL) containing 1X TAE buffer and 10 µl of the PCR products containing 1X loading dye (0.25% bromophenol blue, 0.25% Xylene cyanol FF, 15% Ficoll in water) were loaded into the wells. A molecular weight marker (Hyperladder V, Bioline) was run in a lane alongside the samples on each gel to allow the identification of the size of the products. After electrophoresis at 120 volts for 1 hour the PCR products were visualised under UV light and photographed using an alpha imager system (Alpha Innotech).

Genotyping Sp^{2H} embryos	
Forward Primer Sequence	5' CCTCGGTAAGCTTCGCCCTCTG 3'
Reverse Primer Sequence	5' CAGCGCAGGAGCAGAACCACCTTC 3'
PCR product size	Wild type allele 122bp Mutant allele 90bp
Initial Denaturation Step	94 °C for 4 min
Amplification Cycle	Denaturation at 94 °C for 1 min Annealing at 58 °C for 1 min Extension at 72 °C for 1 min
Number of cycle	30
Final Extension Step	72 °C for 10 min

Genotyping embryonic sex	
Forward Primer Sequence	5' CCTATGAAATCCTTTGCTGCACA 3'
Reverse Primer Sequence	5' AAGATAAGCTTACATAATCACAT 3'
PCR product size	Male allele 370bp Female allele 350bp
Initial Denaturation Step	95 °C for 5min
Amplification Cycle	Denaturation 92 °C for 1 min Annealing 60 °C for 1 min Extension 72 °C for 2 min
Number of cycles	72 °C for 10 min
Final Extension Step	30

Table 2.2. The primer sequences, product sizes and PCR conditions for determining Sp^{2H} genotype and sex.

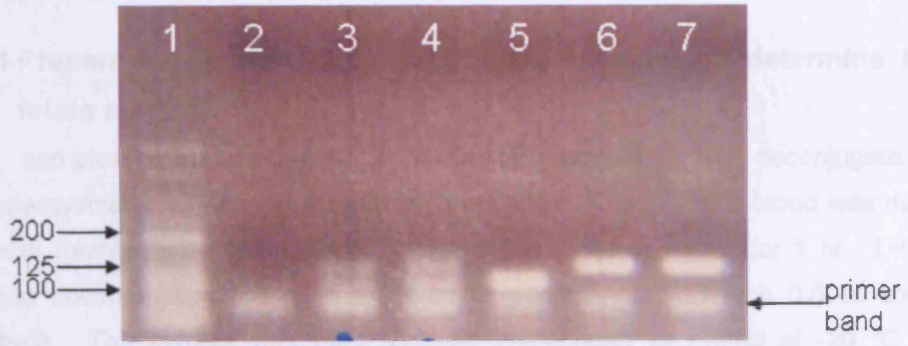

Figue 2.1. Visualisation of *Sp*^{2H} PCR products after agarose gel electrophoresis. Lane 1 contains 5 µl (960 ng DNA) of hyperladder. The negative and positive controls are shown in lane 2 and 3, respectively. The positive control, using heterozygote DNA, illustrates both the wild type allele (the upper band at 122bp) and the mutant allele (the lower band at 90bp). The remaining lanes show the genotyping of wild type (lane 6 and 7), heterozygous (lane 4) and homozygous mutant (lane 5) embryos.

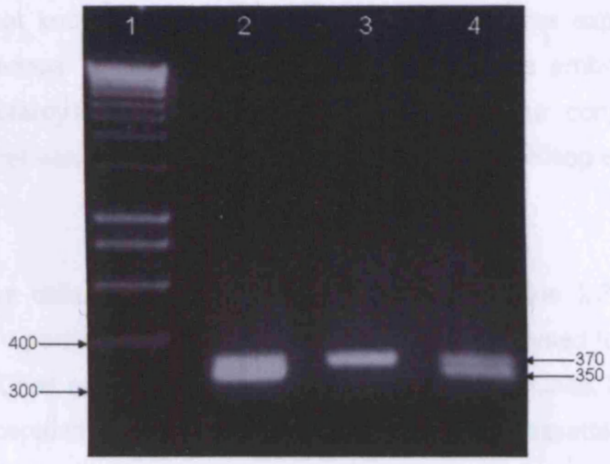

Figue 2.2. Visualisation of *Smcx/Smcy* PCR products after agarose gel electrophoresis. Lane 1 contains 5 µl (960 ng DNA) of hyperladder. Positive controls for male and female embryos are shown in lanes 2 and 3, respectively. The male positive control (Lane 2), using male DNA, contains both the *Smcx* and *Smcy* gene products. The female positive control (Lane 3) using female DNA, contains just the *Smcx* gene product. The remaining lane (Lane 4) shows the genotyping of a male embryo.

2.10 Determination of Folate using the *L. Casei* Microbiological Assay

2.10.1 Preparation of maternal whole blood samples to determine total folate content

Blood samples were defrosted at room temperature. To deconjugate the polyglutamylfolates to assayable monoglutamylfolates, 6 µl of whole blood was diluted 10:1 with freshly made 1% ascorbic acid and incubated at 37 ^{o}C for 1 hr. Directly following deconjugation, 25 µl of the sample was diluted 50:1 with 0.5 % sodium ascorbate. The sample was then assayed immediately or stored at -20 °C until required.

To set-up a sample plate for the whole-blood folate assay, 50 µl of the prepared blood sample was added to each well in one row of a 96-well microplate. Therefore, each sample was analysed in eight replicates enabling up to twelve samples to be analysed per microplate. To each sample well, 50 µl of 0.5 % sodium ascorbate was added using a multichannel pipette.

2.10.2 Preparation of conjugase extract

Since it was not known whether neurulation-stage embryos express the conjugase enzyme, exogenous conjugase extract was added to the embryo homogenates to convert polyglutamylfolates to monoglutamylfolates. The conjugase extract was prepared from rat serum using the method described by McKillop et al. (McKillop et al., 2002).

Rat serum was collected and stored as described (section 2.7) but was not heat deactivated. To partially purify the rat serum, 5 ml was dialysed for 24 hrs at 2-4 °C in 500 ml Hepes/Ches buffer, pH 7.85 (50 mM Hepes, 50 mM Ches, 20 g/L Ascorbic acid, 10 mM 2-mercaptoethanol) using Slide-A-Lyser dialysis cassettes (10,000 molecular weight cut-off; Pierce). The crude rat serum conjugase was then filtered through a 0.2 µm syringe filter (Millipore) and divided into 100 µl portions and stored at -80 °C. The conjugase extract was tested for folate content and no measurable folate was detected.

2.10.3 Preparation of embryo samples to determine folate content

Neurulation-stage mouse embryos (E9.5-E10.5) were sonicated on ice in 100 µl of distilled water, for 10 s at 12 amplitude microns, to produce a homogenate. A 10 µl

aliquot was stored at -20 ^{o}C to determine the protein content in the embryo sample (section 2.10). The homogenate was then diluted 2:1 with 0.5 % sodium ascorbate to stabilise the folates during handling and storage.

To determine monoglutamylfolate content, a 10 µl aliquot was taken from the homogenised embryo sample and diluted 200:1 with 1990 µl of 0.5 % sodium ascorbate to provide sufficient sample for analysis on two different days. The prepared sample was analysed immediately and the remaining sample was stored at -20 °C for analysis on a different day (within a week).

To determine total folate content, a 10 µl aliquot from a homogenised embryo sample was diluted 10:1 with 10 µl of conjugase extract (prepared as described in section 2.10.2) and 80 µl of 1 % ascorbic acid. The solution was incubated at 37 ^{o}C for 60 min to deconjugate polyglutamylfolates to assayable monoglutamyfolates. Following this, the solution was diluted 20:1 with 1900 µl of 0.5% sodium ascorbate to provide sufficient sample for analysis on two different days. The prepared sample was analysed immediately and the remaining sample was stored at -20 °C for analysis on a different day (within a week).

To set-up a sample microwell plate for the assay, 100 µl aliquots of the prepared embryo sample was plated into each well of one lane. The position of each sample on the microplate was recorded along with the sample type (monoglutamylfolate or total folate).

2.10.4 Quality Control

A minimum of two quality controls (QC) were included in each assay run. QCs were prepared by diluting the entire homogenised solution from either one (200 µl) or two (400 µl) embryos with 40 ml of 0.5 % sodium ascorbate to provide a high and a low value QC. 1 ml aliquots of each QC were stored at -80 ^{o}C until required. On the day of analysis an aliquot was freshly defrosted and 100 µl was plated into each well of one row on the sample plate. Following completion of the assay, the folate content was measured from the standard curve and the results recorded.

2.10.5 *L. Casei* Microbiological Assay

2.10.5.1 Preparation of Folate Media

The folate media was made up fresh immediately prior to analysis as follows. To 100 ml of distilled water was added 7 g of folic acid casei media (stored at 4 ^{O}C) and 3 mg of chloramphenicol and mixed gently. The media was warmed for 40 s in a microwave before the addition of 30 µl Tween-80. The media was further heated for approximately 1 min until it boiled and then left to cool at room temperature. Once cooled, 75 mg of ascorbic acid was added.

Immediately prior to plating, a vial of cryopreserved *L.casei* innoculum was removed from the -80 ^{O}C freezer and allowed to thaw. The innoculum was thoroughly mixed by inverting ten times and 200 µl was added to 100 ml of media. The media was placed on a magnetic stirrer and mixed for 10 min before plating.

The above protocol provided 100 ml of media which was enough for 5 plates (4 sample plates and 1 standard plate). For more then five plates, the amount of each reagent was doubled to provide a total of 200 ml of media.

2.10.5.2 Preparation of Folate Working Standard

Solution A (20 µg/ml) was prepared by dissolving 20 mg of folic acid with a few drops of 0.1 M sodium hydroxide and this solution plus the washings were added to 1 L of distilled water. Solution A was diluted 200:1 with 0.5 % sodium ascorbate to give Solution B (100 ng/ml). Solution B was dispensed into 750 µl aliquots and stored at -80 ^{O}C.

The final working standard, called Solution C, was prepared fresh on the day of the assay. An aliquot of Solution B was diluted 200:1 in 50 ml of 0.5 % sodium ascorbate to give a working standard concentration of 500 pg/ml. A series of dilutions were prepared from Solution C to create the standard curve for the assay.

2.10.5.3 Performing the Assay

The sample plates and solutions were prepared as described above. The "standards plate" was then made up by diluting the folate working standard **Solution C,** with 0.5% sodium ascorbate to give a series of concentrations (Figure 2.3). Just before use, the *L. casei* bacterial innoculum was added to the folate media as described (section

2.9.4.2.1) and 200 µl of the inoculated media was added to each well on all plates using a multichannel pipette ensuring the tips did not touch the sample in the wells. Plates were sealed, with the time noted on the plate seal (Perkin-Elmer), and incubated at 37 °C for 42 hr. Following incubation, the OD_{595nm} for each plate was read using a MRX Revelation microplate reader (Dynex Technologies) and the readings were printed out for data analysis.

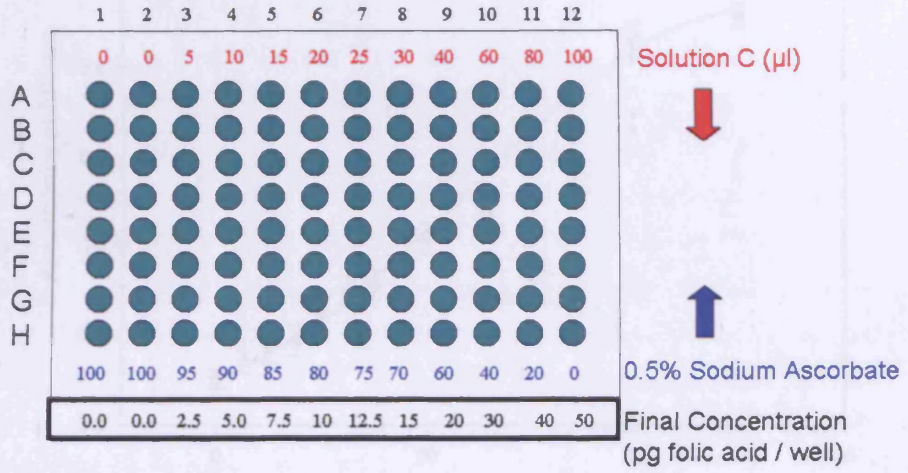

Figure 2.3. Diagram of the "Standards Plate". The standards plate was prepared to give serial dilutions of solution C (500 pg/ml) in 0.5% sodium ascorbate such that each dilution was replicated in eight wells of one column.

2.10.5.4 Data Analysis

Based on readings from the standards plate, a calibration curve was plotted for each assay (Figure 2.4) using the polynomial cubic regression function (Sigma Plot Version 7, SPSS Inc.). To determine folate content in an analytical sample, firstly the average absorbance reading was calculated for the corresponding eight wells. The standard deviation was also noted and if shown to be greater than 0.05 the sample was re-analysed. Using the standard plot equation, the folate content / 100 µl (folate content / well) was calculated from the mean absorbance reading. To determine the folate content in the analytical sample (embryo homogenate or whole blood sample), the folate content / 100 µl was multiplied by the final dilution factor. For embryo samples, the folate per embryo was also normalised to protein content to give the folate concentration in the embryo. Monoglutamylfolate concentrations were quantified in embryo homogenates, in addition to total folate (monoglutamylfolate + polyglutamylfolate). Polyglutamylfolate concentrations were calculated by subtracting the monoglutamylfolate concentration from the total folate. Each sample was assayed

on two different days and the results were compared. If the coefficient of variation between the results from the two different days was greater than 5 % then the sample was analysed again.

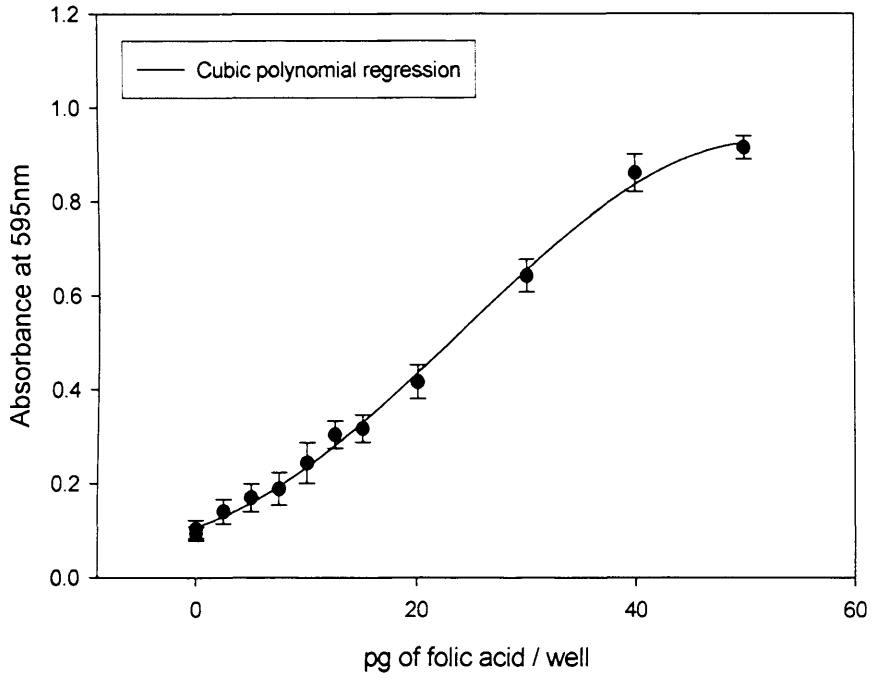

Figure 2.4. Standard curve based on the growth response of *L. casei* to folic acid. Points represent the means +/- standard deviation of eight replicates in the case of the folic-acid containing standards and sixteen replicates for the zero standard.

2.11 Determination of Embryonic Protein Content

From embryo homogenates, 10 µl aliquots were used for the determination of embryonic protein content using the bicinchoninic acid (BCA) protein assay reagent (Pierce) following the manufacturer's instructions for the microplate procedure. Various dilutions (25:1, 50:1, 100:1, 200:1) of the homogenates were prepared to achieve a sample within the standard curve range. A series of standard protein solutions were made, ranging between 0-100 µg/ml, from an initial 2 mg/ml standard protein solution (bovine serum albumin). For the microplate procedure, replicate 25 µl aliquots of each standard or unknown sample were added to each microplate well. The BCA working reagent, a 50:1 mixture of reagents A and B (Pierce), was made fresh for each assay. BCA working reagent (200 µl) was added to each standard/sample well and incubated for 30 minutes at 37 °C. The OD_{562nm} for each well was read using a MRX Revelation

microplate reader, a standard curve was plotted and protein concentration of the samples calculated, using pre-installed software (Revelation Software Version 4.2.1).

2.12 Liquid Chromatography Tandem Mass Spectrometry (LC-MS/MS)

2.12.1 LC-MS/MS Method

Prior to analysis by mass spectrometry, metabolites were separated on a column using a 2795XE high performance liquid chromatography (HPLC) unit with solvent divert valve (Waters, Manchester, UK). The HPLC was coupled to a MicroMass Quattro *micro*™ triple quadrupole tandem mass spectrometer (Waters) operating in the desired ion mode using the following settings (unless stated otherwise): source temperature 150°C, desolvation temperature 350°C, cone gas flow rate 50 L/hr, desolvation gas flow rate 650 L/hr, inter channel delay 0.030 sec, inter scan time 0.030 sec, dwell 0.100 sec and span 0.2 Da. The mass spectrometer was equipped with an electrospray ionisation (ESI) source. In each case, the Selected Reaction Monitoring (SRM) mode was used for quantification and data were acquired and processed using MassLynx software (version 4.0, Waters). Precursor and product ion spectra were obtained at a resolution of 15.0 (LM1, HM1, LM2 and HM2), whilst all other analyses were obtained at a resolution of 13.5 (LM1, HM1, LM2 and HM2).

2.12.2 Calibration curve method for quantification

To generate a calibration curve, the "peak area of the calibrator / peak area of the internal standard" was plotted against increasing concentrations of calibrator spiked into the biological matrix (Figure 3.8 and 7.11). This calibration curve was then used to deduce the endogenous metabolite level in the biological matrix by determining the intercept on the x-axis when y = 0. The endogenous metabolite level was subtracted from each of the calibrators to create a curve that passed through zero on the x-axis. These working calibration curves were then used to quantify the levels of metabolites in samples. Linear regression analysis (un-weighted) was performed using Sigma Plot Version 7.0 (SPSS Inc., Chicago, Illinois).

2.13 Cell culture

2.13.1 Basic cell culture procedures for fetal fibroblasts

Sterile conditions were used throughout the cell culture procedures to minimise the possibility of contamination. Procedures were carried out in a class II microbiological safety cabinet (Envair) and before entering the safety cabinet, all materials were sprayed with 70% industrial methylated spirits (IMS). Solutions were warmed to 37 °C before use. DMEM (Dulbecco's Modified Eagle's Medium) containing 1.5 g/l sodium bicarbonate, 10% fetal calf serum, 2% chicken serum, 100 Units penicillin and 100 µg/ml streptomycin was used as culture medium throughout this study and is referred to as "medium". Medium was made up in 500 ml bottles when needed, sterilised by vacuum driven filtration through a 0.22 µm filter stericup (Millipore) and used or discarded within a two week period. Cells were cultured in a Galaxy R CO_2 incubator (Scientific Laboratory Supplies Ltd.), with 5% CO_2 at 37 °C.

2.13.2 Sample collection and processing of fetal fibroblasts

Samples of amniotic fluid, skin, cord or cartilage were collected with ethical permission by fetal pathologists at University College Hospital, from fetuses aged 12-21 weeks. Samples were allocated to one of two groups, NTD-affected or control (normal fetuses or fetuses affected with malformations other than NTD). The samples were sent to Great Ormond Street Hospital (GOSH) cytogenetics laboratory where fibroblastic cell lines were established.

Human cell lines established by the GOSH Cytogentics Laboratoy were frozen down in medium containing 10% dimethyl sulfoxide (DMSO) and stored in liquid nitrogen until required. Cells were defrosted and immediately placed in 5 ml medium to dilute the DMSO, which could cause cellular damage. The cells were pelleted by centrifugation at 1,000 rpm for 5 minutes. The supernatant was discarded and the cells resuspended in 3 ml of medium then seeded into a 3 cm plate and incubated with 5% CO_2 at 37 °C.

Cells were grown to confluence with changes of medium when necessary. To change the medium, spent medium was removed by aspiration and the cells were washed with 3 ml PBS then 3 ml of fresh medium was added. The growth and health of cultures was checked daily using an inverted microscope (Zeiss).

Once the cells were confluent, they were removed from the culture plates by trypsinisation. A stock solution of 10X trypsin-EDTA was diluted to 1X in PBS and 1 ml was added to the cells for 2-3 minutes at 37 °C until they had rounded up and begun

to detach from the bottom of the flask. The digestion was stopped by centrifuging (1000 rpm, 5 min) and resuspending the cells in 1 ml of medium and subsequently transferring them into a larger 6 cm plate containing 9 ml of medium. Cells were grown again to confluence, passaged by trypsinisation and then each sample was seeded onto 2 plates.

2.13.3 Collecting fetal fibroblast cell pellets

At this stage each sample had been seeded onto two 6 cm plates. Cells were grown to confluence and subsequently, cells on both plates were detached by trypsinisation. The cells from one plate were pelleted by centrifugation for 5 minutes at 1,000 rpm. The supernatant was discarded and the cell pellet was stored at - 80 °C prior to analysis. The cells from the second plate were seeded onto two further 6 cm plates. The plated cells were grown again to confluence and the process repeated to obtain a sufficient cell pellet sample for LC-MS/MS analysis. A homogenised cell pellet (see section 3.3.6) with a protein concentration greater than 1 mg/ml was found to provide sufficient sample for analysis.

2.13.4 Cycloleucine treatment of 3T3 mouse fibroblasts

Frozen aliquots of mouse 3T3 fibroblasts were grown as described in section 4.2.4.2 until they covered approximately three quarters of the surface area of a 6 cm plate. Spent media was replaced with fresh media containing 0, 15, 30 or 60mM cycloleucine and cells were incubated with 5% CO_2 at 37 °C for a further 24 h. Cell pellets from all plates were subsequently collected by trypsinisation as described in section 4.2.4.3.

2.13.5 EBV transformed lymphoblast cell lines

Cell pellets from EBV (Epstein-Barr Virus) transformed lymphoblast cells were prepared by Dr. P. Gustavsson (Karolinska Institute, Sweden). Briefly, peripheral blood was taken from Swedish children with open spina bifida and lymphocytes were separated using Ficoll. EBV was used to transform the cells to generate a population of immortal B lymphocytes. Control cell lines were obtained from normal Swedish blood donors. Cells were grown as a suspension in RPMI (RPMI-1640, Roswell Park Memorial Institute) media supplemented with 10 % fetal calf serum, 100 u penicillin and 100 µg/ml streptomycin. Media was changed twice a week and after four weeks of growth, cells were harvested the morning following the last media change. To harvest the cells, excess media was removed and the remaining media was centrifuged at 1,000 rpm for 5 minutes to collect the suspended cells. The cell pellet was washed with cold PBS and stored at -80 °C prior to analysis of SAM and SAH by LC-MS/MS. All cell pellets were analysed as described in chapter 3.

CHAPTER 3

Quantitative analysis of s-adenosylmethionine and s-adenosylhomocysteine in neurulation-stage mouse embryos by liquid chromatography tandem mass spectrometry.

3.1 Introduction

3.1.1 The Methylation Cycle

The role of folates is to carry one-carbon units, not only for the metabolism of both pyrimidines and purines for DNA synthesis, but also for the methylation of a wide variety of substrates. The methylation cycle involves the transfer of a methyl group from 5-methyltetrahydrofolate to homocysteine by methionine synthase (MS; Figure 3.1). The adenosyl moiety of ATP is then transferred to methionine to form S-Adenosylmethionine (SAM; Figure 3.2) (Lombardini and Talalay, 1971). SAM is the universal methyl donor for methyltransferase-catalysed reactions (Loenen, 2006). Methylation of biomolecules including DNA, RNA, lipids and proteins, is essential for a range of cellular processes including epigenetic control of gene expression (Friso and Choi, 2002) and regulation of protein function (Bergo et al., 2000;Vafai and Stock, 2002).

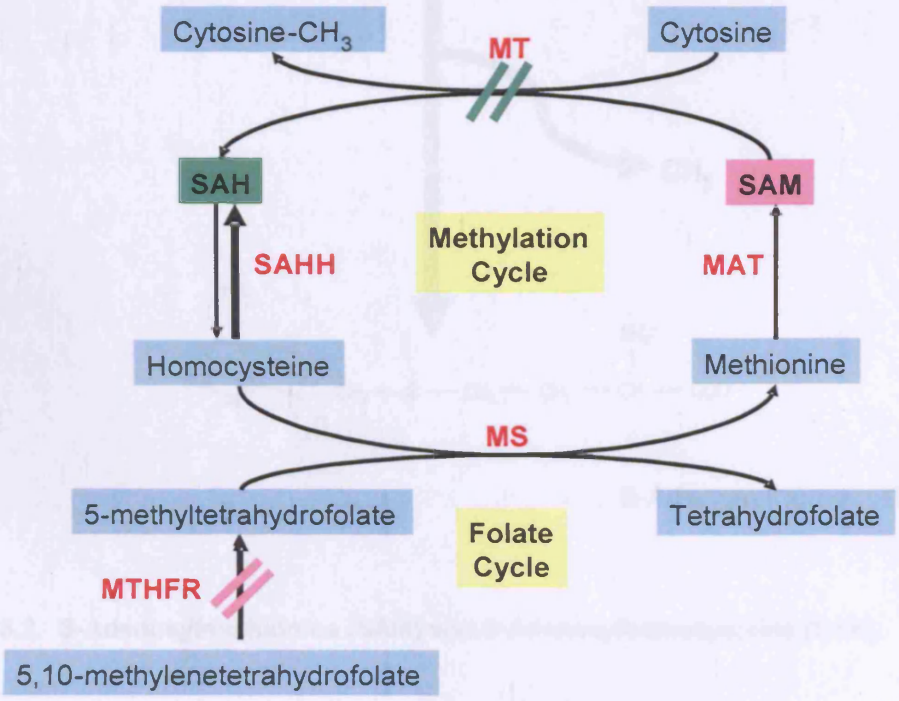

Figure 3.1. The Methylation Cycle. MTHFR; 5,10-Methylenetetrahydrofolate Reductase, MAT; Methionine Adenosyl-transferase, SAHH; SAH Hydrolase, MT; Methyltransferase, MS: Methionine Synthase. Enzyme inhibition by SAM (//) or SAH (//).

S-adenosylhomocysteine (SAH), formed following the donation of the methyl group from SAM (Figure 3.2), acts as a product inhibitor of methyltransferases (De Cabo et al., 1995) such that the ratio of SAM to SAH is crucial for regulation of methylation. SAH must be efficiently recycled, via the production of homocysteine and methionine, for methylation potential to be maintained (Finkelstein, 1998a;Scott, 1999). Thus, the relative abundance of SAM to SAH is not only important for methylation, but can also influence flux through the folate cycle, which is interlinked to the methylation cycle, since SAM is able to inhibit 5,10-methylene tetrahydrofolate reductase (MTHFR; EC1.7.99.5) (Kutzbach and Stokstad, 1971).

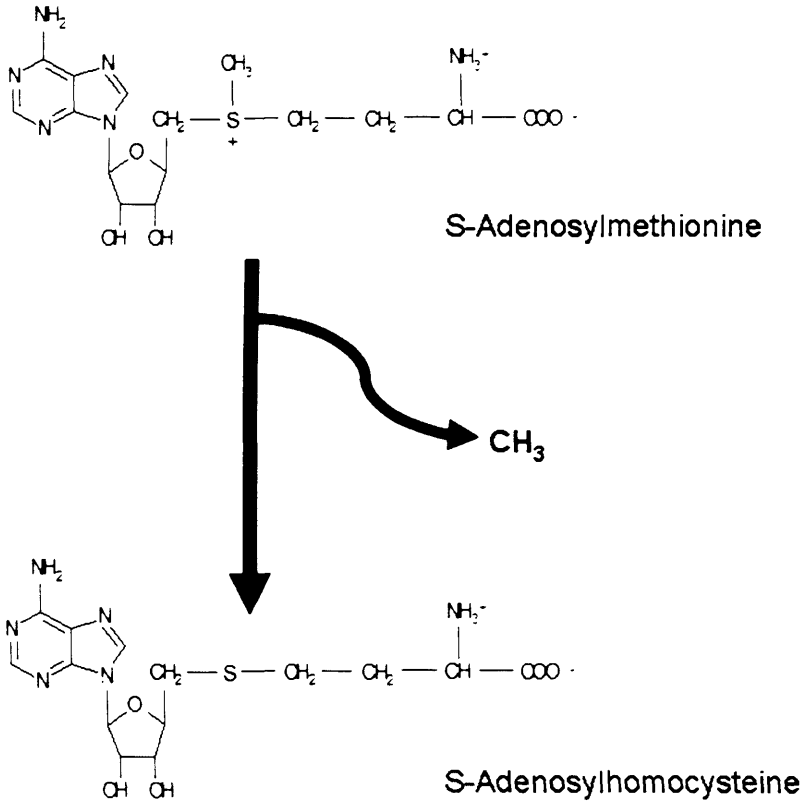

Figure 3.2. S-Adenosylmethionine (SAM) and S-Adenosylhomocysteine (SAH).

3.1.2 Methylation of bio-molecules

DNA methylation involves the addition of a methyl group (donated by SAM) to the 5' carbon position of cytosine, predominantly within a series of cytosine guanine dinucleotides (CpG) in the DNA sequence. Clusters of CpGs found in gene promoter regions, termed "CpG islands", play a key role in epigenetics; modifications of DNA that alter gene transcription without altering the nucleotide sequence (Oommen et al., 2005).

Methylation of CpG islands at the site of transcriptional initiation, an epigenetic modification, is generally capable of silencing gene transcription either by directly impeding the binding of transcription factors, or indirectly, through the binding of methyl-binding proteins which restrict the access of transcription factors to the gene promoter or alter the chromatin structure to a repressive state (reviewed in Newell-Price et al., 2000;Van den Veyver, 2002). DNA methylation is required to silence one allele of imprinted genes (Barlow, 1995) or to silence genes on the inactive X chromosome (Hemberger, 2002). Scattered transposable DNA elements which make up 30% of the genome must also be silenced by DNA methylation as their transcription can disrupt functional genes or induce chromosome rearrangements (Yoder et al., 1997). However, there have been reports of certain proteins exhibiting increased transcription following promoter methylation (Murrell et al., 2001; Hantusch et al., 2007). Furthermore, methylation of CpG islands downstream of transcription initiation does not block elongation in mammalian cells, rather methylation in the transcribed region is often correlated with gene expression (Jones et al., 1999) and hypermethylation of CpG islands has been detected in actively transcribed regions of cancer cells (Liang et al., 1998).

Protein methylation, catalysed by protein methyltransferase enzymes, involves the addition of the methyl-group provided by SAM to arginine or lysine amino acid residues in the protein sequence. Protein methylation may be involved in the ageing/repair of proteins and signal transduction (Grillo and Colombatto, 2005), whilst histone protein methylation is implicated in chromatin remodelling and transcriptional regulation (Martin and Zhang, 2005). Phospholipid methylation provides an alternative pathway, catalysed by phosphatidylethanolamine *N*-methyltransferase (PEMT), for the synthesis of phosphatidylcholine, a structural component of cell membranes (Hartz and Schalinske, 2006).

3.1.3 Investigating the link between methylation and neural tube closure

The ability to accurately measure SAM and SAH in neurulation-stage mouse embryos will provide a means to assess how the methylation capacity of an embryo is affected by genetic and environmental disturbances. Comparisons of SAM and SAH levels between NTD affected embryos and normal embryos, may provide clarification of the role of these two metabolites in the pathogenesis of NTDs. Indeed, the prevention of NTDs by folic acid could be associated with increased flux through the methylation cycle (Blom et al., 2006)

and a change in the levels of SAM and SAH. Provision of SAM for DNA methylation does appear essential for neural tube closure, since NTDs are observed in mouse embryos that are homozygous null for DNA methyltransferase 3b (Okano et al., 1999). Thus, the potential importance of the methylation cycle during embryonic development necessitates the establishment of methodology for an accurate and sensitive assay of SAM and SAH in an embryonic experimental system such as mouse embryos.

3.1.4 Current methods to quantify SAM and SAH

An outline of the methods currently available to measure SAM and SAH is displayed in Table 3.1. Previously, UV detection following HPLC or capillary electrophoresis has been used for the detection of SAM and SAH in tissue samples as well as urine, red blood cells and lymphocytes (She et al., 1994b); (Luippold et al., 1999). Increased sensitivity can be achieved through derivatisation of SAH and SAM followed by fluorescent detection (Capdevila and Wagner, 1998). However, these methods were deemed unsuitable for the analysis of embryonic levels of SAM and SAH due to the requirement for relatively large amounts of tissue sample and limited sensitivity with laborious sample preparation and low recovery.

Recently, liquid chromatography coupled to mass spectrometry (LC-MS) has been utilised for determination of SAM and SAH owing to the high sensitivity of detection and the ability to use stable-isotope-labelled internal standards for precise quantification (Gellekink et al., 2005;Stabler and Allen, 2004;Struys et al., 2000). The previously reported LC-MS method allows assay of tissues (rat liver and lung) as well as fluids (whole blood, plasma, serum and urine) (Stabler and Allen, 2004). In comparison, tandem mass spectrometry (LC-MS/MS) provides enhanced selectivity, less time-consuming sample preparation and has been utilised for plasma and cerebrospinal fluid samples (Gellekink et al., 2005;Struys et al., 2000). The LC-MS/MS method developed by Struys et al. has been used to determine the abundance of SAM and SAH in chick embryos following the application of inhibitors of S-adenosylhomocysteine hydrolase and of methionine adenosyltransferase (Afman et al., 2006). In each case a delay of anterior neuropore closure was observed associated with a decreased SAM/SAH ratio, indicating reduced transmethylation. Here, I developed a modified LC-MS/MS method to allow precise and simultaneous quantification of SAM and SAH in low abundance tissue samples, in this case neurulation-stage mouse embryos (at embryonic day 9.5 and 10.5). The method has also been applied to cell pellets collected from NTD and control patient cell lines, an alternative low abundance tissue sample.

Paper	Method	Tissue	LOD	Linearity	Sample size	Sample Preparation	Run Time	CV	Recovery	Tissue values
She, Q. et al. (1994)	HPLC with UV detection	Rat Liver	25 pmol	50-2000 pmol	50 mg	Deproteinate ($HClO_4$), centrifuge & filter	20 min	Intra-assay 2% SAM 3% SAH	100%	28-95 nmol/g SAM 33-109 nmol/g SAH
Capdevila, A. & Wagner, C. (1998)	HPLC with fluorescent detection	Human Plasma	10 pmol	10-100 pmol	0.5 ml	Deproteinate (TCA), centrifuge, remove TCA using solvent.	33 min	Not stated	65%	0.026-0.110 µM SAM 0.022-0.029 µM SAH
Luippold, G. et al. (1999)	HPLC with UV detection	Rat Kidney & Urine	5 pmol	0.5-100 µM	2ml of urine or tissue extract	Deproteinate ($HClO_4$) centrifuge, adjust pH, SPE	30 min	Not stated	90%	Rat kidney 46.2 nmol/g SAM 0.67 nmol/g SAH
Struys, E. A. et al. (2000)	LC-MS	Plasma & SF	0.005 µM	0.01-0.02 µM	500ul	Deproteinate ($HClO_4$) centrifuge, SPE	3 min	Intra-assay 5.5% SAM* 5.5% SAH* Interassay 5.9% SAM* 5.7% SAH*	93%	Plasma 0.049-0.091 µM SAM 0.019-0.040 µM SAH CSF 0.137-0.385 µM SAM 0.009-0.014 µM SAH
Uthus, E. O. (2003)	Capillary Electrophor-esis	Rat Liver & Kidney, Mouse Liver, Whole Blood	0.01 pmol (unable to detect SAH in whole blood)	1-250 µM	Not stated	Deproteinate ($HClO_4$) centrifuge, filter.	16 min	Intra-assay 1.8% SAM 4.5% SAH Inter-assay 3.6% SAM 6.1% SAH	Not stated	Whole blood 2.2-3.5µM SAM
Stabler and Allen, 2004	LC-MS/MS	Human Serum and Urine, Rat Liver and Lung	5 pmol	Quantified by comparing ratio of peak areas using internal standards	0.5 ml plasma, serum, CSF, 100-300 mg wet weight tissue	Deproteinate ($HClO_4$) SPE	49 min	Intra-assay 5% Inter-assay 17%	95%	Serum 0.071-0.168 µM SAM 0.008-0.026 µM SAH
Gellekink,H. et al. (2006)	LC-MS/MS	Plasma	2.0 nmol/L	5-400 nmol/L	20 µl	SPE columns containing phenylboronic acid	5 min	Intra-assay 4.2% SAM 6.7% SAH Inter-assay 3.9% SAM 8.3% SAH	95%	Plasma Mean 94.5 nmol/L SAM, 12.3nmol/L SAH

Table 3.1. A comparison of published methods to quantify SAM and SAH.

3.2 Materials and Method

3.2.1 Materials

SAM and SAH were purchased from Sigma-Aldrich (Dorset, UK). The internal standard, [$^2H_3$]-SAM, was purchased from CDN Isotopes (Pointe-Claire, Quebec, Canada). Ultra-grade (HPLC) Ammonium acetate, formic acid and heptafluorobutyric acid were purchased from Sigma-Aldrich (Dorset, UK).

3.2.2 Samples

Non-mutant CD1 mouse embryos were collected at embryonic day (E) 9.5 and 10.5 as described (section 2.5 and 2.8). Cell pellets, from NTD and control human cell lines, were also collected for analysis (described in chapter 3).

3.2.3 Preparation of Samples

3.2.3.1. Preparation of neurulation-stage embryos

Embryos at E9.5 or E10.5 were suspended in 200 µl of ice-cold aqueous mobile phase (100% B, see below) containing 1 µM [$^2H_3$]-SAM, and sonicated immediately at 12 micron amplitude for 10 seconds on ice, to produce a homogeneous solution. A 10 µl aliquot was retained for determination of protein concentration using the bicinchoninic acid (BCA) protein assay reagent (section 2.11). Various methods were tested for sample preparation prior to analysis by LC-MS/MS (Table 3.2).

Following testing, heat treatment was chosen as the optimal sample preparation method. This involved heating the sample at 80°C for 5 minutes to precipitate endogenous proteins, cooling immediately on ice for 2 minutes and centrifuging for 15 minutes at 12,000 g to remove any particulate. Prepared samples were subsequently analysed immediately by LC-MS/MS.

3.2.3.2. Preparation of cell pellets

Cell pellets were re-suspended on ice in 200 µl of cold PBS and the protein concentration was assayed using the BCA protein assay in a 10 µl aliquot (section 2.11). Suspensions were pooled to provide approximately 1 mg of protein and subsequently centrifuged for 5 min at 12,000 g. The cell pellet was then re-suspended in 200 µl of ice-cold aqueous

mobile phase (100% B, see below) containing 1 μM [$^2H_3$]-SAM and sonicated immediately at 12 micron amplitude for 10 seconds on ice, to produce a homogeneous solution. The solution was heated at 80°C for 5 minutes to precipitate endogenous proteins, cooled immediately on ice for 2 min and centrifuged for 15 min at 12,000 g to remove any particulate. Samples were analysed immediately by LC-MS/MS.

Method	Sample Volume, μl (No. of embryos per sample)	Description
Acetonitrile	200 (1)	Add 200 μl acetonitrile, mix thoroughly for 2 min and centrifuge for 15 min.
Acetone	200 (1)	Add 200 μl acetone, mix thoroughly for 2 min and centrifuge for 15 min.
Perchloric Acid	200 (1)	Add 200 μl perchloric acid (100 ml/L), mix thoroughly for 2 min and centrifuge for 15 min.
Ethanol	200 (1)	Add 200 μl ethanol, mix thoroughly for 2 min and centrifuge for 15 min.
Spin Column Filtration	400 (2)	Filtered using the Centricon YM-10 Centrifugal Filter Device (Millipore) according to the manufacturer's instructions.
Heat	200 (1)	Heat at 80 °C for 5 min, cool on ice for 2 min and centrifuge for 15 min.

Table 3.2. Sample preparation methods used for the analysis of endogenous SAM and SAH in a pooled sample of homogenised E10.5 embryos. In each case samples were centrifuged at 12,000 g for 15 min prior to analysis to collect precipitated proteins.

3.2.4 Calibration and quantification

In order to quantify endogenous levels of SAM and SAH in whole embryos, the "calibration curve method" was implemented (section 2.12.1) using combined SAM and SAH

calibrators made up in a matrix of pooled mouse embryos. For neurulation stage (E9.5 – E10.5) embryos, calibrators containing 0.5, 1, 2.5, 5, 10, 25 µM of SAM and 0.01, 0.02, 0.05, 0.1, 0.2, 0.5 µM of SAH were utilised. All calibrators contained 1 µM of the internal standard, [$^2H_3$]-SAM. The "calibration curve method" was also used to quantify endogenous levels of SAM and SAH in cell pellets. For cell pellets containing 1 mg/ml protein, calibrators containing 0, 0.25, 0.5, 1, 2 and 5 µM of SAM and 0, 0.01, 0.02, 0.05, 0.1 and 0.2 µM of SAH were utilised. All calibrators contained 1 µM of the internal standard, [$^2H_3$]-SAM.

3.2.5 LC-MS/MS Method

SAM, SAH and [$^2H_3$]-SAM were separated on a pentafluorophenylpropyl (PFPP)-bonded silica column (Discovery HS F5; 50 x 2.1 mm (i.d.); 5 µm bead size; Supelco, Sigma-Aldrich). Solvents for HPLC were: A, 100% methanol; B, 4 mM ammonium acetate, 0.1% formic acid, 0.1% heptafluorobutyric acid (pH 2.5). The F5 column was equilibrated with 40% A: 60% B. The sample injection volume was 40 µl. The HPLC protocol consisted of 40% A: 60% B for 2 minutes, followed by a gradient of 40-100% A over a 2 minute period. The column was then washed with 100% A for 4 minutes before re-equilibration for 7 minutes. The flow rate was 0.5 ml/min and the first 72 seconds after sample injection was diverted to waste, to minimise accumulation of endogenous compounds on the ionisation source which will reduce the performance of the instrument over time. The mass spectrometer was operated in positive-ion mode using the following settings: capillary 3.86 kV, cone voltage 20 V, collision energy 26V. A C8 reverse phase column (Discovery Hypurity C8; 10 x 2.1 mm (i.d.); 5 µm bead size) was also tested for its ability to retain SAM and SAH. Various isocratic and gradient HPLC protocols were tested using the same HPLC solvents and parameters.

3.2.6 Statistical Analysis

Analyte concentrations were compared by One Way ANOVA. Ratios of SAM:SAH (overall and within each sex) were compared by t-test. Statistical tests were computed using SigmaStat Version 2.03 (SPSS Inc.).

3.3. Results

3.3.1. Mass Spectra

The expected $[M+H]^+$ protonated molecules (precursor ions) were m/z 402.2, 399.2 and 385.2 for $^2H_3$-SAM, SAM and SAH, respectively (Figure 3.3). Observed experimental results matched the theoretical masses. Product ion spectra for each of the three molecules yielded a fragment of m/z 136.1 (Figure 3.3), believed to correspond to the adenine backbone (Struys et al., 2000). Thus, the final SRM transitions were as follows: SAM, 399.2 → 136.1; $^2H_3$-SAM, 402.2 → 136.1; SAH 385.2 → 136.1.

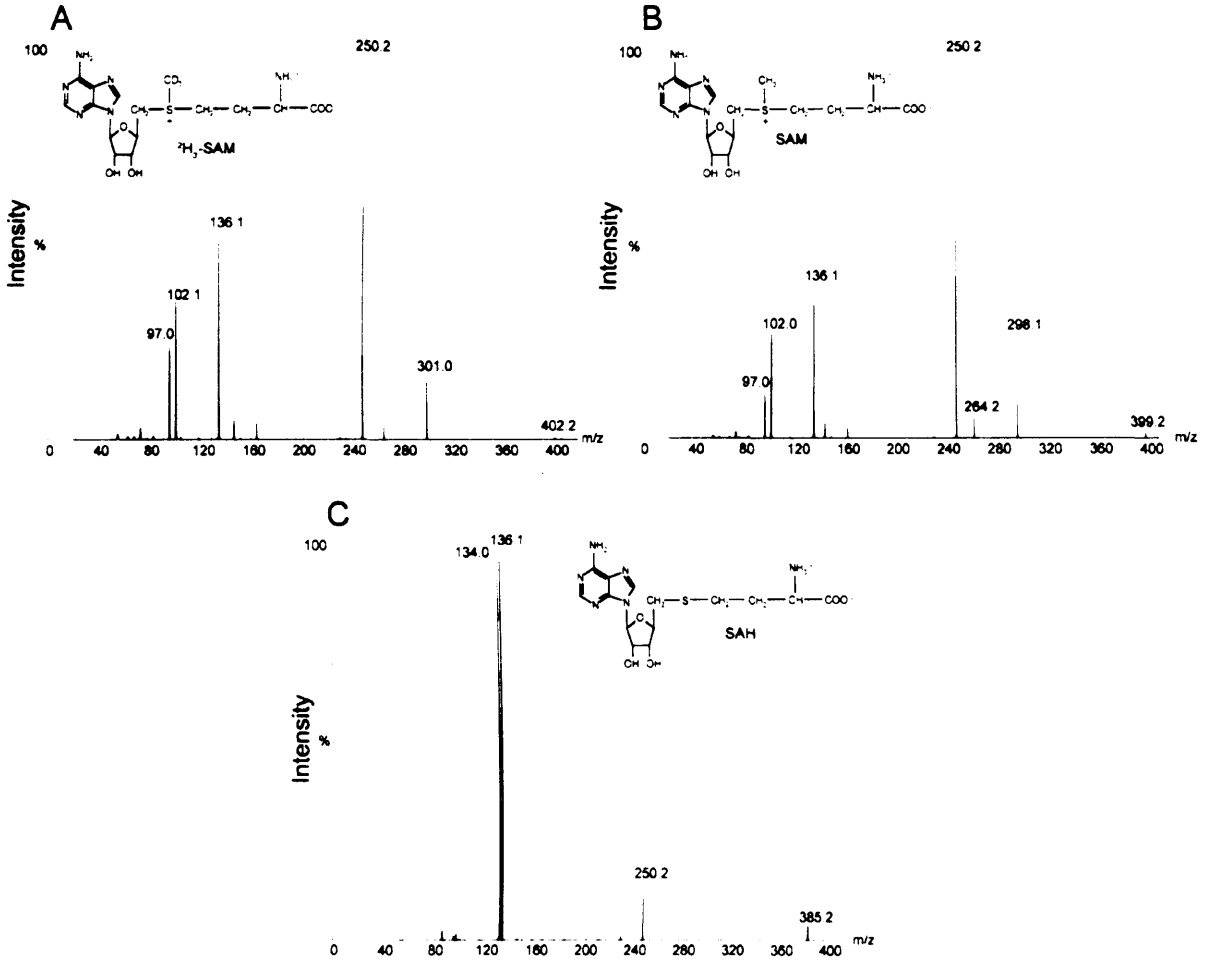

Figure 3.3. Product ion spectra of protonated molecules used for quantification. Precursor ions were at m/z 402.2 for $[^2H_3]$-SAM (A), 399.2 for SAM (B) and 385.2 for SAH (C). In each case the MS/MS conditions were optimised to favour the transition to a major product ion at m/z 136.1, thought to correspond to the adenine backbone (Struys et al., 2000).

3.3.2. Sample Preparation

Embryo tissue samples typically contained approximately 100 or 400 µg protein for E9.5 and E10.5 embryos respectively. Several procedures were evaluated for preparation of samples for LC-MS/MS following homogenisation. These included acetone precipitation, acetonitrile precipitation, ethanol precipitation, heat precipitation, acidification with perchloric acid and filtration on spin-columns (Figure 3.4). All are common methods used to precipitate proteins from solution for the analysis of metabolites. Removal of extraneous matrix components from the sample helps eliminate matrix-induced ion suppression and prevents sample components from blocking the HPLC column. The applicability of a particular sample preparation method depends on efficiency of protein precipitation, recovery losses (loss of material during analysis), compatibility with desired column, convenience of use and type of sample matrix. Solid phase extraction was not suitable, due to low sample volume (200 µl) inherent in the analysis of individual mouse embryos (or other low abundance tissue samples).

Preparation of embryonic samples using the spin columns required twice as much sample due to handling constraints. Thus, in order to achieve the required volume either the embryo sample needed to be diluted which caused a loss of sensitivity or, embryo samples needed to be pooled for analysis. A comparison of peak area to the other methods used demonstrates that filtration on spin-columns did recover sufficient SAM from the pooled sample consisting of two homogenised embryos (Figure 3.4E). However, since this method was being established purposely to measure SAM and SAH in whole embryos, without pooling, this method was not suitable. Precipitation with acetonitrile resulted in poor sample recovery as shown by the smaller peak area in comparison to the other peaks (Figure 3.4A). Overall, the recovery of SAM was greatest when samples were heat or acetone treated to precipitate endogenous proteins (Figure 3.4).

The peak shape of the chromatography was dramatically affected by the sample preparation. Optimum peak shape was achieved with acetone precipitation. A subsequent increase in the flow rate from 0.25 ml/min to 0.5 ml/min was found to reduce peak tailing when samples were prepared by heat treatment. In addition, regular replacement of guard cartridges was required. Heat treatment was chosen as the method of choice as it was convenient, cheap and unlikely to pose any problems with column incompatibility since it did not involve the use of any solvents.

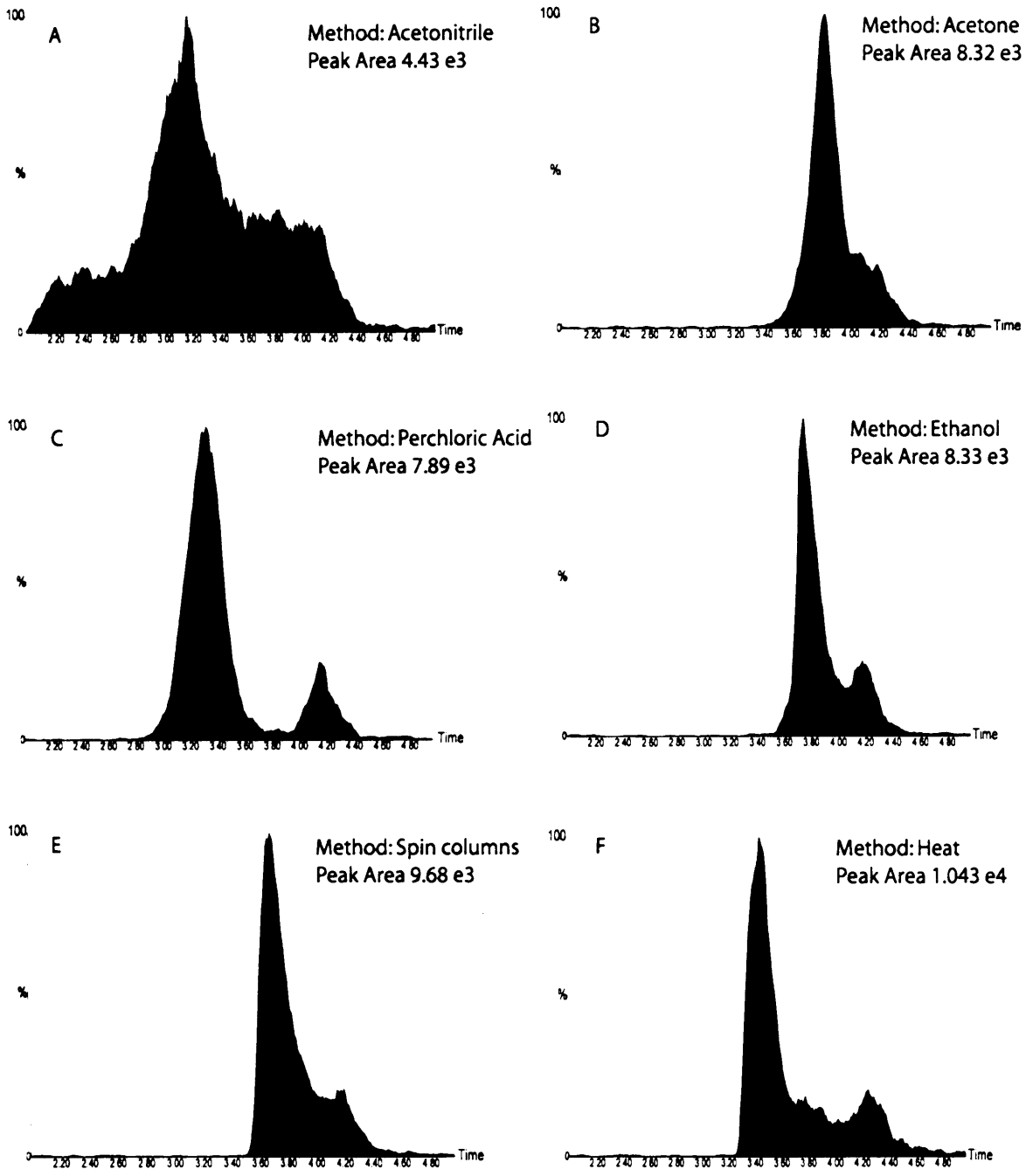

Figure 3.4. Comparison of sample preparation methods for the analysis of SAM. LC-MS/MS chromatograms for SAM obtained in SRM mode using the Discovery HS F5 column (50 x 2.1 mm (i.d.); 5 µm bead size): sample preparation affected both retention time and peak shape. Representative chromatograms are shown for endogenous SAM in a pooled sample of homogenised E10.5 mouse embryos (>35 somites). Samples were prepared using various methods to precipitate proteins (Table 3.2); acetonitrile (A), acetone (B), Perchloric acid (C), Ethanol (D), Spin column filtration (E) and Heat (F). Flow rate = 0.25 ml/min.

Recent reports indicate that, unless acidified, SAM in plasma may be unstable during storage at –20 °C (Gellekink et al., 2005;Stabler and Allen, 2004). For this reason, tissue samples were homogenised in acidified mobile phase (solution B). Additionally, embryos were stored for only short periods at – 80 °C.

To evaluate potential loss of SAM due to heat treatment, control standard samples were divided and analysed with or without the heat step. Using this brief heat treatment and immediate cooling there was no change in signal intensity for SAM, SAH or [$^2H_3$]-SAM compared to non-heat treated samples, indicating that heating for a short period did not cause degradation (Figure 3.5). Peak shape is much improved following heat treatment which suggests that the increased signal intensity following sample preparation is due to the removal of contaminants that cause ion suppression, as opposed to increased recovery.

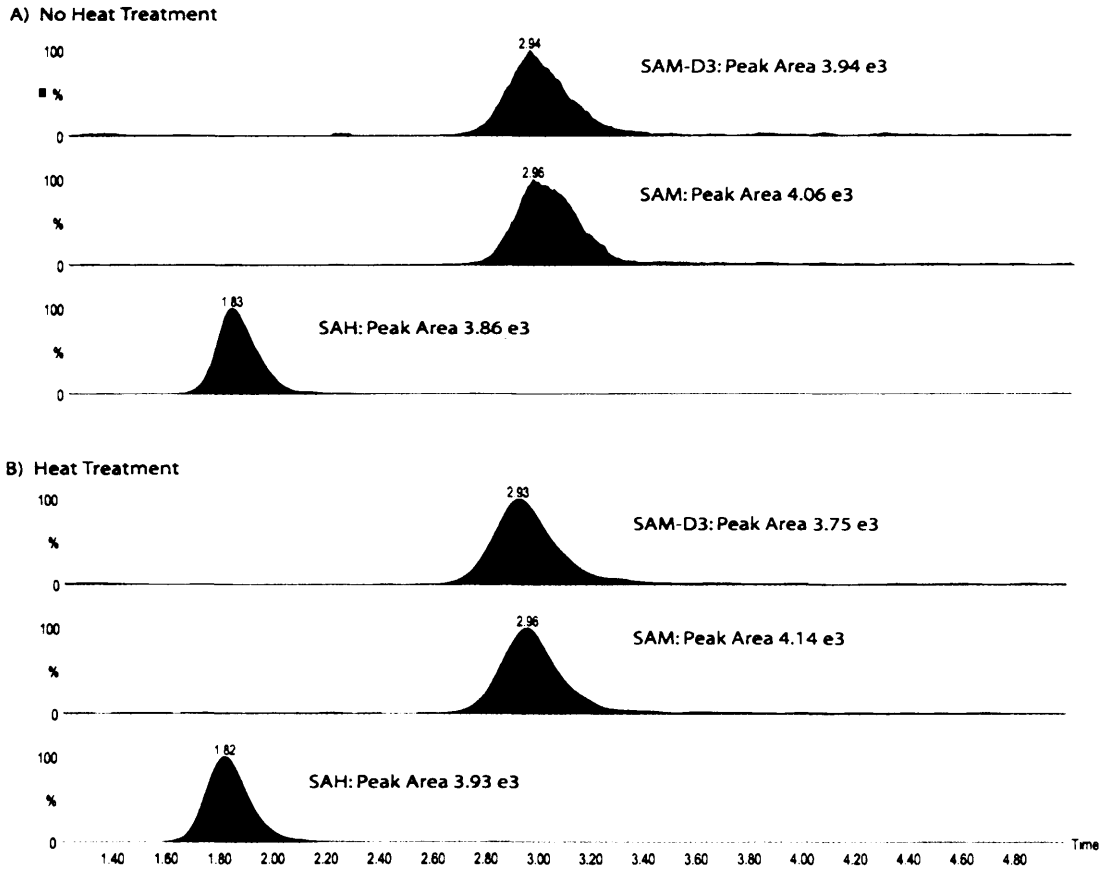

Figure 3.5. The effect of heat treatment on the signal intensity of SAM-D_3, SAM and SAH. Representative chromatograms are shown for 1 µmol/L aqueous standards which were analysed prior to, and following heat treatment at 80 °C for 5 min. Retention times are indicated above peaks.

3.3.3. Chromatography

The retention of SAM and SAH in aqueous solution on a C8 column using reverse phase was 1.02 and 1.85 min, respectively (Figure 3.6). On a column of this dimension (100 x 2.1mm; 5 µm), this suggests that these analytes are not being retained using reverse phase. Gellekink et al. (2005) also reported retention times less than 2 min using a C18 column (100 x 2.1 mm; 5 µm) (Gellekink et al., 2005).

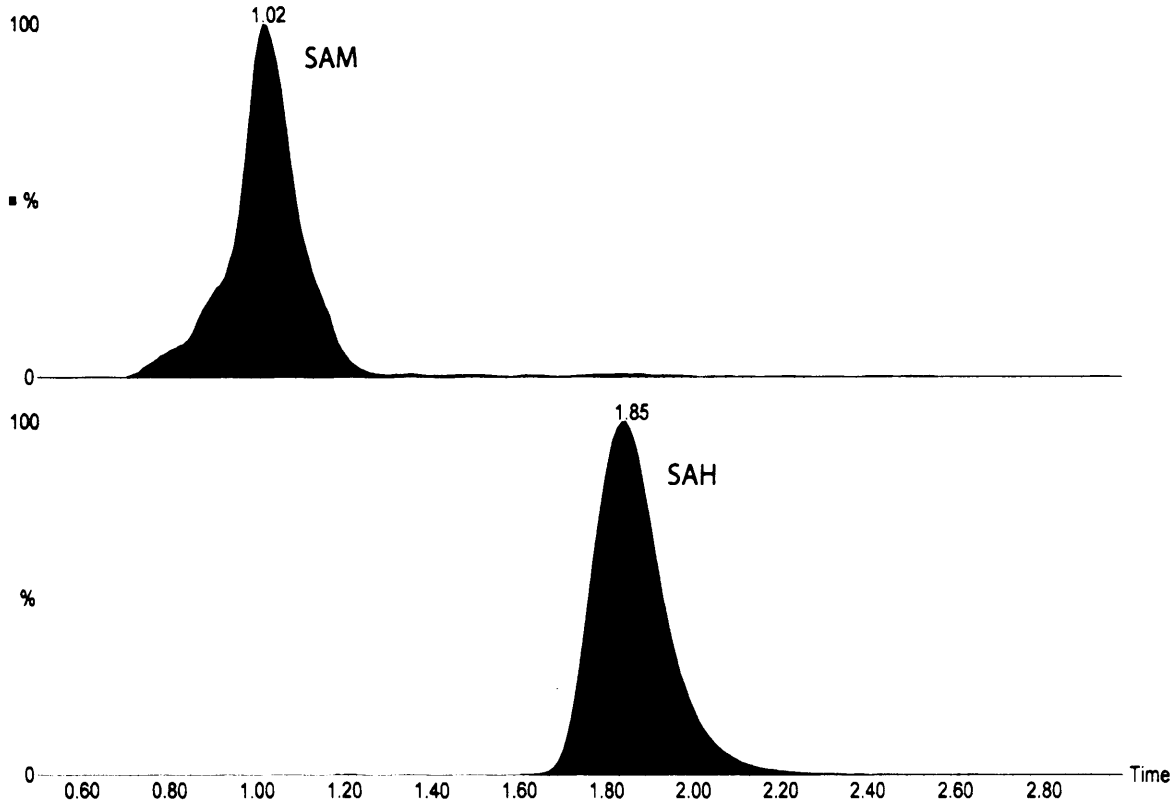

Figure 3.6. LC-MS/MS chromatograms obtained in SRM mode using reverse phase chromatography. Column used: Discovery Hypurity C8 column (100 x 2.1 mm (i.d.); 5 µm bead size). Representative chromatograms are shown for 10 µmol/L aqueous standards. Retention times are indicated above peaks. Mobile phase consisted of 5% A (Methanol):95% B (4 mM ammonium acetate, 0.1% formic acid, 0.1% heptafluorobutyric acid (pH2.5)).

On a pentafluorophenylpropyl-bonded silica (PFPP) column (Figure 3.7), basic analytes exhibit retention that increases with the organic content, with some analytes failing to elute from the column even in 100% organic mobile phase (Needham et al., 2000). This type of retention profile, referred to as a U-shaped retention (Figure 3.7), has been shown to be due largely to ion exchange mechanisms. Retention at high organic percentage is

beneficial for LC-MS/MS experiments since it can lead to an increase in sensitivity through facilitated desolvation and can enhance peak shape. Also, PFPP columns often induce retention otherwise not obtained in reverse phase. Retention aids the elimination of endogenous interferences plus, the use of a solvent-divert valve enables early eluting contaminants to be diverted to waste preventing accumulation on the ion source.

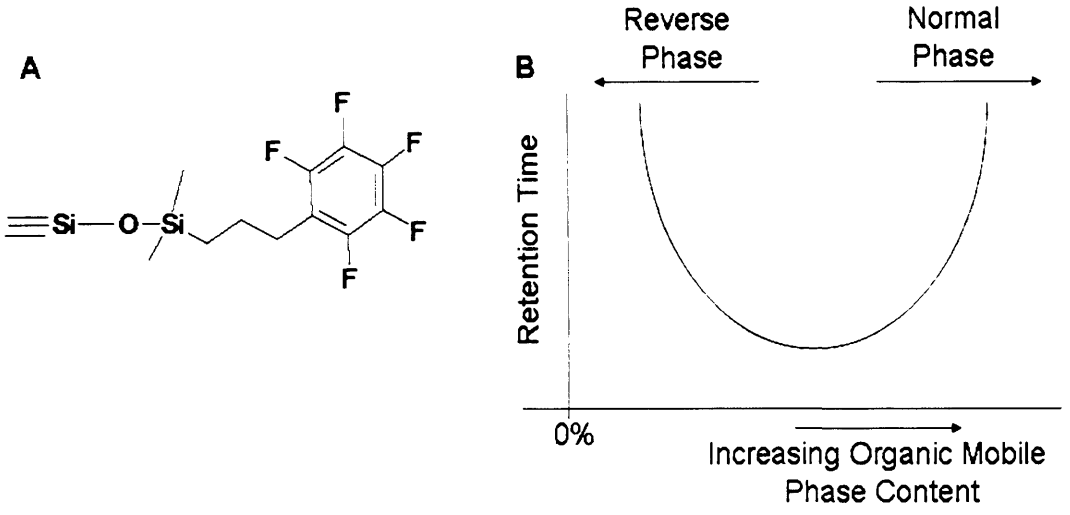

Figure 3.7. The molecular structure (A) and U-shaped retention profile (B) of the pentafluorophenylpropyl-bonded silica, PFPP column.

The retention of SAM and SAH in aqueous solution on a PFPP column using a mobile phase of high organic content was 3.22 and 1.92 min, respectively (Figure 3.8). Thus, the PFPP column was chosen over standard reverse-phase columns due prolonged retention avoiding co-elution with early eluting endogenous compounds and retention in high organic percentage. 0.1% heptafluorobutyric acid was also added to the mobile phase in each case as it results in greater retention due to ion pairing interactions (Struys et al., 2000).

Representative chromatograms of SAM and SAH in both aqueous solution and in an analytical sample prepared by heat treatment, comprising an E10.5 mouse embryo, are

shown (Figure 3.8). In all cases there was a change in the retention time of SAM, SAH and $^2H_3$-SAM, resulting in earlier elution of the three compounds in embryo samples under analysis compared to aqueous standards. Similarly, the spiking of calibrators into pooled embryo matrix resulted in the same change of retention compared to analysis of standards in aqueous solution. The reason for the change in retention time of all three compounds when analysed in an embryo matrix compared to aqueous solution is not clear. I hypothesise that this is due an interaction with unidentified compounds present in the embryo matrix that result in slight changes in the retention time of SAM/SAH on the HPLC column.

3.3.4. Linearity, Limits of Detection and Precision

The internal standard, [$^2H_3$]-SAM, was used for quantification of both SAM and SAH. Calibration curves, made up in a matrix of pooled homogenised embryos, were linear throughout a concentration range of 0.5-25 µM and 0.01-0.5 µM for SAM and SAH, respectively (Figure 3.9). Therefore, it seems that the minor structural difference of [$^2H_3$]-SAM from SAH, which lacks a methyl group, had minimal effect on both the linearity and precision of quantification. Moreover, as the coefficients of variation (CV%) for SAH were comparable to SAM and within acceptable limits (Table 3.5), it was deemed unnecessary to synthesise an additional SAH internal standard.

The range of concentrations used in the calibration curves was found to be suitable for the analysis of individual mouse embryos at E9.5 and E10.5, encompassing the period when neural tube closure is completed in the cranial and spinal regions. The coefficient of linear correlation (r^2) was 0.997 and 0.998 for SAM and SAH, respectively. The limits of detection (determined at a signal-to-noise ratio of 5:1) for SAM and SAH were 10 nmol/L and 2.5 nmol/L, respectively, corresponding to 0.4 pmoles and 0.1 pmoles in the 40 µl injection. The lower and upper limits of quantification for SAM and SAH using this method were 0.02-25 µM and 0.01-10 µM, respectively. Analysis of SAM would be expected to be more sensitive than SAH due to the more polar nature of the molecule. However this is not the case since mass spectromteric analysis of SAH is in fact more sensitive than SAM. The reason for this is unknown.

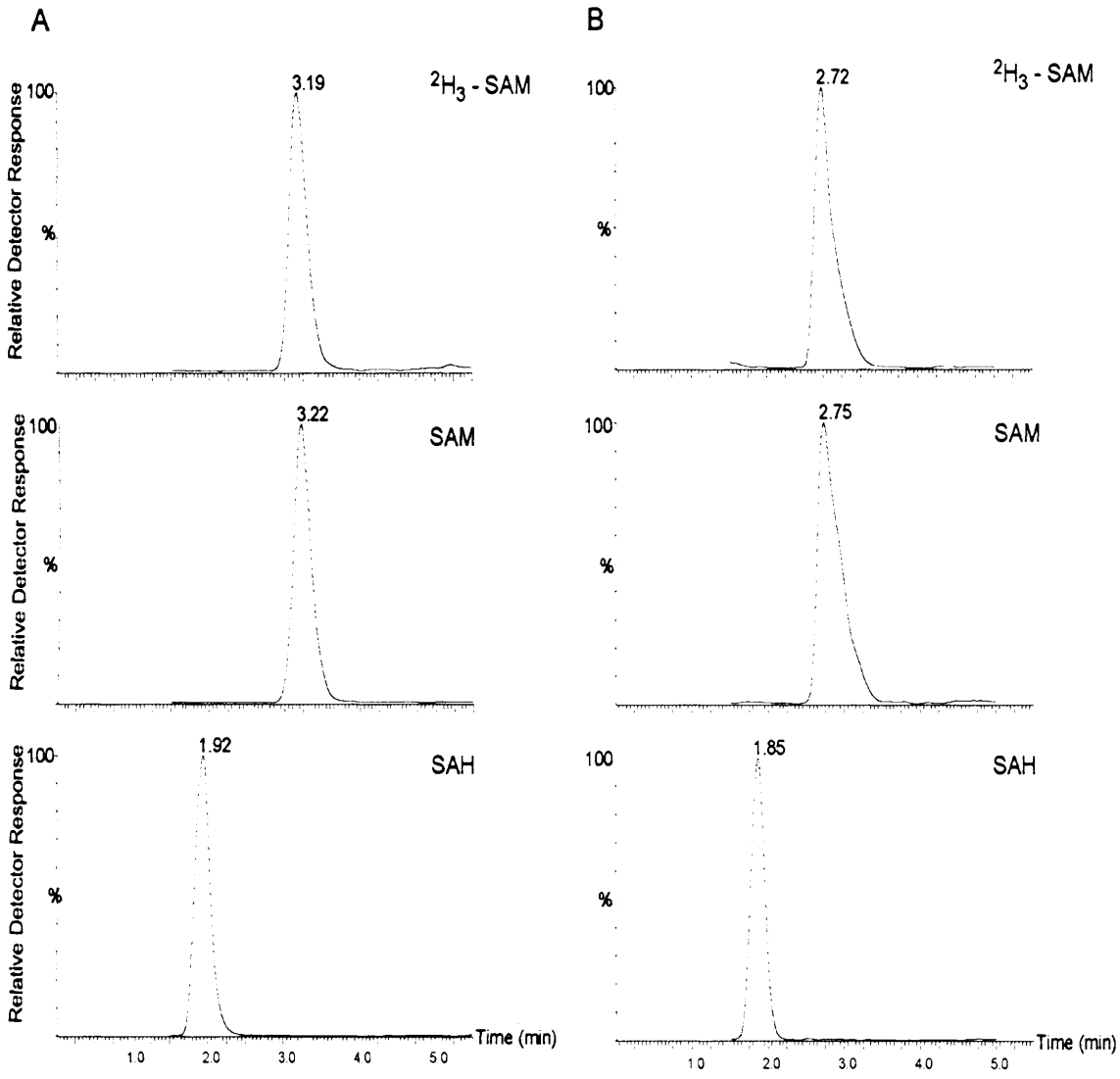

Figure 3.8. LC-MS/MS chromatograms obtained in SRM mode using the Discovery HS F5 column (50 x 2.1 mm (i.d.); 5 µm bead size). Representative chromatograms are shown for, (A) 1 µmol/L aqueous standards and, (B) endogenous SAM and SAH in an E10.5 mouse embryo, containing measured concentrations of 0.766 µmol/L SAM and 0.121 µmol/L SAH. Retention times are indicated above peaks.

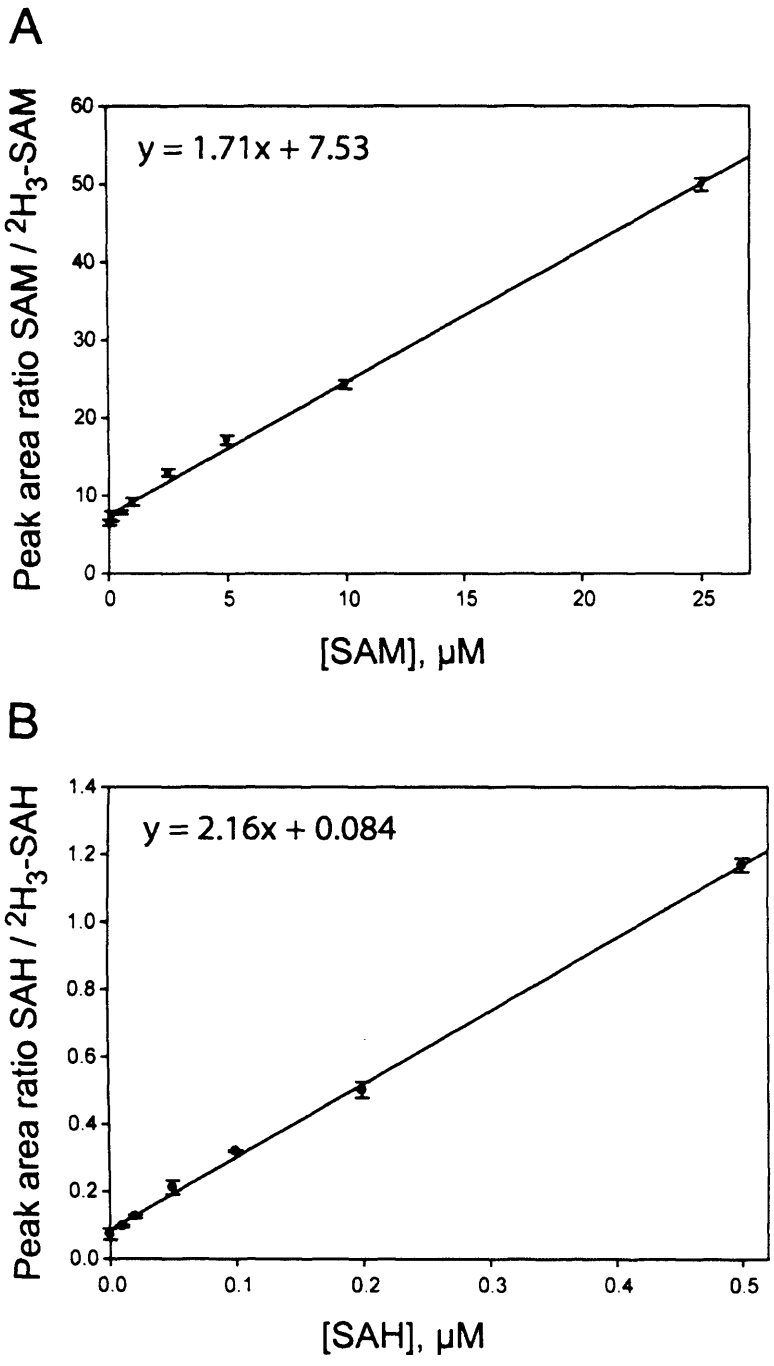

Figure 3.9. Calibration curves of peak-area ratios plotted against concentration of SAM (A) and SAH (B) concentration. Calibrators were made up in a pooled sample of homogenised embryos with 1.0 µmol/L of [$^2H_3$]-SAM (internal standard) added to each sample. SAM data points correspond to 0.5, 1, 2.5, 5, 10, 25 µM of SAM and the SAH data points correspond to 0.01, 0.02, 0.05, 0.1, 0.2, 0.5 µM. Each sample was run in triplicate (n=3).

To determine the precision for analysis of tissue samples, experiments were performed by pooling homogenised whole embryo samples either from E9.5 embryos at the 24-26 somite stage or from late stage E10.5 embryos at the 37 somite stage. All samples contained 1 μM of the internal standard, [$^2H_3$]-SAM. Overall, intra-assay coefficients of variation (CVs) ranged from 4.09-4.13% for SAM and 4.64-5.68% for SAH and inter-assay CVs ranged from 6.34-7.74% for SAM and 11.56-11.93% for SAH in tissue samples (Table 3.3).

Sample	Precision	SAM		SAH	
		Mean concentration (μM ±SD)	CV (%)	Mean concentration (μM ±SD)	CV (%)
E9.5 mouse embryo	Intra-assay (n=12)	2.52 ± 0.10	4.13	0.044 ± 0.002	4.64
E10.5 mouse embryo	Intra-assay (n=12)	11.72 ± 0.48	4.09	0.21 ± 0.01	5.68
E9.5 mouse embryo	Inter-assay (n=8)	2.55 ± 0.20	7.74	0.040 ± 0.005	11.93
E10.5 mouse embryo	Inter-assay (n=8)	12.18 ± 0.77	6.34	0.20 ± 0.02	11.56

Table 3.3. Inter- and Intra-assay precision of the LC-MS/MS method for aqueous and embryonic samples. The precision was determined by repeated assay of standard aqueous solutions and embryo samples, which consisted of pools of homogenised embryos collected at E9.5 and E10.5. CV, coefficient of variation.

Accuracy was evaluated by spiking whole embryo homogenates with increasing concentrations of SAM or SAH, and quantifying the total SAM or SAH (Table 3.4). The measured concentration was expressed as a percentage of the predicted 'nominal' concentration, which was the sum of the added concentration and endogenous level (determined in the 0 μM added sample). In the majority of cases the measured value was greater than 90% of the predicted nominal value (Table 3.4). Recovery was assessed by comparing the response of samples that were spiked before extraction (pre-extraction) to samples that were spiked after extraction (post-extraction) (Matuszewski et al., 2003). Mean recoveries for SAM and SAH from E9.5 and E10.5 pooled mouse embryo matrices were 97 % and 92 %, respectively (Table 3.4).

Sample	*Spiked conc. added (μM)*	*Measured conc. (μM)*	*Accuracy (% Nominal Conc.)*	*Measured conc. (μM)*	*Accuracy (% Nominal Conc.)*	*Recovery (%)*
	SAM Added (μM)	**Spiked pre-extraction**		**Spiked post-extraction**		
E9.5 mouse embryo	0	0.08 ± 0.02				
	0.5	0.57 ± 0.03	98	0.57 ± 0.02	98	100
	1.0	1.06 ± 0.02	98	1.09 ± 0.06	101	97
	2.0	2.08 ± 0.004	100	2.12 ± 0.09	102	98
E10.5 mouse embryo	0	0.79 ± 0.01				
	0.5	1.21 ± 0.01	94	1.19 ± 0.17	92	101
	1.0	1.82 ± 0.04	102	2.03 ± 0.28	113	90
	2.0	2.64 ± 0.04	95	2.83 ± 0.27	101	94
	SAH Added (μM)	**Spiked pre-extraction**		**Spiked post-extraction**		
E9.5 mouse embryo	0	0.11 ± 0.009				
	0.05	0.13 ± 0.002	81	0.14 ± 0.003	88	97
	0.1	0.19 ± 0.001	86	0.21 ± 0.009	100	87
	0.2	0.33 ± 0.027	106	0.35 ± 0.03	113	92
E10.5 mouse embryo	0	0.20 ± 0.03				
	0.05	0.23 ± 0.001	92	0.24 ± 0.006	96	90
	0.1	0.30 ± 0.07	100	0.34 ± 0.03	113	91
	0.2	0.38 ± 0.04	95	0.42 ± 0.05	105	95

Table 3.4. Accuracy and recovery data for the LC-MS/MS quantification of SAM and SAH in mouse embryos. Embryo samples consisted of pools of homogenised embryos collected at E9.5 and E10.5. Accuracy (% nominal concentration) was determined by comparing the measured concentration of SAM or SAH against the nominal concentration (the predicted value equating to the baseline concentration + spiked concentration). Thus, %Nominal concentration = [Measured Conc.]/[Baseline conc. + Spiked conc.] x 100. Recovery was determined by comparing the assay results for embryo samples spiked pre- and post- extraction (n = 3 for each condition). % Recovery = ([Response of Pre-Extracted Spiked Sample] / [Response of Post-Extracted Spiked Sample]) x 100 [as ref. (Luippold et al., 1999)]. Concentration values are given as mean ± standard deviation.

Repeated injections into the mass spectrometer can lead to a build-up of residues on the source, which can affect sample ionisation and subsequently, sensitivity. This loss in sensitivity is increased if the sample preparation is inadequate or if the organic content of the mobile phase is low. The performance of the instrument over a long period of time was evaluated using repeated injections of the same sample. The loss in sensitivity was monitored by calculating the peak area response for the internal standard following the analysis of consecutive embryo samples (Figure 3.10). Thus, repeated injections of sixty samples led to a 25% drop in sensitivity over sixty injections which corresponded to 15 hours of analysis. This loss in sensitivity is generally not a problem, when analysing strong signals, as all compounds should be affected equally. However, since levels of SAM and SAH in embryo samples are limiting, being aware of the limitations of repeated injections is advisable. To overcome reduced sensitivity, long sample lists were avoided and regular cleaning of the source was undertaken.

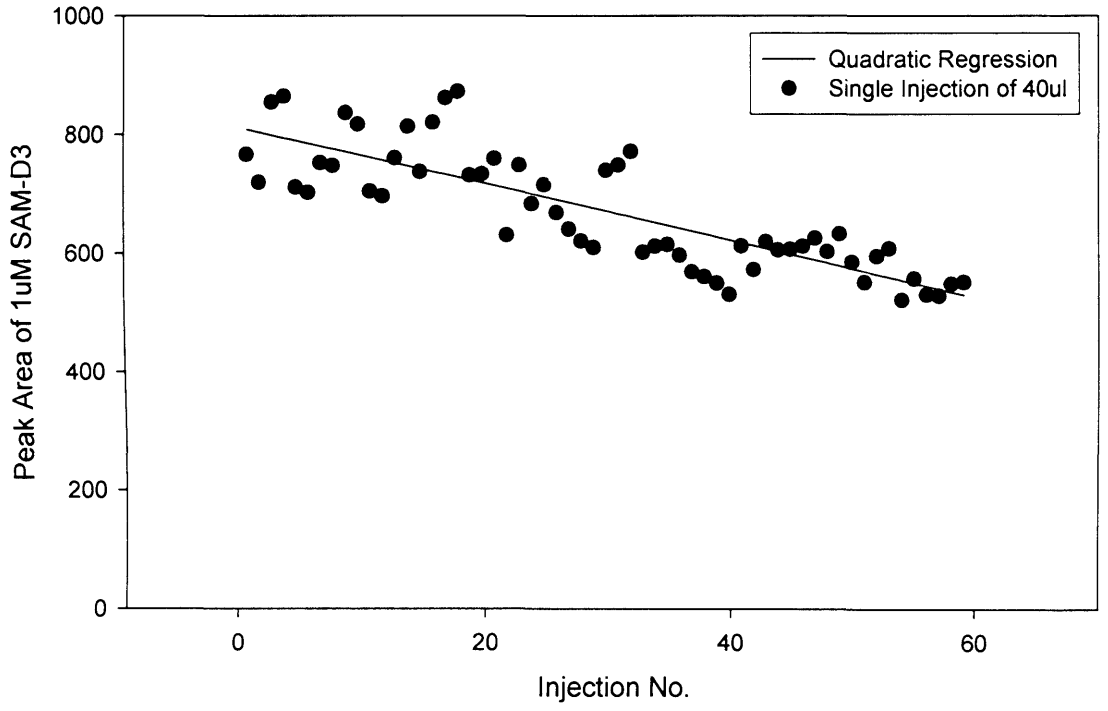

Figure 3.10. Analysis of signal intensity following repeated injections of embryonic samples. The peak area of the 1 μM internal standard, SAM-D_3 was monitored for sixty consecutive injections of embryonic samples. $r^2 = 0.684$.

3.3.5. Mouse embryo samples

A series of non-mutant CD-1 mouse embryos were collected and analysed to establish reference intervals of SAM and SAH. Levels were normalised to protein concentration and correlated with developmental stage (Table 3.5).

Embryonic stage	No. samples	SAM nmol/mg protein	SAH nmol/mg protein	SAM:SAH Ratio
E9.5	**Total (n=24)**	**1.98 ± 0.71**	**0.031 ± 0.011**	**67.8 ± 23.2**
	Male (n=13)	2.23 ± 0.64	0.034 ± 0.012	71.6 ± 24.3
	Female (n=11)	1.69 ± 0.71	0.027 ± 0.009	63.4 ± 22.2
E10.5	**Total (n=26)**	**2.78 ± 0.67****	**0.057 ± 0.029****	**53.0 ± 13.9****
	Male (n=15)	2.75 ± 0.65	0.051 ± 0.021	46.8 ± 13.3
	Female (n=11)	2.83 ± 0.65	0.065 ± 0.023	57.6 ± 12.8

Table 3.5. SAM and SAH abundance in mouse embryos determined by LC-MS/MS. SAM and SAH were quantified in individual CD1 embryos at E9.5 (Mean number of somites 25.7 (standard deviation 1.4)) and E10.5 (Mean number of somites 33.6 (standard deviation 2.4)). Values are given as mean ± standard deviation. ** $p < 0.02$ when compared to E9.5 (unpaired student t-test).

In embryos at E9.5 and E10.5, mean concentrations of SAM were 1.98 and 2.78 nmol/mg protein respectively, while mean concentrations of SAH were 0.031 and 0.057 nmol/mg protein (Table 3.5). Thus, SAM levels are typically 50-70 fold higher than SAH levels in mouse embryos at these stages of development. At a particular stage, comparison of male and female embryos did not indicate any sex difference in SAH or SAM levels (Table 3.5). Moreover, within litters there was no apparent effect of position of the embryo within the uterus as levels were comparable for conceptuses close to the cervix compared with those close to the ovary. Conversely, significant changes occur in the concentration of both SAM and SAH as development proceeds (Table 3.5). Thus, at E10.5 the concentration of both SAM and SAH had increased compared to a day earlier in development. As the abundance of SAH increased to a greater extent than SAM, the SAM:SAH ratio decreased significantly at E10.5 compared to E9.5.

3.3.6 Analysis of cell pellets collected from human cell lines

During the study, a series of lymphoblast and fibroblast cell lines collected from NTD patients became available from which cell pellets were collected as described (Chapter 4). The cell pellet was prepared subsequently for LC-MS/MS analysis using the same approach as that used to analyse neurulation-stage embryos. A representative chromatogram of endogenous SAM and SAH in a cell line sample is shown (Figure 3.12). The retention times of SAM and SAH were comparable to those observed in embryo samples. Calibration curves, made up in a matrix of pooled homogenised cell pellets, were linear throughout a concentration range of 0.25-5 µM and 0.01-0.20 µM for SAM and SAH, respectively (Figure 3.13). This range of concentrations was found to be suitable for the analysis of cell pellets (approx. 1 mg protein) collected from cell lines of fibroblast and lymphocyte origin. As with the analysis of embryo samples, the internal standard, [$^2H_3$]-SAM, was used for quantification of both SAM and SAH. The coefficient of linear correlation (r^2) was 0.995 and 0.999 for SAM and SAH, respectively.

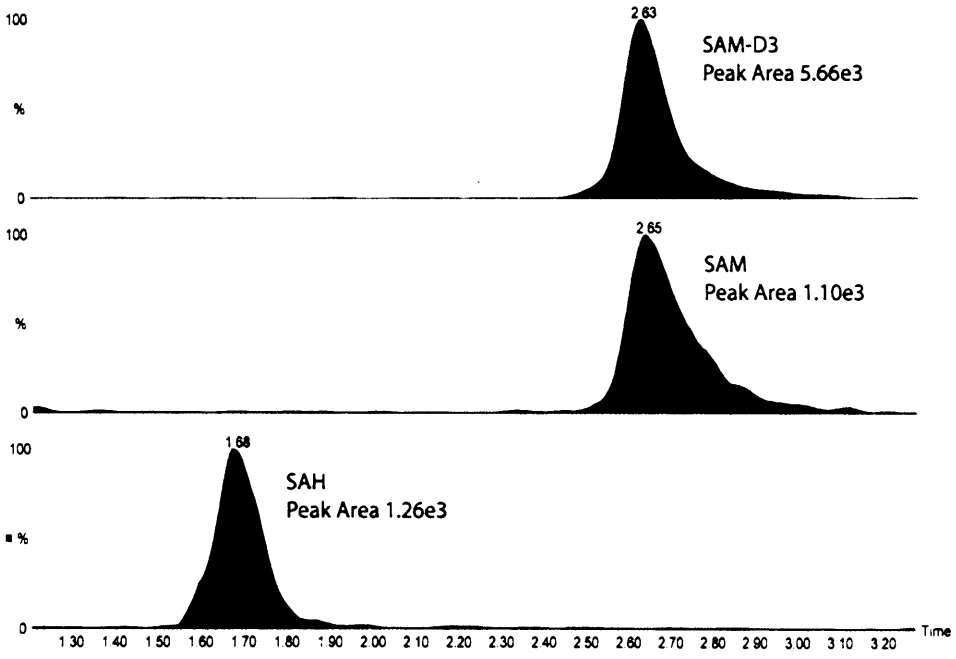

Figure 3.12. LC-MS/MS chromatograms for [$^2H_3$]-SAM, SAM and SAH obtained in SRM mode using the Discovery HS F5 column (50 x 2.1 mm (i.d.); 5 µm bead size). Representative chromatograms are shown for endogenous SAM and SAH in a cell pellet spiked with 1 µM [$^2H_3$]-SAM-D_3. The measured concentrations were 0.323 µmol/L SAM and 0.041 µmol/L SAH. Retention times indicated above peaks.

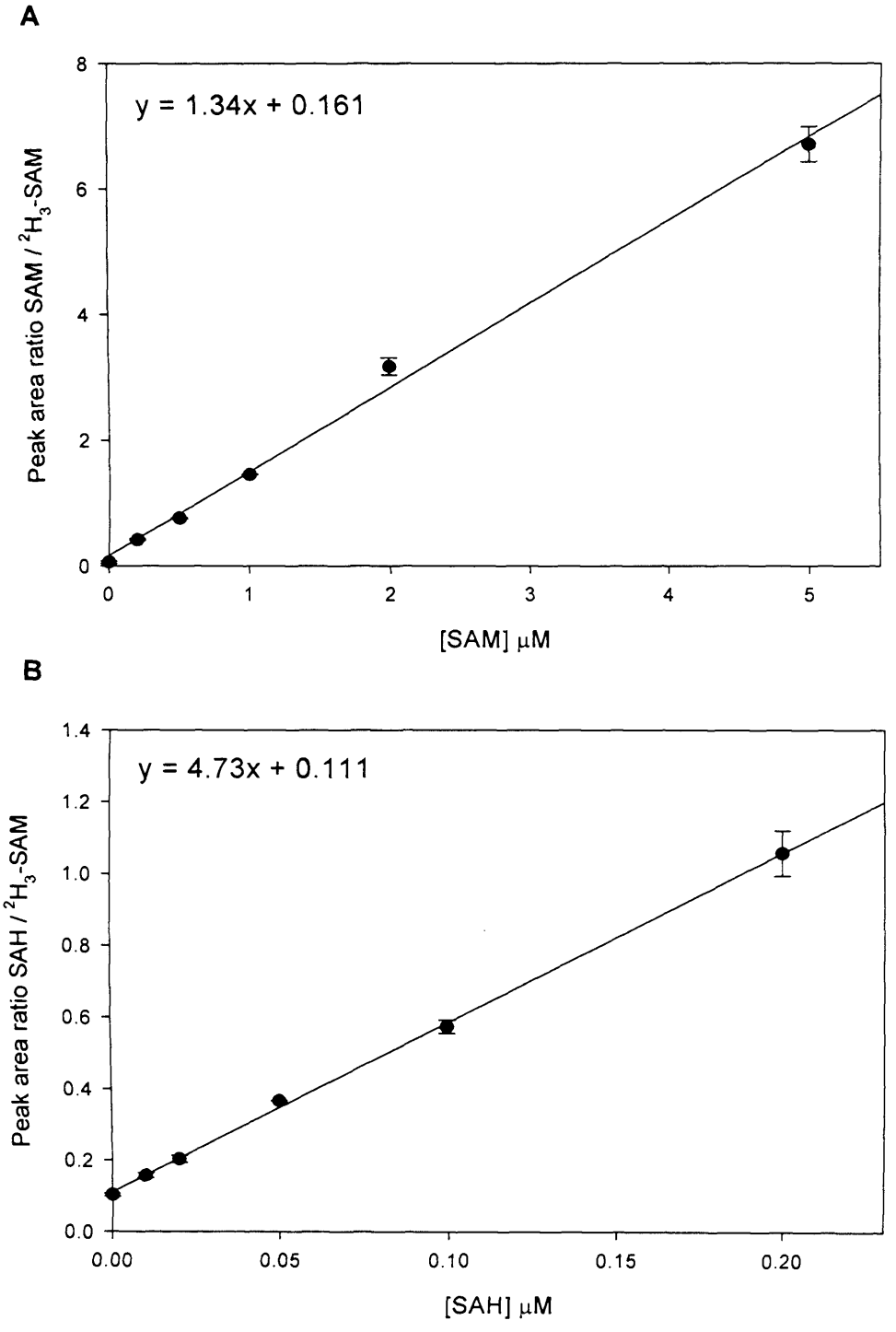

Figure 3.13. Calibration curves of peak-area ratios plotted against SAM (A) and SAH (B) concentration for cell line samples. Calibrators were made up in a pooled sample of cell pellets with 1.0 μmol/L of [$^2H_3$]-SAM (internal standard) added to each. SAM data points correspond to 0, 0.25, 0.5, 1, 2, 5 μM of SAM and the SAH data points correspond to 0, 0.01, 0.02, 0.05, 0.1, 0.2 μM. Each sample was run in triplicate (n=3).

3.4 Conclusion and Discussion

3.4.1 Method Development

SAM and SAH are key metabolites in one-carbon metabolism as their ratio determines the methylation potential in a tissue (Carmel and Jacobsen, 2001;Scott, 1999). Since sub-optimal methylation capacity is associated with various diseases (James et al., 2002;Mattson, 2003;Seshadri et al., 2002), as well as developmental abnormalities, it was necessary to develop new methodology for quantification of SAM and SAH in limiting amounts of sample. For this reason, LC-MS/MS methodology was used for the simultaneous quantification of SAM and SAH in tissue samples. The sample preparation method allowed analysis of tissue quantities (less than 1 mg) considerably lower than used in methods that utilise solid phase extraction (typically 100-300 mg wet weight (Needham et al., 2000)).

Previously, UV detection following HPLC or capillary electrophoresis has been used for detection of SAM and SAH (Luippold et al., 1999;She et al., 1994a;Uthus, 2003). Increased sensitivity can be achieved by the use of coulometric electrochemical detection (Melnyk et al., 2000) or through derivatisation of SAH and SAM followed by fluorescent detection, although this is time-consuming and requires additional sample preparation steps (Capdevila and Wagner, 1998;Weir et al., 1992). Here, a method has been developed that exploits the selectivity and sensitivity of tandem mass spectrometry, yielding a method with limits of detection of 10 nmol/L and 2.5 nmol/L for SAM and SAH, respectively, with very little sample preparation necessary.

Sample preparation is minimised compared to previous MS-based methods, which require solid phase extraction (Gellekink et al., 2005;Struys et al., 2000). Instead, the method developed in this study involved homogenisation of samples in an acidified mobile phase and heat precipitation of proteins. This resulted in increased throughput, reduced sample loss (with a resulting increase in sensitivity) and without degradation of SAM. A single internal standard was used for both assays, since although [$^2H_3$]-SAM is technically a type II internal standard when used in the quantitation of SAH, the inter- and intra-coefficients of variation observed were within acceptable limits of analytical biochemistry. Presumably, this is due to the superior ability of the HS F5 column to retain small, polar metabolites over conventional reverse phase columns, resulting in fewer co-eluting and interfering compounds that can lead to ionic suppression.

In mouse embryos the concentration of SAM detected (2-2.8 nmol/mg protein) was approximately 20-40 times higher than values reported for adult liver and kidney in rats (Luippold et al., 1999;She et al., 1994a). However, the values for adult tissue were expressed per wet weight of tissue, which is not practical with small tissue samples such as embryos. I estimate that SAM levels in embryonic and adult tissue are approximately comparable, based on comparison of protein content and wet weight for a limited number of embryos. SAH concentrations reported in adult rats vary widely between tissues (Luippold et al., 1999;She et al., 1994a), and are similar or an order of magnitude lower than in mouse embryos, although direct comparison is again complicated by normalisation to wet weight rather than protein. However, the concentrations of SAM and SAH detected in neurulation-stage mouse embryos are similar to the levels (also normalised to protein content) measured in a recent study of pooled chick embryos (Afman et al., 2006) A significant increase in the concentration of both SAM and SAH is detected in the period from E9.5 to E10.5, despite the fact that there is a concomitant increase in the protein content of the embryo. At the same developmental period there is a decrease in the SAM:SAH ratio, since the magnitude of the increase in SAH concentration is greater than that for SAM, possibly due to increased demand for SAM in transmethylation reactions or as a precursor in polyamine synthesis.

In summary, the use of LC-MS/MS enables sensitive, precise and accurate quantification of the picomole quantities of SAM and SAH in neurulation-stage mouse embryos. Although, the method was particularly designed for the analysis of individual mouse embryos, it could potentially be applied to any tissue where limited amount of sample is available depending on the matrix and the levels of SAM and SAH in the tissue to be analysed. Indeed, I went on to apply the method to the quantification of SAM and SAH in cell pellets in which the levels were found to be similar to those in embryonic tissue samples. The suitability of this method for cell pellets is demonstrated by the identical retention times observed on the HS F5 column compared to embryonic samples and the linearity of calibration.

3.4.2 Changes in methyltransferase activity with gestation

It remains to be established how variations in the abundance of SAM and SAH through gestation affect the activity of methyltransferases (MT) and the subsequent biological significance. The values for the kinetic constants (K_m value for SAM and K_i value for SAH) are known for several mammalian MT (Carmel and Jacobsen, 2001). The range of K_i

values demonstrates that some MT will be much more sensitive to the inhibitory action of SAH. The catalytic activity of each MT is also dependent on the concentration of SAM since SAH acts as a competitive inhibitor. Using the K_i and K_m stated by Clarke and Banfield, it was possible to calculate relative enzyme activities of each MT at E9.5 and E10.5 (Table 3.6), using the Michalis Menton equation for competitive inhibition (Carmel and Jacobsen, 2001).

Fraction of maximal velocity = [SAM] / (K_m + K_m [SAH]/ K_i + [SAM])
[SAM] = concentration of SAM, [SAH] = concentration of SAH,
K_i = inhibition constant for SAH, K_m = Michaelis constant for SAM.

The percentage activity of each MT at E10.5 relative to E9.5 provides an illustration of how the activity of each MT may change with gestational age (Table 3.6). Thus, enzymes with low K_i values relative to K_m values are more markedly inhibited by a lower SAM/SAH ratio.

The results of this data analysis demonstrate that the activity of some MTs may be relatively unaffected by the change in the abundance of SAM and SAH with gestational age. Examples include three of the MTs involved in RNA processing, tRNA (cytosine-5-)-methyltransferase, tRNA (adenine-*N* 1-)-methyltransferase and rRNA (2'-ribose-*O*-)-methyltransferase, for which the predicted change in activity is less than 10%. By contrast, several other MTs appear to be particularly sensitive to changes in SAM and SAH abundance. At E10.5, the activity of phosphatidylethanolamine methyltransferase, which is involved in phosphatidylcholine synthesis (Hartz and Schalinske, 2006), is predicted to increase by 34%. Similarly, the activity of several N-methyltransferases is increased by over 30%, including glycine methyltransferase which is required for the synthesis of sarcosine and is also involved in the regulation of the methyl- group metabolism (Wagner et al., 1985).

It must be appreciated that the Ki and Km values for these MTs were established in adult tissues of various types. Indeed some of these enzymes may not be present in neurulation stage embryos or the embryonic isoforms of these enzymes may be functionally different. The activity of the methyltransferases may also be subject to additional regulatory influences. Clearly investigations of MT expression and activity in embryonic tissues is required to establish definitively how the activity of each MT is affected by gestational changes and furthermore, to understand changes as a result of a genetic or environmental disturbance.

Methyltransferase	K_m for SAM	K_i for SAH	Fraction of maximal methyltransferase activity		% activity at E10.5 relative to E9.5
			E9.5	E10.5	
DNA					
DNA (cytosine 5-)	1.4	1.4	0.580	0.656	113
RNA					
tRNA (cytosine 5-)	0.5	0.9	0.793	0.839	106
tRNA (guanine-N 1-)	3	0.11	0.340	0.379	112
tRNA (guanine-N 2-)	2	23	0.497	0.581	117
tRNA (adenine-N 1-)	0.3	0.85	0.864	0.897	104
rRNA (2'-ribose-O-)	0.24	0.17	0.875	0.897	103
Lipids					
Phosphatidylethanolamine	18.2	3.8	0.097	0.131	134
Protein					
Carboxyl					
Protein-L-isoaspartate	2	0.08	0.416	0.448	108
Protein S-isoprenylcysteine	2.1	9.2	0.484	0.568	117
Lysine					
Calmodulin-lysine N-	2	15.2	0.497	0.581	117
Histone-lysine N-	12.5	5.9	0.136	0.181	133
Arginine					
[Myelin basic protein]-arginine	4.4	1.8	0.307	0.380	124
Protein arginine I	8	2.3	0.196	0.253	129
Small Molecules					
N-methyltransferase					
Guanidinoacetate	49	16	0.039	0.054	138
Histamine	1.7	11.8	0.537	0.619	115
Glycine	100	35	0.019	0.027	139
Phenylethanolamine	10	1.4	0.162	0.211	130
β-Carboline-2	81	14.8	0.024	0.033	139
Indolethylamine	54.3	8.65	0.035	0.048	138
O-Methyltransferase					
Hydroxyindole	14	2.1	0.122	0.162	132
Catechol	3.1	1	0.383	0.459	120
S-Methyltransferase					
Thiopurine	3	5.8	0.396	0.479	121
Thioether	1	40	0.664	0.735	111

Table 3.6. Sensitivity of methyltransferases to changes in SAM and SAH concentration with gestation. Theoretical activities for methyltransferases were calculated based on known Ki and Km values (Carmel and Jacobsen, 2001) and the measured concentrations of SAM and SAH in E9.5 and E10.5 mouse embryos. Fraction of maximal methyltransferase activity was calculated using the Michaelis Menton equation for competitive inhibition and the concentrations of SAM and SAH at E9.5 and E10.5 stated in Table 3.7.

CHAPTER 4

Impact of methylation cycle perturbation on cranial neural tube closure and the abundance of s-adenosylmethionine and s-adenosylhomocysteine

4.1 Introduction

4.1.1 The Methylation Cycle and NTDs

Several lines of evidence suggest that the methylation cycle (Figure 4.1), plays a key role in determining susceptibility to NTDs. Risk factors for human NTDs include elevated maternal plasma levels of homocysteine and reduced levels of vitamin B_{12}, the co-factor for methionine synthase (Figure 4.1) (Kirke et al., 1993;Steegers-Theunissen et al., 1994). Additionally, a thermolabile polymorphic variant (C677T) of the enzyme MTHFR, which exhibits reduced catalytic activity, causes elevated levels of homocysteine in NTD patients and their mothers (Eskes, 1998). Although homocysteine has been shown to induce NTDs in chick embryos (Rosenquist et al., 1996), similar studies in mammalian embryos have shown that while homocysteine is toxic it does not cause NTDs (Bennett et al., 2005;Greene et al., 2003;VanAerts et al., 1994). Hence, elevated homocysteine may not be the primary factor leading to NTDs in human pregnancy; it may simply be a marker for methylation cycle integrity or another metabolic abnormality.

As homocysteine is the precursor for methionine, high homocysteine levels could be linked with limited production of methionine. Indeed, rat embryos cultured in serum containing low levels of methionine develop cranial NTDs unless methionine is added (Coelho et al., 1989). In humans, low dietary methionine intake is reported to be associated with increased risk of NTDs hence it has been proposed that a high intake of methionine may be protective against NTDs (Shoob et al., 2001). This hypothesis is supported by a study whereby *in vivo* administration of methionine to pregnant dams reduces the incidence of spinal NTDs in the *Axial defects* mutant mouse (Essien, 1992). In contrast, research from our group unexpectedly showed that adding methionine to embryo cultures specifically causes cranial NTDs, in both wild-type (Dunlevy et al., 2006a) and *splotch* embryos (Fleming and Copp, 1998). Thus, it appears that both deficient and excess methionine can cause increases in the incidence of NTDs, suggesting that optimum methionine levels are critical for the closure of the neural tube. Indeed, it has been suggested that methionine may promote DNA methylation yet iocus-specific hypermethylation of DNA could be deleterious (Waterland, 2006).

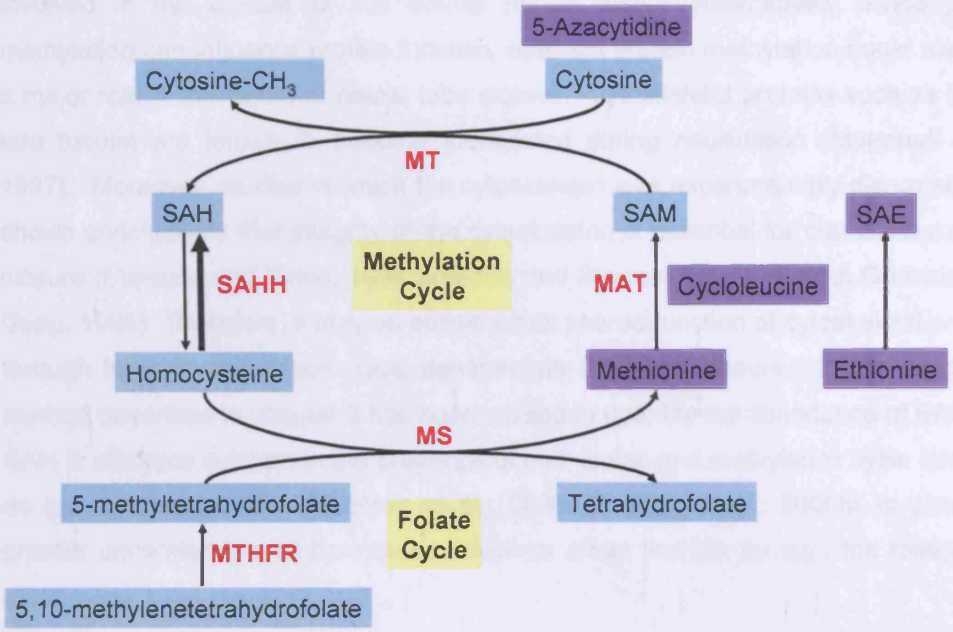

Figure 4.1. Pertubation of the methylation cycle by exogenous agents. Purple boxes highlight exogenous agents used in this study. MTHFR; 5,10-Methylenetetrahydrofolate Reductase, MAT; Methionine Adenosyl-transferase, SAHH; SAH Hydrolase, MT; Methyltransferase, MS: Methionine Synthase.

Previous work from our group has also shown that inhibition of methylation cycle reactions, using ethionine and cycloleucine (see figure 4.1), causes cranial NTDs in wild-type mice (Dunlevy et al., 2006b). Ethionine, a methionine analog, is converted to s-adenosylethionine, which is not utilised by methyltransferases and in turn acts as a competitive inhibitor of methionine adenosyltransferase (MAT; E.C.2.5.1.6)(Cox and Irving, 1977), whereas cycloleucine acts as a direct non-competitive inhibitor of MAT. A similar study in chick recorded a delay in closure of the neural folds following exposure to cycloleucine and inhibitors of SAH hydrolase (Afman et al., 2006). Of note, the conversion of ethionine to s-adenosylethionine by MAT causes depletion of ATP, whereas cycloleucine does not affect ATP levels.

Cranial closure defects following exposure of embryos to methionine and inhibitors of the methylation cycle indicates an essential requirement for the methylation cycle in cranial neurulation. Disruption of the methylation cycle could potentially affect various biochemical processes including DNA and protein methylation. A disturbance of global

DNA methylation could affect the transcriptional control of one or more important genes involved in the closure of the cranial neural tune. Alternatively, since protein methylation can influence protein function, aberrant protein methylation could also play a major role in the failure of neural tube closure. Cytoskeletal proteins such as β-actin and tubulin are known to become methylated during neurulation (Moephuli et al., 1997). Moreover, studies in which the cytoskeleton was experimentally disrupted have shown conclusively that integrity of the cytoskeleton is essential for cranial neural tube closure (Matsuda and Keino, 1994;Smedley and Stanisstreet, 1986;Ybot-Gonzalez and Copp, 1999). Therefore, it may be possible that altered function of cytoskeletal proteins through lack of methylation could detrimentally influence closure. In this study, the method described in chapter 3 has been utilised to quantify the abundance of SAM and SAH in embryos cultured in the presence of methionine and methylation cycle inhibitors as previously described (Dunlevy et al., 2006a;Dunlevy et al., 2006b) to provide a greater understanding of how these inhibitors affect the flux through the methylation cycle.

It has been previously reported that *Mthfr*-deficient mice have a disrupted balance between SAM and SAH due to either a decrease in SAM or an increase in SAH levels, or both, with the effect being dependent on the number of disrupted *Mthfr* alleles (Chen et al., 2001b). The authors went on to demonstrate, using the cytosine-extension assay, that the effect on SAM and SAH levels resulted in a detectable decrease in DNA methylation in the brain and ovaries from both heterozygous and homozygous *Mthfr*-deficient adult mice (Chen et al., 2001b). A second study similarly demonstrated that elevations in plasma homocysteine and SAH levels are associated with a parallel increase in lymphocyte DNA hypomethylation (Yi et al., 2000) To attempt to detect aberrant changes in DNA methylation following exposure to methionine and methylation inhibitors, a method using LC-MS/MS to assess global DNA methylation (Friso et al., 2002) has been adapted for this study at a minimal cost.

4.1.2 DNA Methylation and NTDs

In the mouse, inhibition of DNA methylation following genetic deletion of the DNA methyltransferase Dnmt3b causes exencephaly (Okano et al., 1999). In zebrafish, inhibition of DNA methylation using the inhibitors 5-azacytidine and 5-aza-2-deoxycytidine causes defects in the notochord, somite and muscle development suggesting a requirement for DNA methylation in axial development (Martin et al., 1999). An extensive search of past literature, also reveals that 5-azacytidine, used previously in mouse studies, has been shown to cause exencephaly in mouse embryos

following administration *in utero* (Matsuda, 1990;Takeuchi and Takeuchi, 1985). Similarly, in this study I demonstrate that exposure of CD1 mouse embryos to 5-azacytidine in culture specifically causes a high incidence of exencephaly.

Suppression of DNA methylation could lead to abnormal expression of genes critical for successful closure of the neural tube. An alternative explanation is that inhibition of DNA methylation may cause a build up of SAM due to a lack of substrates for the methyl-group. This could affect the regulation of the methylation cycle, causing a subsequent build up of methionine and homocysteine, which in turn may affect the inter-linked folate cycle. To determine if inhibition of DNA methylation suppresses the methylation cycle, the abundance of SAM and SAH has been quantified in the embryos cultured in the presence of 5-azacytidine. If 5-azacytidine treatment is found to cause exencephaly without disturbing the methylation cycle this would provide substantial evidence for the proposed methylation hypothesis, which suggests that folic acid prevents NTDs by stimulating cellular methylation reactions (Blom et al., 2006).

4.1.3 Biomarkers of Human NTDs

There is now a plethora of evidence implicating the methylation cycle in the susceptibility to NTDs, however this association remains to be definitively elucidated. Two main possibilities exist to explain the elevated homocysteine found in NTD patients and their mothers (Kirke et al., 1993); (i) an altered diet (for example low folate) or, (ii) a genetic defect which affects one-carbon metabolism. In order to assess whether genetically-determined abnormalities in the methylation cycle are associated with increased risk of NTDs in humans, a collection of human cell lines grown under identical conditions have been analysed for the abundance of SAM and SAH.

Firstly, to investigate potential abnormalities in the methylation cycle in the embryo itself, SAM and SAH levels have been quantified in cell pellets of primary fibroblastic cell lines derived from fetuses affected by NTD (Dunlevy et al., 2007). The integrity of the folate cycle in these cell lines has been previously examined using the deoxyuridine (dU) suppression test which measures the ability of deoxyuridine monophosphate (dUMP) to suppress thymidine incorporation into DNA. Briefly, deoxythymidine monophosphate, the precursor of pyrimidines, can be generated from either dUMP (*de novo* pathway catalysed by thymidylate synthase) or by phosphorylation of thymidine (the salvage pathway catalysed by thymidylate kinase). Exogenous dUMP stimulates the *de novo* pathway and thereby suppresses incorporation of thymidine into genomic DNA, provided that the key intermediate 5,10-methylene tetrahydrofolate is available

as part of normal folate metabolism. Cell lines are scored depending on their ability to stimulate the *de novo* pathway and suppress thymidine incorporation.

The deoxyuridine (dU) suppression test demonstrated that a subset of these fetal cell lines from NTD cases exhibited abnormalities in folate-cycling believed to result from as yet unrecognised genetic variants (Dunlevy et al., unpublished). Analysis of SAM and SAH would determine whether the abnormal dU suppression result for NTD cell lines is due to a defect in the methylation cycle. The dU suppression test was unable to detect inhibition of the methylation cycle by cycloleucine treatment, yet quantitative analysis of SAM and SAH using LC-MS/MS (Burren et al., 2006) may be more informative. Alternatively, if the dU suppression test result was normal, a change in the abundance of SAM or SAH would indicate a methylation defect which did not affect the folate cycle, yet could potentially be a contributor to NTD development and/or be rescued by supplemental folate.

Secondly, SAM and SAH have been quantified in a group of immortalised B lymphocyte cell lines collected from Swedish children with open spina bifida. The analysis of a second group of cell lines enables comparison to be made between cell types and, between fetal and adult cells. Changes in the abundance of SAM and SAH in these cell lines would indicate underlying genetic defects which affect the flux through the methylation cycle.

4.2. Materials and Methods

4.2.1. Mouse embryo culture

Embryos were cultured for 18 and 28 hours as described in Chapter 2. At the end of the culture period the embryos were analysed for neural tube defects (described in section 2.8) and other gross morphological defects. The viability (yolk sac circulation and heart beat), growth (crown-rump length) and developmental progression (somite number) of each embryo was recorded (described in section 2.8). Embryos were then rinsed in PBS and stored at -80 °C, prior to analysis of SAM and SAH, or global DNA methylation.

4.2.2 S-Adenosylmethionine and S-Adenosylhomocysteine Assay

Samples consisting of a pool of 2-4 embryos from a specific treatment group were sonicated in 120 µl of aqueous mobile phase (4 mM ammonium acetate, 0.1 % formic acid, 0.1 % heptafluorobutyric acid, pH 2.5) containing 1 µM SAM-D_3 and heat-treated to precipitate proteins. Each sample was then analysed in duplicate by liquid chromatography tandem mass spectrometry, as described previously (Burren et al., 2006). Prior to heat treatment, a 10 µl aliquot was removed to determine protein concentration using the protein assay described in section 2.11.

4.2.3 Method to assess global DNA Methylation

DNA from whole embryos was prepared (see 4.2.3.3) and analysed using an adapted version of the liquid chromatography tandem mass spectrometry method described by Friso et al. (Friso et al., 2002).

4.2.3.1 Apparatus

All analyses were performed on a triple quadrupole tandem mass spectrometer coupled to a HPLC (described in section 2.12.1). A C18 guard cartridge (4mm x 3mm, 5 µm) fitted to a Security Guard holder (Phenomenex, UK) was used and the instrument was operating in positive ion mode.

4.2.3.2 Reagents

2'-deoxycytidine and 5-methyl-2'-deoxycytidine were purchased, along with all other reagents unless stated, from Sigma-Aldrich (Dorset, UK). All solvents and water used were of HPLC grade (Fisher Scientific UK Ltd., Loughborough, UK). The mobile phase consisted of 7 mM ammonium acetate (pH 6.7) with 5% methanol.

4.2.3.3 DNA Extraction and Hydrolysis

To extract the DNA, whole embryos were suspended in 180 µl of PBS and immediately sonicated on ice at 12 µm amplitude for 10 s. Homogenised samples were then incubated overnight at 56 °C with 20 µl of 10 mg/ml proteinase K. Thereafter, 1 µl of 10 mg/ml RNase A was added and incubated for 15 min at 37 °C. The sample mixture was then heated to 100 °C for 5 min and subsequently cooled to room temperature. A 200 µl volume of phenol:chloroform (v/v 50:50) was added to the solution, mixed thoroughly and centrifuged at 12,000 g for 5 min. The aqueous layer was decanted into a clean eppendorf tube, mixed with 200 µl of chloroform and centrifuged again. The aqueous layer was then added to an eppendorf containing 600 µl of 1.3 % potassium acetate dissolved in 95 % ethanol. The mixture was left to incubate at -20 °C for 2 hr or overnight, subsequently centrifuged at 12,000g for 10 min at 4 °C and the resulting supernatant was poured off. The DNA pellet was washed with 70 % ethanol and resuspended in 20 µl of dH_2O. The optical density at 260 nm was measured (UV Mini 1240 Spectrophotometer, Shimadzu) using quartz cuvettes to determine the concentration of DNA.

To hydrolyse the DNA into single bases, 1 µg of DNA was denatured by heating at 100 °C for 3 min and subsequently chilled in ice slush. One-tenth volume of 0.1 M ammonium acetate (pH 5.3) and 2 units of nuclease P1 (Roche Molecular Biochemicals, Manneheim, Germany) were added. The mixture was then incubated at 45 °C for 2 h. To the solution was subsequently added 1/10 volume of 1 M ammonium bicarbonate and 0.002 units of venom phosphodiesterase I. The incubation was continued for an additional 2 h at 37 °C. Thereafter, the mixture was incubated for 1 h at 37 °C with 0.5 units alkaline phosphatase. Hydrolysed samples were stored at -20 °C overnight prior to analysis by LC-MS/MS.

4.2.3.4 LC-MS/MS Procedure

A 20 µl portion of the hydrolysed DNA solution was injected onto the analytical column thermostated at 21 °C. The separation of 2'-deoxycytidine and 5-methyl-2'-deoxycytidine was obtained by isocratic elution. The mobile phase flow rate was 0.3 ml/min and the run time was 2 min. The following settings were used: capillary 3.86 kV, cone voltage 20 V and collision energy 26 V.

4.2.4 Cell Culture

For details of the methods used to culture the cell lines see Chapter 2 (section 2.13) and for the analysis of SAM and SAH in cell pellets refer to Chapter 3 (section 3.3.6).

4.2.5 Statistical Analysis

Statistical analyses were performed using SigmaPlot Version 7, SigmaStat Version 3.5 and SPSS Version 13. To determine the effect of the culture treatments on embryonic growth and development, mean yolk sac circulation, number of somites and crown-rump length were compared to the PBS-treated controls either by group-wise comparisons (methionine, ethionine and cycloleucine) using One-Way ANOVA or by pair-wise comparisons (Azacytidine) using the un-paired student t-test. Incidence of cranial NTDs following exposure to culture treatments was compared to the PBS-treated control either by group-wise comparison using the Chi-square test or by pair-wise comparison using the Fishers Exact test. The effect of culture treatments on the abundance of SAM and SAH, the ratio of SAM/SAH and the peak area ratio of methyl-cytosine/cytosine was compared to PBS-treated controls by pair-wise comparison using the un-paired student t-test. All p-values less than 0.05 were considered significant.

4.3 Results

4.3.1 The effect of methylation cycle perturbation on the incidence of cranial NTDs and the abundance of SAM and SAH in non-mutant, CD1 embryos.

The effect of methionine, ethionine and cycloleucine on the development of neurulation-stage embryos was previously investigated in non-mutant CD1 embryos cultured for 24 hours from E8.5 (4-6 somites) to E9.5 (Dunlevy et al., 2006a;Dunlevy et al., 2006b). Embryo culture experiments were repeated using the same method and the new data are presented herein.

Exposure to 5 mM methionine, 5 mM ethionine or 15 mM cycloleucine for 28 hours did not adversely affect embryo survival, developmental progression (number of somites), growth (crown to rump length) or viability (yolk sac circulation) of the embryos (Table 4.1). Nevertheless, at these concentrations a significant number of embryos exhibited open cranial neural tubes compared to PBS-treated control embryos (Table 4.2). These embryos were classed as exencephalic if they had reached the developmental stage (16 somites or more) when cranial neural tube closure is normally completed in CD1 embryos (Table 4.2 and Figure 4.2).

Culture Treatment	Time in culture (hrs)	No. live embryos (% of total cultured)	Yolk sac circulation	Number of somites	Crown-rump length (mm)
PBS	28	33 (67)	2.94 ± 0.04	19.7 ± 0.49	2.62 ± 0.08
Methionine	28	21 (66)	2.95 ± 0.05	19.7 ± 0.64	2.58 ± 0.08
Ethionine	28	22 (55)	3.00 ± 0.00	20.6 ± 0.51	2.67 ± 0.06
Cycloleucine	28	31 (46)	3.00 ± 0.00	19.8 ± 0.51	2.50 ± 0.08

Table 4.1. Growth and development of mouse embryos following perturbation of the methylation cycle. Non-mutant CD1 embryos were cultured from E8.5 to E9.5 in the presence of PBS (control), 5 mM methionine, 5 mM ethionine or 15 mM cycloleucine for 28 hours. Values are given as mean ± standard error of the mean. Statistical analysis by ANOVA demonstrated no statistical differences ($p > 0.05$) in embryo survival, yolk sac circulation, number of somites or crown-rump length between culture treatments.

Culture Treatment	Time in culture (hrs)	No. live embryos	Open cranial neural tube	No. embryos ≥ 16 somites	Cranial NTDs
PBS	28	33	0 (0.0)	31	0 (0.0)
Methionine	28	21	11 (52.4)	17	7 (41.2)**
Ethionine	28	22	15 (68.2)	22	14 (63.6)**
Cycloleucine	28	31	26 (83.9)	30	25 (83.3)**

Table 4.2. Incidence of neural tube closure abnormalities in mouse embryos following perturbation of the methylation cycle. Non-mutant CD1 embryos were cultured from E8.5 to E9.5 in the presence of PBS (control), 5 mM methionine, 5 mM ethionine or 15mM cycloleucine. Cranial NTDs are defined as failure of cranial neural tube closure in embryos that have completed embryonic turning and have 16 or more somites. This is based on the observation that cranial neural tube closure, in vivo, is completed by the 16 somite stage in CD1 embryos in our laboratory. Data are presented as number of embryos with percentage in each treatment group in parentheses. ** $p < 0.001$ when compared to PBS treated control group (Fishers Exact).

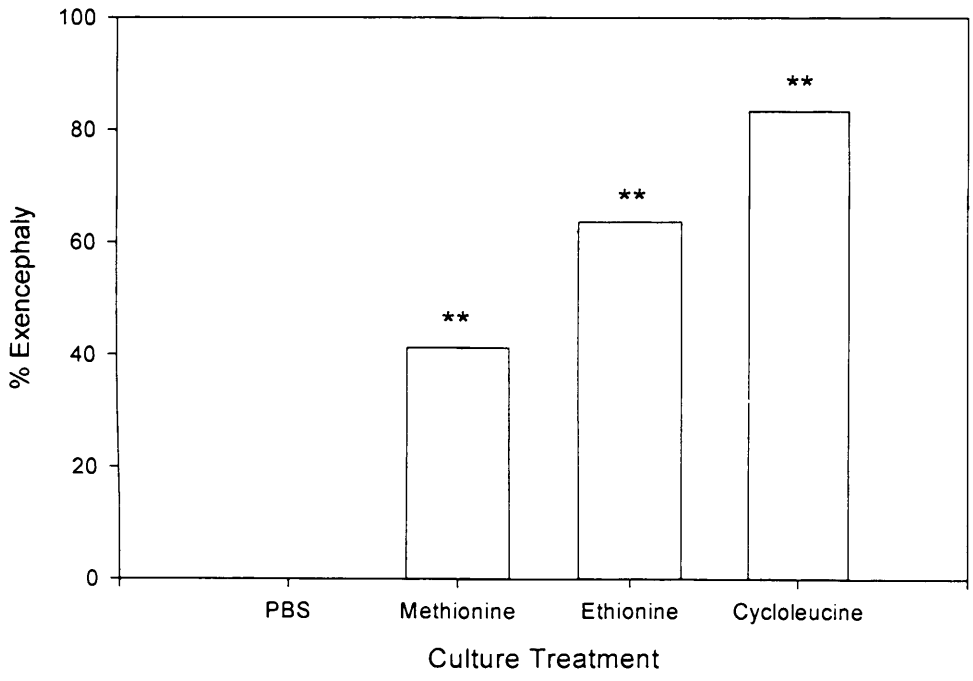

Figure 4.2. Incidence of cranial NTDs in mouse embryos following perturbation of the methylation cycle. Non-mutant CD1 embryos were cultured from E8.5 to E9.5 in the presence of PBS (control), 5 mM methionine, 5 mM ethionine or 15 mM cycloleucine for 28 hours and scored for the presence of exencephaly, defined as persistently open cranial neural folds in an embryo with 16 or more somites. ** $p > 0.001$ when compared to PBS-treated control group (Fishers Exact).

To determine if male and female embryos are equally susceptible to exencephaly induced by methionine, ethionine or cycloleucine, the gender of each embryo was determined through genotyping the SMC locus by PCR (section 2.9, (Agulnik et al., 1999)). Correlation of gender with phenotype revealed that in each treatment group it appears that the female embryos are more susceptible to cranial NTDs (Table 4.3). However, statistical analyses demonstrated that this trend does not reach significance except when treatment groups were pooled.

Culture Treatment	Total no. of male embryos	No. of male embryos with cranial NTDs	Total no. of female embryos	No. of female embryos with cranial NTDs
PBS	22	0 (0)	9	0 (0)
Methionine	16	5 (31)	6	3 (50)
Ethionine	17	11 (65)	11	9 (82)
Cycloleucine	11	8 (73)	20	17 (85)
Total	**66**	**24 (36)**	**46**	**29 (63) ****

Table 4.3. The effect of gender on the incidence of cranial NTDs following perturbation of the methylation cycle. Non-mutant CD1 embryos were cultured from E8.5 to E9.5 in the presence of PBS (control), 5 mM methionine, 5 mM ethionine or 15mM cycloleucine for 28 hours. Data are presented as number of embryos with percentage in each treatment group in parentheses. ** $p < 0.02$ when pair-wise comparisons were made between genders for each culture treatment (Chi-square).

The effect of methionine, ethionine, and cycloleucine on the abundance of SAM and SAH in neurulation-stage embryos was measured using the method described in chapter 3 (Burren et al., 2006). Although the LC-MS/MS method was shown to be suitable for E9.5 CD1 embryos that developed *in vivo*, somite-matched CD1 embryos that have been cultured *in vitro* tended to be smaller such that the abundance of SAH in a single embryo was reduced. Therefore, pools of 2-4 embryos were analysed to ensure that the level of SAH was above the limit of detection (LOD = 2.5 nmol/L). Initially, embryos were cultured as described for 28 hr from E8.5 to E9.5 and analysed for the abundance of SAM and SAH (Table 4.4). Statistical analysis revealed that the changes in metabolite concentrations following exposure to methionine, ethionine or cycloleucine were insignificant, compared to the PBS-treated control embryos.

Culture treatment	No. samples	SAM (nmol/mg protein)	SAH (nmol/mg protein)	Ratio SAM/SAH
PBS	6	2.99 ± 0.61	0.022 ± 0.005	144 ± 1.0
Methionine	7	2.57± 0.47	0.019 ± 0.003	133 ± 0.5
Ethionine	4	1.57 ± 0.25	0.015 ± 0.005	117 ± 1.7
Cycloleucine	5	2.67 ± 0.62	0.024 ± 0.006	119 ± 1.1

Table 4.4. The abundance of SAM and SAH following methylation cycle perturbation: 28 hour culture period. Concentrations of SAM and SAH were determined by LC-MS/MS in mouse embryo samples (pools of 2-4 embryos) following culture from E8.5 to E9.5 for 28 hours in the presence of PBS, 5 mM Methionine, 5 mM Ethionine or 15 mM Cycloleucine. Values are given as mean ± standard error of the mean. $p > 0.05$ compared to PBS control treated embryos (un-paired student t-test).

This finding might suggest that the inhibitors do not affect the abundance of SAM and SAH. Alternatively, the agents may have had an immediate effect but, owing to the long duration of the culture period, the metabolic effect may have worn off, for example over time the embryo may have metabolised and broken down the inhibitors preventing further metabolic effects and the abundance of SAM and SAH may have returned to normal baseline levels. The temperature of the embryo culture chamber could also potentially promote degradation of the exogenous molecules. Thus, in order to detect any earlier effects of methylation cycle perturbation on the abundance of SAM and SAH, non-mutant CD1 embryos were cultured for a shorter period (from late E8.5 to early E9.5) for approximately 18 hours. Cultures were started later (immediately prior to, or during cranial neural tube closure) to measure the metabolic effect at the time of neurulation (Figure 4.3).

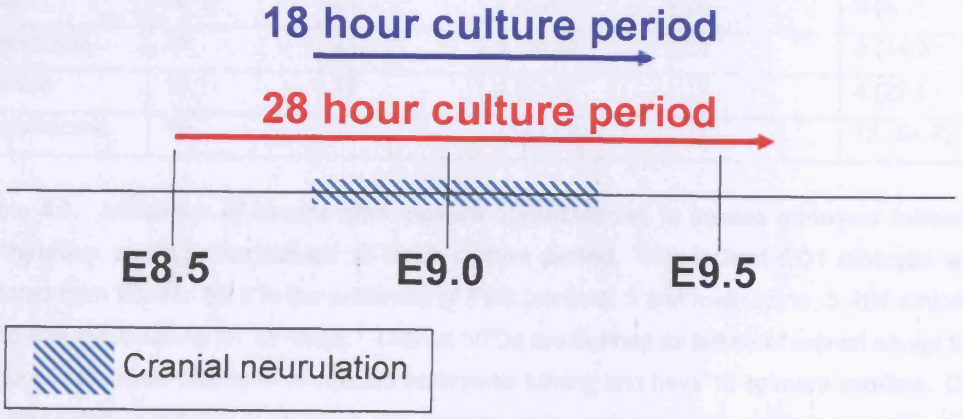

Figure 4.3. Time line depicting the two culture periods used to study perturbation of the methylation cycle.

Consistent with the 28 hr cultures, shorter cultures for 18 hr did not adversely affect the development, growth or viability of the cultured embryos (Table 4.5). However it was expected that since neural tube closure may have already begun at the start of the culture period the incidence rates of exencephaly may differ when compared to 28 hr cultures. In fact, the incidence of neural tube defects was reduced in the methionine, ethionine or cycloleucine treated embryos in 18 hour compared to 28 hour cultures (Table 4.6). These data suggest that older E8.5 embryos are less susceptible to NTDs following exposure to methionine, ethionine and cycloleucine and therefore, exposure at an earlier stage could have targeted a more sensitive period in neurulation.

Culture Treatment	Time in culture (hrs)	No. live embryos (% of total cultured)	Yolk sac circulation	Number of somites	Crown-rump length (mm)
PBS	18	21 (87.5)	2.80 ± 0.11	21.8 ± 0.42	2.61 ± 0.08
Methionine	18	19 (90.1)	2.94 ± 0.05	21.7 ± 0.35	2.74 ± 0.05
Ethione	18	15 (88.2)	2.71 ± 0.19	19.5 ± 1.42	2.36 ± 0.17
Cycloleucine	18	20 (95.2)	2.64 ± 0.18	25.1 ± 1.69	2.09 ± 0.14

Table 4.5. Growth and development of mouse embryos following methylation cycle perturbation: 18 hour culture period. Non-mutant CD1 embryos were cultured from E8.5 to E9.5 in the presence of PBS (control), 5 mM methionine, 5 mM ethionine or 15 mM cycloleucine for 18 hours. Values given as mean ± standard error of the mean. Statistical analysis by ANOVA demonstrated no statistical differences ($p > 0.05$) in yolk sac circulation, number of somites or crown-rump length between culture treatments.

Culture Treatment	Time in culture (hrs)	No. live embryos	Open cranial neural tube	No. embryos ≥ 16 somites	Cranial NTDs
PBS	18	24	2 (8.3)	24	2 (8.3)
Methionine	18	21	3 (14.3)	21	3 (14.3)
Ethione	18	17	4 (23.5)	17	4 (23.5)
Cycloleucine	18	21	15 (71.4)	17	11 (64.7)

Table 4.6. Incidence of neural tube closure abnormalities in mouse embryos following methylation cycle perturbation: 18 hour culture period. Non-mutant CD1 embryos were cultured from E8.5 to E9.5 in the presence of PBS (control), 5 mM methionine, 5 mM ethionine or 15 mM cycloleucine for 18 hours. Cranial NTDs are defined as failure of cranial neural tube closure in embryos that have completed embryonic turning and have 16 or more somites. Data are presented as number of embryos with percentage in each treatment group in parentheses.

Metabolite analysis showed that, in embryos exposed to methionine or cycloleucine for 18 hours, there was a significant decrease in the ratio of SAM/SAH. This difference was mainly due to a significant increase in the abundance of SAH when compared to PBS control treated embryos (Table 4.7 and Figure 4.4). In ethionine-treated embryos, a significant decrease in SAM also contributed to the significant decrease in the ratio of SAM/SAH (Table 4.7 and Figure 4.4).

Culture treatment	No. samples	SAM (nmol/mg protein)	SAH (nmol/mg protein)	Ratio SAM/SAH
PBS	8	3.91 ± 0.38	0.023 ± 0.003	178 ± 11.8
Methionine	5	4.40 ± 0.46	0.043 ± 0.006**	104 ± 4.7**
Ethionine	5	2.67 ± 0.55*	0.034 ± 0.009*	79 ± 3.2**
Cycloleucine	6	4.16 ± 0.73	0.032 ± 0.003*	130 ± 12.1**

Table 4.7. The abundance of SAM and SAH following methylation cycle perturbation: 18 hour culture period. Concentrations of SAM and SAH were determined by LC-MS/MS in mouse embryo samples (pools of 2-4 embryos) following culture from E8.5 to E9.5 for 18 hours in the presence of PBS, 5 mM Methionine, 5 mM Ethionine or 15 mM Cycloleucine. Values are given as mean ± standard error of the mean. * $p < 0.05$, ** $p < 0.01$ when compared to PBS-treated control embryos (un-paired student t-test).

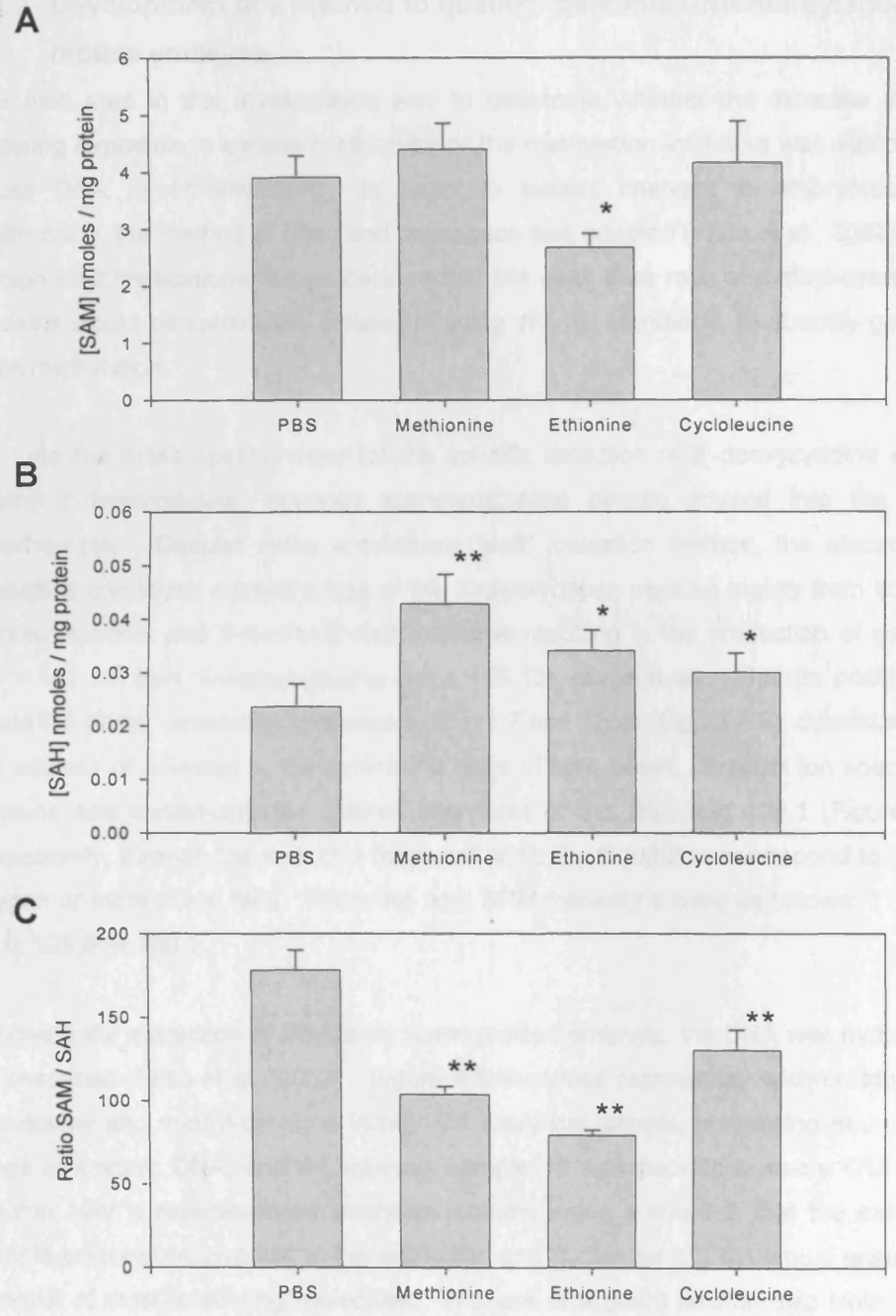

Figure 4.4. Embryonic concentrations of SAM (A), SAH (B) and ratio SAM/SAH (C) following perturbation of the methylation cycle: 18 hour culture period. Concentrations of SAM and SAH were determined by LC-MS/MS in mouse embryo samples (pools of 2-4 embryos) following culture from E8.5 to E9.5 for 18 hours in the presence of PBS, 5 mM Methionine, 5 mM Ethionine or 15 mM Cycloleucine. Values are given as mean ± standard error of the mean. * $p < 0.05$, ** $p < 0.01$ when compared to PBS-treated control embryos (un-paired student t-test).

4.3.2 Development of a method to quantify genomic DNA methylation in mouse embryos

The next step in this investigation was to determine whether the increase in SAH following exposure to excess methionine or the methylation inhibitors was sufficient to cause DNA hypomethylation. In order to assess changes in embryonic DNA methylation, the method of Friso and colleagues was adapted (Friso et al., 2002). Due to high cost implications, it was decided that the peak area ratio of methyl-cytosine to cytosine would be calculated, instead of using internal standards, to quantify genomic DNA methylation.

To tune the mass spectrometer for the specific detection of 2'-deoxycytidine and 5-methyl-2'-deoxycytidine, aqueous standards were directly infused into the mass spectrometer. Despite using a relatively "soft" ionisation method, the electrospray ionisation conditions caused a loss of the 2'-deoxyribose pentose moiety from both the 2'-deoxycytidine and 5-methyl-2'-deoxycytidine resulting in the production of cytosine (wt = 111.10) and 5-methylcytosine (wt = 125.13), respectively. Thus in positive ion mode the $[M+H]^+$ precursor ions were m/z 111.7 and 125.8 (Figure 4.5), consistent with the addition of a proton to the pyrimidine rings of both bases. Product ion spectra for cytosine and methyl-cytosine yielded fragments of m/z 95.0 and 109.1 (Figure 4.5), respectively, through the loss of a fragment of 16 Da thought to correspond to loss of oxygen or more likely, NH_2. Thus, the final SRM transitions were as follows: 111.7 → 95.0; 125.8 → 109.1.

Following the extraction of DNA from homogenised embryos, the DNA was hydrolysed as described (Friso et al., 2002). Figure 4.6 illustrates representative chromatograms of cytosine and methyl-cytosine in both an analytical sample, comprising neurulation-stage embryonic DNA, and an aqueous sample. It was decided to use a C18 guard column over a reverse-phase analytical column since it was felt that the extensive sample preparation involved in the extraction and hydrolysis of DNA would ensure the removal of most interfering molecules. The use of a guard column also limits outlay costs and considerably shortens run times.

A.

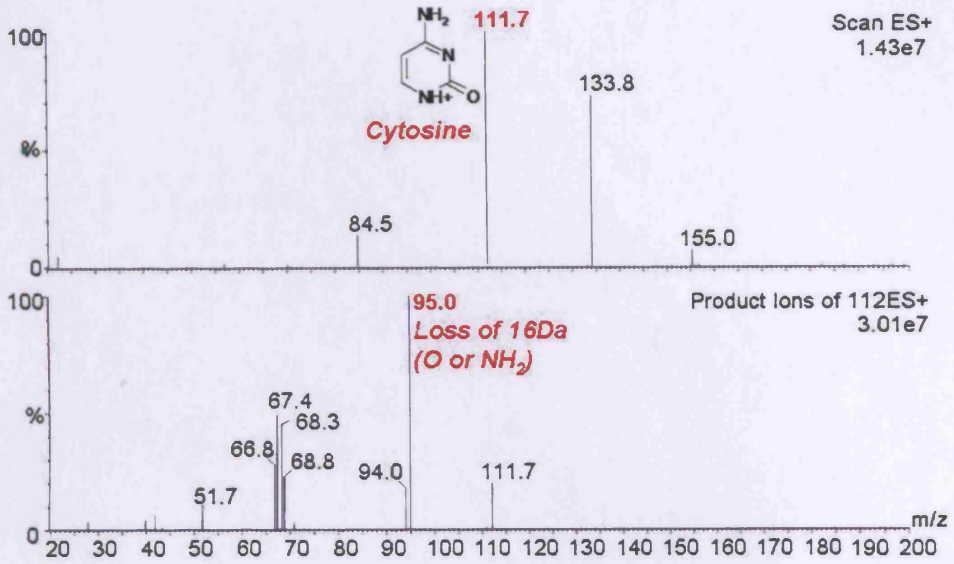

B.

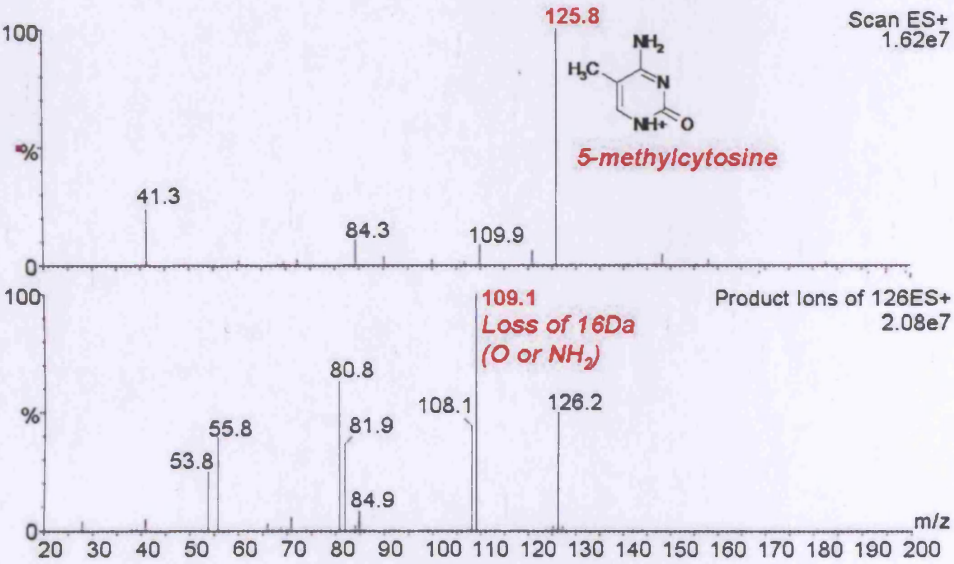

Figure 4.5. Product ion spectra of protonated molecules used for quantification. Precursor ions were at m/z 111.7 for cytosine (A) and 125.8 for 5-methyl cytosine (B). In each case the MS/MS conditions were optimised to favour the transition to the major product ion at m/z 95.0 and 109.1, respectively, due to a loss of 16 Da.

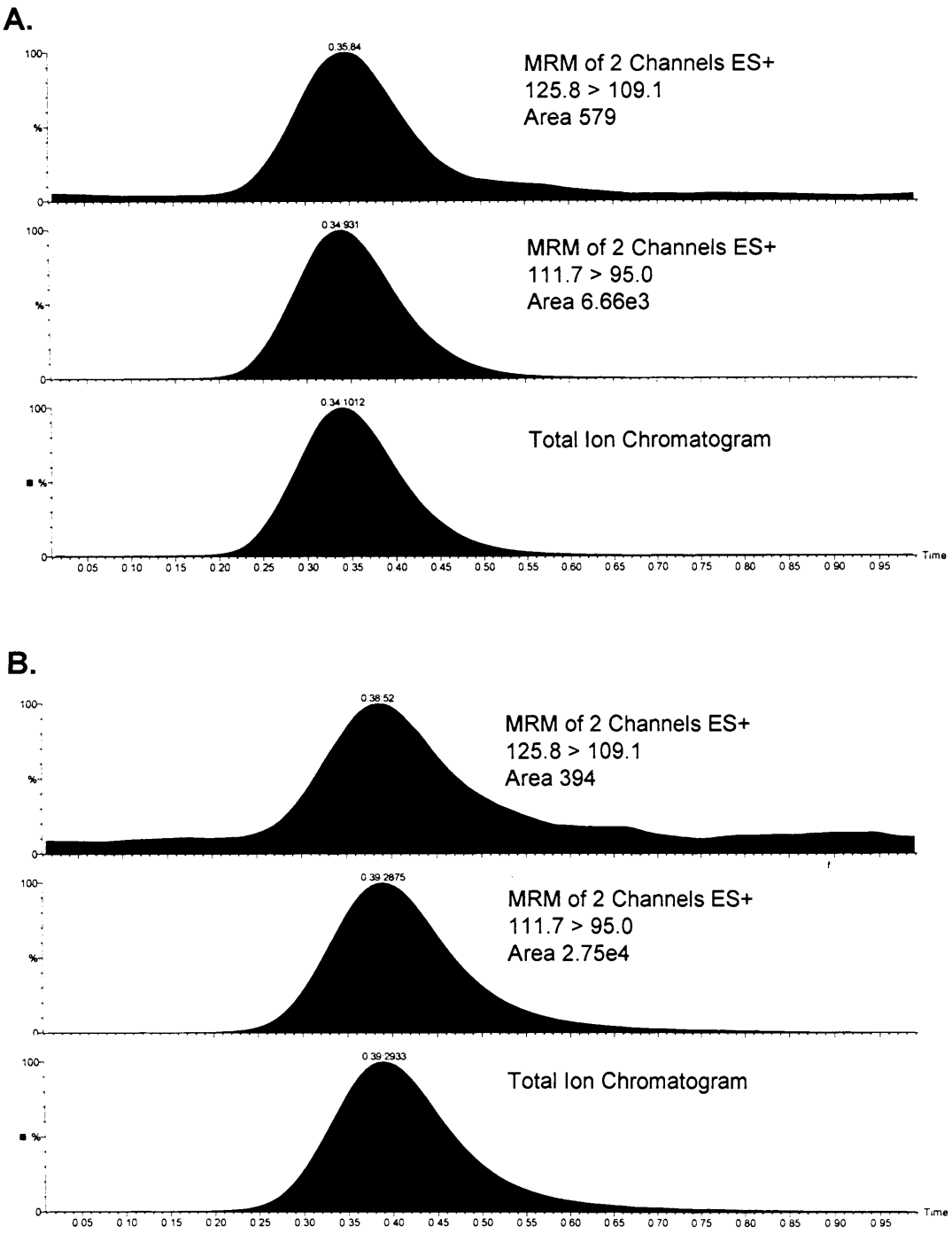

Figure 4.6. LC-MS/MS chromatograms obtained in SRM mode. Representative chromatograms are shown for (A) endogenous 2'-cytosine and 5-methyl-2'-cytosine in hydrolysed neurulation-stage mouse DNA and (B) an aqueous standard containing 0.01 μM 5-methyl-2'-cytosine and 1 μM 2'-cytosine. The ratio of methyl-cytosine / cytosine is (A) 0.09 and (B) 0.01.

Analysis of E9.5 CD1 embryos was undertaken to determine reference intervals of methyl-cytosine and cytosine during neurulation. In all cases, extraction of DNA from a single whole embryo yielded more than the required 1 µg of DNA. Hydrolysis of 1 µg of DNA produced detectable peaks corresponding to methyl-cytosine and cytosine with signal-to-noise ratios in excess of 10:1 (Figure 4.6). Overall, the ratio of methyl-cytosine / cytosine was found to be between 0.06 and 0.10 in all E9.5 embryos analysed.

Once the method had been established, CD1 embryos cultured in the presence of methionine or the methylation cycle inhibitors were analysed to determine the ratio of methyl-cytosine to cytosine (Table 4.8). Statistical analysis revealed that neither methionine, ethionine nor cycloleucine treatment significantly affected the ratio of methyl-cytosine to cytosine compared to PBS control treated embryos (ANOVA; $p = 0.842$). A higher concentration of methionine was also tested but was found to have no further effect. Thus, the results seemed to suggest that perturbation of the methylation cycle, resulting in a subsequent increase in SAH, does not cause a detectable change in DNA methylation.

Culture treatment (conc.)	No. samples	Peak area ratio 5-methyl-2'-cytosine / 2'-cytosine
PBS	10	0.0832 ± 0.0099
Methionine (5 mM)	8	0.0859 ± 0.0084
Methionine (10 mM)	3	0.0937 ± 0.0084
Ethionine	6	0.0736 ± 0.0087
Cycloleucine	4	0.0792 ± 0.0158

Table 4.8. The peak area ratio of methyl-cytosine/cytosine in hydrolysed DNA extracted from whole E9.5 CD1 embryos cultured in the presence of methionine, ethionine or cycloleucine. Values given as mean ± standard error of the mean.

Mthfr-deficient mice represent an ideal positive control to determine whether the LC-MS/MS assay used in this study was sensitive and precise enough to detect changes in DNA methylation relating to methylation cycle perturbation (Chen et al., 2001a). In brain tissue from *Mthfr*-deficient mice, the DNA is hypomethylated due to a decrease the SAM/SAH ratio, resulting from an increase in SAH caused by the genetic disturbance in the folate cycle (Chen et al., 2001a). Thus, DNA was extracted from the brains of heterozygous and homozygous *Mthfr*-deficient mice (donated by Dr. Rima

Rozen) and subjected to hydrolysis and analysis using the described LC-MS/MS method.

The ratio of methyl-cytosine/cytosine in adult mouse brain tissue was found to be similar to values found in neurulation-stage mouse embryos (Table 4.9). As expected, DNA extracted from brain tissue of heterozygous and homozygous *Mthfr*-deficient mice was found to be hypomethylated compared to wild-type mice, as shown by the reduced ratio of 5-methyl-2'-cytosine to 2'-cytosine. However statistical analysis by the student t-test reveals that this decrease is only statistically significant for the heterozygotes ($p = 0.040$), presumably due to the larger standard error of the overall mean for homozygotes and the low sample number.

***Mthfr* genotype**	**No. samples**	**Ratio 5-methyl-2'-cytosine / 2'-cytosine**		
		Sample 1	**Sample 2**	**Mean**
Wild-type	2	0.0965	0.0934	0.0950 ± 0.0022
Heterozygous	2	0.0679	0.0740	0.0710 ± 0.0044*
Homozygous	2	0.0615	0.0786	0.0700 ± 0.0120

Table 4.9. The peak area ratio of methyl-cytosine/cytosine in DNA extracted from brain tissue of *Mthfr*-deficient mice. Values given as mean ± standard error of the mean. * $p < 0.05$ compared to wild-type.

4.3.3 Investigating the effect of inhibition of DNA Methylation on the incidence of cranial NTD and the abundance of SAM and SAH, in non mutant CD1 embryos

A different experimental approach was subsequently undertaken to investigate whether abnormal DNA methylation could be involved in the pathogenesis of NTDs. The DNA methylation inhibitor, 5'-azacytidine, has previously been reported to induce exencephaly (Matsuda, 1990;Takeuchi and Takeuchi, 1985). 5'-Azacytidine is an analogue of cytidine which becomes incorporated into the DNA but cannot be methylated since the 5' carbon has been replaced with a nitrogen. This inhibitor has been well-documented to cause DNA hypomethylation in numerous other systems (Jones et al., 1983).

AZA conc. (mM)	Duration of culture (hrs)	n=	Yolk sac circulation	Number of somites	Crown-rump length (mm)
0.0	28	5	3.00 ± 0.0	20.2 ± 0.58	2.67 ± 0.09
0.8	28	2	3.00 ± 0.0	21.5 ± 0.50	2.83 ± 0.17
2.0	28	5	2.20 ± 0.4	19.0 ± 1.05	2.32 ± 0.08
0.0	18	5	2.80 ± 0.20	19.6 ± 0.98	2.20 ± 0.17
2.0	18	14	3.00 ± 0.00	19.7 ± 0.87	2.25 ± 0.08

Table 4.10. Growth and development of mouse embryos following exposure to an inhibitor of DNA methylation. Non-mutant CD1 embryos were cultured from E8.5 to E9.5 in the presence of PBS (control) or 5'-azacytidine (AZA) for 18 hours. Values are given as mean ± standard error of the mean. $p > 0.05$ compared to PBS control treated embryos (unpaired student t-test).

AZA conc. (mM)	Duration of culture (hrs)	No. live embryos	Cranial neural tube open	No. embryos ≥ 16 somites	Cranial NTDs
0.0	28	5	0 (0.0)	5	0 (0.0)
0.8	28	2	1 (50.0)	2	1 (50.0)
2.0	28	5	5 (100.0)	5	4 (80.0)*
0.0	18	5	0 (0.0)	5	0 (0.0)
2.0	18	14	8 (57.1)	14	8 (57.1)*

Table 4.11. Incidence of neural tube closure abnormalities in mouse embryos following exposure to an inhibitor of DNA methylation. Non mutant CD1 embryos were cultured from E8.5 to E9.5 in the prescence of PBS (control) or 5'-azacytidine (AZA). Cranial NTDs are defined as failure of cranial neural tube closure in embryos that have completed embryonic turning and have 16 or more somites. Data are presented as number of embryos with percentage in each treatment group in parentheses. * $p < 0.05$ when compared to PBS control treated embryos (Fisher Exact test).

A series of non mutant CD1 embryos were cultured for 28 hours in the presence of 5-azacytidine at the doses stated in previous studies (Matsuda and Yasutomi, 1992). Exposure to azacytidine concentrations of 0.8 mM and 2 mM did not result in embryotoxicity as shown by absence of an effect on yolk sac circulation scores (Table 4.10). Embryos showed normal developmental progression, as indicated by comparable somite numbers among azacytidine-treated embryos and embryos

cultured with PBS (Table 4.10). There were no differences in the mean crown-rump length between the treatment groups suggesting that azacytidine treatment does not cause growth retardation at these concentrations (Table 4.10). At the higher concentration (2 mM) a significant number of embryos exhibited open cranial neural tubes compared to PBS-treated control embryos (Table 4.11). These embryos were classed as exencephalic if they had reached the developmental stage (16 somites or more) when cranial neural tube closure is normally completed in CD1 embryos.

The effect of azacytidine exposure on the levels of SAM and SAH was measured using the method described in chapter 3 (Burren et al., 2006) in embryo samples (pools of 2-4 embryos) following short 18 hr cultures. Cultures were started immediately prior to, or during cranial neural tube closure to measure the metabolic effect at the time of neurulation (as in section 4.3.1). Consistent with the 28 hr cultures, shorter cultures for 18 hr did not adversely affect the development, growth or viability of the cultured embryos (Table 4.10). There was a 22.9% decrease in the incidence of NTDs in embryos treated for just 18 hours compared to 28 hours (Table 4.11). This suggests that older E8.5 embryos are less susceptible to NTD following azacytidine exposure, as in short cultures, embryos were not placed in culture until the 8-10 somite stage compared to 5-7 somite stage for 28 hour cultures.

In azacytidine-treated embryos there was no significant change in the abundance of SAM, SAH or the ratio of abundance of SAM to SAH, compared to PBS-treated control embryos (Table 4.12 and Figure 4.7). Failure to detect a change in SAM and SAH implies that 5'-azacytidine does not affect the methylation cycle and any effect on DNA methylation is downstream of the methylation cycle.

AZA conc. (µg/ml)	**No. samples**	**SAM (nmol/mg protein)**	**SAH (nmol/mg protein)**	**Ratio SAM/SAH**
0.0	7	5.40 ± 0.78	0.035 ± 0.005	155 ± 8.3
2.0	5	4.29 ± 0.74	0.026 ± 0.005	166 ± 8.5

Table 4.12. The abundance of SAM and SAH in mouse embryos following exposure to an inhibitor of DNA methylation. Concentrations of SAM and SAH were determined by LC-MS/MS in mouse embryos (pools of 2-4 embryos) following culture from E8.5 to E9.5 for 18 hours in the presence of PBS (control) or 2 mM Azacytidine (AZA). Values are given as mean ± standard error of the mean. No significant differences were detected (un-paired student t-test).

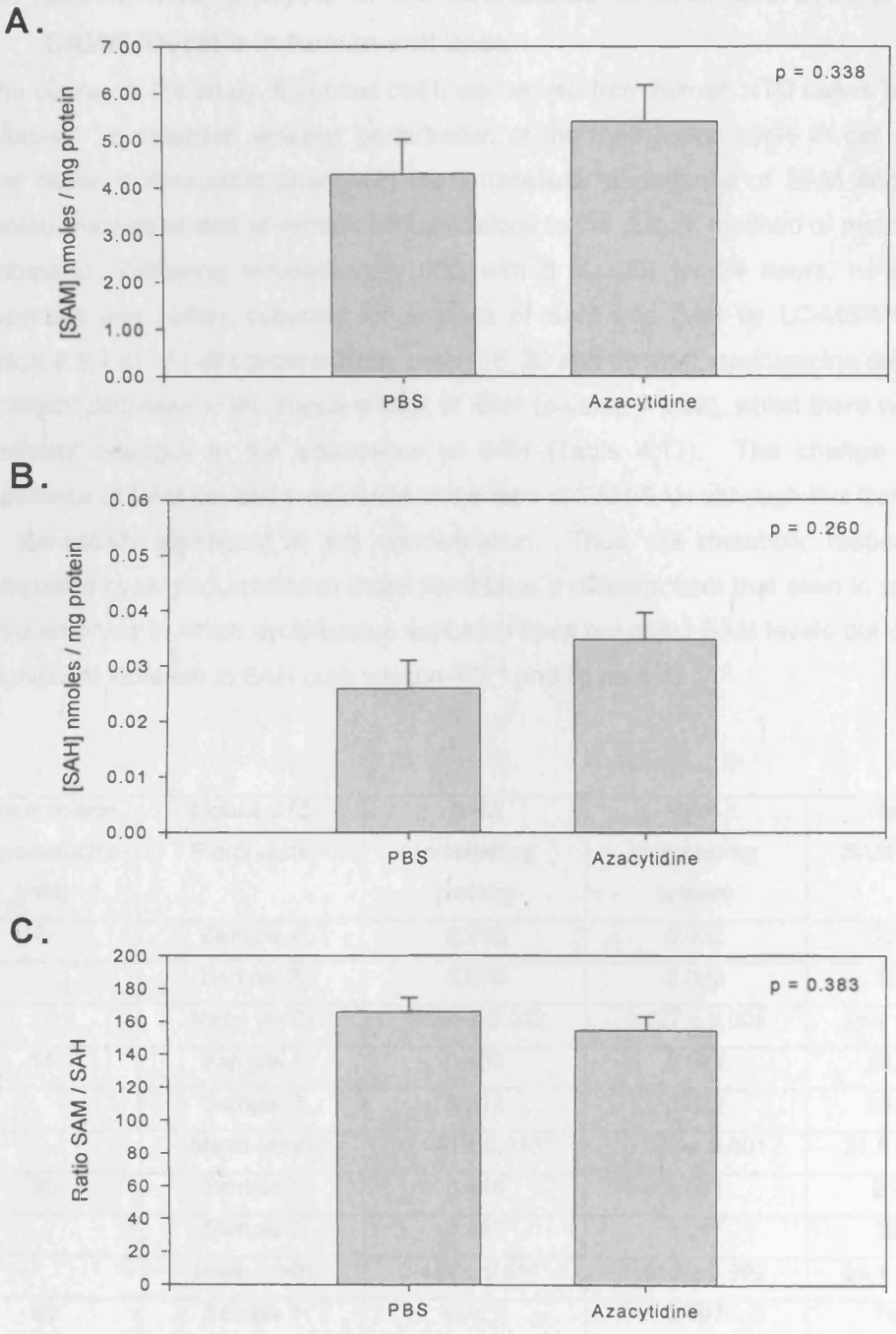

Figure 4.7. The abundance of SAM and SAH in mouse embryos following exposure to an inhibitor of DNA methylation. Concentrations of SAM and SAH were determined by LC-MS/MS in mouse embryos (pools of 2-4 embryos) following culture from E8.5 to E9.5 for 18 hours in the presence of PBS (control) or 2 mM Azacytidine (AZA). Values are given as mean ± standard error of the mean. The p-value (t-test) is displayed in the top RHS of each graph.

4.3.4 Biochemical analysis of the abundance of SAM and SAH and the SAM/SAH ratio in human cell lines.

In the course of the study, fibroblast cell lines derived from human NTD cases became available. To establish whether perturbation of the methylation cycle in cell culture could cause a detectable change in the intracellular abundance of SAM and SAH, cycloleucine was added at various concentrations to the culture medium of mouse 3T3 fibroblasts. Following incubation at 37°C with 5 % CO_2 for 24 hours, cells were trypsinised and pellets collected for analysis of SAM and SAH by LC-MS/MS (see section 4.2.4.4). At all concentrations used (15, 30 and 60 mM), cycloleucine caused a significant decrease in the concentration of SAM (p-value < 0.02), whilst there were no significant changes in the abundance of SAH (Table 4.13). The change in the abundance of SAM caused a decrease in the ratio of SAM/SAH although this trend was not statistically significant at any concentration. Thus, the metabolic response to methylation cycle perturbation in these fibroblasts is different from that seen in cultured whole embryos in which cycloleucine exposure does not affect SAM levels but causes a significant increase in SAH (see section 4.3.1 and figure 4.4).

Concentration of cycloleucine (mM)	Mouse 3T3 Fibroblasts	SAM (nmoles/mg protein)	SAH (nmoles/mg protein)	Ratio SAM/SAH
0	Sample 1	0.716	0.032	22.3
	Sample 2	0.672	0.022	30.6
	Mean (n=2)	0.694 ± 0.022	0.027 ± 0.005	26.4 ± 4.1
15	Sample 1	0.480	0.024	20.04
	Sample 2	0.512	0.022	23.05
	Mean (n=2)	0.496 ± 0.016*	0.023 ± 0.001	21.5 ± 1.5
30	Sample 1	0.446	0.021	21.6
	Sample 2	0.423	0.017	25.2
	Mean (n=2)	0.434 ± 0.017*	0.019 ± 0.002	23.4 ± 1.8
60	Sample 1	0.427	0.027	16.0
	Sample 2	0.401	0.030	13.6
	Mean (n=2)	0.414 ± 0.035*	0.028 ± 0.001	14.8 ± 1.2

Table 4.13. Concentration of SAM, SAH and the ratio of SAM/SAH in mouse 3T3 fibroblasts exposed to cycloleucine for 24hr at various concentrations. Mean values are given as mean ± standard error of the mean. * $p < 0.05$ when compared to untreated control, 0 mM (unpaired student t-test).

To investigate whether disturbances in the abundance of SAM or SAH are commonly seen in human NTDs, the concentrations of SAM and SAH were quantified in individual fetal cell lines from NTD cases and a subset of controls (Figure 4.8). As cell lines were cultured under identical conditions, it was reasoned that any abnormality in the ratio of methylation cycle intermediates would be due to a genetic variation. The integrity of the folate cycle in these cell lines had been previously examined by Dr. L. P. E. Dunlevy using the dU suppression test (Dunlevy et al., 2006c). Cell lines were scored depending on their ability to stimulate the *de novo* pathway and suppress ^{3}H-thymidine incorporation. A low score, representing a low ^{3}H-thymidine suppression value, was indicative of reduced efficacy of folate metabolism.

The mean dU suppression test score was significantly lower in NTD cases than control cell lines. When all cell lines were considered together the lowest quartile of scores all corresponded to NTD cell lines, whereas none of the control cell lines had a suppression score within this lowest quartile (Dunlevy et al., 2006c). When the NTD cell lines were ranked in order of dU suppression score, with the lowest corresponding to abnormal folate metabolism, there was no apparent correlation between the results of the dU suppression test and the abundance of SAM or SAH (Figure 4.8). In fact overall, there was very little variation in metabolite levels between cell lines with most values being less than one standard deviation from the mean. The only result that did highlight a potential disturbance in the methylation cycle was the NTD sample with the tenth lowest dU suppression score which had an unusually high SAM/SAH ratio due to both a high concentration of SAM and a low concentration of SAH. However, as the dU suppression score was in the 'normal' range shared by cases and controls it is unlikely that the altered SAM/SAH ratio affected performance of folate metabolism.

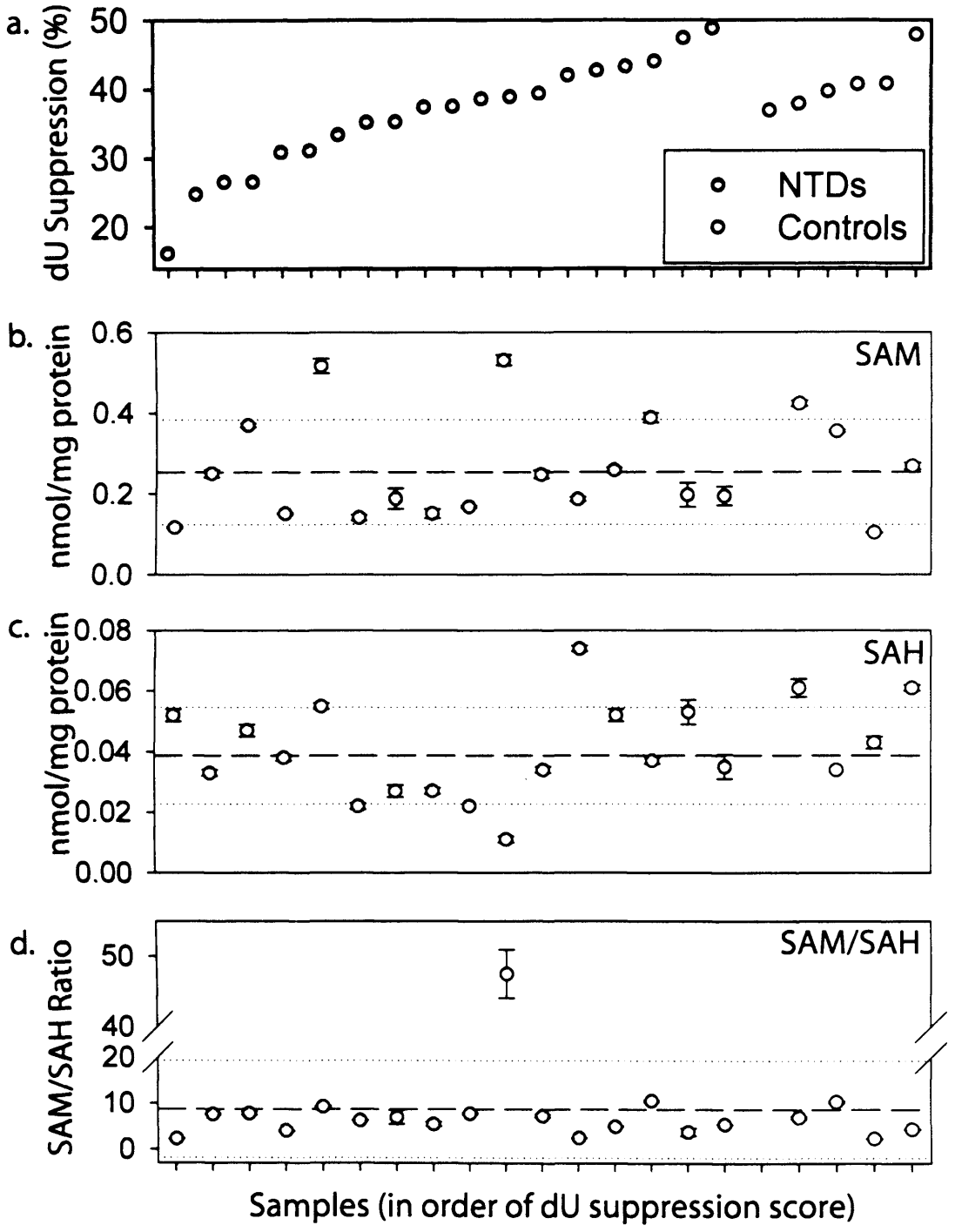

Figure 4.8. A comparison between dU suppression result and abundance of SAM and SAH in fibroblastic fetal cell lines. (a) dU suppression rank, (b) abundance of SAM, (c) abundance of SAH and (d) ratio of abundance of SAM/SAH. Samples were ranked in order of dU suppression score (dU suppression rank), with the 6 NTD samples with the lowest scores (*1-6*), exhibiting apparent abnormalities in folate metabolism. Figure taken from Dunlevy et al., 2006c (unpublished). Data presented in 4.15a provided by Louisa Dunlevy.

Comparing the mean concentration of SAM and SAH in fetal fibroblast cell lines (Table 4.14) reveals that the concentration of SAM (p-value = 0.645), SAH (p-value = 0.223) and the SAM/SAH ratio (p-value = 0.634) is not significantly different between NTD and control cell lines. Thus overall, it appears that fibroblasts taken from NTD affected fetuses do not have a reduced efficacy of the methylation cycle, compared to normal controls.

Patient Type	n=	SAM (nmoles/mg protein)	SAH (nmoles/mg protein)	Ratio SAM/SAH
NTD	16	0.254 ± 0.032	0.0387 ± 0 0040	8.7 ± 2.6
Control	4	0.288 ± 0.069	0.0497 ± 0.0067	6.1 ± 1.7

Table 4.14. A comparison of the mean concentration of SAM and SAH, and the mean SAM/SAH ratio between NTD and control sample cell pellets from fetal fibroblast cell lines. Values are given as the mean ± the standard error of the mean. * $p < 0.05$, ** $p < 0.02$ when compared to control samples (un-paired student t-test).

	Patient Type	NTD	Control
	n=	28	10
SAM (nmoles/mg protein)	Mean ± SEM	0.145 ± 0.009	0.148 ± 0.020
	Range	0.075 – 0.255	0.054 – 0.240
SAH (nmoles/mg protein)	Mean ± SEM	0.0121 ± 0.0010	0.0115 ± 0.0017
	Range	0.0051 – 0.0304	0.0055 – 0.0221
Ratio SAM/SAH	Mean ± SEM	13.0 ± 0.82	13.3 ± 1.24
	Range	5.8 – 20.9	7.8 – 17.6

Table 4.15. A comparison of the mean concentration of SAM and SAH, and the mean SAM/SAH ratio between NTD and control sample cell pellets from EBV transformed B lymphocyte cell lines collected from Swedish children. Values are given as the mean ± the standard error of the mean. $p > 0.05$ when compared to control samples (un-paired student t-test).

A second population of cell lines of a different cell type was then studied. In this case immortalised B-lymphocyte cell lines were analysed to provide reference levels of SAM and SAH in lymphocytes and potentially reveal differences between NTD affected and normal cell lines. These cell pellets were provided by Dr. P. Gustavvson and concentrations of SAM and SAH were quantified using the method described in chapter 3. A comparison of the mean concentration of SAM and SAH, and the mean SAM/SAH ratio from the NTD and control patient EBV transformed cell lines reveals no

statistically significant differences in metabolite concentrations between patient types (Table 4.15). Overall, this finding would suggest that collectively B lymphocytes from Swedish children with open spina bifida do not have a defect in the methylation cycle.

Concentrations of SAM, SAH and the SAM/SAH ratio in individual samples were analysed further to identify isolated cases with potential genetic disturbances in the methylation cycle (Figure 4.9). Three NTD samples (13, 24 and 27) and three control samples (2, 5 and 6) had SAM concentrations greater than one standard deviation from the mean, whilst five NTD samples (10, 11, 19, 20 and 21) and three control samples (3, 7 and 10) had SAM concentrations less than one standard deviation from the mean. Thus, it appears that the concentration of SAM is not atypical in NTD samples. Sample number 24 (highlighted in figure 4.9 by the vertical blue dotted line), an NTD cell line, had the highest concentration of SAM, yet the concentration of SAH was very close to the overall mean resulting in a high SAM/SAH ratio. This result is analogous to that seen in 3T3 mouse fibroblast cultures following exposure to the methylation cycle inhibitor, cycloleucine (Table 4.13).

Two NTD samples (13 and 27) and two control samples (6 and 9) had SAH concentrations greater than one standard deviation from the mean, whilst one NTD sample (11) and two control samples (3 and 10) had SAH concentrations less than one standard deviation from the mean (Figure 4.9). Thus, concentrations of SAH in NTD samples are not indifferent to SAH concentrations in control samples. Likewise, it appears that an increased abundance of SAH is not a common feature in these human NTD samples, as was seen in mouse embryos following perturbation of the methylation cycle (see section 4.3.1. and figure 4.4). Sample number 13 (highlighted in figure 4.9 by the vertical red dotted line) had the highest concentration of SAH although the ratio of SAM/SAH was not particularly low since the concentration of SAM was above the overall mean.

Two NTD samples (22 and 24), but no control samples, had a SAM/SAH ratio greater than one standard deviation from the mean, whilst seven NTD samples (1, 2, 13, 17, 19, 20 and 21) and two control samples (7 and 9) had a SAM/SAH ratio less than one standard deviation below the mean (Figure 4.9). Thus, a trend appears to be developing whereby the outlying SAM/SAH ratios are more likely to be attributable to NTD cases as opposed to control cases. Likewise, analysis of the range of SAM/SAH ratios for NTD and control samples demonstrates a greater range in NTD samples compared to control samples (Table 4.15).

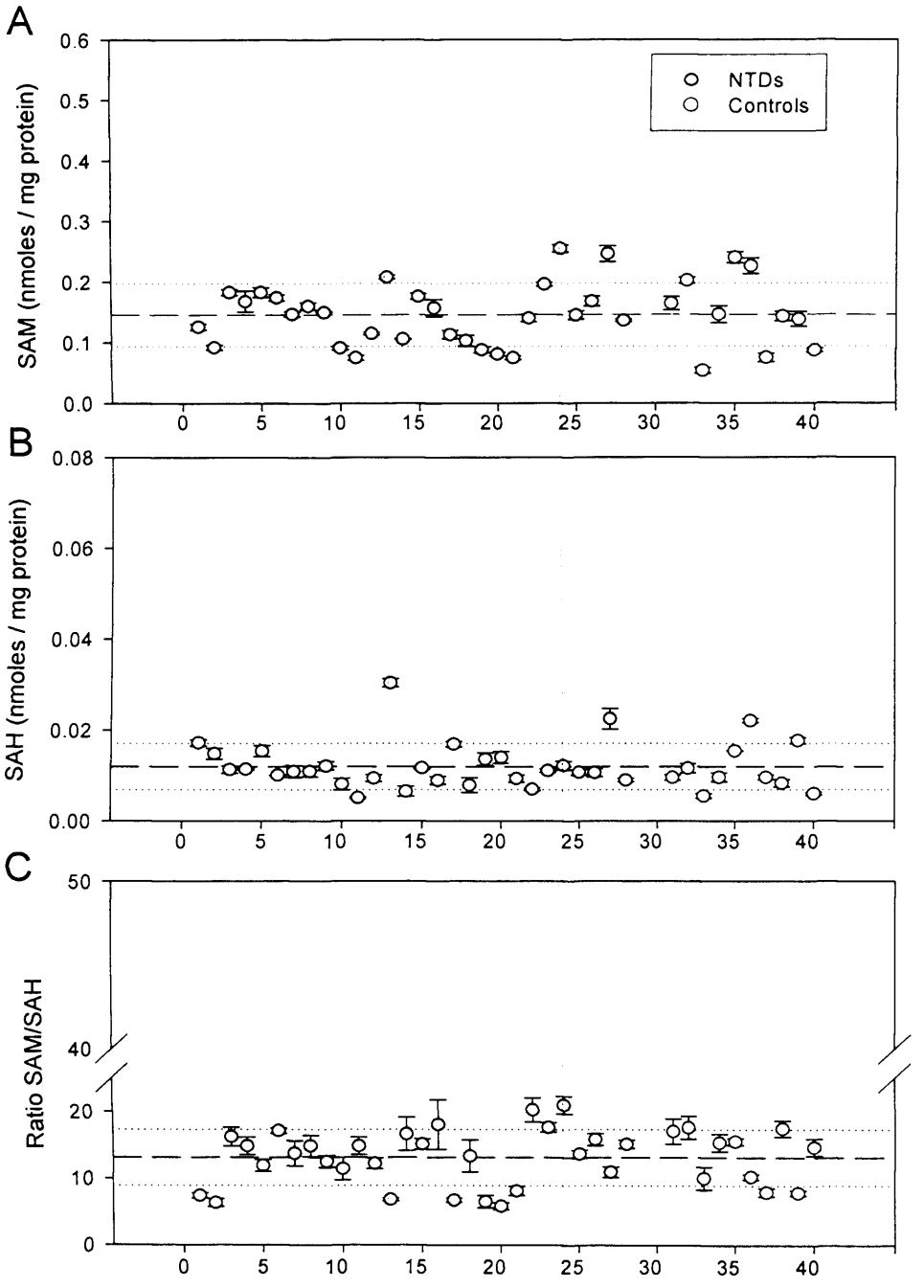

Figure 4.9. A comparison of the concentration of SAM and SAH in EBV transformed B lymphocyte cell lines from Swedish children with open spin bifida and normal Swedish controls. The (A) concentration of SAM, (B) concentration of SAH and (C) ratio of SAM/SAH are plotted. In each graph the overall mean value (dashed line) and 1 standard deviation (dotted line) of all samples are indicated. The vertical red and blue dotted lines indicate the samples with the highest concentration of SAM and SAH, respectively.

4.3 Conclusion and Discussion

4.3.1 Integrity of the methylation cycle is critical for cranial neurulation

Induction of exencephaly by exposure of embryos to excess methionine and inhibitors of the methylation cycle indicates an essential requirement for the methylation cycle in cranial neurulation. Furthermore, exposure to inhibitors of DNA methylation pinpoints a requirement for DNA methylation. In many cases in which exencephaly is induced experimentally by exogenous agents it is associated with lethality prior to closure, or generalised retardation of embryonic growth or developmental progression (Copp et al., 1990). However, none of the teratogens used in this study caused embryonic lethality or, suppressed growth or development at doses required to induce a significant incidence of exencephaly, suggesting a specific effect on cranial neurulation processes.

Ethionine and cycloleucine are both inhibitors of MAT. Ethionine was found to cause a significant decrease in the abundance of SAM, the product of this enzyme, and an increase in the level of SAH. Previous studies utilising ethionine in adult mice have demonstrated a 10-fold increase in the ratio of s-adenosylethionine (SAE) to s-adenosylmethionine (SAM) associated with the production of methyl-deficient DNA in the liver (Cox and Irving, 1977). Cycloleucine, however, did not affect the abundance of SAM but did cause a significant increase in the level of SAH. The increased abundance of SAH following inhibition of MAT is presumably due to feedback regulation around the methylation cycle, whereby the reversible reaction between homocysteine and SAH, catalysed by SAH hydrolase, favours the production of SAH (Finkelstein, 1998). The net effect is that both ethionine and cycloleucine cause a decrease in the SAM/SAH ratio, which is indicative of poor cellular methylation potential (James et al., 2002). Investigations using methyl-deficient cystathionine-β-synthase heterozygous mice have demonstrated that elevation of intracellular SAH concentration and, to a lesser extent, decreased SAM/SAH ratio are biomarkers of global DNA hypomethylation, whereas changes in intracellular concentrations of SAM are not associated with changes in DNA methylation (Caudill et al., 2001). Thus, although cycloleucine did not apparently affect SAM levels in cultured mouse embryos, the significant effects on SAH concentration and SAM/SAH ratio strongly suggest that methylation reactions are suppressed.

Miller and colleagues demonstrated in the adult rat liver, that ethionine treatment, through the production of s-adenosylethionine, is an activator of cystathionine β-synthase and effectively promotes the catabolism of homocysteine through

cystathionine (Miller et al., 1994). However, only adult tissues such as the liver, pancreas, kidney and brain that express CBS would be responsive to CBS regulation (James et al., 2002). In fact at this stage of embryonic development cells do not express CBS and therefore may be more sensitive to accumulation of SAH (VanAerts et al., 1995).

Consistent with metabolite concentrations in mouse embryos, a study of SAM and SAH levels in chick reported a mean SAM concentration of 1.12 nmol/mg protein and a mean SAH concentration of 0.06 nmol/mg protein in neurulation-stage embryos. In accordance with the findings from this study, treatment with cycloleucine also resulted in a decrease in the SAM/SAH ratio (Afman et al., 2006). Thus, at the same embryonic stage, there is little variation between mouse and chick in the global abundance of SAM and SAH and the metabolic response to methylation cycle perturbation with cycloleucine is similar.

In contrast to mouse embryos, exposure of mouse 3T3 fibroblasts to cycloleucine in this study caused a decrease in the concentration of SAM with no detectable change in the abundance of SAH. Thus, there appears to be a difference in regulation with no feedback mechanism causing a build-up of SAH to inhibit methylation. Since fibroblasts lack the transsulfation pathway, two possible mechanisms exist to avert potential intracellular accumulation of free SAH. First, at high levels, SAH can be exported out of the cell into the culture medium. Second, the lack of SAH accumulation may be due to facile transport of homocysteine across the plasma membrane (James et al., 2002). This may be more likely because the concentration of plasma homocysteine far exceeds that of SAH.

Methionine treatment was predicted to increase flux through the methylation cycle (Coelho et al., 1989), and the finding that excess methionine actually induces a significant incidence of cranial NTDs without affecting embryonic viability, growth or development, was therefore unexpected (Dunlevy et al., 2006a). Analysis of SAM and SAH levels in this study revealed that methionine has a similar metabolic effect to cycloleucine, causing a highly significant increase in SAH. It is presumed that this is again due to feedback suppression of the conversion of homocysteine to methionine, in turn leading to an increase in SAH (Finkelstein, 1998). The overall decrease in the SAM/SAH ratio due to a large increase in SAH is predicted to inhibit methyltransferase reactions (Caudill et al., 2001).

4.4.2 Is maintenance of DNA methylation critical for cranial neural tube closure?

A possible mechanism envisaged to cause NTDs through suppression of the methylation cycle is aberrant DNA methylation (McKay et al., 2004). In this study, a method was adapted to assess genomic DNA methylation in neurulation stage mouse embryos using high performance liquid chromatography tandem mass spectrometry. However, analysis of the ratio of methyl-cytosine to cytosine in non-mutant CD1 embryos cultured in the presence of methionine and the methylation inhibitors, ethionine and cycloleucine, did not reveal any detectable differences in global DNA methylation.

Subtle changes in global DNA methylation may have been below the limits of detection, although it was demonstrated that the method was sufficiently sensitive to detect significant changes in DNA methylation in brain tissue from *Mthfr*-deficient mice. An alternative explanation is that certain tissues would be more sensitive to the increase in SAH, such that DNA methylation may be maintained in some tissues at the expense of others. Indeed, changes in DNA methylation in *CBS*- and *Mthfr*-deficient mice are tissue specific (Chen et al., 2001a;Choumenkovitch et al., 2002). Assessment of DNA methylation in whole embryos provides an overview of embryonic metabolism which, depending on the number of tissues affected and the extent of the change, may not detect tissue specific DNA methylation. Due to the small size of mouse embryos it would be exceedingly difficult to assess DNA methylation in individual tissues using current methodologies.

In this study exencephaly was observed in mouse embryos following exposure to 5-azacytidine, as previously reported (Matsuda, 1990;Takeuchi and Takeuchi, 1985). It could be predicted that inhibition of DNA methylation may affect the regulation of other important reactions connected to the methylation cycle including polyamine synthesis, protein synthesis and folate metabolism. However, this study observed no change in the abundance of SAM or SAH in mouse embryos cultured in the presence of 5-azacytidine using the same conditions that were used with the methionine and the methylation inhibitors. The absence of an effect of 5'-azacytidine on the SAM/SAH ratio, suggests that this inhibitor is acting downstream of the methylation cycle presumably through inhibition of DNA methylation. The idea that DNA methylation is essential for processes underlying neural tube closure is consistent with exencephaly observed in *Dnmt3b*-deficient embryos, where changes in DNA methylation are thought to affect gene regulation (Okano et al., 1999). It remains to be established whether particular tissues or cell types are more sensitive to changes in DNA methylation

following exposure to 5-azacytidine and furthermore, whether these cell types are involved in cranial neural tube closure.

4.4.3 Investigating methylation cycle integrity in human NTDs

Overall, there is now considerable evidence using experimental models that suppression of the methylation cycle can contribute to increased risk of NTDs. Levels of SAM and SAH are ideal markers of intracellular methylation potential. SAH-mediated DNA hypomethylation and associated alterations in gene expression may be the key to understanding the pathogenesis of NTDs related to risk factors such as sub-optimal folate, high homocysteine and reduced vitamin B12 (Kirke et al., 1993;Kirke et al., 1996;Steegers-Theunissen et al., 1994). To extrapolate this study to human cases of NTDs, the abundance of SAM and SAH was quantified in cells from NTD affected patients to determine any potential abnormalities in the methylation cycle.

Analysis of the abundance of SAM and SAH in fetal fibroblast cell lines revealed no correlation with dU suppression score. Thus, overall it appears that the abnormal dU suppression result obtained in the previous study (Dunlevy et al., 2006c) is unlikely to result from a defect in the methylation cycle. Metabolite analysis led to the detection of a NTD sample with increased abundance of SAM which could be a potential biomarker for a genetically-determined disturbance in the methylation cycle. A high SAM/SAH would suggest that methylation was unaffected (Dunlevy et al., 2006c) therefore this result is unlikely to be biologically significant. More samples need to be analysed to establish the relevance of this finding.

A comparison of mean values demonstrated that NTD fetal samples have similar concentrations of SAM and SAH compared to control fetal samples. There was also no differences detected in mean concentrations of SAM and SAH between NTD and control samples in the second set of cell lines analysed: the immortalised B lymphocytes collected from Swedish children with open spina bifida compared to normal Swedish controls. Comparisons between the two cell types revealed that fetal fibroblasts have a 2-4 fold higher concentration of SAM and a 3-6 fold higher concentration of SAH compared to B lymphocytes collected from children (compare Table 4.14 and 4.15). The SAM/SAH ratio is approximately 1.5-fold lower in the fetal fibroblast cells. Thus it is apparent that metabolite concentrations do vary between cell types and/or with human development. This supports the previous hypothesis that different tissues may be more sensitive to changes in methylation cycle perturbation.

To date there seems to have been a general lack of studies investigating the relationship between the abundance of SAM and SAH in human NTD cases. In part, this may have been due to lack of availability of a sufficiently sensitive and robust assay method. A recent publication reported increased levels of SAH and decreased SAM in plasma collected from women with an NTD affected pregnancy (Zhao et al., 2006). This study highlighted NTD samples with potential genetically-determined disturbances in the methylation cycle, however it is not clear how physiologically relevant these changes in SAM and SAH levels are, and whether they are indeed risk factors for human NTDs. A large-scale investigation of SAM and SAH levels in human NTD cases is required to determine whether altered levels are associated with NTDs.

CHAPTER 5

Investigating the relationship between maternal dietary folate intake, embryonic one carbon metabolism and the incidence of neural tube defects in the splotch NTD mouse model.

5.1 Introduction

5.1.1 Dietary folate deficiency in mouse models

Burgoon and colleagues undertook research using wild-type mice to evaluate changes in maternal folate, homocysteine and reproductive outcome caused by a diet deficient in folic acid (Burgoon et al., 2002). They reported biochemical characteristics similar to human folic acid deficiency, including decreased plasma and red blood cell folate, and increased plasma homocysteine. Reproductive outcome was poor with increased rate of fetal deaths, decreased fetal weight and delay in embryonic development of the heart and palate. Notably, folate deficiency did not cause NTDs in wild-type mice. An analogous investigation by Heid and co-workers reported that folate deficient dietary conditions resulted in a high rate of resorption with fewer and smaller embryos yet, similarly, folate deficiency did not cause NTDs in wild-type mice (Heid et al., 1992).

A different approach would be to use an NTD mutant mouse strain to enable any interaction between folate deficiency (environmental factor) and a mutation causing an NTD phenotype (genetic factor) to be assessed. In this chapter, this study uses the folate-preventable *splotch* (Sp^{2H}) NTD mutant mouse model to demonstrate that a folate-deficient (FD) diet causes increased incidence of exencephaly in Sp^{2H} homozygous and heterozygous embryos, which can be rescued in utero by folic acid supplementation, but not by thymidine. Additionally, a diet deficient in both folate and inositol is shown to cause exencephaly in all Sp^{2H} homozygous embryos.

Many bacterial species, including several present in the large intestine, are capable of synthesising folate, which can be absorbed across the large intestine and incorporated into tissue (Asrar and O'Connor, 2005). Thus to ensure a folate-deficient diet effectively reduces maternal folate status, it is recommended that an antibiotic is included to kill the gut bacteria and prevent the absorption of bacterially synthesised folate (Burgoon et al., 2002). To highlight potential adverse outcomes of adding the antibiotic to the diet, two control diets have been used to assess the effects of bacterial folate deficiency versus dietary folate deficiency. The bacterial folate deficient (BFD) diet used contained sufficient dietary folic acid but had the antibiotic added to exclude bacterial folate supplies. Therefore, this diet was sufficient in dietary folate but deficient in bacterial folate. In contrast, the dietary folate deficient (DFD) diet did not contain the antibiotic and the dietary folic acid was removed. Therefore, this diet was sufficient in bacterial folate but deficient in dietary folate.

5.1.2 The folate-preventable *splotch* NTD mouse model

The *splotch* (*Sp*) mutation was originally identified in a mouse colony as a spontaneous semi-dominant allele (Russell, 1947). Since then multiple alleles at the same locus on murine chromosome 1 have arisen, including the radiation-induced Sp^{2H} allele (Beechey and Searle, 1986). The Sp^{2H} allele encodes a 32 nucleotide deletion in the *Pax3* gene resulting in a truncated protein lacking the C-terminal homeodomain, while the octapeptide motif and paired domain remain intact (Epstein et al., 1991). Most homeodomains recognise DNA sequences containing the TAAT motif, however the homeodomain found in the Pax-3 protein enables co-operative dimerisation on a distinct palindromic DNA sequence not bound by other homeodomains (Chi and Epstein, 2002). The Sp^{2H} mutation is thought to result in a functionally null protein.

The role of *Pax3* during neural tube closure remains to be definitively identified, however the pattern of expression suggests functional importance in this process. *Pax3* is expressed prior to closure at the dorsal aspect of the prosencephalon, the point of Closure site II, with expression extending to the posterior neuropore (Goulding et al., 1991). The migratory population of neural crest cells emerge from this *Pax3* expressing domain. Neural crest cells migrate throughout the developing embryo and differentiate into many cell types, contributing to multiple organs (Chi and Epstein, 2002).

Heterozygous *splotch* mice have a characteristic white patch on their belly due to the failure of neural crest cell derived melanocytes to migrate (Auerbach, 1954). Homozygous *splotch* mice develop spina bifida and/or exencephaly, in addition to abnormalities of neural crest migration including congenital heart disease which results in embryonic death at E14 (Auerbach, 1954). Historically, 40% of Sp^{2H}/Sp^{2H} embryos develop cranial and spinal NTDs, 25% develop isolated spinal NTDs and the remaining 35% develop normally (Fleming and Copp, 1998). Humans with Waardenburg syndrome (types I and III) with mutations in *PAX3* have an increased prevalence of NTDs in homozygotes, although *PAX3* mutations do not appear to be associated with familial NTDs in humans (Chatkupt et al., 1995;Read and Newton, 1997).

Folic acid and thymidine administration both in vivo and in vitro reduce the incidence of NTDs by 35-45% among homozygous Sp^{2H} mouse embryos, whilst methionine has an exacerbating effect (Fleming and Copp, 1998). Using the deoxyuridine suppression test (for further details see section 4.3.4), a disturbance in folate metabolism has also been identified in homozygous Sp^{2H} embryos developing in vitro (Fleming and Copp, 1998). The excessive incorporation of [H^3]-thymidine indicated a metabolic deficiency

in the supply of folate for the biosynthesis of pyrimidine. Unlike homozygous Sp^{2H} embryos, studies using the *Sp* mouse colony found that folic acid does not rescue either spontaneous or arsenic-induced NTDs in *Sp* homozygotes (Gefrides et al., 2002). In addition, the analysis of mice with both *Sp* and *Mthfr* mutations demonstrated that there were no differences in the incidence or severity of NTDs in embryos from double-mutant mating pairs compared to those from single *Sp* mutants (Li et al., 2006), suggesting there is no interaction between the *Sp* mutation and folate metabolism.

5.1.3 Biomarkers of folate metabolism

In addition to studying the incidence of NTDs following dietary intervention, this study has also focused on the biochemical effects of the diets on folate and one-carbon metabolism in $Sp^{2H}/+$ dams and their embryos. In order to study embryonic folate metabolism and to determine maternal folate levels, a suitably sensitive and accurate method was required to measure folate. Of the procedures currently in use, the method of choice is the *L.casei* microbiological assay (Shane et al., 1980). This method is based on the folate-dependent growth of the bacterium *Lactobacillus casei*, which can be measured spectro-photometrically. An advantage of the *L.casei* microbiological method is that it is sensitive to all monoglutamylfolate species, and therefore provides a means to assess the monoglutamylfolate content within a biological sample. In addition to this, specific sample preparation enables the determination of polyglutamylfolate levels following enzymatic hydrolysis of the glutamate chain to produce the assayable monoglutamate folate species (Pfeiffer and Gregory, 1996). This well-established assay has been used to measure folate content in plasma, serum, whole blood and various tissue samples (Horne, 1997;Molloy and Scott, 1997). However, the present study was the first time it had been applied to measure folate in whole embryo samples. Therefore, for the purposes of this study, the method was suitably adapted to quantify both the abundance of monoglutamyl- and polyglutamylfolate in neurulation-stage whole embryos.

Whole blood and embryonic concentrations of folate are used to give direct measures of folate status in the dam and the embryo following exposure to folate deficiency. A functional biomarker of folate status is a parameter that reflects the integrity of a biochemical system that is dependent on folate (Mason, 2003). Plasma homocysteine and embryonic SAM and SAH have been selected for this study as functional biomarkers. An elevation in homocysteine is a sensitive indicator of folate depletion because the re-methylation of homocysteine to methionine is a folate-dependent process (Burgoon et al., 2002). The concentrations of SAM and SAH are determined

largely by adequate methionine and homocysteine availability, therefore they constitute a functional reflection of one-carbon nutrient status. Additionally, the measurement of SAM and SAH is a functional indicator of methylation capacity (Mason, 2003).

5.2 Materials and Methods

5.2.1 Mouse diets

Female Sp^{2H}/+ mice were placed on five different diets, outlined in Table 5.1, to test the embryonic effects of folate deficiency. The folate-deficient diet (FD) was a rodent diet (Harlan) adapted to contain no folic acid and to include 1 % succinyl sulfathiazole (SST). Succinyl sulfathiazole is an antibiotic that reduces the gut flora responsible for the synthesis of a significant amount of folate.

Four additional diets were used in the study (all produced by Harlan). The first was a normal breeding rodent diet (ND), containing no SST and 2.7 mg FA/kg diet. The second was a control diet used to study solely the effects of bacterial folate deficiency but with normal dietary folate supply. Thus, a group of mice was fed a diet containing 1% SST and 2.7 mg FA/kg diet (bacterial folate deficient, BFD). A third control diet was used to study solely the effects of dietary folate deficiency. Therefore, although these mice had no supply of dietary folate, they were able to absorb folate produced by their gut flora. Thus, a group of control mice was placed on a diet containing no SST and no folic acid (dietary folate deficient, DFD). A fourth diet was used to investigate the effect of both folate and inositol deficiency. Thus, a group of mice was fed a diet that contained no folic acid, 1% SST and no inositol (folate and inositol deficient, FID).

All mice were fed their respective diet for a minimum of 3 consecutive weeks, while being housed in standard breeding cages in a room with a 14-hr light/10-hr dark cycle. After three weeks on their respective diets, females were mated with male Sp^{2H}/+ mice overnight and checked the following morning for the presence of a copulation plug. Plug day was termed embryonic day 0.5 (E0.5). Mice remained on the different diets until they were killed at E10.5-E11.5. At that time, numbers of implantations and resorption sites were determined and fetuses were examined for neural tube defects and gross malformations. All viable fetuses at E10.5 and E11.5 were rinsed with PBS and stored at -80 ^{0}C prior to analysis of embryonic folate or SAM/SAH levels.

To attempt to rescue cranial NTDs, pregnant mice on the folate deficient diet received an interperitoneal (i.p.) injection of 10 mg folic acid / kg body weight (FD+FA) or 1 mg thymidine / kg body weight (FD+THY) at embryonic days E7.5, 8.5, 9.5 and 10.5. Mice fed the folate and inositol diet (FID) were supplemented with 10 mg FA / kg body weight at embryonic days E7.5, E8.5, E9.5 and E10.5 to determine the effects of inositol deficiency on the rescue of cranial NTDs by folic acid.

Diet	FA (mg/kg)	Inositol (g/kg)	SST (g/kg)	Supplements (per kg body weight)	Description
ND	2.7	1.9	X	None	Normal Diet
FD	X	1.9	10	None	Folate-deficient Diet
BFD	2.7	1.9	10	None	Bacterial Folate-deficient Diet
DFD	X	1.9	X	None	Dietary Folate-deficient Diet
FID	X	X	10	None	Folate- and Inositol-deficient Diet
FD+FA	X	1.9	10	10 mg folic acid	Folate-deficient Diet + FA
FD+THY	X	1.9	10	1 mg thymidine	Folate-deficient Diet + THY
FID+FA	X	X	10	10 mg folic acid	Folate- and Inositol-deficient Diet + FA

Table 5.1. Details of the experimental diets fed to female Sp2H/+ mice. Supplements were administered by i.p. injection at embryonic day E7.5, 8.5, 9.5 and 10.5.

5.2.2 Metabolite Analysis

Maternal blood was collected and plasma prepared as described in section 2.4. Maternal whole blood and embryonic folate concentrations were measured by the *Lactobacillus casei* microbiological assay using the method described in section 2.10. Total plasma homocysteine levels (free + protein-bound) were determined as described in section 2.4. Plasma homocysteine and whole blood folate were not measured in the same samples due to limited volume of blood. Embryonic SAM and SAH were analysed in individual whole embryos as detailed in chapter 3.

5.2.3 Statistical Analysis

Statistical analyses were performed using SigmaPlot Version 7, SigmaStat Version 3.5 and SPSS Version 13. Maternal whole blood folate and plasma homocysteine concentrations were compared with respect to the normal diet (ND) using the un-paired student t-test. To determine the effect of the different diets on reproductive success, the mean values for number of implants per litter and number of resorptions per litter were compared between groups by ANOVA followed by pair-wise analysis using the Holm-Sidak statistical test. The incidence of NTDs following dietary intervention and supplementation was compared using the chi-square statistical test followed by the Fishers Exact test for pair-wise comparisons. To determine the effect of dietary intervention on developmental progression, the mean number of somites developed by embryos from the ND and the FD diets were compared using the un-paired student t-

test. Mean values for total folate content, total folate concentration, SAM, SAH and SAM/SAH ratio were compared between dietary groups by ANOVA followed by pair-wise analysis using the Holm-Sidak statistical test. All p-values less than 0.05 were considered significant.

Multiple linear regression was applied to all scatter-plot graphs in section 5.3.8 and 5.3.9. The p-value was calculated using the equation $y = c + mx + \beta z + \gamma zx$, where y = folate, x = somite and z = diet group (folate deficient diet = 0, normal diet = 1). The p-value represents the significance of the constant γ, and therefore the significance of the difference between the gradients of the two graph lines. All p-values less than 0.05 were considered significant.

5.3 Results

5.3.1 Effect of folate deficiency on maternal folate and homocysteine.

After consumption of the folate-deficient diet for a minimum of three consecutive weeks, $Sp^{2H}/+$ dams had a whole blood folate concentration only 35% of that in $Sp^{2H}/+$ dams fed the normal diet (Table 5.2). This decrease in maternal folate caused by the folate-deficient diet was statistically significant ($p < 0.001$). Folic acid supplementation (E7-E10) of dams fed the folate-deficient diet caused a significant increase ($p < 0.001$) in maternal folate (E11) compared to dams fed the folate-deficient diet only. Thus, supplemental folic acid administered by intra-peritoneal injection successfully increases maternal folate status.

Diet	Whole Blood Folate (µg/ml)		Plasma Homocysteine (µmol/L)	
	n=	Mean ± SEM	n=	Mean ± SEM
ND	17	0.43 ± 0.021**	4	1.46 ± 0.64
FD	14	0.15 ± 0.010##	6	9.23 ± 2.49##
BFD	10	0.23 ± 0.023**##	5	2.66 ± 0.23
DFD	11	0.17 ± 0.012##	5	6.37 ± 0.24##
FID	8	0.23 ± 0.012**##		
FD+FA	4	0.28 ± 0.030**##		

Table 5.2. Maternal whole blood folate and plasma homocysteine concentration following dietary intervention. FD, Folate-deficient Diet; ND, Normal Diet; BFD, Bacterial Folate-deficient Diet; DFD, Dietary Folate-deficient Diet; FID, Folate- and Inositol- deficient Diet; FD+FA, Folate-deficient Diet + FA. ** p-value < 0.02 when compared to FD dietary group, ## p-value < 0.02 when compared to ND dietary group (un-paired student t-test).

Similar to the folate-deficient diet, $Sp^{2H}/+$ dams fed the dietary folate-deficient diet (DFD) had a whole blood folate concentration only 40% of that in dams fed the normal diet. In contrast, the whole blood folate concentrations in dams fed the bacterial folate deficient diet (BFD) had only declined to 0.23 µg/ml, a level 53% of that in dams fed the normal diet. Thus, the dietary folate deficient diet had a greater effect on maternal folate than the bacterial folate deficient diet (Table 5.2). Statistical analyses demonstrated that the maternal blood folate level was significantly lower in dams fed the dietary folate-deficient diet compared to dams feds the bacterial folate-deficient diet ($p < 0.05$). In dams fed the folate and inositol deficient diet (FID), the whole blood folate concentration was 0.23 µg/ml, a level 53% of that in dams fed the normal diet.

Thus, inositol deficiency had no further detrimental effect on maternal folate levels compared to the three folate depleted diets (BFD, DFD and FD) (Tables 5.2).

Plasma homocysteine concentrations also varied among the different diet groups, with the lowest levels in dams fed the normal diet and highest levels in dams fed the folate-deficient diet (Table 5.2). The dams fed the dietary folate deficient diet had intermediate homocysteine levels, whilst the bacterial folate deficient diet did not significantly increase maternal homocysteine compared to the normal diet. Overall, maternal biochemical analyses showed that the folate-deficient diet used in this study lowered maternal folate status and increased levels of homocysteine. Bacterial folate deficiency was sufficient to affect maternal blood folate levels but not homocysteine levels. By comparison, dietary folate deficiency affected both blood folate and homocysteine but was not as effective as combined bacterial and dietary deficiency.

It is possible that Sp^{2H}/+ dams have a defect in folate metabolism or are unable to uptake sufficient folate from the diet. To investigate this hypothesis maternal folate levels in Sp^{2H}/+ dams were compared to CD1 dams, a non-mutant control strain assumed to have no folate-related defect. There was no difference in the whole blood folate concentration under normal and folate-deficient dietary conditions between the two strains (Figure 5.1) suggesting that Sp^{2H}/+ dams do not have an abnormality in the uptake of folate from the diet.

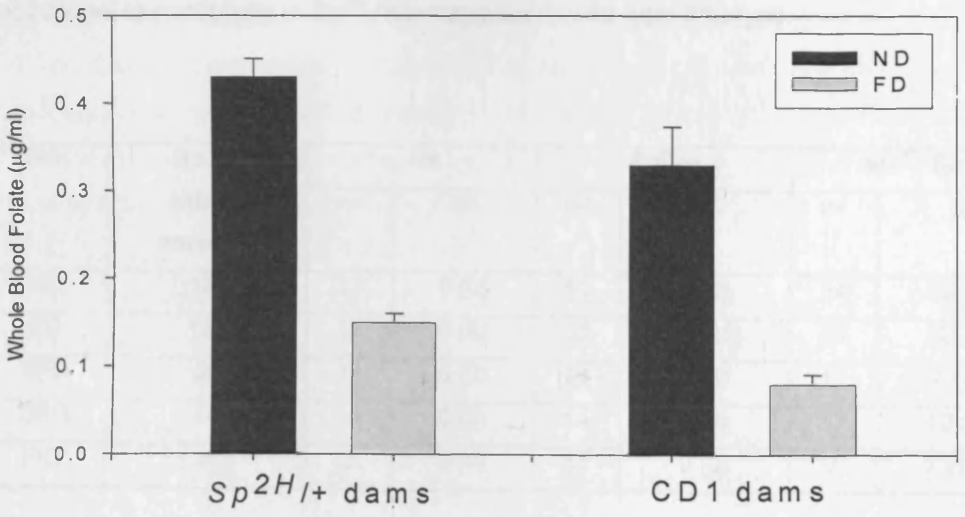

Figure 5.1. A comparison of maternal whole blood folate levels between Sp^{2H}/+ and CD1 dams. Values are given as mean ± standard error of the mean. ND: Normal Diet, FD: Folate Deficient diet. $p > 0.05$ when compared between strains for each dietary group (un-paired student t-test).

5.3.3 Effect of folate deficiency on the incidence of NTDs in *splotch* embryos

The incidence of NTDs among E10.5 – E11.5 *splotch* litters following maternal dietary intervention was noted and correlated with genotype (Table 5.4). The folate-deficient diet caused a 14% increase in exencephaly in Sp^{2H} homozygous embryos compared to normal dietary conditions, whilst Sp^{2H} heterozygous embryos in our colony have never previously been reported to develop isolated cranial NTDs but under folate-deficient conditions 25% of Sp^{2H} embryos developed exencephaly. Pair-wise statistical analyses using the chi-square test demonstrated that the increased incidence of cranial NTDs in Sp^{2H} heterozygous embryos was significant ($p < 0.001$) whilst the increased incidence of cranial NTDs in Sp^{2H} homozygous embryos was not significant ($p = 0.339$). Loss of bacterial folate (BFD) unexpectedly reduced the incidence of exencephaly in Sp^{2H} homozygous embryos compared to normal dietary conditions ($p = 0.037$), but did cause exencephaly in one Sp^{2H} heterozygous embryos. In contrast, loss of dietary folate (DFD) did not affect the incidence of exencephaly in either Sp^{2H} homozygous or heterozygous embryos compared to the normal diet group.

Combined folate and inositol deficiency (FID) caused 100% exencephaly in Sp^{2H} homozygous embryos. However, pair-wise statistical analyses using the Fishers Exact test demonstrated that the increased incidence of NTDs was not significant ($p = 0.075$) compared to Sp^{2H} homozygous embryos from the normal diet group, presumably due to insufficient sample size. Notably, combined folate and inositol deficiency (FID) did not cause exencephaly in Sp^{2H} heterozygous or wild-type embryos.

Diet	No. of viable embryos	+/+		Sp^{2H}/+		Sp^{2H}/ Sp^{2H}	
		n=	EX	n=	EX	n=	EX
ND	122	27	0 (0)	61	0 (0)	34	20 (59)
FD	123	28	0 (0)	53	13 (25)	30	22 (73)
BFD	59	18	0 (0)	24	1 (4)	17	4 (24)
DFD	45	14	0 (0)	14	0 (0)	17	10 (59)
FID	21	3	0 (0)	11	0 (0)	7	7 (100)

Table 5.4. Incidence of neural tube closure abnormalities in E10.5-E11.5 *splotch* embryos following dietary intervention. Data are presented as number of embryos with percentage in each treatment group in parentheses. EX; exencephaly. FD, Folate-deficient Diet; ND, Normal Diet; BFD, Bacterial Folate-deficient Diet; DFD, Dietary Folate-deficient Diet; FID, Folate- and Inositol-deficient Diet.

For the purposes of this study embryos were collected to study the relationship between folate deficiency, embryonic one-carbon metabolism and the incidence of neural tube defects. Additional embryos were collected and analysed by Dr. N. D. E. Greene (Table 5.5). The data collected by Dr. Greene shows that the folate-deficient diet caused a 27% increase in the incidence of exencephaly among Sp^{2H} homozygous embryos compared to the normal diet.

Diet	No. of viable embryos	+/+		$Sp^{2H}/+$		Sp^{2H}/Sp^{2H}	
		n=	cNTD	n=	cNTD	n=	cNTD
ND	103	35	1 (3)	45	0 (0)	23	14 (61)
FD	139	25	0 (0)	77	1 (1)	37	29 (88)
BFD	8	3	0 (0)	2	0 (0)	3	1 (33)
DFD	4	0	0 (0)	2	0 (0)	2	0 (0)

Table 5.5. Incidence of neural tube closure abnormalities in *splotch* embryos following dietary intervention: data collected by Dr. N. D. E. Greene. Data are presented as number of embryos with percentage in each treatment group in parentheses. cNTD; cranial neural tube defect (exencephaly). FD, Folate-deficient Diet; ND, Normal Diet; BFD, Bacterial Folate-deficient Diet; DFD, Dietary Folate-deficient Diet.

As embryos were collected by myself and Dr. Greene from the same mouse colony and during the same period it was deemed appropriate to combine the data from Tables 5.4 and 5.5 in order to increase the sample size, and therefore, the power of each statistical test. Analysis of the combined data (Table 5.6) using the chi-square test showed significant differences between the incidence of exencephaly in Sp^{2H} homozygous embryos among the various dietary groups ($p < 0.001$).

Pair-wise comparisons demonstrated that the incidence of cranial NTDs among Sp^{2H} homozygous embryos in the folate-deficient diet group was significantly greater than the incidence among embryos in the normal diet ($p = 0.033$) and the bacterial folate-deficient diet ($p < 0.001$) but not the dietary folate-deficient diet ($p = 0.083$) groups. There were no significant differences in incidence between Sp^{2H} homozygous embryos from the normal diet and the dietary folate-deficient diet groups ($p = 0.603$), although the incidence of exencephaly among Sp^{2H} homozygous embryos from the bacterial folate-deficient diet group had significantly decreased compared to the normal diet group ($p = 0.010$). As demonstrated previously, the incidence of cranial NTDs in Sp^{2H} heterozygous embryos from the folate-deficient diet group was significantly greater ($p =$

0.004) than the normal diet group. Notably, folate deficiency did not induce NTDs among wild-type embryos. Overall, these results show removal of both bacterial and dietary sources of folate causes an increased incidence of cranial NTDs, whereas removal of only bacterial or dietary folate does not increase NTD frequency. In addition, embryos must carry at least one mutant *Pax3* allele.

Diet	No. of viable embryos	+/+		Sp^{2H}/+		Sp^{2H}/ Sp^{2H}	
		n=	cNTD	n=	cNTD	n=	cNTD
ND	225	62	1 (2)	106	0 (0)	57	34 (60)
FD	262	53	0 (0)	130	13 (10)	67	51 (76)
BFD	67	21	0 (0)	26	1 (4)	20	5 (25)
DFD	49	14	0 (0)	16	0 (0)	19	10 (53)
FID	76	16	0 (0)	38	0 (0)	22	21 (95)

Table 5.6. Incidence of neural tube closure abnormalities in *splotch* embryos following dietary intervention: combined data from Table 6.4 and 6.5. Data are presented as number of embryos with percentage in each treatment group in parentheses. cNTD; cranial neural tube defect (exencephaly). FD, Folate-deficient Diet; ND, Normal Diet; BFD, Bacterial Folate-deficient Diet; DFD, Dietary Folate-deficient Diet; FID, Folate- and Inositol-deficient Diet.

The increased incidence of NTDs in Sp^{2H} homozygous embryos in the folate- and inositol-deficient diet group (FID) compared to the normal diet group was highly significant (Fisher Exact; $p < 0.001$). Additionally, the incidence of NTDs in Sp^{2H} homozygous embryos in the folate- and inositol-deficient group (FID) was 19 % greater than in the folate-deficient diet group however statistical analyses demonstrates that this difference is not significant (Fisher Exact; $p = 0.060$). These results suggest that inositol deficiency, in combination with folate deficiency, is a risk factor for exencephaly in Sp^{2H} homozygous mutant embryos.

5.3.4 Analysing the development and size of splotch embryos

During collection of embryos, differences in size of embryos developing under varying dietary conditions were apparent (Figure 5.2). Thus, embryos from the folate-deficient diet group, were seen to be smaller than *splotch* embryos from the normal, bacterial folate-deficient and dietary folate-deficient groups.

Figure 5.2. High magnification photographs of E10.5 *splotch* embryos following dietary intervention. (A) Sp^{2H}/Sp^{2H} embryo (30 somites) with an open posterior neuropore from the normal diet group (ND), (B) Sp^{2H}/Sp^{2H} embryo (30 somites) with exencephaly (solid arrow) and an open posterior neuropore from the folate deficient diet (FD) group, (C) Sp^{2H}/Sp^{2H} embryo (29 somites) with an open posterior neuropore from the bacterial folate deficient diet (BFD) group and (D) Sp^{2H}/Sp^{2H} embryo (32 somites) with an open posterior neuropore from the dietary folate deficient diet (DFD) group. Dashed arrows indicate open posterior neuropore. Scale bar is equivalent to 1mm.

Thus, in addition to analysing embryos for NTDs, the developmental progression and size was also monitored by recording the number of somites an embryo had developed and by measuring the crown-rump length (Table 5.7). Somites are units of mesenchymal cells that arise in a periodic manner as the embryo grows and develops. Somitogenesis occurs within the same embryonic period of development as neurulation, such that counting somites provides a simple approach to quantitate developmental progression.

At E10.5, *splotch* embryos from the folate-deficient diet group were significantly smaller ($p < 0.001$) and developmentally retarded ($p < 0.001$) than *splotch* embryos from the normal diet group (Table 5.7). In comparison to the normal diet group, the bacterial and dietary folate deficient diet did not detrimentally affect embryonic size or development (Table 5.7). Thus, both control diets appear to provide sufficient folate, either from the diet or from the gut bacteria, to enable normal growth and development.

The folate- and inositol-deficient diet caused a significant decrease in embryonic size ($p = 0.001$) and development ($p = 0.001$) compared to embryos from the normal diet group. Moreover, in comparison to folate-deficient embryos, the folate- and inositol-deficient diet caused a significant decrease in the mean number of somites at E10.5, although the decrease in mean crown rump length was not significant ($p = 0.07$). This

suggests that inositol deficiency, in addition to folate deficiency, further delayed development.

Diet	Gestational Age	n=	Crown Rump Length (mm)	Number of somites
ND	E10.5	80	3.97 ± 0.06	29.3 ± 0.28
FD	E10.5	82	2.78 ± 0.07**	23.5 ± 0.39**
BFD	E10.5	26	4.36 ± 0.07	29.9 ± 0.70
DFD	E10.5	18	4.08 ± 0.18	30.6 ± 1.28
FID	E10.5	14	2.46 ± 0.12**	20.1 ± 0.75**##
ND	E11.5	20	5.86 ± 0.19	39.6 ± 1.07
FD	E11.5	49	4.57 ± 0.11**	32.7 ± 0.48**

Table 5.7. Size and development of *splotch* embryos following dietary intervention. All genotypes were pooled for analysis. Values given as mean ± standard error of the mean. ** $p < 0.02$ when compared to ND, ## $p < 0.001$ when compared to FD (un-paired student t-test). FD, Folate-deficient Diet; ND, Normal Diet; BFD, Bacterial Folate-deficient Diet; DFD, Dietary Folate-deficient Diet; FID, Folate- and Inositol-deficient Diet.

To determine whether the *Pax3* mutation summates with folate deficiency to affect embryonic size and development, the data was divided according to genotype for further analysis (Table 5.8). At E10.5, Sp^{2H}/Sp^{2H} embryos had significantly fewer somites than heterozygous ($p = 0.020$) and wild-type ($p = 0.025$) embryos under normal dietary conditions, yet the crown-rump length of embryos was comparable between genotypes (Table 5.8). Although Sp^{2H}/Sp^{2H} embryos had significantly fewer somites at E10.5 this finding is not consistently observed with the Sp^{2H} colony (Greene, N., personal communication) and the biological relevance of this observation is unclear. The similar mean crown rump length of embryos of different genotypes suggests comparable growth. The size and development of Sp^{2H} homozygous and heterozygous embryos was indistinguishable from that of wild-type under folate-deficient conditions (Table 5.8). Therefore, overall, there appears to be no interaction between diet and genotype to further affect the size and development of *splotch* embryos.

Genotype	Diet	n=	% cranial NTD	Crown rump length (mm)	Number of somites
+/+	ND	13	0	49.3 ± 1.25	30.4 ± 0.27
Sp^{2H}/+	ND	53	0	48.1 ± 0.90	29.5 ± 0.28
Sp^{2H}/ Sp^{2H}	ND	14	50	44.4 ± 2.31	27.6 ± 1.08*
+/+	FD	16	0	32.8 ± 1.55	23.6 ± 0.80
Sp^{2H}/+	FD	32	32	31.8 ± 1.00	22.5 ± 0.52
Sp^{2H}/ Sp^{2H}	FD	26	69	34.7 ± 1.07	22.9 ± 0.61
Sp^{2H}/ Sp^{2H}	FD	8	0	36.9 ± 1.44	23.6 ± 0.89
Sp^{2H}/ Sp^{2H}	FD	18	100	33.8 ± 1.45	22.5 ± 0.83

Table 5.8. Size and development of E10.5 *splotch* embryos following dietary intervention: analysis by genotype. Values given as mean ± standard error of the mean. Mixed; embryos with normal and NTD phenotypes were pooled for analysis. FD, Folate-deficient Diet; ND, Normal Diet. * $p < 0.05$ when comparing wild-type to Sp^{2H}/+ under normal dietary conditions (ND).

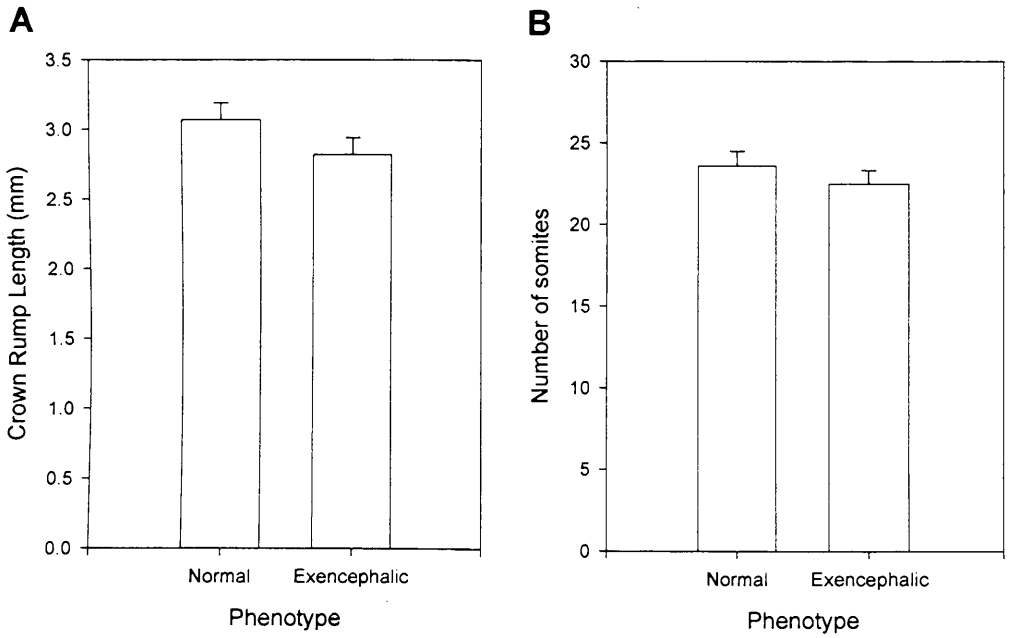

Figure 5.3. Size and development of E10.5 Sp^{2H}/Sp^{2H} embryos from the folate deficient diet group (FD): analysis by phenotype. Values given as mean ± standard error of the mean.

In order to determine whether folate deficiency causes NTDs in the smaller and more developmentally delayed embryos, the size and development of exencephalic and normal homozygous embryos were compared (Table 5.8 and Figure 5.3). At E10.5, exencephalic Sp^{2H}/Sp^{2H} embryos from the folate-deficient diet group appeared to have a shorter mean crown rump length and fewer somites than unaffected Sp^{2H}/Sp^{2H} embryos from the folate-deficient diet group. However, statistical analyses using the student t-test demonstrated that this difference in size ($p = 0.181$) and development ($p = 0.454$) was not statistically significant. Thus, these results do not clarify whether the NTD is due to growth and developmental delay as a result of the folate deficient diet or if the NTD arises independent of the growth and developmental delay.

Later in gestation, at E11.5, *splotch* embryos from the folate-deficient diet group were significantly smaller ($p < 0.001$) and developmentally ($p< 0.001$) retarded compared to embryos from the normal diet group, as at E10.5 (Table 5.7). There are two possible explanations which could explain the observed growth and developmental retardation; (i) the folate deficient embryos were growing and developing at a slower rate or, (ii) the folate deficient embryos grew at comparable rates during neurulation but were already behind in growth and development due to an event which happened prior to neurulation. To investigate this hypothesis the extent of growth and developmental retardation has been analysed at E10.5 and E11.5. At E10.5 (Table 5.7) *splotch* embryos from the normal diet group had developed approximately six more somites and were 5.8 mm longer than *splotch* embryos from the folate-deficient diet group. At E11.5 (Table 5.7) *splotch* embryos from the normal diet group had developed approximately seven more somites and were 6.9 mm longer than *splotch* embryos from the folate-deficient diet group. Thus, the extent of growth and developmental retardation appeared to be getting progressively worse with gestational age. Overall, this data suggests that the embryos from the folate-deficient diet group were growing and developing at a slower rate during the period of neural tube closure.

5.3.5 Effect of folic acid and thymidine supplementation on the incidence of NTDs in folate deficient *splotch* embryos

To determine the potential for prevention of cranial NTDs by supplemental folic acid (FA) and thymidine (THY), dams fed the folate-deficient diet were treated with FA (FD+FA) or THY (FD+THY) at E7.5, E8.5, E9.5 and E10.5 by intra-peritoneal injection. The dams were then sacrificed at E11.5 and the embryos collected for analysis. The incidence of cranial NTDs in Sp^{2H}/Sp^{2H} embryos following supplementation with FA was

48% compared to 100% in untreated folate-deficient embryos (Table 5.9). Thus, supplemental folic acid caused a significant decrease in the incidence of NTDs.

The incidence of cranial NTDs in Sp^{2H}/Sp^{2H} embryos following supplementation with thymidine was 86% compared to 100% in untreated folate-deficient Sp^{2H} homozygous embryos. Thus, treatment with thymidine did not significantly reduce the incidence of cranial NTDs (Table 5.9). However it became apparent that thymidine treatment reduced the severity of the cranial NTDs such that there was only a small opening visible at E11.5 (Figure 5.4).

Supplement	No. embryos	+/+		$Sp^{2H}/+$		Sp^{2H}/Sp^{2H}	
		n	cNTD	n	cNTD	n	cNTD
ND	22	7	0 (0)	7	0 (0)	8	4 (50)
FD	27	6	0 (0)	16	2 (13)	5	5 (100)
FD+FA	70	15	0 (0)	32	0 (0)	23	11 (48)#
FD+THY	36	9	0 (0)	20	0 (0)	7	6 (86)

Table 5.9. Incidence of NTD in folate-deficient E11.5 *splotch* embryos following dietary supplementation with folic acid or thymidine. Data are presented as number of embryos with percentage in each treatment group in parentheses. cNTD; cranial neural tube defect (exencephaly). # $p < 0.05$ when compared to FD (Fishers Exact). FD, Folate-deficient Diet; ND, Normal Diet; FD+FA, Folate-deficient Diet + FA; FD+THY, Folate-deficient Diet + THY.

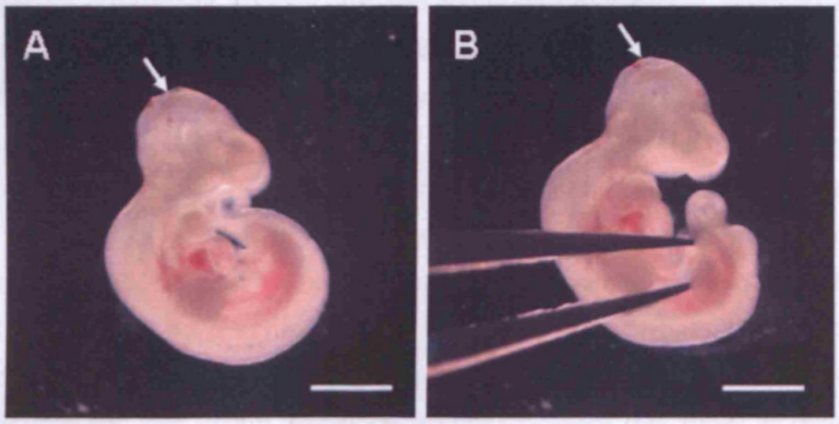

Figure 5.4. High magnification photographs (x1.25) of an E11.5 Sp^{2H}/Sp^{2H} embryo, (35 somites) from the folate-deficient diet group supplemented with thymidine (FD+THY). Arrow highlights the small opening in the cranial neural tube. Scale bar is equivalent to 1mm at x2.0 magnification.

Analysis of size and developmental progression of these embryos demonstrated that, although FA reduces the incidence of NTD, there is no improvement in the size or development compared to un-supplemented folate-deficient embryos (Table 5.10). In contrast, THY significantly increased the size and developmental progression of the treated embryos in comparison to un-supplemented folate-deficient (FD) embryos. Thus, improving growth and development may assist closure (see figure 5.4) but it does not appear sufficient to prevent NTDs.

Supplement	Gestational Age	No. embryos	Crown Rump Length (mm)	Number of somites
ND	E11.5	22	6.49 ± 0.11	40.8 ± 0.40
FD	E11.5	18	4.52 ± 0.14	32.6 ± 0.69
FD+FA	E11.5	20	4.28 ± 0.09	31.2 ± 0.49
FD+THY	E11.5	13	5.02 ± 0.01$^{\#\#}$	35.5 ± 0.31$^{\#\#}$

Table 5.10. Size and development of folate deficient *splotch* embryos following dietary supplementation with folic acid and thymidine. Values given as mean ± standard error of the mean. $^{\#\#}p < 0.02$ when compared to FD (Holm-Sidak). FD, Folate-deficient Diet; ND, Normal Diet; FD+FA, Folate-deficient Diet + FA; FD+THY, Folate-deficient Diet + THY.

5.3.6 Investigating the relationship between embryonic growth and development following maternal dietary intervention.

To attempt to understand further how the folate-deficient diet is affecting embryonic growth and development at E10.5 and E11.5, embryos that had developed under folate-deficient and normal dietary conditions were analysed for protein content and number of somites, as a measure of growth and developmental progression, respectively. A graphical plot of protein content against somite number of each embryo (Figure 5.5), illustrates that the relationship between growth and development is unaffected by maternal diet. For example, a thirty somite embryo from the folate-deficient diet group had a similar protein content to a thirty somite embryo from the normal diet group. However, as shown in section 5.3.4, a thirty somite embryo from the folate-deficient diet group would be approximately a day older in gestation age (E11.5) than a thirty somite embryo from the normal diet group (E10.5). Thus collectively the results suggest that it is the relationship between growth/development and time (gestational age) which is perturbed by the folate-deficient diet.

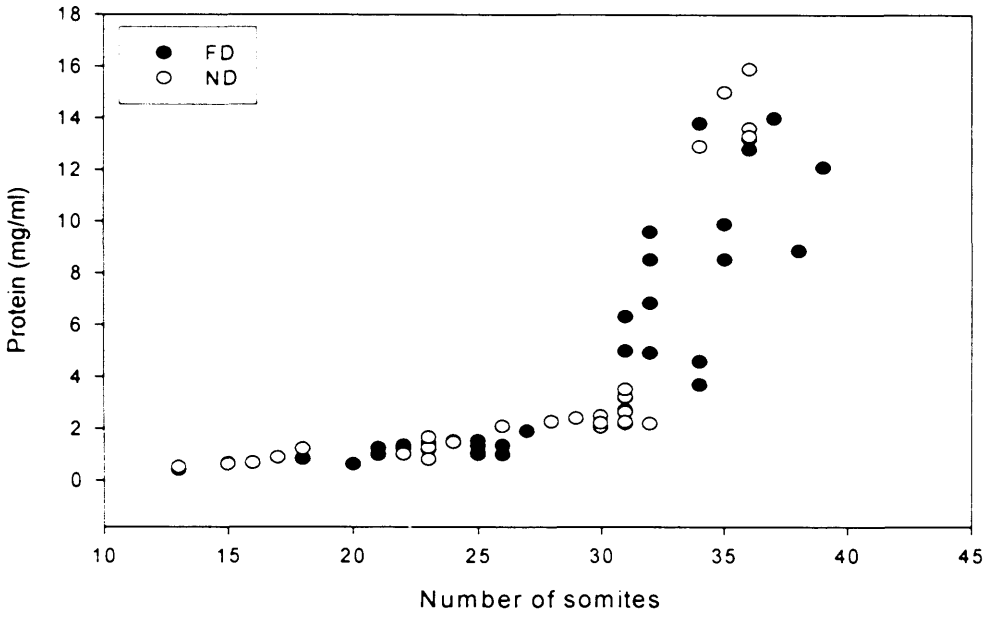

Figure 5.5. The relationship between embryonic growth (protein concentration) and development (somite number) for *splotch* embryos from the folate-deficient (FD) and normal (ND) diet groups. All genotypes were pooled together for analysis.

5.3.7 Development of *L.Casei* microbiological assay for the measurement of folate levels in neurulation-stage embryos

In order to study embryonic folate levels following maternal dietary intervention, the *L.Casei* microbiological assay was adapted to allow measurement of mono- and polyglutamylfolate levels in individual whole neurulation-stage embryos. Briefly, whole mouse embryos were sonicated to produce a homogeneous solution suitable for analysis. Aliquots from the homogenised solution then needed to be diluted to be within the read-out range of an assay. Folates are unstable and require antioxidants when extracted and assayed from tissues, and sodium ascorbate was therefore used as the diluent. The pH of the sodium ascorbate solution was also predicted to inhibit the activity of endogenous conjugase enzymes (Pfeiffer and Gregory, III, 1996) that may be present in the embryo, thereby preventing deconjugation and enabling monoglutamylfolate levels to be measured.

To determine polyglutamylfolate levels, an aliquot of embryo homogenate was incubated with conjugase extract (partially purified rat serum) and diluted with ascorbic acid to achieve optimal pH for the reaction (Pfeiffer and Gregory, 1996). The

conjugase enzyme removes the glutamate chain to form assayable monoglutamates from the polyglutamates. Therefore, when this sample is analysed the result is the summation of the monoglutamyl- and polyglutamylfolate embryonic content. In order to calculate the polyglutamylfolate levels, the monoglutmylfolate level (measured in the absence of conjugase) is then subtracted.

To ensure that sonicating the embryo was a suitable method for production of a completely homogenised uniform solution, all ten aliquots from a single embryo sample were analysed in parallel to determine if there was any significant variation between aliquots (Figure 5.6). Statistical analysis by ANOVA indicated that the fluctuations in folate content between the aliquots were insignificant ($p = 0.438$). The mean folate content was 7.52 pg of folate per well with a standard deviation of 0.35 pg of folate per well. The coefficient of variation (CV%) was equal to 4.60%. Hence, sonicating the embryo was found to be a suitable procedure to produce a uniform solution for the analysis of folate.

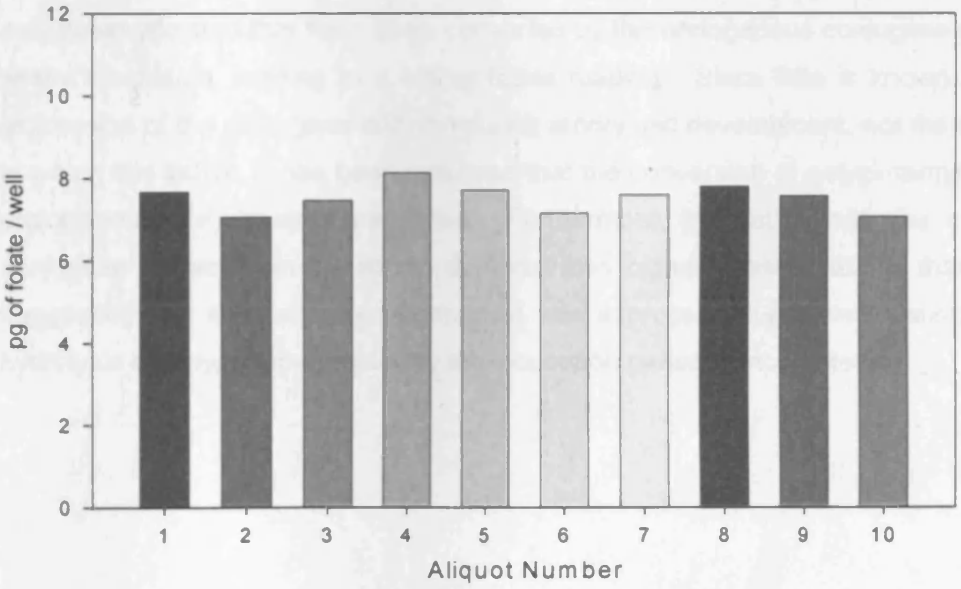

Figure 5.6. Variation in monoglutamylfolate content between sample aliquots. An E10.5 non-mutant CD-1 embryo was homogenised in 100 µl and separated into ten 10 µl aliquots for analysis.

To establish whether the assay was suitable to analyse polyglutamylfolate levels, in addition to monoglutamylfolate, in mouse embryos, an E9.5 CD1 mouse embryo was treated with the conjugase extract for varying time intervals (as described in section

2.10.3). Incubation with conjugase over time resulted in an increasing concentration of measurable folate with time (Figure 5.7) since the polyglutamylfolates present in the embryo sample were being progressively de-conjugated to assayable monoglutamylfolates. After 30 min a plateau was reached when presumably all polyglutamylfolates present had been de-conjugated to monoglutamylfolates. The conjugase extract (partially purified rat serum) was dialysed to remove all small molecules including folate and analysis of extract alone confirmed that there was no detectable folate present in the serum. Analysis of the same embryo sample using the monoglutamylfolate analysis conditions (stated in section 2.10.3) revealed that the concentration of monoglutamylfolate was 19.8 ng folate / mg protein. This is similar to the concentration found at the initial time point (zero) using the polyglutamylfolate analysis conditions.

Of note, it is possible that neurulation-stage embryos endogenously express conjugase enzyme (gamma-glutamylhydrolase) which during the assay incubation period at 37 °C converts embryonic polyglutamylfolates to monoglutamylfolates. This would mean that the method used to quantify monoglutamylfolate levels may also detect some polygluatmylfolates that have been converted by the endogenous conjugase during the assay incubation, leading to a higher folate reading. Since little is known about the expression of the conjugase enzyme during embryonic development, nor the conditions at which it is active, it has been assumed that the conversion of polyglutamylfolates by endogenous conjugase is negligible. Furthermore, incubation with the exogenous conjugase extract from rat serum demonstrates higher folate readings than without, suggesting that if enodgneous conjugase was expressed during neurulation then the hydrolysis of polyglutamates during the incubation period is incomplete.

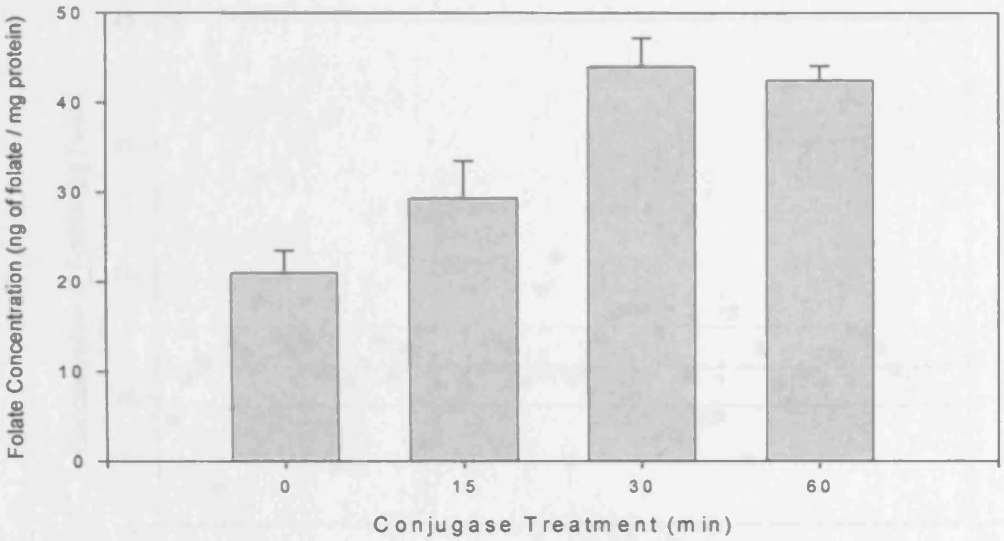

Figure 5.7. Incubation with conjugase over time resulted in increasing concentrations of measurable folate. An E9.5 CD1 mouse embryo sample was incubated with conjugase extract for increasing time periods. Aliquots were removed at intervals and assayed for folate content. Values are given as mean ± standard error of the mean.

Despite following a standardised protocol, some variation was observed within and between assays. This is because the bacteria are extremely sensitive to small changes in assay conditions, both between wells and plates and from day to day. This can be due to pipetting errors, variation in oven temperature, weighing errors, variations in the composition of all reagents and insufficient plate sealing, all of which can affect the growth of the bacteria. This can change the plot equation for the standard curve and/or the results obtained for a sample read-out. Although sufficient measures were taken to minimise these problems, variation still occurred and this needed to be monitored. To do this two quality control samples (pools of sonicated E9.5 and E10.5 CD1 embryos) were included in each assay and guidelines were in place for qualifying variation between sample results (see section 2.10.4). The graph below illustrates how the measured folate content varied in the E9.5 quality control between assays (Figure 5.8). If there was a large variation in both QC results from a single assay compared to other assays, the subsequent results for the analytical samples run on the same day were discarded (see section 2.10.5.4 for further details).

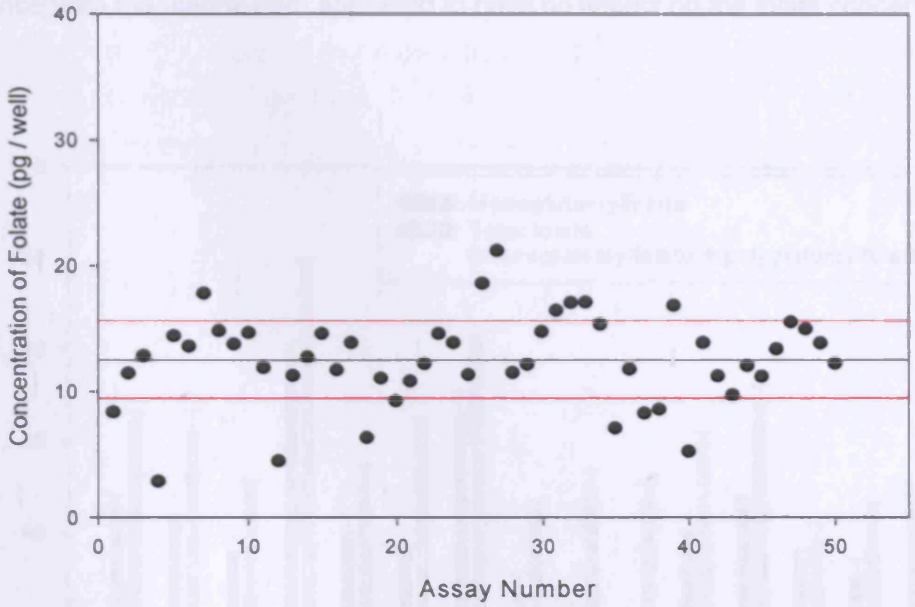

Figure 5.8. Inter-day variation in measured total folate content of an E9.5 QC sample. The QC was prepared as stated in section 2.10.4. The black line represents the mean, with the red lines representing 1xSD.

Since there was little data available concerning folate content in neurulation stage mouse embryos, it was decided to establish some basic parameters using the non-mutant CD-1 mouse strain. Firstly, the variation within a litter was evaluated. Secondly, the effect of position of each embryo within the uterine horn on embryonic folate content was established. Thirdly, the relationship between monoglutamylfolate and polyglutamylfolate levels was investigated. To do this, monoglutamylfolate and total folate levels were assayed in each embryo from a non-mutant CD1 litter (Figure 5.9). Embryonic folate levels were normalised to protein to adjust for variability in embryo size.

The results show that both the monoglutamylfolate and total folate concentration is highly variable within a single litter. This removes the need in later studies to cluster data from different litters for statistical analyses but emphasises the need for analysis of several embryos for a particular experimental condition. In the majority of embryos the total folate concentration was higher than the monoglutamylfolate concentration in each embryo. However, the embryos in position 13 and 15 had virtually equal concentrations of monoglutamylfolate and total folate, suggesting low levels of polyglutamylfolate. The mean ratio of monoglutamylfolate / total folate

(monoglutamylfolate + polyglutamylfolate) is 0.70. Position within the uterus or distance from the uterine horn appeared to have no impact on the folate concentration.

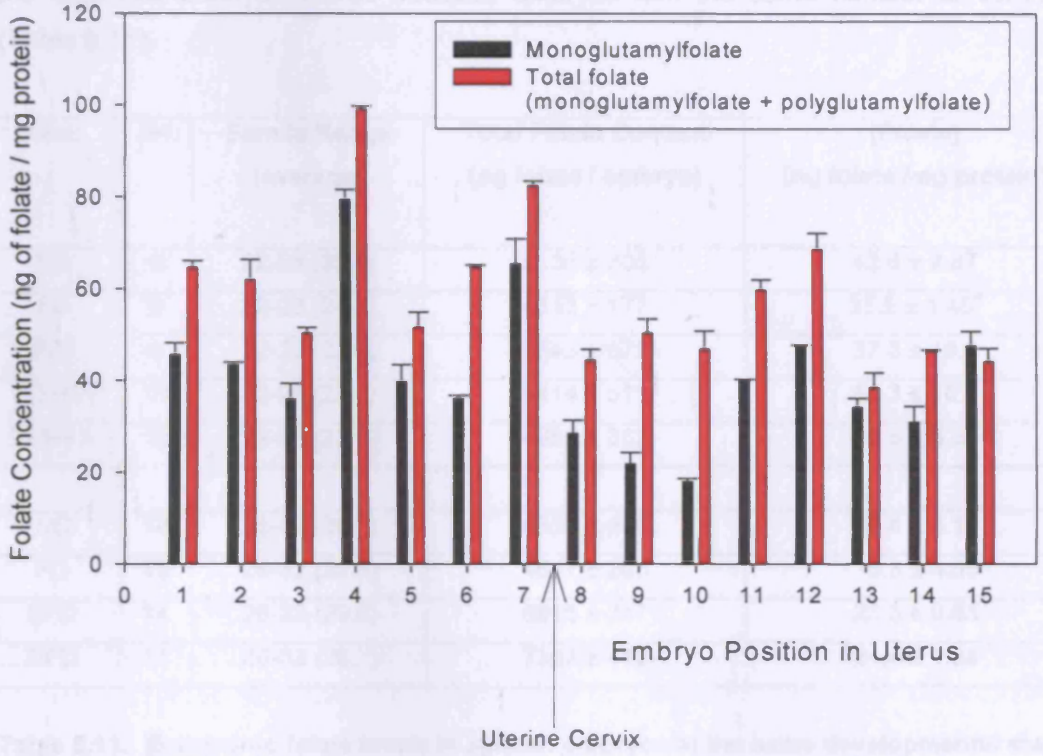

Figure 5.9. Monoglutamylfolate and total folate concentrations vary between embryos within a litter. The litter was collected an E9.5 from a wild-type CD-1 dam. The uterine position is numbered, starting with 1, from one end of the uterine horn going towards the uterine cervix and then back up the uterine horn in a sequential order.

5.3.8 Investigating embryonic folate levels following dietary intervention.

Once the *L.casei* microbiological assay had been adapted to measure embryonic folate, it was used to study folate levels in *splotch* embryos that developed under different dietary conditions. One approach to study the effects of all the different diets and supplements on embryonic folate levels would be to compare splotch embryos at the same gestational age. However, it must be appreciated that embryos from the FD and FID group are significantly smaller and developmentally retarded compared to the ND group (section 5.3.4). Therefore, changes in folate content would simply reflect

changes in size whereas, when normalised to protein, the FD embryos may appear to have a greater folate concentration because they are smaller and developmentally retarded. Therefore, the total folate (monoglutamylfolate + polyglutamylfolate) content and concentration was determined in splotch embryos collected at E10.5-E11.5 and the data has been compared between embryos with the same number of somites (Table 5.11).

Diet	n=	Somite Range (average)	Total Folate Content (pg folate / embryo)	[Folate] (ng folate /mg protein)
ND	6	22-26 (23.0)	5135 ± 305	42.6 ± 2.87
FD	9	22-26 (24.1)	4613 ± 177	35.5 ± 1.46#
FID	5	22-26 (23.4)	3743 ± 679	37.3 ± 10.2
FD+FA	11	22-26 (23.6)	5414 ± 511	50.3 ± 10.0
FID+FA	9	22-26 (23.8)	4955 ± 352	48.5 ± 3.35
ND	14	26-32 (30.1)	8857 ± 650	36.4 ± 3.14
FD	10	26-32 (29.6)	4647 ± 205	16.3 ± 4.55
BFD	14	26-32 (29.6)	6916 ± 317	23.3 ± 0.65
DFD	11	26-32 (28.7)	7347 ± 412	24.4 ± 1.34

Table 5.11. Embryonic folate levels in *splotch* embryos at the same developmental stage (the same number of somites). Folate values are given as mean ± standard error of the mean. # $p < 0.05$ when compared to ND. FD, Folate-deficient Diet; ND, Normal Diet; BFD, Bacterial Folate-deficient Diet; DFD, Dietary Folate-deficient Diet; FID, Folate- and Inositol-deficient Diet, FD+FA, Folate-deficient Diet + FA, FID+FA, Folate- and Inositol-deficient Diet + FA.

In *splotch* embryos that have developed between 22 and 26 somites (Table 5.11), the folate content per embryo was lower in embryos from the folate-deficient diet than the normal diet group but the difference was not significant ($p = 0.136$). In contrast, the folate concentration per mg of protein was also significantly reduced ($p = 0.03$) by the folate-deficient diet. Inositol- and folate-deficiency (FID) had no further effect on embryonic folate content ($p = 0.080$) or concentration ($p = 0.305$), compared to folate deficiency alone (FD).

Maternal folic acid supplementation of *splotch* embryos in the folate-deficient diet group (FD+FA) caused an increase in total folate content of 801 pg and an increase in folate concentration of 14.8 ng folate / mg protein (Table 5.11). However statistical analysis

demonstrated that this change in embryonic folate content ($p = 0.080$) and concentration ($p = 0.305$) was not statistically significant compared to folate-deficient embryos. Similarly, maternal folic acid supplementation to embryos in the folate and inositol deficient diet (FID+FA) caused a non-significant increase in folate content and concentration of 342 pg/embryo ($p = 0.192$) and 13.0 ng folate/mg protein ($p = 0.201$), compared to offspring of the FID fed dams. The lack of statistical significance is most likely to be due to the variation of embryonic folate levels. This would suggest that the response of individual embryos to maternal supplementation varies, and this could explain why neural tube closure occurs in some embryos following supplementation but not in others.

To further study the effects of the bacterial and dietary folate-deficient diet, *splotch* embryos that had developed between 26 and 32 somites were also grouped for analysis (Table 5.11). At this later stage of neurulation, *splotch* embryos from the folate-deficient diet had a significantly reduced folate content (Holm-Sidak; $p < 0.001$) and folate concentration ($p < 0.001$) compared to embryos developing under normal diet conditions.

There were no significant differences in embryonic folate content and concentration between embryos from the bacterial or the dietary folate-deficient diet. However, the total folate content of embryos from the bacterial and the dietary folate-deficient diet groups was significantly lower ($p = 0.001$ and $p = 0.03$, respectively) than for the normal diet group and significantly greater ($p = 0.001$ and $p < 0.001$, respectively) than for the folate-deficient diet. Similarly, embryonic folate concentrations from the bacterial and the dietary folate-deficient diet groups were significantly lower ($p < 0.001$ and $p = 0.003$, respectively) than for the normal diet group. Thus, embryonic folate levels for these two control diets are intermediate between the embryonic folate levels for the folate-deficient and the normal diet (Table 5.11). Overall, these results reveal that in order to have the maximum effect on embryonic folate status the diet needs to be deficient in both dietary and bacterial folate content.

A

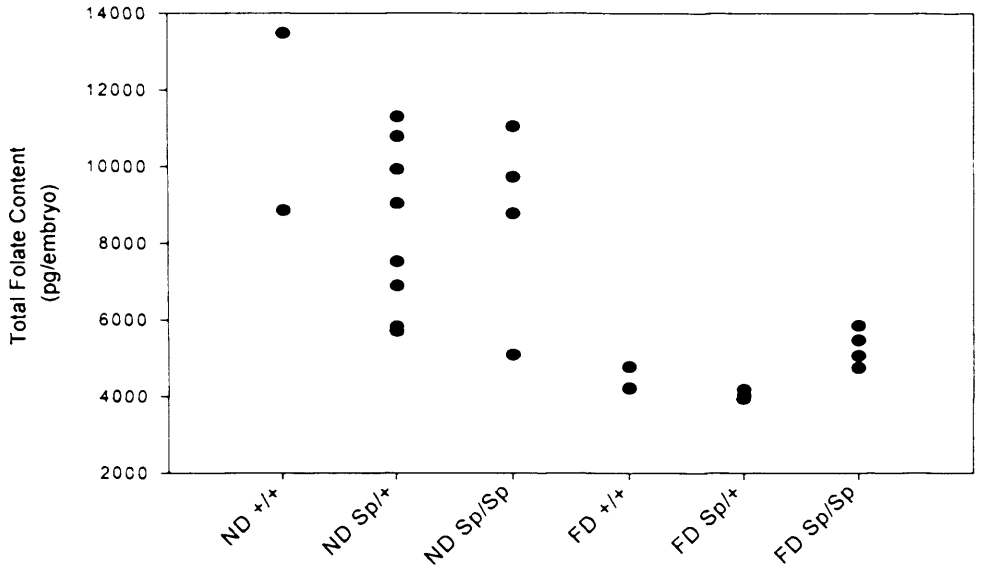

B

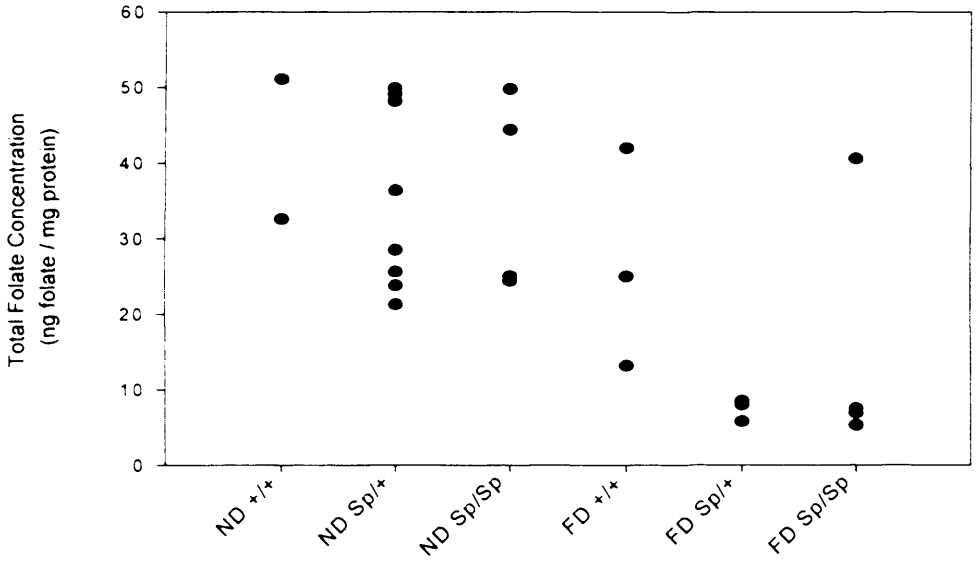

Figure 5.10. Mean total folate content (pg/embryo) and folate concentration (ng folate / mg protein) in *splotch* embryos that have developed between 26-32 somites following dietary intervention and supplementation: analysis by genotype. Each data point represents an individual embryo. ND, normal diet, FD, folate deficient diet.

Analysis of embryonic folate levels by genotype demonstrated that embryonic folate content and concentration are randomly distributed irrespective of genotype (Figure 5.16). Hence, the Sp^{2H} mutation has no apparent effect on embryonic folate status, under either normal or folate deficient dietary conditions. Thus, it appears to be a summation of the embryonic genotype and folate status which is responsible for the

increased incidence of cranial NTDs among *Pax3* deficient embryos when the diet is deficient of folate.

5.3.9 Detailed analysis of mono- and polyglutamylfolate levels with respect to developmental stage in *splotch* embryos

To illustrate how the embryonic monoglutamylfolate content and concentration change with development under different dietary conditions, the data was plotted against somite number (Figure 5.11). As expected, the total monoglutamylfolate content increases with development under normal dietary conditions, presumably since a larger and more developed embryo would have a greater folate content (Figure 5.11A). Up to approximately the thirty somite stage, embryos from the FD and ND dietary groups have similar levels of monoglutamylfolate, but as development proceeds the monoglutamylfolate content fails to increase under folate-deficient conditions. Indeed in the FD group, the monoglutamylfolate content appears to decrease with development such that more developed embryos contain less folate. For statistical purposes, the data was analysed by linear regression (see section 5.2.3) and the gradients of the graph lines were found to be significantly different ($p = 0.005$).

When folate levels were normalised to protein content (Figure 5.11B), the embryonic monoglutamylfolate concentration was found to decrease with development under normal dietary conditions. Thus, there was less folate available per mg of tissue suggesting a rapid turnover of folate metabolites at this stage of development or insufficient regulation of folate to keep pace with the rapid growth. Under folate-deficient conditions, the embryonic monoglutamylfolate concentration also decreased with development but the rate of decrease (gradient of the graph line) is slightly greater. At some stages of development, for example when the embryos have developed 23 somites, embryos appear to have the same folate concentration irrespective of dietary conditions, whereas when comparing embryos with 30 or more somites, the embryos from the normal diet group seem to have a higher folate concentration compared to embryos from the folate-deficient diet group. Statistical analysis by linear regression (see section 5.2.3) demonstrates that the gradients of the two graphs are significantly different (p-value < 0.001).

A

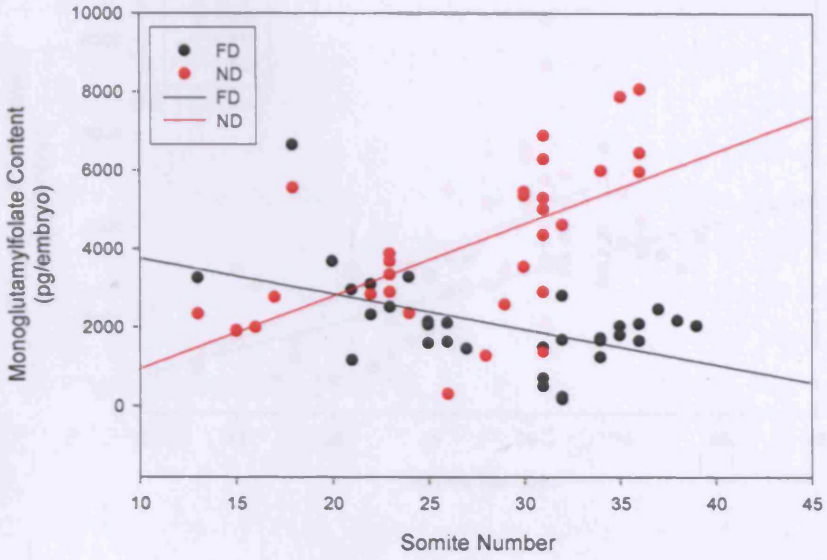

B

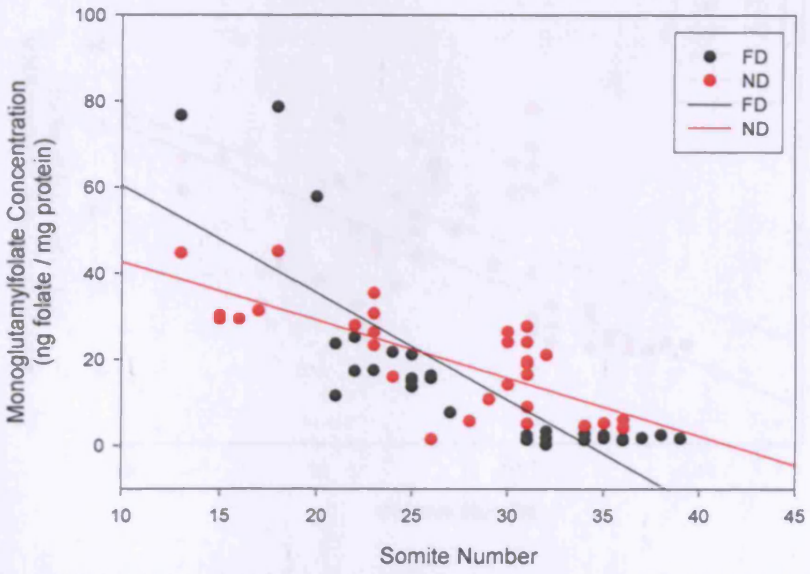

Figure 5.11. Comparison of monoglutamylfolate levels in *splotch* embryos between the folate-deficient (FD) and the normal diet (ND) group. The graphs show (A) monoglutamylfolate content per embryo (pg of folate / embryo) vs. somite number, and (B) embryonic monoglutamylfolate concentration (ng folate / mg protein) vs. somite number. •, splotch embryos from the folate deficient group, •, splotch embryos from the normal diet group, Each data point represents an individual embryo (all splotch genotypes were pooled for analysis). Linear regression analysis demonstrates that the gradients of the graph lines are statistically different in 5.23.A (see section 5.2.3).

A

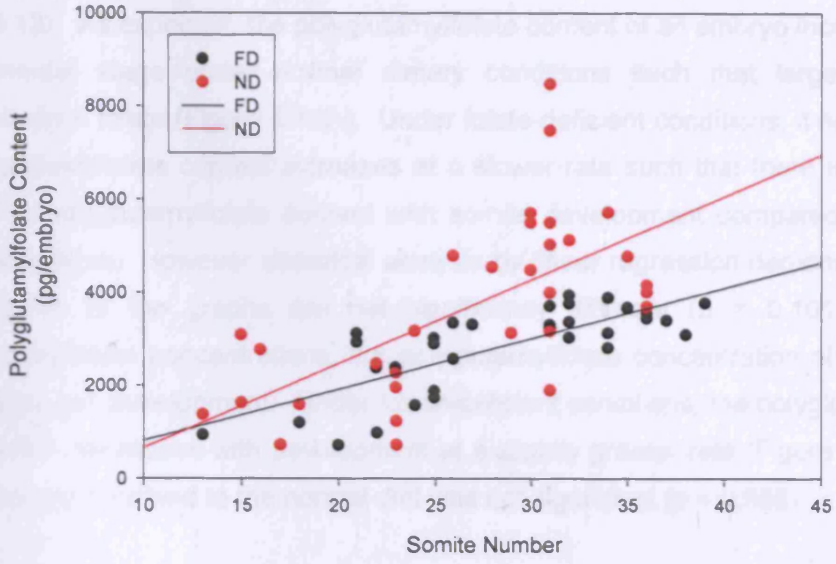

B

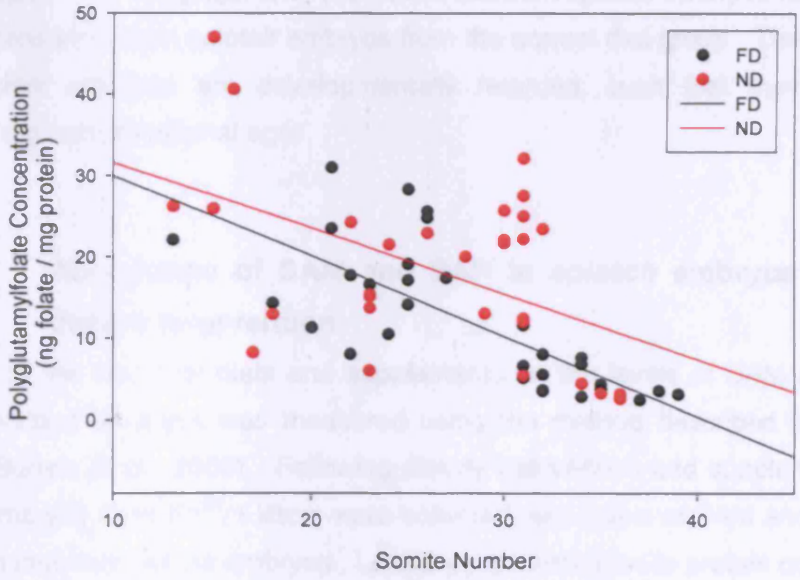

Figure 5.12. Comparison of polyglutamylfolate levels in *splotch* embryos between the folate deficient (FD) and the normal diet (ND) group. The graphs show (A) polyglutamylfolate content per embryo (pg of folate / embryo) vs. somite number, and (B) embryonic polyglutamylfolate concentration (ng folate / mg protein) vs. somite number. ●, splotch embryos from the folate deficient group, ●, splotch embryos from the normal diet group, Each data point represents an individual splotch embryo (all splotch genotypes were pooled for analysis). Linear regression analysis demonstrates that the gradients of the graph lines are not statistically different (see section 5.2.3).

It was next determined how the embryonic total polyglutamylfolate content and polyglutamylfolate concentration changes with somite number (developmental stage) (Figure 5.12). As expected, the polyglutamylfolate content of an embryo increased with developmental stage under normal dietary conditions such that larger embryos contained more folate (Figure 5.12A). Under folate-deficient conditions, it appears that the polyglutamylfolate content increases at a slower rate such that there is a smaller increase in polyglutamylfolate content with somite development compared to normal dietary conditions. However statistical analysis by linear regression demonstrates that the gradients of the graphs are not significantly different ($p = 0.101$). As for monoglutamylfolate concentrations, the polyglutamylfolate concentration also appears to decrease with development. Under folate-deficient conditions, the polyglutamyfolate concentration decreases with development at a slightly greater rate (Figure 5.12B) but the difference compared to the normal diet was not significant ($p = 0.555$).

If embryonic folate concentrations were to be compared for embryos at the same gestational age (Figure 5.11B and 5.12B) the data presented would show, due to the negative gradient of the graph line, that folate-deficient splotch embryos had a greater folate concentration than *splotch* embryos from the normal diet group. This is because folate-deficient embryos are developmentally retarded, such that they have less somites at a given gestational age.

5.3.10 Abundance of SAM and SAH in *splotch* embryos following dietary intervention

The effect of the maternal diets and supplements on the levels of SAM and SAH in neurulation-stage embryos was measured using the method described in chapter 3 (also see Burren et al., 2006). Following dietary intervention and supplementation, a series of embryos from Sp^{2H}/+ litters were collected, and levels of SAM and SAH were analysed in individual whole embryos. Levels were normalised to protein concentration and correlated with developmental stage (Table 5.12) to show the abundance of embryonic SAM and SAH, and the SAM/SAH ratio (Figure 5.13), in each dietary group.

In embryos at E10.5 and E11.5, SAM levels were typically 100-140 fold higher than SAH levels in *splotch* embryos. As gestation proceeded, the concentration of SAM did not significantly change ($p = 0.887$) whilst the concentration of SAH increased significantly ($p = 0.012$). Due to the increased abundance of SAH, the ratio of SAM/SAH was significantly lower at E11.5 than at E10.5 ($p = 0.013$).

Maternal Treatment Group	n=	Age	Somite Number	SAM (nmoles/mg protein)	SAH (nmoles/mg protein)	Ratio SAM/SAH
ND	40	E10.5	29.7 ± 0.3	3.35 ± 0.26	0.024 ± 0.002	147 ± 6.8
ND	14	E11.5	40.1 ± 0.64	3.28 ± 0.29	0.033 ± 0.0037**	111 ± 18.1**
FD	18	E11.5	29.6 ± 0.9	2.94 ± 0.23	0.050 ± 0.011**	96 ± 12.4**
FD+FA	29	E11.5	28.7 ± 0.7	3.29 ± 0.35	0.041 ± 0.005	97 ± 14.2
FD+THY	13	E11.5	35.5 ± 0.3	3.58 ± 0.20	0.063 ± 0.004	59 ± 3.6##

Table 5.12. SAM and SAH abundance determined by LC-MS/MS in *splotch* embryos from each maternal treatment group. SAM and SAH were quantified in individual whole embryos. Values are given as mean (standard error of the mean. ND; Normal Diet, FD; Folate deficient Diet, FD+FA; Folate deficient Diet + Folic Acid; FD+THY; Folate deficient Diet + Thymidine. ** $p < 0.02$ when compared to ND at E10.5, ## $p < 0.02$ when compared to FD. All genotypes were pooled for analysis.

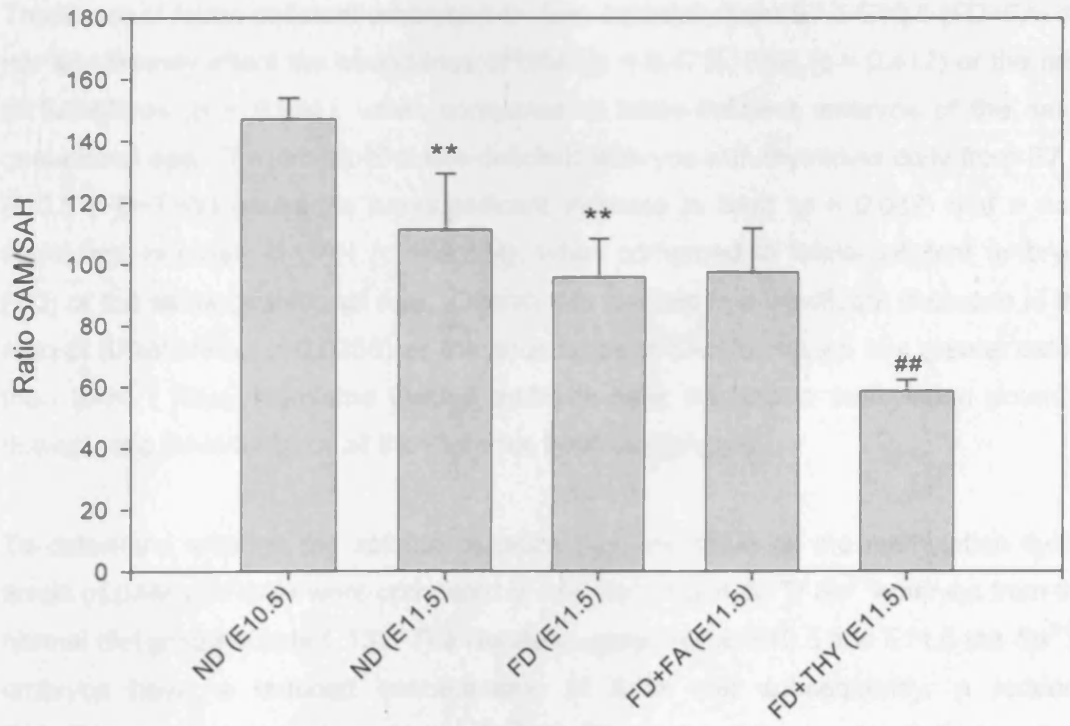

Figure 5.13. SAM/SAH ratio in *splotch* embryos from each maternal treatment group. Values are given as mean ± standard error of the mean. ** $p < 0.02$ when ND (E11.5) or FD compared to ND (E10.5), ## $p < 0.02$ when FD+THY compared to FD. All genotypes were pooled for analysis.

When comparing *splotch* embryos at the same developmental stage (with the same mean number of somites) from the normal diet group to embryos from the folate-deficient diet, folate deficiency appeared to reduce the level of SAM but this reduction was not statistically significant, yet the level of SAH did significantly increase by two-fold ($p = 0.002$). This slight decrease in SAM together with the increased SAH caused a significant decrease in the ratio of SAM/SAH ($p < 0.001$) in folate-deficient *splotch* embryos compared to *splotch* embryos developing under normal dietary conditions.

When comparing *splotch* embryos at the same gestational age (with different mean number of somites) from the normal diet and folate-deficient diet groups there was no significant difference in the level of SAM ($p = 0.307$) or SAH ($p = 0.213$). Similarly, the ratio of SAM/SAH, when comparing embryos at E11.5, was unchanged by folate deficiency ($p = 0.417$). Therefore despite folate-deficient *splotch* embryos being smaller and developmentally retarded, the abundance of SAM and SAH was consistent with gestational age therefore the methylation potential was reduced at an earlier stage of embryonic development as defined by somite number.

Treatment of folate-deficient embryos with folic acid daily from E7.5-E10.5 (FD+FA) did not significantly affect the abundance of SAM ($p = 0.472$), SAH ($p = 0.412$) or the ratio of SAM/SAH ($p = 0.934$), when compared to folate-deficient embryos of the same gestational age. Treatment of folate-deficient embryos with thymidine daily from E7.5-E10.5 (FD+THY) caused a non-significant increase in SAM ($p = 0.062$) and a non-significant increase in SAH ($p = 0.334$), when compared to folate-deficient embryos (FD) of the same gestational age. Overall this resulted in a significant decrease in the ratio of SAM/SAH ($p = 0.0258$) as the abundance of SAH increased to a greater extent than SAM. Thus, thymidine treated embryos have the lowest methylation potential (lowest ratio SAM/SAH) of all the maternal treatment groups.

To determine whether the *splotch* mutation had any effect on the methylation cycle, levels of SAM and SAH were compared in +/+, Sp^{2H}/+ and Sp^{2H}/ Sp^{2H} embryos from the normal diet group (Table 5.13). The results suggest that at E10.5 and E11.5 the Sp^{2H}/+ embryos have a reduced concentration of SAM and subsequently, a reduced SAM/SAH ratio compared to +/+ and Sp^{2H}/ Sp^{2H} embryos. However, statistical analysis demonstrates that this is not significant at either embryonic day (ANOVA; $p > 0.02$). Thus, there was no apparent effect of *splotch* genotype on the abundance of SAM and SAH, or the ratio of SAM/SAH.

Although the *splotch* genotype did not affect the abundance of SAM or SAH under normal dietary conditions, it is possible that the *splotch* genotype could further affect the abundance of SAM and SAH under folate-deficient conditions. To investigate this hypothesis, the abundance of SAM, SAH and the ratio of SAM/SAH in Sp^{2H}/Sp^{2H} embryos was analysed (Table 5.13). Overall, this revealed similar results to the analysis of all *splotch* genotypes pooled together (Table 5.13).

Genotype of embryo	Diet	n=	Age	Somite Number	SAM (nmoles/ mg protein)	SAH (nmoles/ mg protein)	Ratio SAM/SAH
+/+	ND	5	E10.5	30.8 ± 0.4	3.59 ± 0.71	0.021 ± 0.005	183 ± 20.4
$Sp^{2H}/+$	ND	29	E10.5	29.7 ± 0.3	3.28 ± 0.30	0.025 ± 0.002	137 ± 7.4
Sp^{2H}/Sp^{2H}	ND	6	E10.5	28.7 ± 0.6	3.44 ± 0.87	0.021 ± 0.005	168 ± 15.6$^{\#\#}$
+/+	ND	5	E11.5	40.2 ± 1.1	3.22 ± 0.23	0.031 ± 0.006	125 ± 33.7
$Sp^{2H}/+$	ND	3	E11.5	39.3 ± 0.3	2.43 ± 0.02	0.027 ± 0.000	91 ± 0.7
Sp^{2H}/Sp^{2H}	ND	6	E11.5	40.5 ± 0.7	3.75 ± 0.34$^{\#\#}$	0.037 ± 0.004**	110 ± 15.3**
Sp^{2H}/Sp^{2H}	FD	4	E11.5	31.5 ± 2.0	2.56 ± 0.31	0.030 ± 0.008	98 ± 17.6
Sp^{2H}/Sp^{2H}	FD+FA	12	E11.5	27.5 ± 1.2	3.30 ± 0.46	0.046 ± 0.011	87 ± 11.1
Sp^{2H}/Sp^{2H}	FD+THY	2	E11.5	35.0 ± 0.0	2.73 ± 0.20	0.047 ± 0.017	66 ± 19.9

Table 5.13. SAM and SAH abundance determined by LC-MS/MS in +/+, $Sp^{2H}/+$ and Sp^{2H}/Sp^{2H} embryos. SAM and SAH were quantified in individual whole embryos. Values are given as mean (standard error of the mean). ** $p < 0.02$ when compared to ND at E10.5. $^{\#\#}$ $p < 0.02$ when compared to FD.

5.4 Conclusion and Discussion

5.4.1 Folate deficiency affects maternal folate metabolism

Female Sp^{2H} heterozygous mice fed the folate-deficient diet exhibited decreased whole blood folate and increased plasma homocysteine. The lowered maternal folate and the increase in homocysteine reported in this dietary study was consistent with previous results obtained in wild-type mice and rats fed similar folate deficient diets (Burgoon et al., 2002;Sohn et al., 2003). These changes in maternal folate and homocysteine, which can be rescued by folic acid, support the idea that the diets directly affect maternal folate metabolism.

5.4.2 Folate deficiency causes NTDs in Sp^{2H} embryos

This study demonstrates that a lack of maternal folate uptake via the diet increased the incidence of exencephaly among Sp^{2H} homozygotes and Sp^{2H} heterozygotes, without affecting litter size or resorption rate. Previously, low incidences of NTDs in heterozygous *splotch* have been reported only when mice also harboured a mutation in one Nf1 allele, identifying Nf1 as a genetic modifier (Lakkis et al., 1999). Recent research by Li and colleagues using the *splotch* (*Sp*) mouse demonstrated that the incidence or severity of NTDs was not affected by a diet deficient in folic acid (Li et al., 2006). In contrast, this study uses the folate-sensitive Sp^{2H} mouse model in which NTDs have been previously shown to be rescued following folic acid supplementation (Fleming and Copp, 1998).

Other studies using folate-deficient diets (Burgoon et al., 2002;Heid et al., 1992) demonstrate that folate deficiency does not cause an increase in the incidence of NTDs in wild-type mice. Similarly, in this study, folate-deficient wild-type mice from Sp^{2H} litters did not develop NTDs. The incidence of NTDs in wild type mice under normal breeding conditions is approximately 0.3-4.2 per 1000 embryos (Sakai, 1989). Thus, in order to detect the 14-27% fold increase in incidence demonstrated in mutant embryos in this study, it would be necessary to analyse a vast number of wild-type embryos. Therefore, the possibility that folate deficiency may cause NTDs in a very small percentage of wild-type embryos cannot be excluded.

Comparison of maternal folate levels in *splotch* compared to other strains suggests that maternal uptake of folate is not affected by *Pax3* deficiency. Additionally, analysis by embryonic genotype shows that the genetic mutation in *Pax3* does not affect embryonic folate levels, the abundance of SAM or SAH or, growth and development.

Thus, it appears that the folate deficient diet affects folate metabolism and embryonic growth and development independent of *Pax3* deficiency. However the alternative, that folate deficiency enhances the detrimental effect of *Pax3* deficiency on neurulation, may be true. Since the mechanism underlying the neural tube defect in Sp^{2H} homozygotes remains unclear, it is difficult to investigate this hypothesis. Overall, the etiology of NTDs in folate-deficient Sp^{2H} embryos appears to be multifactorial in nature, possessing both genetic (*Pax3* mutation) and environmental (dietary folate content) components.

5.4.3 Bacterial and dietary folate sources of folate need to be removed to induce effective folate deficiency

Research using radio-labelled precursors of bacterially synthesised folate has shown that at least 18% of the dietary folate requirement can be met by folate absorption across the large intestine (Asrar and O'Connor, 2005). For these reasons this study included an antibiotic in the diet to kill the gut bacteria which provide a major source of folate. Investigation of maternal biomarkers reveals that a diet deficient in both bacterial and dietary folate is required to have maximal effects on maternal folate and homocysteine. Also for folate deficiency to interact with the Sp^{2H} mutation to increase the incidence of NTDs the diet needs to lack both forms of folate. The bacterial (BFD) and dietary folate deficient diets (DFD) did not detrimentally affect embryonic growth and development and had intermediate effects on embryonic folate status.

Burgoon et al. reported no differences in red blood cell folate, plasma folate, plasma homocysteine, resorptions or fetal weight between the normal breeding diet and the same diet with the antibiotic added. They conclude that the antibiotic could be removed, providing the mice remained on wire mesh floor to prevent coprophagy. Indeed it has been shown that fecal levels of folic acid can be 14-fold higher than that found in the diet (Ebino et al., 1988). Wire mesh cages were not used in this investigation, such that mice did have access to folate in their feces which presumably accounts for a proportion of the residual folate in dams and embryos. The fecal supply of folate may have been sufficient to prevent the poor reproductive outcome which was witnessed in other studies in which wire mesh flooring was utilised (Burgoon et al., 2002;Heid et al., 1992) and enabled the incidence of NTDs to be assessed. Alternatively, discomfort to the mice caused by long term housing on wire mesh flooring may have increased the rate of resorptions.

The folate deficient diet used by Li et al. in their study of folate deficiency in *Sp* mice did include an antibiotic, but not all of the dietary folate was removed (the "severely folic acid deficient diet" used contained 0.3 mg FA / kg diet) and it appears the mice were housed in normal breeding cages such that the dams had access to both dietary and fecal folate. Although it was shown that maternal homocysteine levels were significantly increased by the diet, my study demonstrates that changes in homocysteine do not necessarily predict a change in the incidence of NTD, as shown using the diet deficient in dietary folate (DFD). Thus, it is unclear whether the study by Li et al. induced folate deficiency to an extent which would be necessary to increase the incidence of NTDs in *Sp* embryos.

5.4.4 Folate deficiency causes retardation of embryonic growth and developmental progression

Overall, growth and developmental examinations revealed that *splotch* embryos from the folate-deficient diet group were growing and developing at a slower rate. Indeed evidence from this study appears to show that folate controls the rate of embryonic growth and development, yet the relationship between growth and development is unchanged. Therefore, when a folate-deficient embryo reaches the appropriate developmental stage at which neural tube closure occurs, the correct amount of cells should be present but the embryo would be older by gestational age. It is not yet fully understood if a disturbance of the time window in which neural tube closure occurs could affect the highly complex events, at the cellular, biochemical and molecular level, required for successful neurulation such as a dissociation between growth and correct gene expression.

An alternative explanation is that during neurulation embryos are growing and developing at the normal rate but they are delayed in growth and development due to an event which happened prior to neurulation. This raises the possibility of a critical period in early gestation when folate deficiency might retard growth and development, subsequently resulting in defective neurulation. However, the extent of growth and developmental retardation appears to be getting progressively worse with gestational age suggesting that this is not the case.

Embryonic growth and developmental delay caused by folate deficiency was shown to be independent of splotch genotype in this study. Copp and Fleming likewise demonstrated that the growth profile (DNA content plotted against somite number) of Sp^{2H} homozygotes and heterozygotes was indistinguishable from that of wild type on a

normal breeding diet (Fleming and Copp, 1998). Thus, it appears that *Pax3* deficiency in Sp^{2H} embryos does not affect embryonic growth or development. Research by Bennett and colleagues using *Sp* mice also demonstrated that under normal dietary conditions the overall growth, measured by somite number, does not differ between *Sp* genotypes during neural tube closure (Bennett et al., 1998). However a detailed evaluation of progression through neural tube closure in *Sp* embryos collected at several time-points during the period of neural tube closure revealed that there was a significant delay in the time taken to close the neural tube in both *Sp/+* and *Sp/Sp* embryos (Bennett et al., 1998). Therefore, the increased incidence of cranial NTDs among *splotch* embryos could be explained by an extended delay in neural tube closure which is worsened by a lack of folate.

It remains to be fully established whether folate deficiency affects neurulation directly or indirectly via retardation of growth and development. The diets deficient in either bacterial (BFD) or dietary (DFD) folate, which did not detrimentally affect embryonic growth or development, failed to increase the incidence of NTD. However, analysis of size and developmental progression between affected and unaffected Sp^{2H} homozygous embryos revealed that the smaller and developmentally retarded embryos were not necessarily the ones affected by an NTD. This suggests that under these conditions, when growth and development is unaffected, other factors are important in the etiology of NTDs.

5.4.5 Folate deficiency affects embryonic one-carbon metabolism

None of the previous studies to date have measured embryonic folate levels following folate deficiency or supplementation. By adapting the *L.casei* microbiological folate assay, I was able to demonstrate that the folate content increases during neurulation but the concentration of folate (normalised to protein) decreases with development. The concentration of SAH was also found to increase during neurulation, causing a decrease in the SAM/SAH ratio. These findings suggest that after neurulation embryos have a reduced folate concentration and methylation potential, which is further reduced by the folate-deficient diet.

In folate-deficient embryos the rate of increase in embryonic folate content with development was lower than under normal dietary conditions, whereas the folate concentration (normalised to protein) decreased at a slightly greater rate. When comparing embryos with the same number of somites, the folate-deficient embryos had

a lower mean folate content and concentration compared to the normal diet embryos such that during neural tube closure there would be less folate available.

Under folate-deficient conditions it seems as if embryonic growth and folate content have become unsynchronised such that the folates appear to be 'diluted' by more cells. This imbalance may be the cause of the reduced rate of embryonic growth and development. There are several potential outputs from the folate cycle which could affect embryonic growth and development including nucleotide synthesis and methylation. Analysis of methylation cycle metabolites revealed that the abundance of embryonic SAH was increased by the folate-deficient diet, resulting in a decrease in the SAM/SAH ratio. Increased SAH could potentially inhibit methyltransferases involved in the methylation of genes or proteins required for embryonic growth and development.

5.4.6 Possible mechanisms of folate-sensitive NTDs in *splotch* embryos

Mechanisms leading to cranial NTDs are not clear. Proposed mechanisms include faulty release of neural crest cells from the margins of the cranial neural folds (Copp et al., 2003) or imbalance of extracellular matrix components in the neural folds (Bennett et al., 1998). A further mechanism arose from an investigation which revealed that neuroepithelial cells in *splotch* (*Sp*) embryos undergo unscheduled apoptosis at the site of the neural tube prone to defects (Phelan et al., 1997). This led to a study whereby p53 deficiency, caused by either a genetic mutation or use of a chemical inhibitor, rescued not only apoptosis but also NTDs in *Sp* homozygous embryos, suggesting that Pax-3 regulates neural tube closure by inhibiting p53-dependent apoptosis (Pani et al., 2002).

It is possible that all of the above proposed mechanisms could be worsened by growth and developmental delay caused by the folate-deficient diet. If an embryo is growth retarded and receives a genetic insult, it may not then be able to successfully repair itself or undergo 'catch-up' growth (Shum and Sadler, 1988). For example, if excess apoptosis does occur in splotch mice (Pani et al., 2002), the embryo may be able to undergo catch-up growth under normal dietary conditions to prevent the increased apoptosis from affecting neural tube closure. In contrast, under folate-deficient conditions, the lack of folate metabolites may prevent catch-up growth and thereby cause an increased incidence of NTD.

5.4.7 How does folic acid rescue NTDs in folate-deficient *splotch* embryos?

A key outstanding question is how folic acid prevents NTDs. In this study I investigated possible mechanisms by which folic acid prevents NTDs induced by folate deficiency, focussing on possible effects on growth or methylation. Maternal folic acid supplementation was found to increase maternal whole blood folate and reduce the incidence of NTDs in folate-deficient embryos. Whereas, maternal thymidine supplements did not reduce the incidence of NTDs in folate-deficient embryos, they apparently reduced the severity of the cranial defect. Interestingly, folic acid did not stimulate growth, whilst thymidine did stimulate growth. This suggests a possible protective effect of growth stimulation on the severity of the NTD, whereas folic acid may have had a localised effect on proliferation enabling cranial neural tube closure to occur successfully.

Embryonic metabolic analysis showed that folic acid supplements did not significantly affect embryonic folate status and there was no detectable change in the abundance of SAH or the SAM/SAH ratio. Confusingly, treatment with thymidine was found to decrease the methylation potential, which could be postulated to be due to scavenging of folate metabolites away from the methylation cycle, thereby causing a build-up of homocysteine which is converted to SAH. Perhaps inhibition of the methylation cycle counteracts the beneficial effect on embryonic growth and therefore, combined supplementation with thymidine and folic acid may have been a better preventative treatment. In summary, the data is not conclusive of either argument.

5.4.8 Summation of the effect of folate and inositol deficiency

A diet deficient in inositol as well as folate (FID) was found to increase the incidence of exencephaly to 95%-100% among Sp^{2H} homozygotes, yet there was no further change in maternal and embryonic folate status compared to the folate deficient diet (FD). This indicates that inositol deficiency does not affect maternal or embryonic folate metabolism but there is an indirect interaction between inositol and folate metabolism to increase the risk of NTDs among Sp^{2H} embryos. The folate and inositol deficient diet (FID) did not cause cranial NTDs in wild-type or Sp^{2H} heterozygous embryos. Thus, the interaction between folate and inositol deficiency represents a summation of the effects of each deficiency to produce a disturbance of cranial neurulation in homozygous Sp^{2H} embryos that is greater than with either deficiency alone.

5.4.9 A mouse model of folate-responsive neural tube defects

In summary, the *splotch* mouse model described in the present study shows that folate deficiency causes developmental delays that may be related to increased incidence of neural tube defects. In this model reduced embryonic folate status and poor methylation capacity correlate with decreases in maternal folate and increases in homocysteine. This model also affords the opportunity to test the effects of supplemental vitamins to determine the potential for neural tube defect prevention.

CHAPTER 6

Investigating the relationship between maternal dietary folate intake, embryonic one carbon metabolism and the incidence of neural tube defects in the *curly tail* NTD mouse model

6.1 Introduction

6.1.1 Folate resistant NTDs

The UK Medical Research Council trial demonstrated that folic acid prevented up to 70% of recurrent NTDs (Wald et al., 1991). This result highlights the possibility that the remaining cases are resistant to folate. Indeed there have been reports of multiple NTD pregnancies within a single family despite high intake of folic acid (Cavalli and Copp, 2002; unpublished findings). This resistance to the prevention of NTDs by folic acid has been mirrored in several mutant mouse strains including the *Ephrin A5*, *curly tail* and *Bent tail* mouse models (Holmberg et al., 2000; Seller, 1994; Essien and Wannberg, 1993).

6.1.2 The *curly tail* NTD mouse model

The *curly tail* (*ct*) mutant mouse, originally identified in 1950, was first described by Hans Grüneburg (Gruneberg, 1954). Since then it has been maintained as a random bred closed colony whereby all individuals are assumed to be homozygous for the *ct* mutation. The *ct* mutant phenotype is incompletely penetrant and has variable expressivity, whereby 50% of homozygous embryos develop a curled tail which is accompanied with spina bifida in 10-20% of these embryos. A small proportion of curly tail embryos also develop exencephaly, yet relatively large variations in the frequency of this phenotype, ranging from 0-9%, have been reported (Van Straaten and Copp, 2001).

The *curly tail* mutant mouse has been the focus of over 50 papers, despite the *ct* gene only recently being identified (Ting et al., 2003). The interest in this mouse model is in part due to its striking resemblance to human NTDs. Indeed, the *curly tail* mouse model was the first example of a closure failure during primary neurulation at the level often seen in human cases of spina bifida. Incomplete penetrance with major effect of genetic and environmental factors resembles multifactorial etiology of human NTDs. Also, there is increased alphafetoprotein (AFP) in the amniotic fluid (Adinolfi et al., 1976) and maternal serum (Jensen et al., 1991), as demonstrated for anencephaly and spina bifida in humans. In addition several studies have shown that exencephaly is more common in females whilst males show a slight preponderance to spina bifida, as is seen in humans (Copp and Brook, 1989;Embury et al., 1979;Seller et al., 1979). Also, there is an association of spina bifida with hydrocephalus in *ct* embryos, as in humans (Van Straaten and Copp, 2001).

The first sign of an abnormality in *curly tail* embryos is the reduced cell proliferation in the hindgut and notochord at the 27-29 somite stage (E10.5) (Copp et al., 1988a) and in the dorsal tailbud at E9.5 (Peeters et al., 1996). The growth imbalance causes a ventral curvature of the caudal axis which opposes closure of the neural tube and thus delays posterior neuropore closure (Brook et al., 1991). Delayed closure results in the curled tail phenotype, whereas a more prolonged delay prevents closure of the posterior neuropore leading to spina bifida. At the 27-29 somite stage, expression of *RARβ* in the hindgut and *RARγ* in the tail bud is reduced (Chen et al., 1995). The expression of *RARβ* is known to play a key role in cell proliferation, and down-regulation of *RARβ* may therefore be responsible for the cell proliferation defect and the subsequent growth imbalance in caudal tissues.

6.1.3 Prevention of NTDs in curly tail

Treatment of *curly tail* embryos with folic acid or other folate derivatives was found to have no effect on the incidence of NTDs (Seller, 1994b). Methionine was also found to be ineffective at reducing the frequency of NTDs and methionine loading did not result in an aberrant rise in homocysteine (Seller, 1994b;Van Straaten et al., 1995). Furthermore, the deoxyuridine suppression test detected normal folate cycling in *curly tail* embryos (Fleming and Copp, 1998). Thus, the *curly tail* mouse has become known as a genetic model of "folate resistant" NTDs. It is believed to represent a possible paradigm for the sub-category of human NTDs which do not respond to folic acid (Van Straaten and Copp, 2001), estimated at around 30-50% (Wald et al., 2001).

Folate-resistant NTDs in the *curly tail* mouse can be prevented by inositol. A possible role for inositol in NTDs was first suggested by studies in which embryos were cultured in the absence of specific vitamins during cranial neurulation. Deficiency of inositol caused exencephaly, and among mouse strains tested, *curly tail* was particularly sensitive with 71% of embryos developing exencephaly (Cockroft et al., 1992). This study prompted Greene and Copp (1997) to test whether inositol might prevent spinal NTDs, and they showed a significant protective effect both in embryo culture and following maternal supplementation. Since myo-inositol treatment causes up-regulation of *RARβ* (Greene and Copp, 1997), it has been hypothesised that inositol rescues closure defects by promoting cell proliferation (Van Straaten and Copp, 2001). Future studies of cell proliferation in caudal tissues would provide further clarification.

6.1.4 Genetics of *curly tail*

Genetic analysis has demonstrated that the *ct* mutation is semi-dominant since the curly tail phenotype is occasionally observed in heterozygous embryos (Gruneberg, 1954), whilst the penetrance of the NTD phenotype is highly influenced by genetic background (Embury et al., 1979;Neumann et al., 1994). For example, crosses to other strains have resulted in low NTD frequencies (Neumann et al., 1994). Indeed, three modifier loci have been identified which affect the incidence of NTDs (Letts et al., 1995;Neumann et al., 1994).

The lack of a wild-type control strain, and the fact that all mice in the *curly tail* colony are homozygous, poses potential difficulties in interpreting the results of research on *curly tail* NTDs. To overcome this problem, a partially congenic strain has been developed by successive backcrosses which is wild-type (SWR strain) throughout the mapped *ct* genetic region on chromosome 4 but shares more than 90% of its genetic background with the *curly tail* stock (G. Pavlovska and A.J. Copp, unpublished). The *curly tail* congenic mouse model ($+/+^{ct}$) will be used as a control strain herein.

6.1.5 Investigating folate deficiency in *curly tail*

As described previously in chapter 5, folate-deficiency increased the incidence of exencephaly in folate-sensitive *splotch* embryos. It was originally hypothesised that folate deficiency would not affect the incidence of exencephaly among *curly tail* embryos, owing to the resistance of spina bifida in this model to the preventative effects of folic acid. However, unexpectedly this study demonstrates that induction of folate deficiency by dietary intervention does cause a high frequency of exencephaly in so-called "folate-resistant" curly tail embryos. Also, for the first time, dietary folate deficiency is shown to cause NTDs in wild-type congenic embryos and remarkably these folate-deficiency induced NTDs can be rescued with exogenous inositol. This study has used the analytical techniques described in chapter 5 to investigate the biochemical effects of the diets on folate and one-carbon metabolism in *curly tail* dams and their embryos. Overall, the findings of this study emphasise that folate deficiency increases the risk of cranial NTDs and suggest that inositol may be a possible therapy to use in conjunction with folic acid to prevent more cases of NTDs.

6.2 Materials and Methods

6.2.1 Mouse diets

Female *ct/ct* and *+/+*^{ct} mice were maintained on five different diets, as described in section 5.2.1, to test the effects of folate deficiency on developing embryos. To attempt to rescue the NTDs, pregnant mice on the folate deficient diet received an interperitoneal (i.p.) injection of 10 mg FA / kg body weight (FD+FA), 20 mg FA / kg body weight (FD++FA) or 400 mg myo-inositol (MI) / kg body weight (FD+MI) at embryonic days E7.5, E8.5, E9.5 and E10.5 (Table 6.1).

Diet	FA (mg/kg)	Inositol (g/kg)	SST (mg/kg)	Supplements (per kg body weight)	Description
FD+FA	X	1.9	10	10 or 20 mg folic acid	Folate-deficient Diet + FA
FD+MI	X	1.9	10	400 mg myo-inositol	Folate-deficient Diet + MI

Table 6.1. Details of the experimental diets fed to female *curly tail* mice. Supplements were administered by i.p. injection at embryonic day E7.5, E8.5, E9.5 and E10.5.

6.2.2 Metabolite Analysis

Maternal blood was collected and plasma prepared as described in section 2.4. Maternal whole blood and embryonic folate concentrations were measured by the *Lactobacillus casei* microbiological assay using the method described in section 2.10.5. Total plasma homocysteine levels (free + protein-bound) were determined by the method described in section 2.4. Plasma homocysteine and whole blood folate were able to be measured in the same samples from a population of dams following optimisation of the blood collection method. Embryonic SAM and SAH were analysed in individual whole embryos as detailed in chapter 3.

6.2.3 Statistical Analysis

As described in section 5.2.3.

6.3 Results

6.3.1 The effect of folate deficiency on maternal folate and homocysteine.

A statistical comparison of whole blood folate and plasma homocysteine concentrations between *ct/ct* and $+/+^{ct}$ dams fed either diet (Table 6.2) did not reveal any differences between mouse strains indicating that the *ct* genetic defect does not affect maternal uptake of folate or maternal homocysteine metabolism compared to $+/+^{ct}$ dams.

Diet	Mouse Model	Whole Blood Folate (µg/ml)		Plasma Homocysteine (µmol/L)	
		n=	Mean ± SEM	n=	Mean ± SEM
ND	*ct/ct*	8	0.58 ± 0.05	7	3.53 ± 0.07
	$+/+^{ct}$	16	0.50 ± 0.03	5	3.54 ± 0.35
FD	*ct/ct*	12	0.18 ± 0.03$^{\#\#}$	7	20.20 ± 5.32$^{\#\#}$
	$+/+^{ct}$	8	0.11 ± 0.02$^{\#\#}$	5	14.09 ± 4.15$^{\#}$
BFD	*ct/ct*	9	0.37 ± 0.01$^{\#\#}$**	6	6.41 ± 0.46$^{\#\#}$
	$+/+^{ct}$	6	0.27 ± 0.07$^{\#\#}$**	6	5.66 ± 0.08$^{\#\#}$
DFD	*ct/ct*	10	0.19 ± 0.02$^{\#\#}$	4	13.91 ± 1.70$^{\#\#}$
	$+/+^{ct}$	9	0.17 ± 0.02$^{\#\#}$	5	12.80 ± 3.15$^{\#\#}$
FID	*ct/ct*	5	0.11 ± 0.02$^{\#\#}$		
	$+/+^{ct}$	3	0.09 ± 0.02$^{\#\#}$		

Table 6.2. Maternal whole blood folate and plasma homocysteine concentration following dietary intervention. Statistical analyses using the student t-test were between diet groups for each separate mouse model. FD, Folate-deficient Diet; ND, Normal Diet; BFD, Bacterial Folate-deficient Diet; DFD, Dietary Folate-deficient Diet; FID, Folate- and Inositol-deficient Diet. ** p-value < 0.02 when compared to FD group, $^{\#}$ p-value < 0.05 when compared to ND group, $^{\#\#}$ p-value < 0.02 when compared to ND group.

Analysis of the effects of dietary intervention on maternal folate levels in each mouse model (*ct/ct* and $+/+^{ct}$) did reveal significant changes (Table 6.2). After consumption of the folate-deficient diet for three consecutive weeks, *ct/ct* and $+/+^{ct}$ dams had a level only 22-31% of that in dams fed the normal diet (Table 6.2). Thus, whole blood folate levels were significantly reduced by the folate-deficient diet compared to the normal diet in both $+/+^{ct}$ ($p < 0.001$) and *ct/ct* ($p < 0.001$) dams. Similarly, $+/+^{ct}$ and *ct/ct* dams fed the dietary folate-deficient diet had a level only 33-34 % of that in dams fed the normal diet. In contrast, whole blood folate concentrations in the bacterial folate-deficient diet fed dams had only declined to 54-64% of that in dams fed the normal diet. Thus, the DFD reduced maternal folate to a lower level in both the *ct/ct* and $+/+^{ct}$ dams

compared to the BFD. In *ct/ct* and $+/+^{ct}$ dams fed the folate and inositol deficient diet, the whole blood folate concentration was 18-19% of that in dams fed the normal diet. This was the lowest folate level of all the diets studied, yet statistical analysis revealed that inositol deficiency had no further detrimental effect on maternal folate levels compared to the folate-deficient diets.

Plasma homocysteine concentrations varied among the different diet groups for each mouse model, with the lowest levels in *ct/ct* and $+/+^{ct}$ dams fed the normal diet and highest levels in *ct/ct* and $+/+^{ct}$ dams fed the folate-deficient diet (Table 6.2). The *ct/ct* and $+/+^{ct}$ dams fed the dietary folate deficient diet and the bacterial folate deficient diet had intermediate homocysteine levels. Overall, as with the *splotch* mouse model, maternal biochemical analyses showed that the folate-deficient diet resulted in lowered maternal folate status and increased levels of homocysteine. Bacterial folate deficiency (BFD) was sufficient to affect maternal folate but not homocysteine levels. Dietary folate deficiency affected both blood folate and homocysteine but was not as effective as combined bacterial and dietary deficiency.

To illustrate the inverse relationship between folate and homocysteine in maternal mice, the blood collection method was optimised to ensure sufficient blood was collected from a population of *ct/ct* and $+/+^{ct}$ dams to enable the measurement of both whole blood folate and plasma homocysteine in a single sample. This direct comparison between folate and homocysteine levels for each dam sacrificed shows that the higher the plasma homocysteine concentration, the lower the whole blood folate concentration (Figure 6.1). It also demonstrates that the order of severity of each diet on maternal folate and homocysteine levels is FD, DFD, BFD and ND, with the highest homocysteine and lowest folate levels found in the FD dietary group.

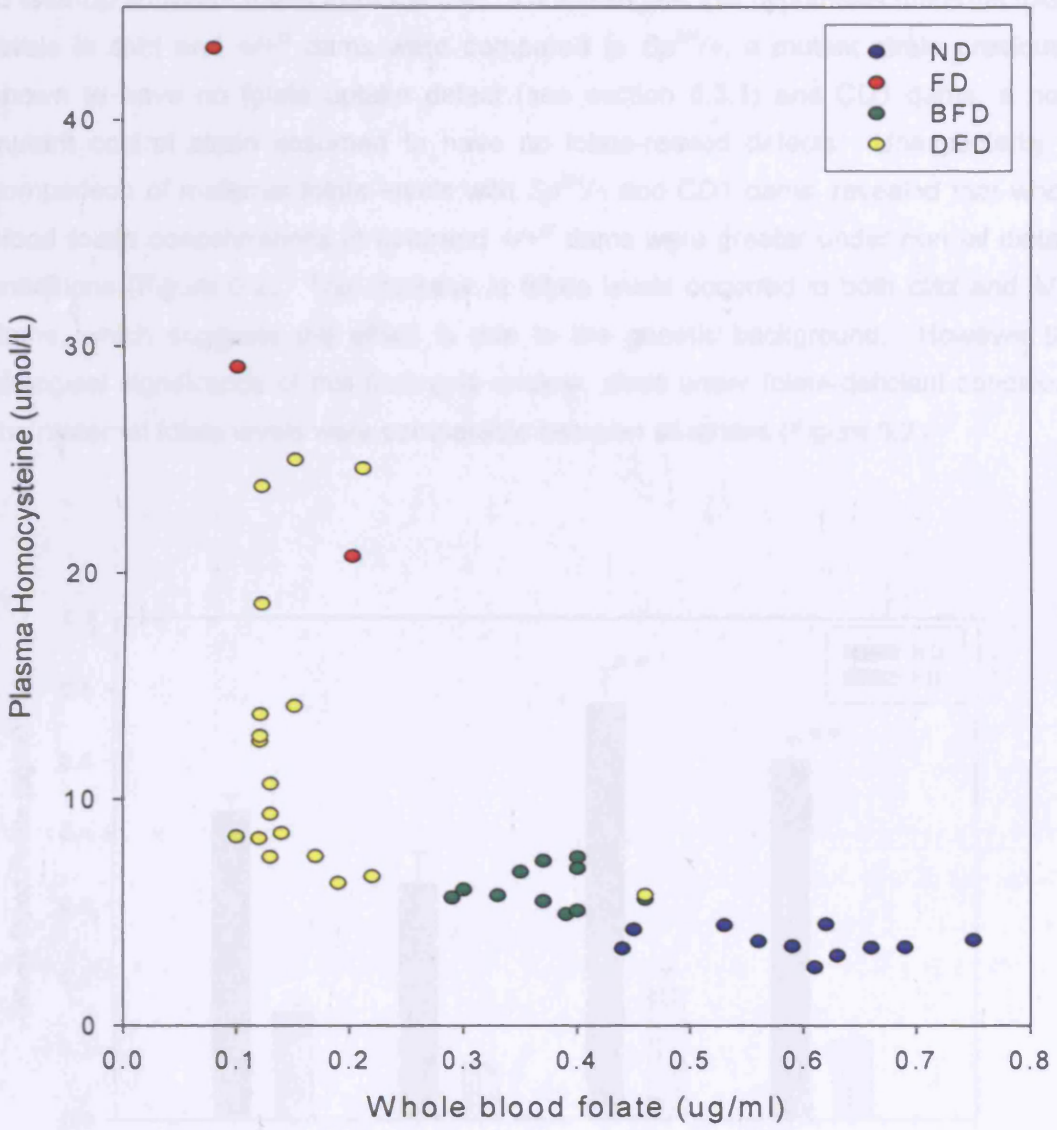

Figure 6.1. A direct comparison of whole blood folate and plasma homocysteine levels in *ct/ct* and +/+^{ct} dams following dietary intervention. Each data point represents the folate and homocysteine level within a single blood sample collected from each dam sacrificed. FD, Folate-deficient Diet; ND, Normal Diet; BFD, Bacterial Folate-deficient Diet; DFD, Dietary Folate-deficient Diet.

It is possible that *ct/ct* and *+/+^{ct}* dams have a defect in folate metabolism or are unable to take up sufficient folate from the diet. To investigate this hypothesis maternal folate levels in *ct/ct* and *+/+^{ct}* dams were compared to *Sp^{2H}/+*, a mutant strain previously shown to have no folate uptake defect (see section 5.3.1) and CD1 dams, a non-mutant control strain assumed to have no folate-related defects. Unexpectedly, a comparison of maternal folate levels with *Sp^{2H}/+* and CD1 dams, revealed that whole blood folate concentrations in *ct/ct* and *+/+^{ct}* dams were greater under normal dietary conditions (Figure 6.2). The increase in folate levels occurred in both *ct/ct* and *+/+^{ct}* dams, which suggests the effect is due to the genetic background. However the biological significance of this finding is unclear, since under folate-deficient conditions the maternal folate levels were comparable between all strains (Figure 6.2).

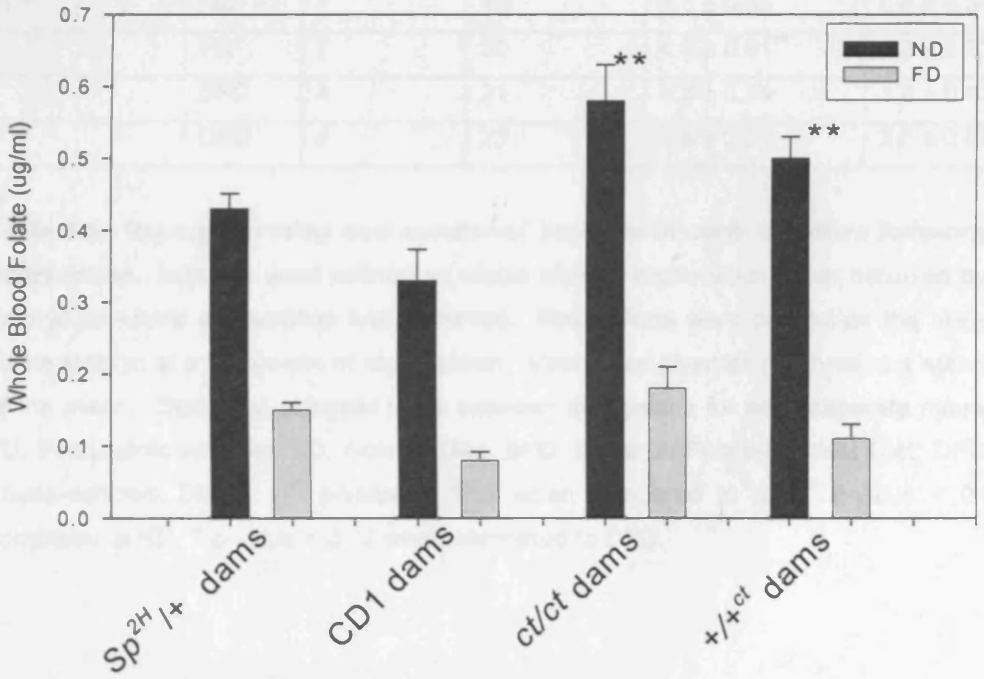

Figure 6.2. A comparison of maternal whole blood folate levels between mouse strains. Values given as mean ± standard error of the mean. FD, Folate-deficient Diet; ND, Normal Diet. ** p-value < 0.02 when compared to CD1 dams fed the normal diet (ND).

6.3.2 The effect of folate deficiency on reproductive success

The mean number of implants per litter and the mean number of resorptions per litter (Table 6.3) in *ct/ct* dams compared to $+/+^{ct}$ dams were not significantly different, irrespective of dietary conditions (ANOVA analysis of all data groups and Holm-Sidak pair-wise analysis).

Mouse Model	Diet	No. of litters	No. of total implants	No. of implants per litter[a]	No. of resorptions per litter[b]
ct/ct	ND	9	65	7.8 ± 0.13	0.6 ± 0.17
	FD	14	77	5.5 ± 0.53$^{\#\#}$	2.4 ± 0.43$^{\#}$
	BFD	6	41	6.8 ± 0.28	1.0 ± 0.16"
	DFD	5	33	6.8 ± 0.28	2.3 ± 0.17$^{\#\#}$
$+/+^{ct}$	ND	7	45	6.8 ± 0.83	0.6 ± 0.34
	FD	7	30	4.0 ± 0.91$^{\#\#}$	2.3 ± 0.72$^{\#\#}$
	BFD	4	21	5.3 ± 0.74	1.0 ± 0.17
	DFD	4	23	5.8 ± 0.31	2.0 ± 0.38

Table 6.3. Resorption rates and number of implants in *curly tail* litters following dietary intervention. Implants were defined as visible sites of implantation either occupied by a viable embryo or where a resorption had occurred. Resorptions were defined as the absence of a viable embryo at a visible site of implantation. Values are given as mean value ± standard error of the mean. Statistical analyses were between diet groups for each separate mouse model. FD, Folate-deficient Diet; ND, Normal Diet; BFD, Bacterial Folate-deficient Diet; DFD, Dietary Folate-deficient Diet. $^{\#\#}$ p-value < 0.02 when compared to ND, $^{\#}$ p-value < 0.05 when compared to ND, " p-value < 0.02 when compared to DFD.

Following dietary intervention it was apparent by observation that the folate deficient (FD) diet affected reproductive success in both mouse strains. Statistical analysis confirmed that the mean number of resorptions per litter under folate-deficient conditions was significantly greater than under normal dietary conditions in both *ct/ct* (Holm-Sidak; $p < 0.001$) and $+/+^{ct}$ (Holm-Sidak; $p = 0.006$) litters (Table 6.3). Correlating with this finding, the mean number of implants per litter under folate-deficient conditions was significantly decreased compared to normal dietary conditions in *ct/ct* litters (Holm-Sidak; $p < 0.001$) and $+/+^{ct}$ (Holm-Sidak; $p = 0.004$) (Table 6.3). To conclude, folate deficiency significantly affected reproductive success in both *ct/ct* and $+/+^{ct}$ litters. Since this effect was seen in both *ct/ct* and $+/+^{ct}$ mouse models it suggests

that it is due to the closely similar genetic background, rather than an effect of the folate-deficient diet on all strains as reproductive success was unaffected in *splotch* litters (see section 5.3.2).

In both *ct/ct* and $+/+^{ct}$, the dietary folate-deficient and the bacterial folate-deficient diets increased the number of implants per litter and decreased the number of resorptions per litter compared to the folate deficient diet (Table 6.3). However, the reproductive success was not as great as that recorded in the normal diet group. Statistical analysis demonstrates that the number of resorptions per *ct/ct* litter in the dietary folate-deficient diet was significantly less than for the normal diet (DFD vs. ND; Holm-Sidak $p = 0.001$) and, the bacterial folate-deficient diet (DFD vs. BFD; Holm-Sidak $p = 0.004$). The same trend was apparent in $+/+^{ct}$ litters but the results were not significant. Thus, it appears that the removal of folate from the diet had a worse effect on reproductive success than the addition of an antibiotic which eliminates bacterial sources of folate.

6.3.3 The effect of folate deficiency on the incidence of NTDs in *curly tail* embryos

The incidence of NTDs among both *ct/ct* and $+/+^{ct}$ litters at E10.5-E11.5 was noted following dietary intervention (Table 6.4). Unexpectedly, group-wise statistical analysis demonstrated that there was a significant effect of diet on the incidence of exencephaly in both *ct/ct* litters (Chi-square; $p < 0.001$) and $+/+^{ct}$ litters (Chi-square; $p = 0.001$).

The folate-deficient diet caused a significant increase in the incidence of exencephaly among *ct/ct* embryos, compared to *ct/ct* embryos in the normal diet group (Fishers Exact; $p < 0.001$). The folate-deficient diet also caused a significant number of $+/+^{ct}$ embryos to develop exencephaly, compared to $+/+^{ct}$ embryos from the normal diet group (Chi-square pair-wise; $p < 0.001$). In both *ct/ct* and $+/+^{ct}$, the extent of increase in NTD incidence was approximately 30%.

The incidence of exencephaly among embryos from the dietary folate-deficient and the bacterial folate-deficient litters was lower than among the folate deficient litters for both *ct/ct* and $+/+^{ct}$ litters. With the exception of *ct/ct* embryos from the bacterial folate-deficient diet group, the incidence of exencephaly was greater among embryos from the dietary folate-deficient and the bacterial folate-deficient litters in comparison to embryos from the normal diet group. Statistical analysis demonstrated that among *ct/ct* embryos the rate of exencephaly on the bacterial folate-deficient diet was significantly lower than for the folate-deficient diet (BFD vs. FD; Chi-square pair-wise; $p < 0.001$)

and, the dietary folate-deficient diet (BFD vs. DFD; Fishers Exact; p = 0.01). The same trend was apparent in $+/+^{ct}$ litters but the results were not statistically significant. Thus, it appears that the removal of folate from the diet has a greater effect on the incidence of exencephaly than the addition of antibiotic, which eliminates bacterial sources of folate.

Diet	*ct/ct*		$+/+^{ct}$	
	n=	EX	n=	EX
ND	48	9 (19)	42	0 (0)
FD	74	42 (57)##	38	11 (29)##
BFD	36	2 (6)**''	17	1 (6)
DFD	23	10 (44)	15	2 (13)

Table 6.4. Incidence of exencephaly (EX) in *curly tail* embryos following dietary intervention. Data are presented as number of embryos with percentage in each treatment group in parentheses. Exencephaly is defined as failure of cranial neural tube closure in embryos that have completed embryonic turning and have 18 or more somites. This is based on the observation that cranial neural tube closure, in vivo, is completed by the 18 somite stage in *ct/ct* and $+/+^{ct}$ embryos in our laboratory. FD, Folate-deficient Diet; ND, Normal Diet; BFD, Bacterial Folate-deficient Diet; DFD, Dietary Folate-deficient Diet. Statistical analyses using the Chi-square or Fisher's exact test were between diet groups for each separate mouse model. ## p-value < 0.02 when compared to ND, ** p-value < 0.02 when compared to FD, '' p-value < 0.02 when compared to DFD.

6.3.4 Analysing the development of *curly tail* embryos

After collecting litters from the folate-deficient diet groups, it became apparent that the diet affected the size and developmental progression of both *ct/ct* and $+/+^{ct}$ embryos (Figure 6.3). Folate-deficient embryos from E11.5 litters resembled embryos from normal E10.5 litters. Furthermore, there was wide variation in the size and development of folate-deficient embryos within a litter. Thus, some folate- deficient embryos were severely growth and developmentally restricted, while others were less affected. In the most severely affected embryos, morphological features were indistinct, which may indicate that the embryo was dying and would have been resorbed if development was allowed to continue.

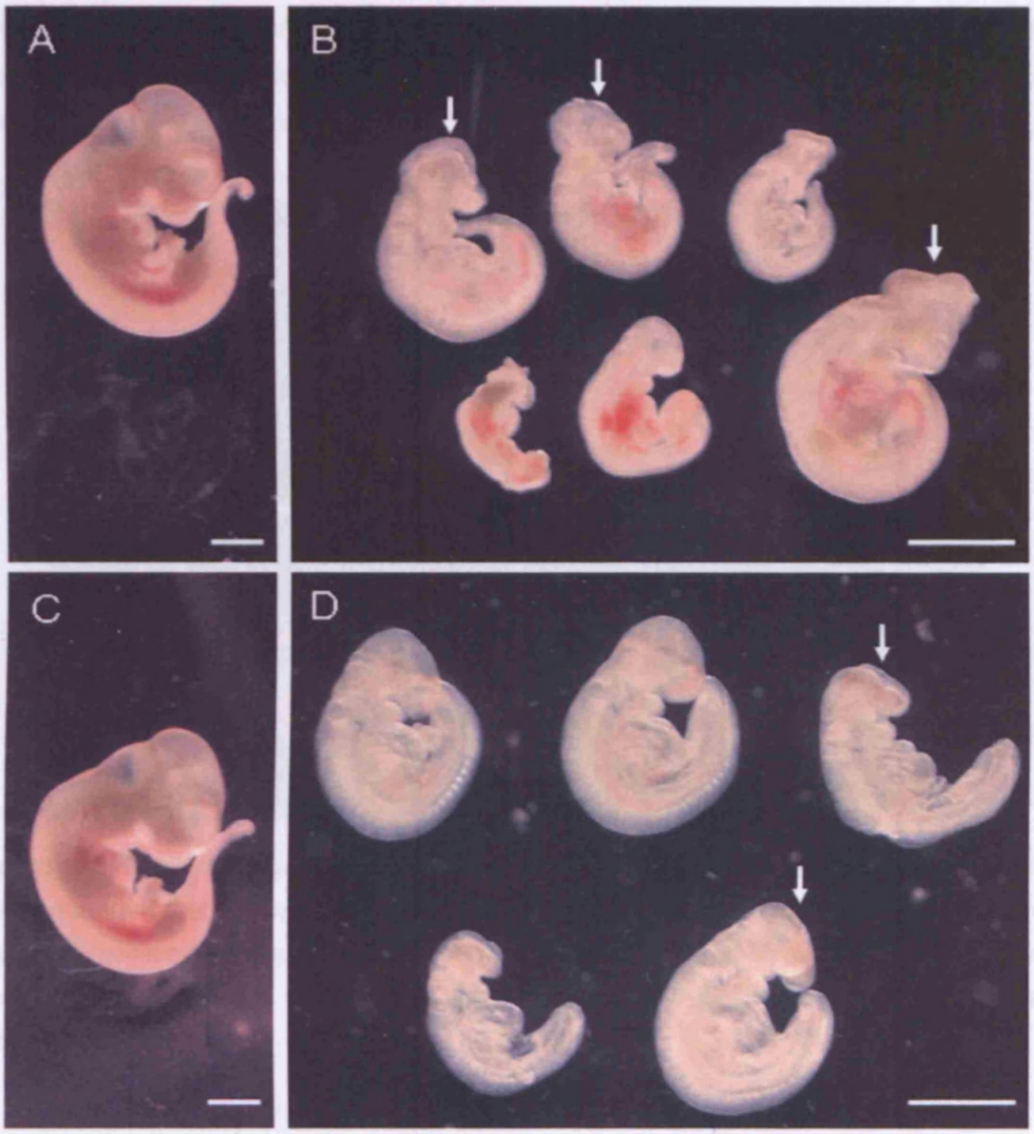

Figure 6.3. E11.5 *curly tail* embryos following dietary intervention. (A) *ct/ct* embryo (38 somites) with a curled tail from the normal diet group (ND), (B) a typical litter of *ct/ct* embryos (10-32 somites) from the folate deficient diet (FD) group, (C) $+/+^{ct}$ embryo (40 somites) with a normal, straight tail from the normal diet (ND) and (D) a typical litter of $+/+^{ct}$ embryos (24-32 somites) from the folate deficient diet (FD) group. Solid arrow indicates exencephaly, defined as persistently open cranial neural folds in an embryo with 18 or more somites. Scale bar is equivalent to 1mm.

A direct comparison of embryos from the bacterial and dietary folate-deficient diet groups (Figure 6.4) clearly shows that the removal of dietary folate, as opposed to the removal of bacterial folate, had the greater effect on embryonic growth and developmental retardation.

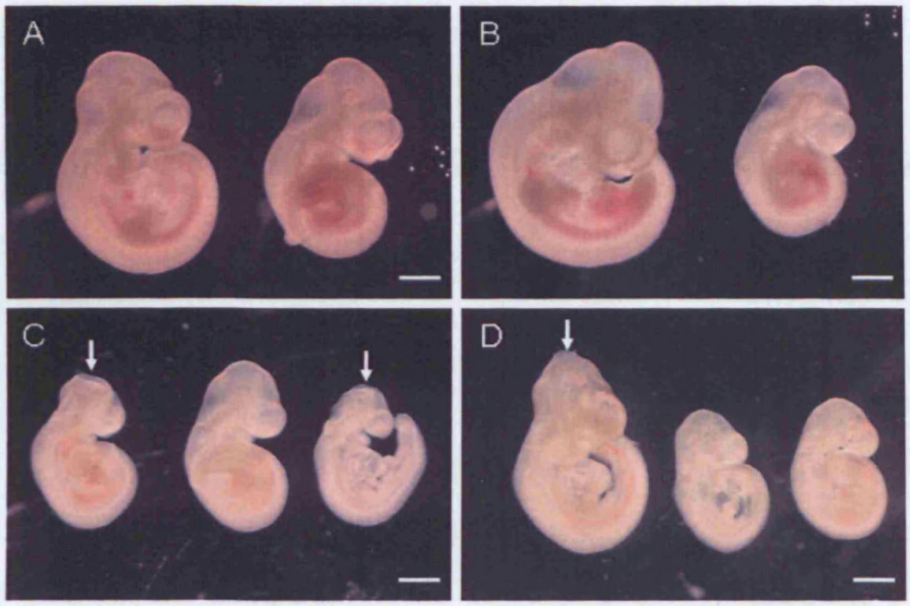

Figure 6.4. E10.5 *curly tail* embryos from the bacterial folate deficient (BFD) and dietary folate deficient diet (DFD) groups. (A) *ct/ct* embryos and (B) $+/+^{ct}$ embryos from the bacterial folate deficient diet (BFD) group. (C) *ct/ct* embryos and (D) $+/+^{ct}$ embryos from the dietary folate deficient diet (DFD) group. Solid arrow indicates exencephaly. Scale bar is equivalent to 1 mm at x2.0 magnification.

In order to make quantitative comparisons of embryonic developmental progression and size, the number of somites and the crown-rump length were recorded for E10.5 embryos (Table 6.5). Under normal dietary conditions (ND), the mean number of somites and crown-rump length was comparable between E10.5 *ct/ct* and $+/+^{ct}$ embryos. Similarly, under folate-deficient conditions, there was no significant difference in the mean number of somites and crown-rump length between E10.5 *ct/ct* compared to $+/+^{ct}$ embryos. Indeed developmental stage differences are not consistently observed between *ct/ct* and $+/+^{ct}$ embryos (N. Greene, personal communication).

Group-wise statistical analysis demonstrated significant variation in the size and development of E10.5 embryos following dietary intervention (ANOVA; $p < 0.001$). At E10.5, *ct/ct* and $+/+^{ct}$ embryos from the folate-deficient diet group were significantly

smaller and developmentally retarded than *ct/ct* and +/+^{ct} embryos from the normal diet group (Table 6.5). Folate deficient *ct/ct* and +/+^{ct} embryos were also significantly smaller and developmentally retarded compared to *ct/ct* and +/+^{ct} embryos from DFD and BFD litters (Table 6.5). Thus, the combined elimination of both dietary and bacterial forms of folate in the folate deficient (FD) diet has an acute effect on embryonic growth and development.

Diet	n=	Crown-rump length (mm)	n=	Number of somites
		ct/ct		
ND	31	3.84 ± 0.11**	24	31.3 ± 1.06**
FD	27	2.17 ± 0.07##	34	19.5± 0.84##
BFD	34	3.73± 0.09**	34	28.4 ± 0.44**
DFD	13	3.20 ± 0.18**##	13	26.4 ± 0.87**##
		+/+^{ct}		
ND	16	3.85 ± 0.12**	16	29.5 ± 0.53**
FD	14	2.19 ± 0.04##	10	15.9 ± 2.26##
BFD	8	3.47 ± 0.21**	8	26.9 ± 1.17**
DFD	7	3.90 ± 0.25**	7	28.9 ± 1.16**

Table 6.5. Development of E10.5 *curly tail* embryos following dietary intervention. Values given as mean ± standard error of the mean. FD, Folate-deficient Diet; ND, Normal Diet; BFD, Bacterial Folate-deficient Diet; DFD, Dietary Folate-deficient Diet. Statistical analyses using the Student t-test were between diet groups for each separate mouse model. ** $p < 0.02$ when compared to FD, ## $p < 0.02$ when compared to ND (Holm-Sidak).

The bacterial folate-deficient diet did not significantly affect embryonic growth and development compared to the normal diet group, in either *ct/ct* or +/+^{ct} (Table 6.5). In comparison, E10.5 *ct/ct* embryos from the dietary folate-deficient diet group were significantly smaller and developmentally retarded compared to E10.5 *ct/ct* embryos from the normal diet group (Table 6.5). However, +/+^{ct} embryos from the dietary folate-deficient diet group, were comparable in size and development to +/+^{ct} embryos from the normal diet group (Table 6.5). Notably, the DFD diet also had a greater effect on the incidence of exencephaly in *ct/ct* embryos than in +/+^{ct} embryos (Table 6.4).

6.3.5 The effect of folic acid and inositol supplementation on the incidence of NTD in folate deficient *curly tail* embryos.

The potential for NTD prevention of maternal supplemental folic acid (FA) and myo-inositol (MI) was tested in folate-deficient *ct/ct* and $+/+^{ct}$ embryos. Thus, dams fed the folate-deficient diet were treated with folic acid (at 10 or 20 mg/kg body weight) or *myo*-inositol (at 400 mg/kg body weight) at E7.5, E8.5, E9.5 and E10.5 by i.p. injection. The dams were sacrificed at E11.5 or E13.5 and the embryos collected for analysis. A dose of 10 mg/kg body weight was chosen as this was found to prevent NTDs in *splotch* (Fleming and Copp, 1998).

In comparison to un-supplemented *ct/ct* embryos from the folate-deficient diet group (FD), low dose supplemental folic acid (10 mg/kg) did not reduce the incidence of exencephaly (Table 6.6). Doubling the dose of folic acid to 20 mg/kg did reduce the incidence of exencephaly in *ct/ct* embryos, but the change was not significant ($p = 0.523$). The incidence of exencephaly among offspring of folate-deficient *ct/ct* dams supplemented with *myo*-inositol was higher than in unsupplemented folate-deficient litters but this was not statistically significant (Fishers Exact; $p = 0.118$, Table 6.6). Among folate deficient $+/+^{ct}$ embryos, the incidence of exencephaly following supplementation with 10 mg/kg folic acid was reduced but this was not significant (Fishers Exact; $p = 0.303$). Unexpectedly, none of the folate- deficient $+/+^{ct}$ embryos receiving *myo*-inositol supplementation developed NTDs (Fishers Exact; compared to FD, $p = 0.011$, compared to ND, $p = 1.00$).

Supplement	*ct/ct*		$+/+^{ct}$	
	n=	EX	n=	EX
ND	61	9 (15)	42	0 (0)
FD	82	42 (52)	38	11 (29)
FD+FA (10 mg/kg)	8	5 (63)	17	2 (12)
FD+FA (20 mg/kg)	11	4 (36)	-	-
FD+MI (400mg/kg)	7	6 (86)	18	0 (0)**

Table 6.6. Incidence of NTDs in folate deficient *curly tail* embryos following dietary supplementation with folic acid (FA) or myo-inositol (MI). Data are presented as number of embryos with percentage in each treatment group in parentheses. ND; Normal Diet, FD; Folate deficient Diet, FD+FA; Folate deficient Diet + Folic Acid; FD+MI; Folate deficient Diet + Myo-Inositol. Embryos were treated at E7.5, 8.5, 9.5, 10.5 (AM) and collected at E10.5 (PM) or E11.5. ** $p < 0.02$ when compared to FD.

To determine if supplemental folic acid or myo-inositol reduced the developmental delay caused by folate-deficiency, the number of somites at E11.5 was recorded. At E11.5, *ct/ct* and $+/+^{ct}$ embryos from the folate-deficient diet group (FD) were significantly developmentally retarded ($p<0.001$ and $p<0.001$, respectively) compared to embryos from the normal diet group (ND), as at E10.5 (Table 6.7). Among both folate deficient *ct/ct* and $+/+^{ct}$ embryos, neither supplemental folic acid (FD+FA) nor myo-inositol (FD+MI) had a significant effect on embryonic development compared to unsupplemented folate deficient (FD) embryos.

Diet	*ct/ct*		$+/+^{ct}$	
	n=	Number of somites	n=	Number of somites
ND	25	41.0 ± 0.47	14	36.9 ± 1.37
FD	33	27.7 ± 0.95$^{\#\#}$	17	27.6 ± 1.33$^{\#\#}$
FD+FA	17	29.2 ± 2.79$^{\#\#}$	8	27.8 ± 3.01$^{\#\#}$
FD+MI	6	25.8 ± 2.20$^{\#\#}$	13	30.3 ± 1.93$^{\#\#}$

Table 6.7. Developmental stage of folate deficient *curly tail* embryos at E11.5 following dietary supplementation with folic acid and myo-inositol. Values given as mean ± standard error of the mean. ND; Normal Diet, FD; Folate deficient Diet, FD+FA; Folate deficient Diet + Folic Acid; FD+MI; Folate deficient Diet + Myo-Inositol. $^{\#\#}p < 0.001$ when compared to ND (Holm-Sidak). Of note when comparing somite matched embryos, folate-deficient embryos are of a younger gestational age.

At E13.5, exencephalic and curled tail phenotypes were observed in both folic acid and myo-inositol supplemented *ct/ct* embryos (Figure 6.5). It also became apparent that the folate-deficient diet was affecting eye development in exencephalic embryos. Thus, embryos appeared to have smaller eyes compared to litter mates, and moreover, in some cases one eye was more affected than the other eye. At E13.5, no neural tube defects were observed in myo-inositol supplemented folate-deficient $+/+^{ct}$ embryos (Figure 6.6). Eye defects were also apparent in supplemented and unsupplemented folate deficient $+/+^{ct}$ embryos. Hence, it appears the folate deficient diet is affecting eye development in both mouse strains.

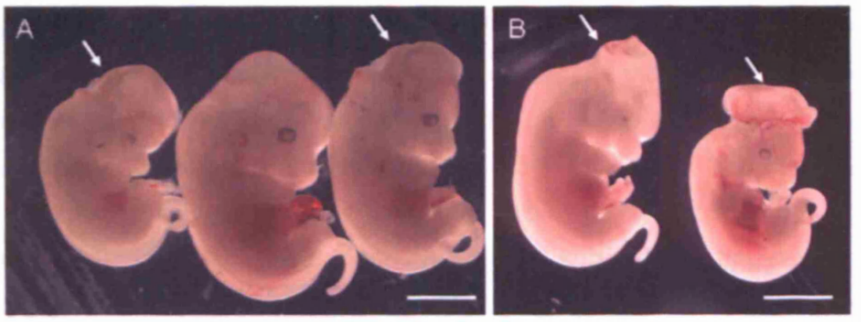

Figure 6.5. Folate-deficient E13.5 *curly tail* embryos supplemented with folic acid and myo-inositol. (A) Folate-deficient *ct/ct* embryos supplemented with folic acid (FD+FA) and (B) folate-deficient *ct/ct* embryos supplemented with *myo*-inositol (FD+MI). Solid arrow indicates the exencephaly. Scale bar is equivalent to 1 mm.

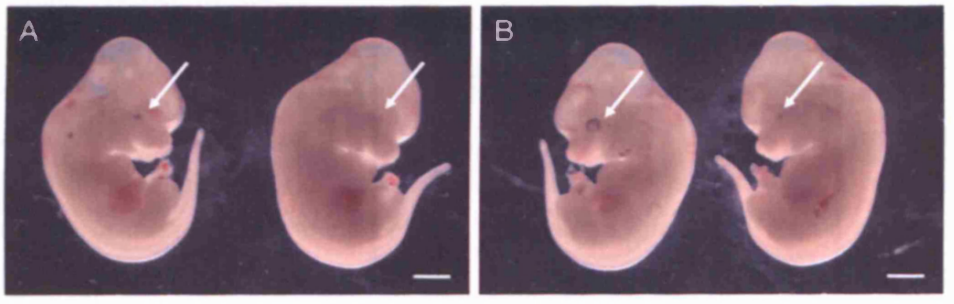

Figure 6.6. Folate-deficient E13.5 *congenic curly tail* embryos supplemented with myo-inositol. (A) right, and (B) left view of folate deficient $+/+^{ct}$ embryos supplemented with myo-inositol (FD+MI). Scale bar is equivalent to 1 mm. Solid arrow indicates eye defects.

Mouse Model	Diet	No. of litters	No. of embryos per litter	No. of resorptions per litter
ct/ct	FD	6	0.75 ± 0.42	5.75 ± 1.28
	FD+FA	3	5.33 ± 0.88	1.00 ± 0.58
	FD+MI	5	2.20 ± 0.37	3.00 ± 1.22
$+/+^{ct}$	FD	4	0.33 ± 0.21	5.50 ± 0.56
	FD+FA	2	2.50 ± 1.50	1.00 ± 0.00
	FD+MI	1	3.00 ± 0.00	0.00 ± 0.00

Table 6.8. Survival of *curly tail* embryos following dietary intervention. Resorptions were defined as the absence of a viable embryo at a visible site of implantation. Values are given as mean per litter ± standard error of the mean. FD; Folate deficient Diet, FD+FA; Folate deficient Diet + Folic Acid; FD+MI; Folate deficient Diet + Myo-Inositol.

Under normal dietary conditions $+/+^{ct}$ embryos survive into adulthood (N.Greene, personal communication). Likewise, since the *ct* gene mutation is not embryonic lethal, the majority of *ct/ct* embryos will survive until birth despite the presence of any NTDs. Following the collection of litters later in gestation, it became apparent that very few folate-deficient embryos were surviving past E13.5 (Table 6.8). The high number of visible resorptions suggested that embryos were dying around this stage of development (Table 6.8). Preliminary analysis of survival in supplemented litters suggests that both folic acid and myo-inositol both improved embryonic survival as shown by the increased mean number of live embryos at E13.5 and the reduction in the mean number of visible resorptions (Table 6.8). However, further work is required to clarify this finding.

6.3.6 Investigating the relationship between growth and development in *curly tail* embryos.

To attempt to understand further how the folate-deficient diet affected embryonic growth and development during neurulation, embryos that had developed under folate-deficient and normal dietary conditions were analysed for protein content and somite number, as a measure of growth and development, respectively. Upon observation there appears to be a disturbance of the relationship between growth and development for both *ct/ct* and $+/+^{ct}$ (Figure 6.11). Thus, folate-deficient *ct/ct* and $+/+^{ct}$ embryos appear to have a lower protein content compared to *ct/ct* and $+/+^{ct}$ embryos from the normal diet group with the same number of somites (Figure 6.11).

To investigate whether somite-matched folate-deficient embryos are growth retarded compared to embryos from the normal diet group, the mean growth (protein content) of embryos that had developed between 22-26 somites was compared (Table 6.9). Somite-matched folate-deficient *ct/ct* embryos had a lower protein content than *ct/ct* embryos from the normal diet (ND) group, however statistical analysis demonstrated that this difference was not significant (Student t-test; $p = 0.422$). A greater effect on growth was observed in the congenic wild-type strain, for which somite-matched folate deficient $+/+^{ct}$ embryos had statistically lower protein content than $+/+^{ct}$ embryos from the normal diet group (Student t-test; $p < 0.001$). Thus, folate deficient $+/+^{ct}$ embryos are smaller for both gestational age and developmental stage. This is in contrast to the *splotch* NTD mouse model where the folate deficient diet did not affect the relationship between growth and development such that embryos with the same number of somites had the same protein content.

A

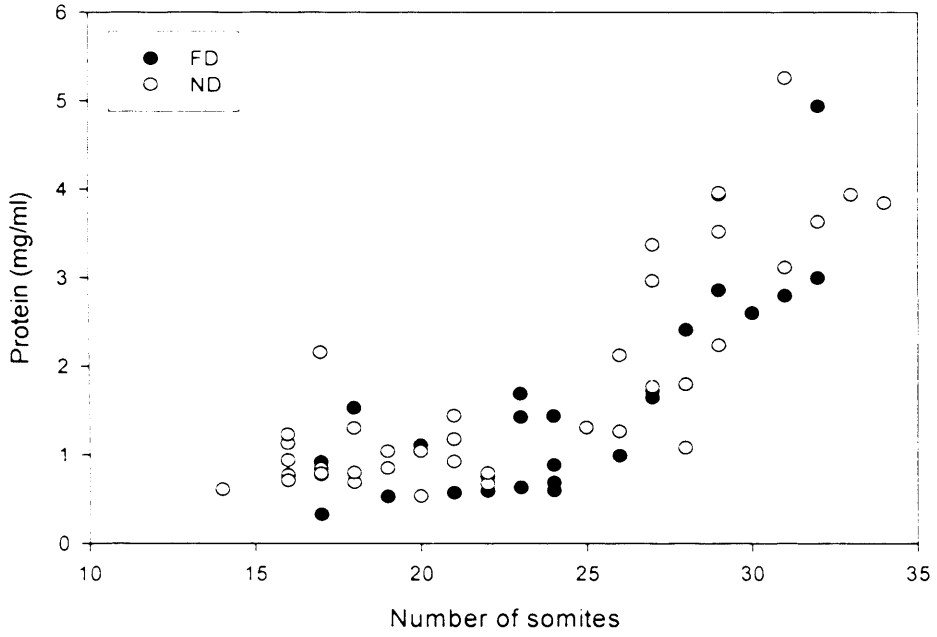

B

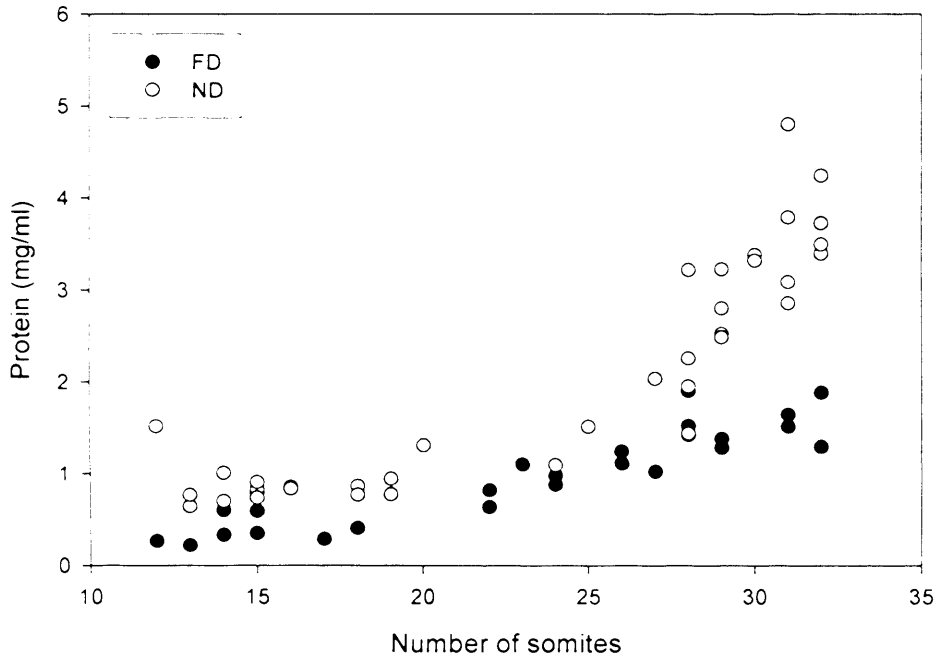

Figure 6.7. The relationship between embryonic growth (protein content) and development (somite number) for *ct/ct* (A) and +/+^{ct} (B) embryos from the folate deficient (FD) and normal (ND) diet groups. Each dot represents a single embryo.

Mouse Model	Diet	n=	Mean number of somites	Protein Concentration (mg/ml)
ct/ct	ND	14	28.4	3.47 ± 0.76
	FD	10	29.1	2.69 ± 0.36
$+/+^{ct}$	ND	19	29.7	3.05 ± 0.19
	FD	13	28.0	1.40 ± 0.08$^{\#\#}$

Table 6.9. A comparison of protein content between somite-matched *ct/ct* and $+/+^{ct}$ embryos following dietary intervention. Protein concentration was determined in homogenised embryos which had developed between 22-26 somites. Values are given as mean ± standard error of the mean. ND; Normal Diet, FD; Folate deficient Diet. $^{\#\#}$ p-value < 0.02 when compared to ND. Of note, FD and ND embryos were of the same gestational age.

6.3.7 Investigating embryonic folate levels following dietary intervention.

As with the *splotch* mouse model (chapter 5), the total folate (monoglutamylfolate + polyglutamylfolate) content and concentration was determined in *ct/ct* and $+/+^{ct}$ embryos collected at E10.5-E11.5 and the data has been compared between embryos with the same number of somites.

Mouse Model	Diet	n=	Somite Range (average)	Total Folate Content (pg folate / embryo)	[Folate] (ng folate / mg protein)
ct/ct	ND	10	26-32 (28.4)	8822 ± 1527	28.8 ± 3.20
	FD	14	26-32 (29.1)	5065 ± 419$^{\#\#}$	23.4 ± 5.58
	FD+FA	7	26-32 (28.1)	8877 ± 975*	56.0 ± 7.91**
$+/+^{ct}$	ND	18	26-32 (29.8)	8244 ± 445	30.1 ± 3.31
	FD	13	26-32 (28.0)	5184 ± 282$^{\#}$	37.3 ± 1.27
	FD+FA	5	26-32 (28.8)	13675 ± 598**$^{\#\#}$	49.0 ± 9.18$^{\#\#}$

Table 6.10. Embryonic folate levels in *ct/ct* and $+/+^{ct}$ embryos at the same developmental stage (the same number of somites). Folate values are given as mean ± standard error of the mean. ND; Normal Diet, FD; Folate deficient Diet, FD+FA; Folate deficient Diet + Folic Acid. $^{\#}$ $p < 0.05$ when compared to ND, $^{\#\#}$ $p < 0.02$ when compared to ND, * $p < 0.05$ when compared to FD, ** $p < 0.02$ when compared to FD. Of note when comparing somite matched embryos, folate-deficient embryos are of an older gestational age.

In *ct/ct* embryos that had developed between 26 and 32 somites (Table 6.10), the folate-deficient diet caused a significant decrease in the folate content per embryo (Holm-Sidak; p = 0.007) compared to *ct/ct* embryos from the normal diet (ND) group. However, the folate concentration was not significantly affected by the folate-deficient diet (p = 0.719). Likewise, the folate-deficient diet significantly reduced the folate content (p = 0.05) in $+/+^{ct}$ embryos that had developed between 22 and 26 somites compared to $+/+^{ct}$ embryos developing under normal dietary (ND) conditions (Table 6.10). The folate concentration in $+/+^{ct}$ embryos was also unaltered by the folate deficient diet (p = 0.128). Thus, it appears that the folate deficient diet restricts growth such that the embryo cannot grow or develop unless the required folate concentration is available.

Treating the folate-deficient *ct/ct* embryos with folic acid from E7.5 to E10.5 (FD+FA) led to a significant increase in folate concentration (p = 0.005). Additionally, folic acid treatment also significantly increased the folate content per embryo compared to folate-deficient embryos (p = 0.025) (Table 6.10). Treatment of folate-deficient $+/+^{ct}$ with folic acid from E7.5 to E10.5 led to a large, significant increase in folate content compared to $+/+^{ct}$ embryos from the folate-deficient diet group (p < 0.001) and the normal diet group (p < 0.001) (Table 6.10). There was also a significant increase in the folate concentration (p = 0.006) between supplemented (FD+FA) and $+/+^{ct}$ embryos from the normal diet group (ND). Thus, although folic acid supplementation did not affect embryonic development (number of somites; section 6.3.5), it did significantly increase the amount of folate per mg of protein, in both *ct/ct* and $+/+^{ct}$ embryos.

6.3.8 In-depth analysis of mono- and polyglutamylfolate levels in *curly tail* embryos

The previous section investigated how total folate levels differed between embryos of the same developmental stage. As described (section 1.4.1), total folate consists of two different forms; monoglutamylfolate and polyglutamylfolate. To illustrate how embryonic mono- and polyglutamylfolate content and, concentration change with development under different dietary conditions, the data was plotted against somite number (Figures 6.8 - 6.11).

In *ct/ct* embryos, as expected, the monoglutamylfolate content of an embryo increased as the embryo developed under normal dietary conditions, presumably since a larger and more developed embryo has a greater folate content (Figure 6.8A). Under folate-deficient conditions, the monoglutamylfolate content also increased with development

but at a slower rate as shown by the shallower gradient of the linear regression plot. There was a wide variation in monoglutamylfolate content per embryo, for example some *ct/ct* embryos from the normal diet group had a monoglutamylfolate content similar to that of folate deficient *ct/ct* embryos and vice-versa. However, overall it appears that at all stages of development folate-deficient *ct/ct* embryos have a lower monoglutamylfolate content. Statistical analysis of the graphical data by linear regression (see section 5.2.3) demonstrated that the gradients of the graph lines were not significantly different ($p = 0.390$).

When folate levels were normalised to protein content (Figure 6.8B), the monoglutamylfolate concentration in *ct/ct* embryos was found to decrease with development under normal dietary conditions. Thus, there was less folate available per mg of tissue suggesting a rapid turnover of folate metabolites at this stage of development. Alternatively, rapid growth occurs which outpaces the rate of folate uptake. Under folate-deficient conditions, the embryonic monoglutamylfolate concentration also decreased with development but the gradient of the graph line was shallower, presumably due to the lower growth rate. At some stages of development, for example the 15-18 somite stage, *ct/ct* embryos from the normal diet group seem to have a higher folate concentration compared to *ct/ct* embryos from the folate-deficient diet group. In contrast, when comparing embryos with 25 or more somites, *ct/ct* embryos appear to have the same folate concentration irrespective of dietary conditions. Statistical analysis by linear regression demonstrated that the gradients of the graphs are not significantly different ($p = 0.400$)

It was next determined how the embryonic polyglutamylfolate content and polyglutamylfolate concentration changes with developmental progression (as indicated by somite number) among *ct/ct* embryos (Figure 6.9). As expected, the polyglutamylfolate content of *ct/ct* embryos increased with developmental stage under normal dietary conditions such that larger embryos contained more folate (Figure 6.9A). Under folate-deficient conditions, the data points representing *ct/ct* embryos from the two dietary groups overlay and it is not possible to distinguish one group from another. However, the shallower gradient of the linear regression plot for the folate-deficient diet group appears to suggest that the polyglutamylfolate content is increasing at a slower rate such that there is a smaller increase in polyglutamylfolate content with somite development compared to normal dietary conditions. Statistical analysis by linear regression (see section 5.2.3) demonstrated that the gradients of the two graphs are significantly different (p-value = 0.010).

A

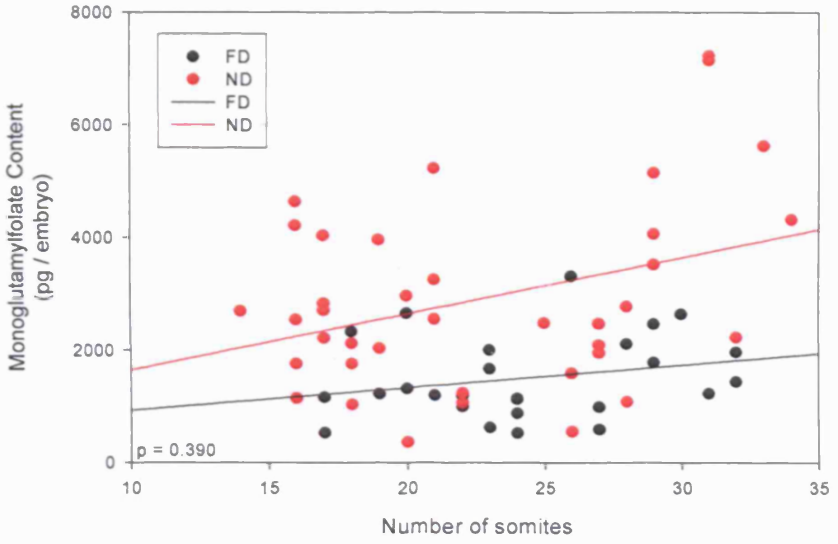

B

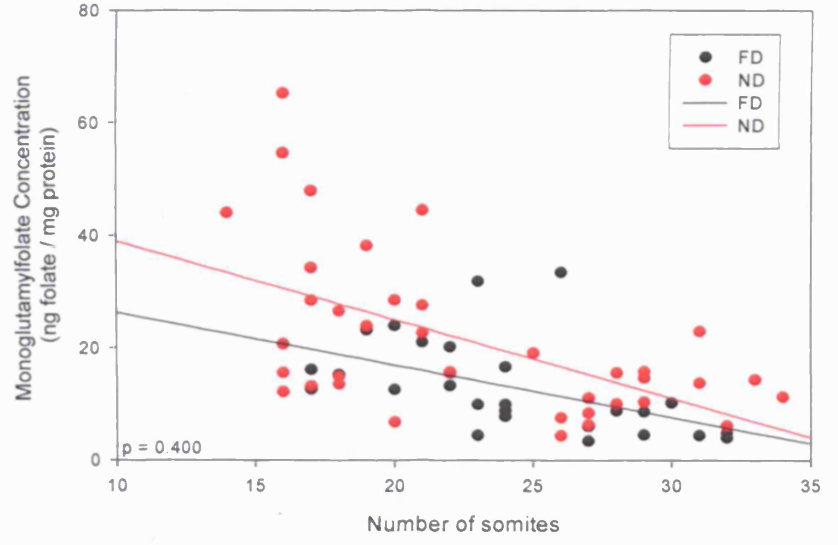

Figure 6.8. Comparison of monoglutamylfolate levels in *ct/ct* embryos from the folate deficient (FD) and normal diet (ND) groups. The graphs show (A) monoglutamylfolate content per embryo (pg of folate/embryo) vs. somite number, and (B) embryonic monoglutamylfolate concentration (ng folate/mg protein) vs. somite number. ●, *ct/ct* embryos from the folate deficient group; ●, *ct/ct* embryos from the normal diet group, Each data point represents an individual embryo. The p-value represents the significance of the difference between slopes of the graph lines (see section 6.2.3).

A

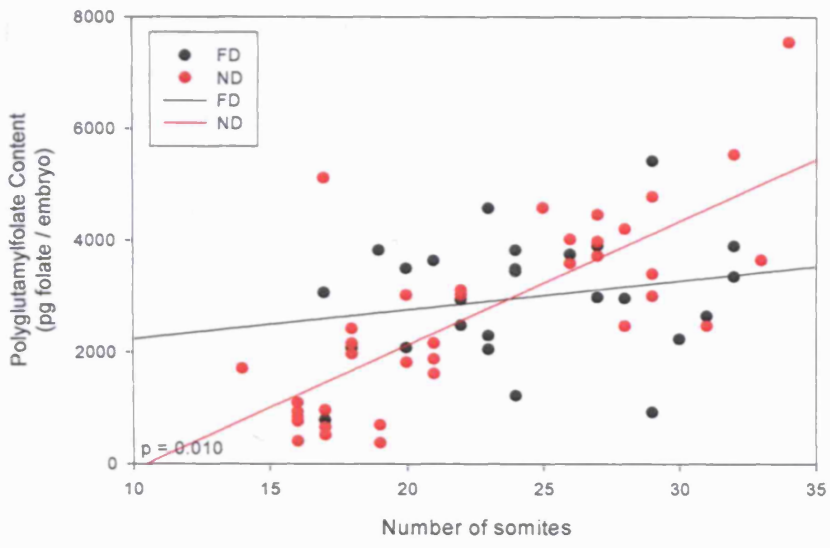

B

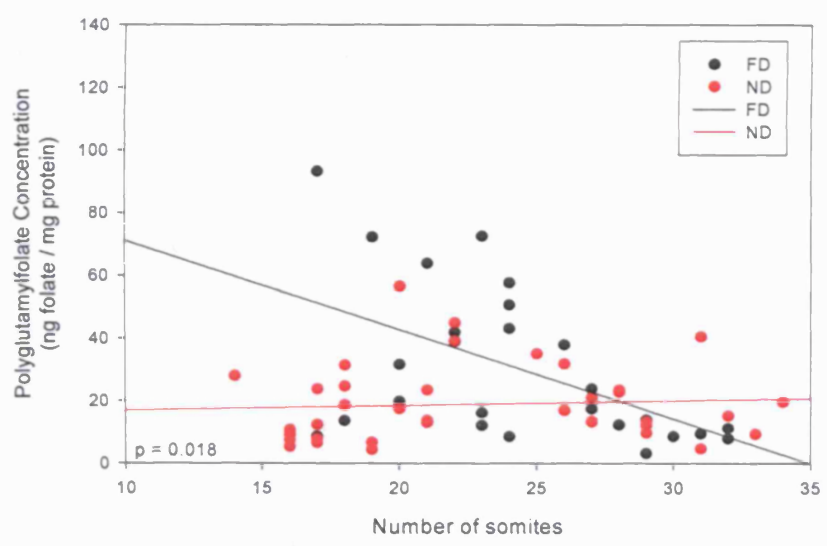

Figure 6.9. Comparison of polyglutamylfolate levels in *ct/ct* embryos from the folate deficient (FD) and the normal diet (ND) groups. The graphs show (A) polyglutamylfolate content per embryo (pg of folate/embryo) vs. somite number, and (B) embryonic polyglutamylfolate concentration (ng folate/mg protein) vs. somite number. •, *ct/ct* embryos from the folate deficient group; •, *ct/ct* embryos from the normal diet group, Each data point represents an individual embryo. The p-value represents the significance of the difference between slopes of the graph lines (see section 6.2.3).

Under normal dietary conditions, the polyglutamylfolate concentration appears to remain constant with development among *ct/ct* embryos (Figure 6.9B) whilst under folate deficient dietary conditions, the polyglutamyfolate concentration decreases with development. Statistical analysis by linear regression showed that the difference between the gradients of these graphs is significant ($p = 0.018$). The polyglutamylfolate concentration in normal diet group *ct/ct* remains approximately 10-20 ng/mg protein, perhaps at a concentration which is sufficient to enable embryonic growth and development. Unexpectedly, folate-deficient *ct/ct* embryos with between 15-19 somites have a higher polyglutamylfolate concentration, compared to *ct/ct* embryos developing under normal dietary conditions. It is difficult to understand why *ct/ct* embryos have a greater polyglutamylfolate concentration under folate deficient dietary conditions. Possibly this represents a scavenging mechanism which enables *ct/ct* embryos to accumulate folate under limiting conditions. Also, somite-matched folate-deficient *ct/ct* embryos are older than normal diet *ct/ct* embryos therefore they would have had more time to accumulate folate stores.

Analysis of mono- and polyglutamylfolate in $+/+^{ct}$ embryos reveals identical patterns to those described in *ct/ct* embryos (Figure 6.10 and 6.11). Monoglutamylfolate content increases with development in both diets yet, at all stages of development folate-deficient $+/+^{ct}$ embryos have lower monoglutamylfolate content (Figure 6.10A). However, the gradients of the graph lines are not significantly different ($p = 0.840$). The monoglutamylfolate concentration decreases with development yet there is little variation between dietary groups (Figure 6.10B). Indeed, statistical analysis demonstrates that the gradients of the graph lines are not significantly different ($p = 0.743$). The polyglutamylfolate content increases with development under normal dietary conditions, but increases at a slower rate in folate-deficient $+/+^{ct}$ embryos (Figure 6.11A). The gradients of the graph lines were found to be significantly different ($p = 0.010$). Finally, the polyglutamylfolate concentration remains constant under normal dietary conditions, yet decreases with development under folate-deficient conditions due to the high polyglutamylfolate concentration in folate-deficient $+/+^{ct}$ embryos with 12-18 somites (Figure 6.11B). The difference in the gradients of the graph lines was highly significant ($p < 0.001$). The comparable relationships between folate and growth/development in *ct/ct* and $+/+^{ct}$ suggests that the *ct* mutation does not affect embryonic folate status.

A

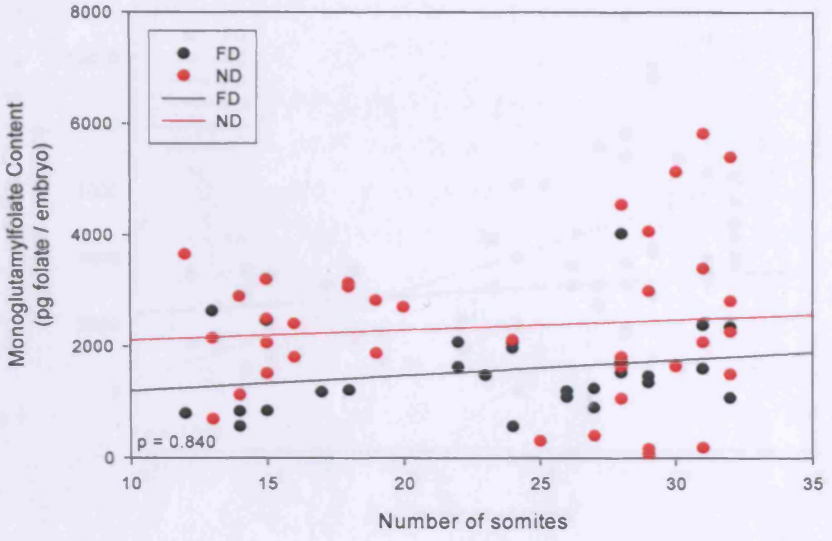

B

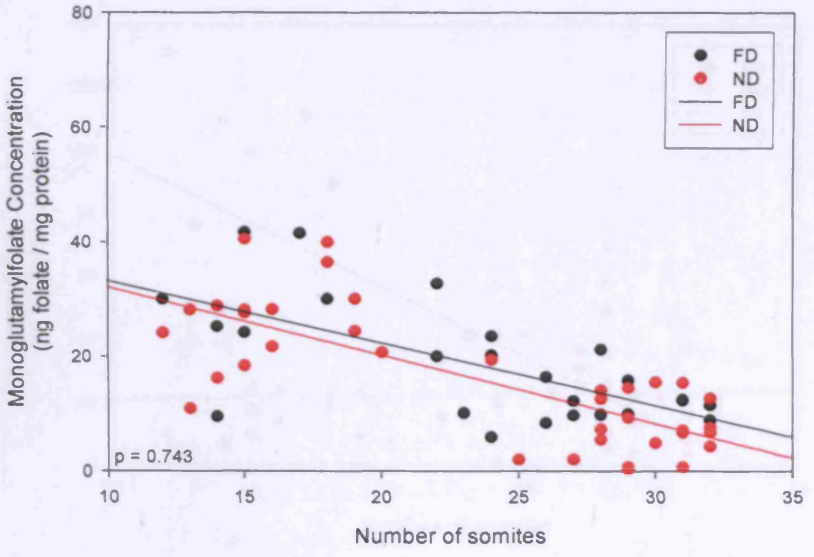

Figure 6.10. Comparison of monoglutamylfolate levels in +/+^{ct} embryos from the folate deficient (FD) and normal diet (ND) groups. The graphs show (A) monoglutamylfolate content per embryo (pg of folate / embryo) vs. somite number, and (B) embryonic monoglutamylfolate concentration (ng folate / mg protein) vs. somite number. ●, +/+^{ct} embryos from the folate deficient group, ●, +/+^{ct} embryos from the normal diet group, Each data point represents an individual embryo. The p-value represents the significance of the difference between slopes of the graph lines (see section 6.2.3).

A

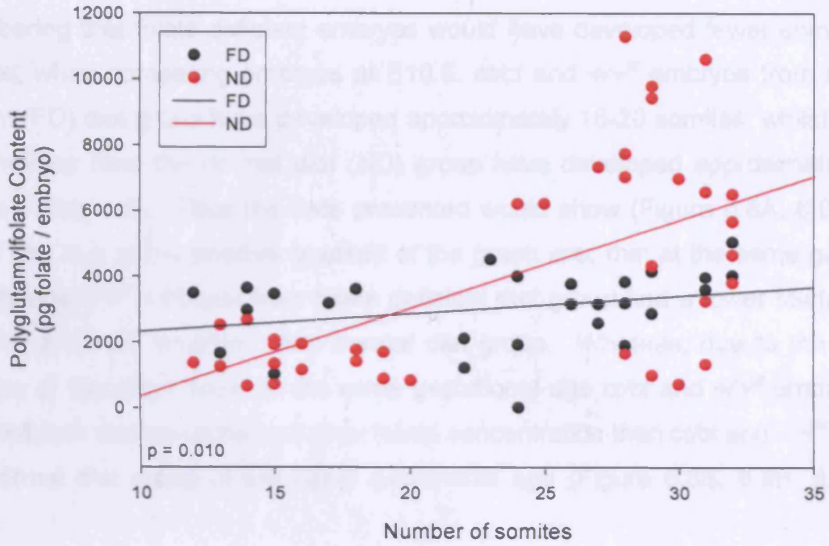

B

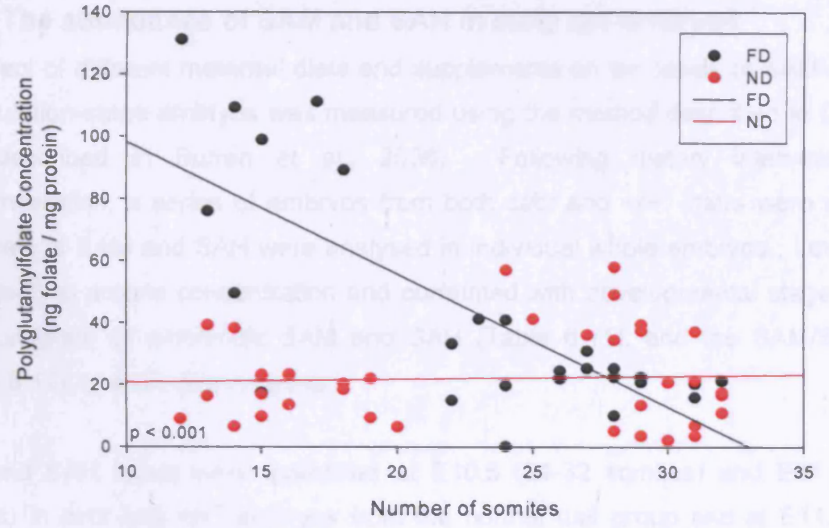

Figure 6.11. Comparison of polyglutamylfolate levels in +/+^{ct} embryos from the folate deficient (FD) and normal diet (ND) groups. The graphs show (A) polyglutamylfolate content per embryo (pg of folate / embryo) vs. somite number, and (B) embryonic polyglutamylfolate concentration (ng folate / mg protein) vs. somite number. ●, +/+^{ct} embryos from the folate deficient group, ●, +/+^{ct} embryos from the normal diet group, Each data point represents an individual embryo. The p-value represents the significance of the difference between slopes of the graph lines (see section 6.2.3).

Using the graphs it was then possible to compare mono- or polyglutamylfolate concentrations and content between embryos of the same gestational age, remembering that folate deficient embryos would have developed fewer somites. For example, when comparing embryos at E10.5, *ct/ct* and $+/+^{ct}$ embryos from the folate deficient (FD) diet group have developed approximately 16-20 somites, whilst *ct/ct* and $+/+^{ct}$ embryos from the normal diet (ND) group have developed approximately 30-31 somites (Table 6.5). Thus the data presented would show (Figure 6.8A, 6.9A, 6.10A and 6.11A), due to the positive gradient of the graph line, that at the same gestational age *ct/ct* and $+/+^{ct}$ embryos from folate deficient diet group had a lower folate content than *ct/ct* and $+/+^{ct}$ embryos from normal diet group. Whereas, due to the negative gradients of the graph lines, at the same gestational age *ct/ct* and $+/+^{ct}$ embryos from folate deficient diet group had a higher folate concentration than *ct/ct* and $+/+^{ct}$ embryos from normal diet group of the same gestational age (Figure 6.8B, 6.9B, 6.10B and 6.11B).

6.3.9 The abundance of SAM and SAH in *curly tail* embryos

The effect of different maternal diets and supplements on the levels of SAM and SAH in neurulation-stage embryos was measured using the method described in Chapter 3 (also described in Burren et al., 2006). Following dietary intervention and supplementation, a series of embryos from both *ct/ct* and $+/+^{ct}$ litters were collected, and levels of SAM and SAH were analysed in individual whole embryos. Levels were normalised to protein concentration and correlated with developmental stage to show the abundance of embryonic SAM and SAH (Table 6.11), and the SAM/SAH ratio (Figure 6.12), in each dietary group.

SAM and SAH levels were quantified at E10.5 (24-32 somites) and E11.5 (38-42 somites) in *ct/ct* and $+/+^{ct}$ embryos from the normal diet group and at E11.5 (22-34 somites) in *ct/ct* and $+/+^{ct}$ embryos from the folate-deficient diet group. E11.5 embryos from the folate-deficient diet group are somite-matched to E10.5 embryos from the normal diet group. SAM and SAH levels were also analysed in E11.5 folate-deficient embryos treated with folic acid (19-34 somites) and *myo*-inositol (34-37 somites).

Mouse Model	Diet	n=	Age	Somite Number	SAM (nmoles/mg protein)	SAH (nmoles/mg protein)	Ratio SAM/SAH
ct/ct	ND	15	E10.5	29.5 ± 0.32	3.27 ± 0.25**	0.044 ± 0.004	76 ± 3.4**
	ND	9	E11.5	39.8 ± 0.76	2.84 ± 0.27**	0.027 ± 0.003	119 ± 19.4
	FD	16	E11.5	29.8 ± 1.40	5.18 ± 0.75	0.045 ± 0.012	195 ± 42.7
	FD+FA	9	E11.5	27.6 ± 0.80	2.98 ± 0.24**	0.025 ± 0.004	152 ± 37.8
$+/+^{ct}$	ND	15	E10.5	29.2 ± 0.54	2.81 ± 0.18**	0.031 ± 0.002**	93 ± 5.4**
	ND	8	E11.5	38.6 ± 0.86	1.98 ± 0.08**	0.025 ± 0.001**	79 ± 2.8**
	FD	7	E11.5	32.6 ± 1.23	4.01 ± 0.47	0.116 ± 0.030	48 ± 10.7
	FD+FA	5	E11.5	31.4 ± 0.87	2.44 ± 0.16**	0.029± 0.003**	87 ± 5.9**
	FD+MI	5	E11.5	33.2 ± 1.93	2.38 ± 0.16**	0.030 ± 0.008**	104 ± 25.6**

Table 6.11. SAM and SAH abundance determined by LC-MS/MS in *curly tail* embryos (all genotypes included) from each maternal treatment group. SAM and SAH were quantified in individual whole embryos. Values are given as mean ± standard error of the mean. ND; Normal Diet, FD; Folate deficient Diet, FD+FA; Folate deficient Diet + Folic Acid; FD+MI; Folate deficient Diet + Myo-Inositol. ** $p < 0.02$ when compared to FD.

In embryos at E10.5 and E11.5 under normal dietary conditions, SAM levels were typically 75-105 fold, and 80-90 fold higher than SAH levels in *ct/ct* and $+/+^{ct}$ embryos, respectively, at these stages of development. In *ct/ct* embryos, the concentration of SAM and SAH decreased as gestation progressed leading to an increase in the ratio of SAM/SAH since the concentration of SAH decreased by the greatest extent. In $+/+^{ct}$ embryos, the concentration of SAM and SAH also decreased as gestation proceeded, however this led to a decrease in the ratio of SAM/SAH since the concentration of SAM decreased to a greater extent compared to SAH.

When comparing *ct/ct* embryos from the normal diet group (ND) to embryos from the folate-deficient diet (FD) at the same developmental stage (with the same mean number of somites), the folate-deficient diet significantly increased the concentration of SAM ($p = 0.007$), yet the concentration of SAH remained unchanged. Overall, the increase in SAM caused a significant increase in the ratio of SAM/SAH ($p = 0.005$) in folate-deficient *ct/ct* embryos compared to *ct/ct* embryos developing under normal dietary conditions. Similarly, when comparing *ct/ct* embryos from the normal diet group (ND) to embryos from the folate-deficient diet (FD) at the same gestational age (with different mean number of somites), there was a significant increase in the concentration of SAM ($p = 0.004$) whilst there was no significant change in the

concentration of SAH. The ratio of SAM/SAH, when comparing embryos of the same gestational age, appeared to be increased by the folate-deficient diet but this change was not significant. Thus, overall, the folate-deficient diet caused an increased concentration of SAM in *ct/ct* embryos. Treatment of folate-deficient *ct/ct* embryos with folic acid daily from E7.5-E10.5 (FD+FA) significantly decreased the concentration of SAM ($p = 0.007$) to near ND levels, when compared to folate-deficient embryos (FD) of the same gestational age.

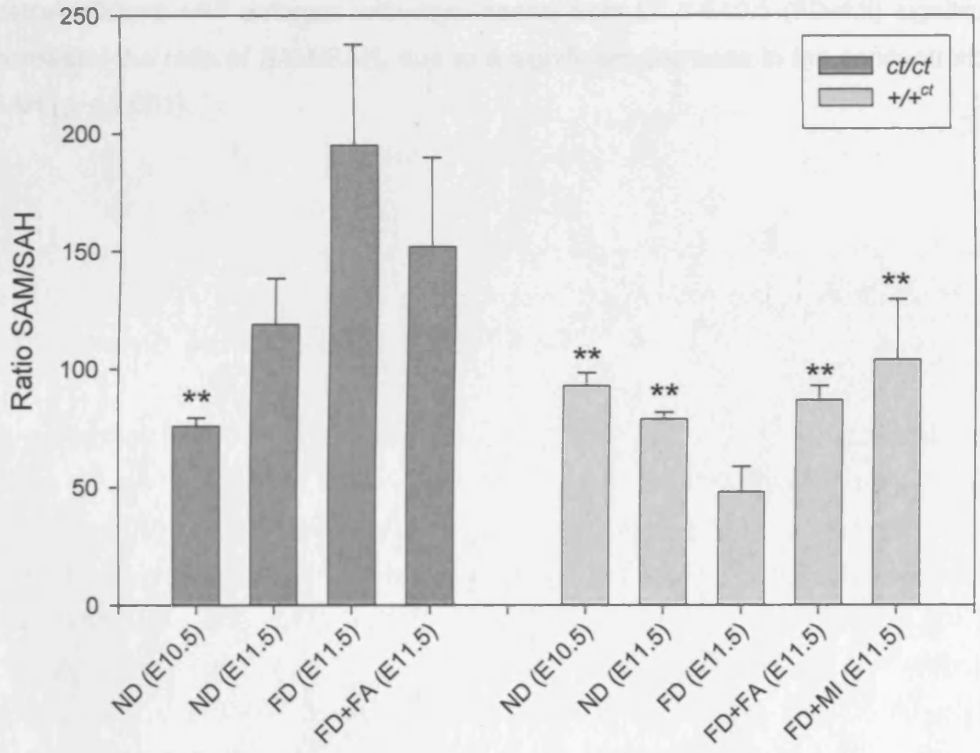

Figure 6.12. SAM/SAH ratio in *ct/ct* and +/+^{ct} embryos from each maternal treatment group. Values are given as mean ± standard error of the mean. ** $p < 0.02$ when compared to FD.

When comparing +/+^{ct} embryos from the normal diet group (E10.5) to embryos from the folate-deficient diet (E11.5) at the same developmental stage (with the same mean number of somites), the folate-deficient diet significantly increased the concentration of SAM ($p<0.001$) and SAH ($p<0.001$). Overall, the extent of change in the concentration of SAH was greatest, causing a significant decrease in the ratio of SAM/SAH ($p < 0.001$) in folate deficient +/+^{ct} embryos compared to +/+^{ct} embryos developing under normal dietary conditions. Similarly, when comparing +/+^{ct} embryos from the normal

diet group (E11.5) to embryos from the folate-deficient diet (E11.5) at the same gestational age (with different mean number of somites), there was a significant decrease in SAM/SAH ratio due to a significant increase in the concentration of SAH ($p < 0.001$). To conclude, the folate-deficient diet caused a significant increase in the concentration of SAH in $+/+^{ct}$ embryos. Treatment of folate-deficient $+/+^{ct}$ embryos with folic acid daily from E7.5-E10.5 (FD+FA) significantly decreased the concentration of SAM ($p < 0.001$) and SAH ($p < 0.001$), when compared to folate-deficient embryos (FD) of the same gestational age, leading to an increase in the SAM/SAH ratio since the concentration of SAH was reduced by a greater extent. Similarly, treatment of folate-deficient $+/+^{ct}$ embryos with myo-inositol from E7.5-E10.5 (FD+MI) significantly increased the ratio of SAM/SAH, due to a significant decrease in the concentration of SAH ($p < 0.001$).

6.4 Conclusions and Discussion

6.4.1 Folate deficiency affects maternal folate metabolism

The folate-deficient diet, which was deficient in both bacterial and dietary forms of folate, effectively changed maternal folate status, causing decreased whole blood folate levels and increased homocysteine in both *ct/ct* and $+/+^{ct}$ dams. Elimination of either bacterial folate or dietary folate alone reduced maternal folate and increased homocysteine, but not to the same extent as combined elimination of dietary and bacterial folate.

In this study an inverse relationship was apparent between maternal folate and homocysteine levels. Homocysteine and folate levels are usually inversely related and dietary supplementation with folate lowers homocysteine levels, restores normal folate levels (Daly et al., 2002) and reduces the risk for NTDs (Wald et al., 1991). In mice, a recent study by Ernest et al. also demonstrated an inverse relationship between folate and homocysteine levels in both wild-type and *Crooked tail* mutant embryos following dietary intervention (Ernest et al., 2006).

A comparison of folate levels with other available strains, such as the *splotch* NTD mouse model and the CD1 wild-type mouse strain, revealed that folate levels are higher in *ct/ct* and $+/+^{ct}$ dams. Furthermore, plasma homocysteine concentrations were also considerable higher in *ct/ct* and $+/+^{ct}$ than those measured in *splotch* dams, both under folate-deficient and normal dietary conditions (compare Table 5.2 and 6.2). Since elevated folate and homocysteine were recorded in both *ct/ct* and $+/+^{ct}$ dams this appears to suggest that the effect is due to the genetic background of the *ct* strain. Hyperhomocysteinemia has previously been demonstrated in *ct/ct* mice when compared to wild-type C57Bl/6 mice, under both folate-deficient and normal dietary conditions (Tran et al., 2002). These authors also reported that homocysteine:cysteine ratios were comparable between *ct/ct* and C57Bl/6 mice indicating that similar proportions of total homocysteine are metabolised through the transsulfation pathway to cysteine. Therefore, it is likely that the differences in homocysteine levels reflect differences in the remethylation cycle.

6.4.2 Folate deficiency causes NTDs in *curly tail* embryos

This study has shown that folate deficiency by maternal dietary intervention increases the incidence of exencephaly in *curly tail* embryos. This was unexpected since the *curly tail* mutant is well-known as a model of neural tube defects which are not

preventable by folic acid (Seller, 1994b). Thus, it was presumed that folate deficiency would not affect the incidence of NTDs. It is important to note, however, that folic acid was administered to prevent spina bifida in *curly tail* embryos (Seller, 1994b) whilst in this study folate deficiency was shown to cause exencephaly. Another striking finding from this study was the occurrence of exencephaly in congenic embryos, $+/+^{ct}$, which have a 95% similar genetic background to the *curly tail* mutant but are wild-type at the *ct* gene locus (Van Straaten and Copp, 2001). To date, the occurrence of NTDs in this control mouse strain has not been reported, however $+/+^{ct}$ embryos have a longer posterior neuropore compared to somite-matched wild type CD1 mouse embryos (Prof. Andrew J. Copp, personal communication).

Tran et al. investigated the incidence of NTDs among *ct/ct* embryos following dietary intervention (Tran et al., 2002). Four synthetic diets were used (a folate-deficient diet, a folate/choline-deficient diet, a folate-supplemented diet and a control diet) but none of these significantly affected the incidence of NTDs. However, it is unclear whether the folate-deficient diet used by Tran et al. effectively caused folate deficiency since changes in maternal folate and homocysteine were not reported. In addition, the minimum level of folic acid was 0.3 mg/kg and no antibiotic was added to eliminate bacterial folate. After eight weeks on the folate/choline-deficient diet homocysteine levels in *ct/ct* dams had increased twofold, in association with increased liver S-Adenosylhomocysteine and decreased SAM/SAH ratios. In contrast, in the present study, the folate-deficient diet resulted in four-fold and sixteen-fold increases in homocysteine level in *ct/ct* and $+/+^{ct}$, respectively. The changes in homocysteine reported by Tran et al. could be due to the lack of choline in this diet as reducing dietary choline would further increase homocysteine abundance as less betaine would be available for the remethylation of homocysteine to methionine catalysed by BHMT. Nonetheless, their work suggests that altered homocysteine metabolism is present in *ct/ct* mice and could therefore contribute to the pathogenic mechanism of the *ct* defect.

The folate-deficient diet caused exencephaly in $+/+^{ct}$ embryos which are wild-type at the *ct* locus: $+/+^{ct}$ embryos have normal expression levels of the *curly tail* gene, believed to be *Grhl3* (Ting et al., 2003). This implies that risk factors in the genetic background play a role in the susceptibility of cranial neural tube closure to folate-deficiency. Indeed, the presence of at least three modifier loci that influence the incidence of NTD have been demonstrated in the *curly tail* mice (Neumann et al., 1994). In this study, aside from the increased SAM concentration in *ct/ct* embryos, all other metabolic effects induced by the folate deficient diet were comparable highlighting the important involvement of the genetic background on NTD risk.

The risk of exencephaly in the SELH/Bc mouse inbred strain is determined by a combination of genes across about 3 loci and dietary content (Harris and Juriloff, 2005;Juriloff et al., 2001). Thus, exencephaly seems to occur when the timing of cranial neural tube elevation is delayed beyond the critical threshold time due to multi-factorial traits (Gunn et al., 1995;MacDonald et al., 1989). Perhaps *ct* background modifier genes affect the timing of cranial neural tube closure but not enough to cause the development of cranial NTDs under normal dietary conditions. Whereas under folate deficient conditions neural tube closure could be delayed beyond the critical threshold time causing exencephaly. This could be due to the embryonic growth and developmental retardation observed under folate deficient conditions. Significantly, that the incidence of exencephaly increased to the same extent in *ct/ct* and $+/+^{ct}$ embryos under folate deficient conditions indicating that the same underlying mechanism may be responsible.

6.4.3 Folate deficiency causes retardation of embryonic growth and developmental progression

As I found in the *splotch* mouse (Chapter 5), the folate-deficient diet retarded embryonic growth and development. However, in contrast to *splotch*, the fundamental relationship between growth and development was altered in *curly tail* such that embryonic growth was affected to a greater extent than developmental progression. Thus, *ct/ct* and $+/+^{ct}$ embryos from the folate-deficient group with a particular number of somites have a lower protein concentration than *ct* embryos from the normal diet group. This raises the possibility that the effect of folate deficiency in the *ct/ct* and $+/+^{ct}$ embryos reflects an effect of growth retardation as opposed to a specific defect in neurulation. Furthermore, the folate-deficient *ct/ct* and $+/+^{ct}$ dams appear to have a poor reproductive outcome again suggesting the folate-deficient diet may have caused severe growth retardation perhaps due to interaction with genetic risk factors in the *ct* background. It appears unlikely that there is generalised toxicity as the folate-deficient diet (FD) did not increase the incidence of neural tube defects in wild-type CD1 or folate-responsive *cited-2* null embryos (personal communication, Dr. Nicholas Greene).

Previous studies of *curly tail* mice demonstrated that treatment with the DNA synthesis inhibitor, hydroxyurea, on embryonic day 8 increased the proportion of *curly tail* mice affected with exencephaly, whilst hydroxyurea reduced the incidence of NTDs when administered on day 9, mainly through a reduction of posterior neuropore defects (Seller and Perkins, 1983). Similar effects were also produced in *curly tail* mice with two other inhibitors of DNA synthesis; mitomycin C and 5-fluorouracil (Seller,

1983;Seller and Perkins, 1986). Work by Copp et al. identified a cell-type specific cell proliferation abnormality that affects *ct/ct* embryos developing spinal NTDs but not their normally developing littermates (Copp et al., 1988a). In a subsequent study spinal NTDs in *ct/ct* embryos were prevented by growth retardation caused by food deprivation (Copp et al., 1988b). Thus, it appears that growth retardation exacerbates the incidence of exencephaly yet prevents the development of spinal NTDs in *curly tail* mice. It was not possible to study spinal neural tube closure in folate-deficient *curly tail* embryos due to poor reproductive success and survival. However, with further work it would be possible to study the effects of a less severe folate-deficient diet on spinal neurulation, such as the bacterial or dietary folate deficient diets.

6.4.4 Folate deficiency affects embryonic one-carbon metabolism

In this study, embryonic folate status was analysed in *ct/ct* and $+/+^{ct}$ embryos under normal and folate deficient dietary conditions. Mean folate content was reduced by the folate deficient diet in both *ct/ct* and $+/+^{ct}$ embryos that had developed between 26-32 somites. In contrast, the folate concentration was unchanged yet folate-deficient embryos took longer to reach this developmental stage. This suggests that the total folate concentration needs to remain at a critical level to enable development to proceed. Therefore to maintain the critical embryonic folate concentration under folate limiting conditions, growth and development must be slowed. Treatment with exogenous folic acid dramatically increased the folate content and concentration, and reduced the incidence of cranial NTDs. However, improvement in embryonic growth and development was not detectable although this may become apparent later in development. Alternatively, a subtle effect on proliferation, perhaps in certain tissues, allowed neural tube closure to occur.

I found that mono- and polyglutamylfolate content increased with development. This was expected, since more developed embryos would be larger and therefore would be envisaged to contain more folate. Under normal dietary conditions the embryonic monoglutamylfolate concentration decreased with development, as seen in *splotch* embryos (chapter 5), indicating that at this stage of development the demand for monoglutamylfolate exceeds the supply. The same relationship was observed under folate-deficient conditions, however younger embryos had a lower monoglutamylfolate concentration compared to embryos from the normal diet such that the rate of decrease was less.

Under normal dietary conditions, the polyglutamylfolate concentration remained constant as development proceeded. Thus, it seems that in order to meet the demand for biologically active polyglutamylfolates, monoglutamylfolates are being taken up into the cell, resulting in the observed decrease in monoglutamylfolate concentration with development. Under folate-deficient conditions, the polyglutamylfolate concentration decreases with development perhaps because there is less monoglutamylfolate available for uptake. However, confusingly, the polyglutamylfolate concentration is greater in folate-deficient embryos with 15-20 somites compared to embryos from the normal diet. This might represent a type of scavenging mechanism whereby the embryo, under folate limiting conditions, is able to store excess folate for future development. Uptake of folate by placental receptors might be more efficient when maternal folate concentrations are decreased (Antony, 2007). Alternatively, since folate deficient embryos took longer to develop, they would have had longer to uptake folate. However, it is not clear why development does not proceed in folate-deficient embryos despite the high polyglutamylfolate concentration.

In *splotch* and $+/+^{ct}$ embryos, the folate deficient diet (FD) led to a decrease in the ratio of SAM/SAH primarily due to high embryonic concentrations of SAH. Unexpectedly, in *ct/ct* embryos the response was reversed such that the SAM/SAH ratio increased due to high concentrations of SAM in folate deficient *ct/ct* embryos. To explore this difference further, work could be undertaken to analyse concentrations of SAM and SAH in younger embryos to determine the metabolic response as neurulation occurs. The analysis of SAM and SAH levels in E10.5 folate deficient *ct/ct* embryos may provide further insight, although embryos would need to be pooled due to their small size.

PCMT-null mice, which lack a protein methyltransferase enzyme required for protein repair, have a high SAM/SAH ratio (Kim et al., 1997). This raises the possibility that *ct/ct* mice may have a methylation defect whereby they are unable to utilise available methyl groups causing a build-up of SAM. In such a model, the build-up of SAM is envisaged to be minimal under normal dietary conditions whereas under folate deficient conditions the build-up of SAM becomes apparent. This could explain why folic acid treatment does not rescue NTDs in *ct/ct* embryos as exogenous folic acid may not rescue the methylation defect. Alternatively, this may suggest that folate-sensitive NTDs do not have defects in the methylation cycle.

6.4.5 Alternative mechanisms underlying folate-sensitive NTDs in *curly tail* embryos

The evidence appears to suggest that growth and developmental retardation play a role in the mechanism underlying folate-sensitive NTDs in *curly tail* embryos. However, other possible mechanisms should also be considered. Reduced expression of *RARβ* in the hindgut endoderm of affected *ct/ct* embryos correlates with decreased cell proliferation in this tissue (Chen et al., 1994). Administration of retinoic acid or inositol leads to an upregulation of *RARβ* expression in the hindgut endoderm. This is proposed to enhance cell proliferation in the hindgut and rescue spinal NTDs, although a causative link has not been proven (Chen et al., 1994;Greene and Copp, 1997). Further work analysing *RARβ* expression and cell proliferation in folate-deficient *curly tail* embryos could provide insight into the mechanism underlying folate-sensitive cranial NTDs. However, the mechanisms of closure in the cranial and caudal regions involve different developmental processes and the mechanism of NTD induction may differ (Copp, 2005). Despite this, the biochemical pathways of retinoic acid and homocysteine have some overlap, since homocysteine has been shown to disrupt conversion of retinal to the biologically active derivative, retinoic acid, *in vitro*. Limpach et al. proposed this as the mechanism of NTD induction by homocysteine in avian embryos (Limpach et al., 2000). Thus, higher levels of homocysteine in *ct/ct* and $+/+^{ct}$ mice could potentially affect NTD risk by blocking the synthesis of retinoic acid.

6.4.6 How does *myo*-inositol rescue cranial NTDs in $+/+^{ct}$ embryos?

The protective effect of inositol on spinal neurulation in *ct/ct* embryos depends on activation of protein kinase C (PKC), which stimulates cell proliferation in the hindgut (Cogram et al., 2004;Greene and Copp, 1997). Evidence suggests that neurulation does not depend on PKC activation, and defective closure in *curly tail* embryos is unlikely to result from a deficiency in specific PKC isoforms (Cogram et al., 2004). Rather exogenous inositol is thought to operate through the stimulation of the cell cycle that requires activation of specific PKC isoforms In particular, the activity of PKC isoforms βI and γ are essential, whereas other isoforms (α, βII, δ, ε) were found to be dispensable (Cogram et al., 2004). Over-expression of PKCβI has been shown to lead to increased proliferation of aortic endothelial cells (Rosales et al., 1998) and vascular smooth muscle cells (Yamamoto et al., 1998). Thus, if a similar effect is present in cranial tissues, activation of PKCβI by *myo*-inositol may increase cell proliferation and enable cranial neural tube closure to occur. Further studies are required to determine whether the protective action of inositol in folate deficient $+/+^{ct}$ involves stimulation of proliferation via the activation of PKC isoforms.

In this study, *myo*-inositol treatment did not rescue cranial NTDs in folate deficient *ct/ct* embryos. Perhaps the unknown underlying mechanism could have been further disrupted due to combination of the *ct* mutation and the folate deficient diet, as indicated by the increased frequency of NTDs. Therefore, higher doses of *myo*-inositol, or the use of D-*chiro*-inositol may be required especially since it has been proven that the prevention of NTDs in *ct* embryos by inositol is dose- and epimer-dependent (Cogram et al., 2002). Indeed, higher doses of folic acid were required to rescue folate deficiency in *ct/ct* embryos. Higher doses of *myo*-inositol, or the use of D-*chiro*-Inositol, may also prevent the severe and frequent NTDs observed in *Grhl3-/-* mice (Ting et al., 2003).

6.4.7 Summary

In humans, folic acid has been shown to be highly effective at preventing NTDs and sub-optimal folate status is a known risk factor for NTD. Although folic acid also has a preventative action in some mouse models, there are several models, including the *curly tail* mutant mouse, in which the NTDs are resistant to rescue by FA therapy. This has led to the term "folate-resistant" NTD. Here I show that folate deficiency by effective dietary intervention causes exencephaly in "folate-resistant" curly tail embryos. I also demonstrate for the first time that dietary folate deficiency causes NTDs in wild-type congenic embryos and show that these folate-deficient NTDs can be rescued by inositol. Our findings highlight that folate deficiency increases the risk of NTD and suggest that inositol may be a possible therapy to use in conjunction with folic acid to prevent more cases of NTDs.

CHAPTER 7

Developing a quantitative method for the analysis of myo-inositol in urine by liquid chromatography tandem mass spectrometry.

7.1 Introduction

7.1.1 *Myo*-Inositol

Myo-Inositol (MI), a six-carbon sugar alcohol is the most abundant of the nine epimers of inositol in cells. As a constituent of living cells, inositol plays a important role in numerous biological functions. Free inositol is implicated in the control of cell volume and cell osmolarity (Kane et al., 1992). Inositol phosphates and their derivatives are involved in signalling pathways (Shears, 1998;Stuart et al., 1993), arachidonic acid metabolism, the modulation of membrane bound enzymes, mediation of transmembrane passage (Holub, 1986), cytoskeletal and endomembrane regulation (Dove and Michell, 2000) and insulin signalling (Alessi and Downes, 1998). In addition, many proteins are bound to the cell surface by a glycosylphosphatidylinositol (GPI) linkage (Brown and Waneck, 1992;Hooper, 1997;Low, 1989).

Human adults consume approximately 1 g of inositol per day in different biochemical forms (Holub, 1986). Free inositol is actively transported across the intestinal wall by a mechanism dependent on sodium and energy, a process that can be inhibited by glucose (Caspary and Crane, 1970;Scalera et al., 1991). Inositol is transported in blood plasma at a concentration of approximately 30 μM in healthy subjects (Clements and Diethelm, 1979). Circulating free inositol is taken up by most tissues by a membrane-associated sodium-dependent inositol co-transporter that is temperature-dependent, energy-dependent and saturable (Holub, 1986;Kane et al., 1992). Inositol penetrates the blood-brain barrier poorly (Spector, 1988;Spector and Lorenzo, 1975), such that a dose of 12 g for 7 days is needed to raise cerebrospinal fluid levels in human subjects by 70% (Levine et al., 1993). Several mammalian tissues such as the testes, mammary gland, brain, liver and kidney are able to synthesise inositol from glucose (Hooper, 1997). In particular, it is estimated that one kidney can synthesise approximately 2 g of inositol per day.

7.1.2 Prevention of neural tube defects by inositol

Considerable evidence has now accumulated to indicate the need and appropriateness of a clinical trial to assess whether inositol is capable of preventing FA-resistant NTDs in humans, as in mice. These several lines of evidence can be summarised as:

1. Inositol deficiency is the only 'vitamin' deficiency that leads to NTDs in mice (Cockroft, 1988;Cockroft et al., 1992).

2. Significantly lower inositol concentration is present in the blood of mothers carrying NTD fetuses than in normal pregnancies (Groenen et al., 2003). The inositol:creatine ratio in the brain of hydrocephalic fetuses was found to be significantly lower than in normal fetuses (Kok et al., 2003). Hence, human NTDs may be associated with inositol deficiency.

3. Inositol supplementation of the NTD mutant mouse model *curly tail* during pregnancy, significantly reduces the frequency of NTDs (Cogram et al., 2002;Greene and Copp, 1997), a finding that has been replicated recently in another laboratory (Ting et al., 2003).

4. In a single case study, a woman took 0.5 g *myo*-inositol per day in the first trimester of her third pregnancy, after two previous pregnancies were terminated because of NTDs (she took FA in both). The third pregnancy was uneventful, and a normal baby was born (Cavalli and Copp, 2002). Since then four more women, all at high risk of NTD recurrence, have taken 0.5 g *myo*-inositol per day and gone on to have pregnancies without NTDs (Dr Pietro Cavalli, personal communication, 2005).

Inositol therapy appears safe during mouse pregnancy. Detailed pathological analysis of inositol-treated *curly tail* mice revealed no major fetal defects and no increase in fetal loss (Cogram et al., 2002). Treated pregnant females showed no adverse effects. Regarding the safety of inositol in human pregnancy, the mother who took inositol in a third pregnancy reported no side effects (Cavalli and Copp, 2002). Trials in adults for depressive pychiatric disorders (Levine et al., 1995), to improve insulin sensitivity in polycystic ovary syndrome (Nestler et al., 1999), and to ameliorate psoriasis in patients on lithium therapy (Allan et al., 2004) have all identified beneficial effects of inositol with no major side effects. In children, inositol has been used to treat autism (Levine et al., 1997) and to reduce the severity of respiratory distress syndrome in premature babies (Hallman et al., 1992). Relatively high inositol doses have been used; up to 20 g per day in adults and 200 mg/kg in children. Inositol is a constituent of living cells, is widespread in many foods, and is an essential nutrient included in the culture medium of many cell lines. Thus, it seems unlikely that exogenous inositol therapy will pose a risk to the mother and/or embryo/fetus.

7.1.3 The PONTI (Prevention Of Neural Tube defects by Inositol) study

The PONTI study, a randomised, double blind clinical trial, has been set-up to compare (i) FA (folic acid) plus placebo, and (ii) FA plus MI, for prevention of NTD recurrence.

The aim is to evaluate the effectiveness of MI in the context of co-administration with FA. Hence, a simple two-arm trial protocol has been adopted, in which all subjects receive identical FA supplementation at the 'high dose' level of 5 mg/day, typically used in pregnancies at risk of NTDs. The MI dose level is set at 1 g/day. Placebo is used instead of MI in the control group. Women are recruited into the trial who are planning a pregnancy and who have a history of one or more NTD pregnancies. Supplementation begins prior to conception and continues until the 12th week of pregnancy. Pregnancy outcome is determined by second trimester ultrasound scanning plus follow up of term pregnancies. Compliance is to be monitored by the collection of urine samples prior to trial entry, 2 weeks after trial entry and following conception at the first antenatal clinic.

7.1.4 Monitoring compliance

The kidneys play a major role in the regulation of plasma inositol concentration; besides being able to synthesise inositol, they are the primary sites of clearance. The kidney is the only organ containing inositol oxygenase, the rate limiting enzyme in the catabolism of inositol (Bry and Hallman, 1991). Clearance of inositol by the human kidney was found to be 1 g/day, rising to 21 g/day in cases of hyperinositolaemia. Thus, it was expected that the concentration of MI in urine would be within a detectable range and would be a good marker of physiological changes in MI levels. Additionally, PONTI trial participants would be able to collect the urine sample themselves and post it to the laboratory for analysis, overcoming the need to arrange blood collection.

Methods for the quantitation of MI in urine, plasma and tissue samples have been developed using gas chromatography/mass spectrometry (GC-MS) (Lee and Chung, 2006;Tetsuo et al., 1999), LC-MS (Perello et al., 2004) and LC-MS/MS (Kindt et al., 2004;Perello et al., 2004). It is also possible to measure MI by enzymatic assay (Ashizawa et al., 2000;Kouzuma et al., 2001) or by magnetic resonance imaging (Srinivasan et al., 2004)). Initial investigations demonstrated that the LC-MS/MS method described by Kindt et al. (2004) is not applicable to samples which contain glucose due to suppression of the *myo*-inositol signal. Therefore, a new method has been developed for the quantitative analysis of MI by LC-MS/MS which uses a HPLC to separate these two metabolites. This has been applied to urine but could potentially be used to analyse other tissue samples which contain high concentrations of glucose, such as serum. In particular, the specificity of the method has been thoroughly investigated since inositol has the same molecular weight as other common hexose monosaccharides. Furthermore, the LC method was tested for its ability to separate

other inositol epimers, which the mass spectrometer is unable to differentiate due to identical SRM transitions.

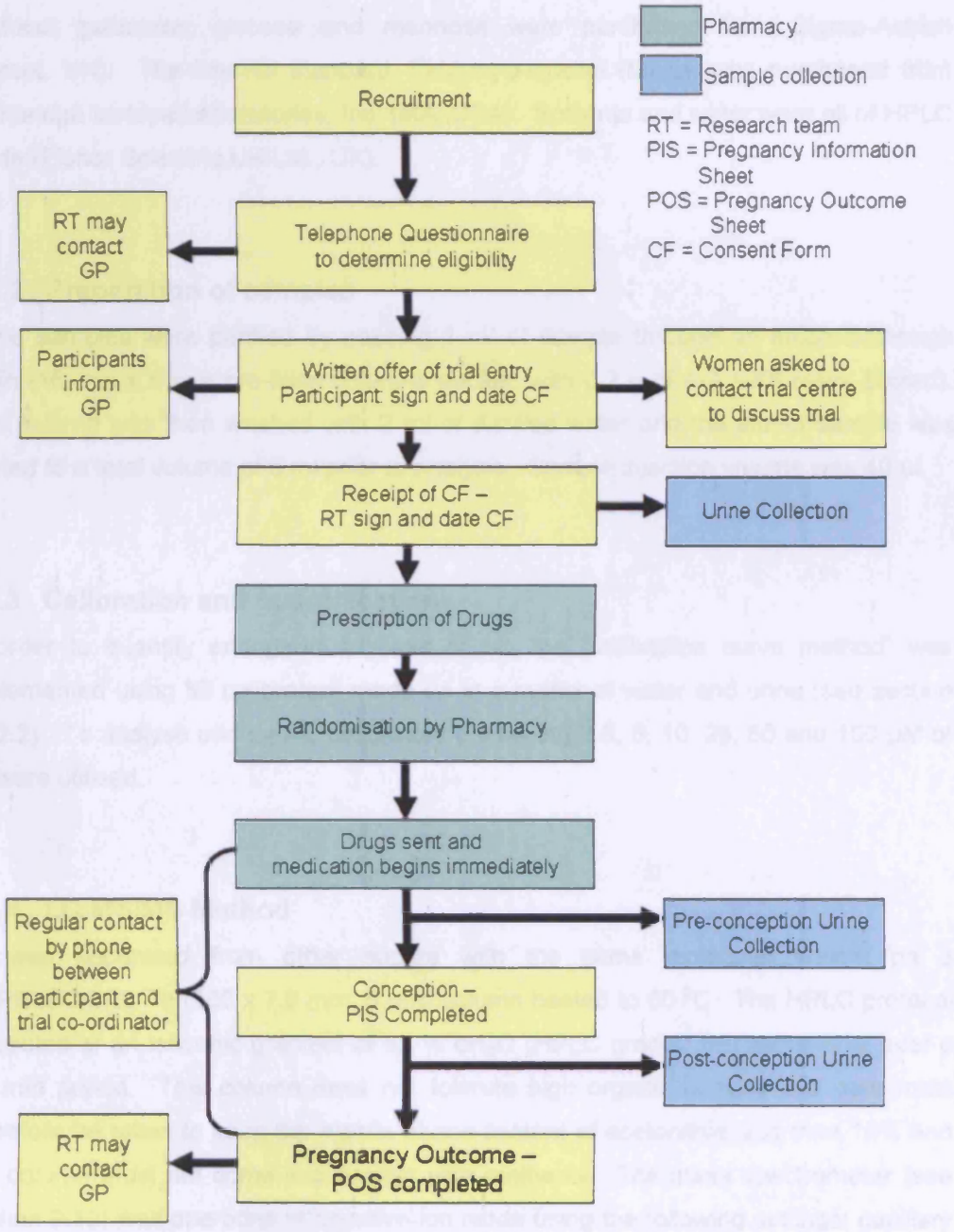

Figure 7.1. Flow chart of procedures for the PONTI Study.

7.2 Materials and Methods

7.2.1 Materials

Readily available inositol epimers (*myo-*, *allo-*, *muco-*, D-*chiro*, L-*chiro-* *scyllo-*,), fructose, galactose, glucose and mannose were purchased from Sigma-Aldrich (Dorset, UK). The internal standard, [$^2H_6$]-*myo*-inositol (MID_6), was purchased from Cambridge Isotope Laboratories, Inc. (MA, USA). Solvents and water were all of HPLC grade (Fisher Scientific UK Ltd., UK).

7.2.2 Preparation of samples

Urine samples were purified by passing 1 ml of sample through an anion-exchange resin (16 mm x 5 mm pre-filled columns packed with 0.2 g of AG 1-X8 resin, Biorad). The column was then washed with 2 ml of distilled water and the eluted sample was diluted to a total volume of 5 ml prior to analysis. Sample injection volume was 40 µl.

7.2.3 Calibration and quantification

In order to quantify endogenous levels of MI, the "calibration curve method" was implemented using MI calibrators made up in a matrix of water and urine (see section 2.12.2). To analyse urinary MI, calibrators containing 2.5, 5, 10, 25, 50 and 100 µM of MI were utilised.

7.2.4 LC-MS/MS Method

MI was separated from other sugars with the same molecular weight on a SUPELCOGEL Pb (300 x 7.8 mm; 5 µm) column heated to 60 °C. The HPLC protocol consisted of an isocratic gradient of 95 % dH_2O (HPLC grade): 5% acetonitrile over a 40 min period. This column does not tolerate high organic content and care must therefore be taken to keep the mobile phase content of acetonitrile less than 10% and the column must not come into contact with methanol. The mass spectrometer (see section 2.12) was operating in negative-ion mode using the following settings: capillary 3.75 kV, cone voltage 19 V, collision energy 19 V, cone gas flow rate 90 L/hr and desolvation gas flow rate 900 L/hr.

7.3 Results

7.3.1 Mass Spectra

A greater signal to noise ratio was apparent following the direct infusion of MI and [$^2H_6$]-MI into the MS/MS in negative ion mode, compared to positive ion mode. Thus MS/MS conditions were optimised for the predicted [M-H]$^-$ deprotonated molecule of m/z 178.8 for MI and m/z 184.9 for $^2H_6$-MI (Figure 7.2). Of note, the [$^2H_6$]-MI internal standard is deuterated on the carbon backbone, therefore the deprotonated molecule corresponds to a loss of a hydrogen ([M-H]$^-$) as opposed to a loss of deuterium ([M-D]$^-$). Product ion spectra for MI and [$^2H_6$]-MI yielded specific fragment ions of m/z 86.4 and 88.5, respectively (Figure 7.2). Although the most abundant product ion for MI and [$^2H_6$]-MI were m/z 160.8 and 166.8, respectively, further analysis of this reaction (178.8 → 160.8) in urine samples demonstrated poor signal intensity, peak shape and reproducibility compared to the more specific reaction (178.8 → 86.4). Thus, the final SRM transitions were as follows: MI, 178.8 → 86.4; [$^2H_6$]-MI, 184.9 → 88.5.

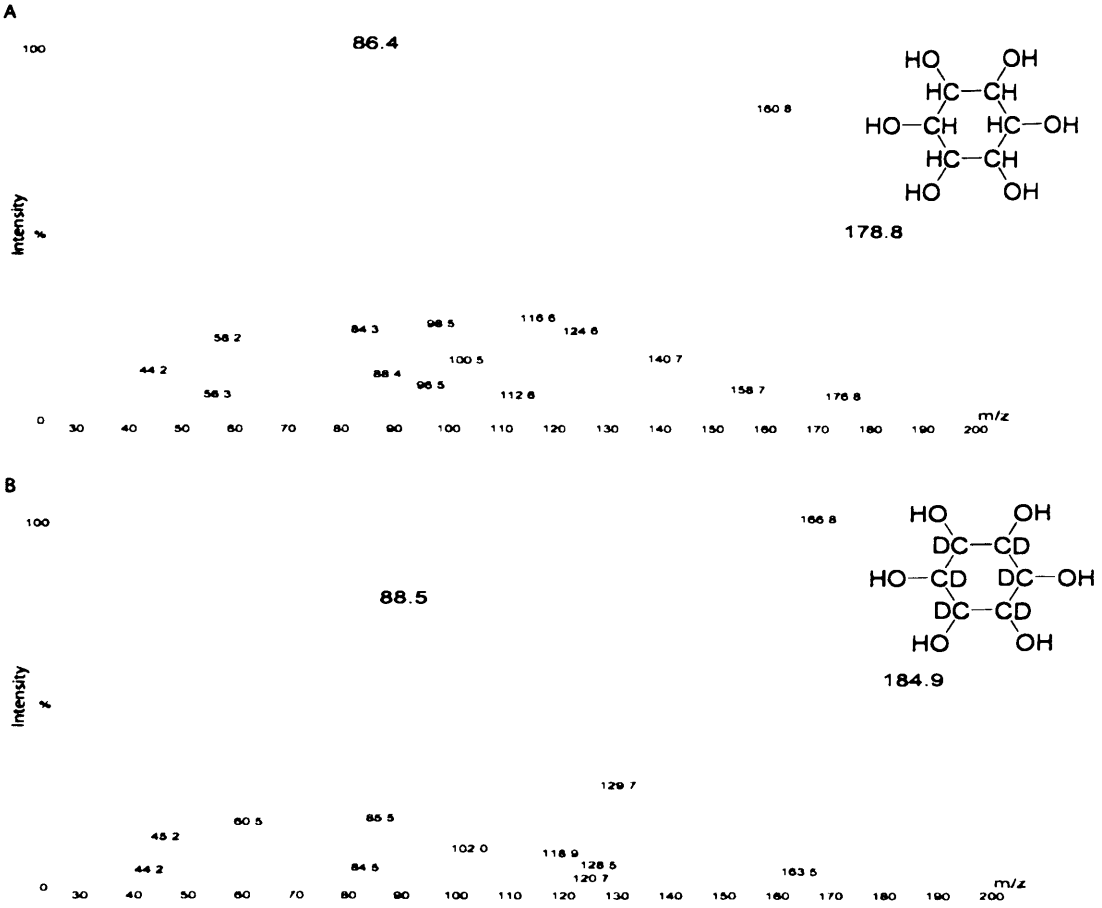

Figure 7.2. Negative ion spectra of [M-H]$^-$ used for quantification. Molecular ions were at m/z 178.8 for MI (A) and 184.9 for [$^2H_6$]-MI (B). The MS/MS conditions were optimised to favour the transition to major product ions at m/z 86.4 (A) and 88.5 (B).

Since other common endogenous hexose monosaccharides have the same molecular weight as MI, the specificity of the tandem mass spectrometer and selectivity of the HPLC method was investigated. To do this, MS/MS conditions in negative ion mode were optimised for the expected $[M-H]^-$ deprotonated molecular ions of m/z 179.0, 178.8, 178.8 and 178.8 for glucose, galactose, fructose and mannose, respectively. Observed experimental results matched the theoretical masses (Figure 7.3). Product ion spectra for glucose, galactose, fructose and mannose yielded specific abundant fragments of m/z 88.8, 88.3, 88.3 and 88.3, respectively (Figure 7.3). The final SRM transitions for the five monosaccharides were; glucose, 179.0 → 88.8; galactose 178.8 → 88.3; fructose 178.8 → 88.3; mannose 178.8 → 88.3. Although galactose, fructose and mannose have identical molecular ions to MI, the product ion of m/z 88.3 was not apparent in the product ion spectra for MI. This demonstrates that tandem mass spectrometry is able to specifically analyse metabolites with the same molecular weight due to variations in fragmentation patterns.

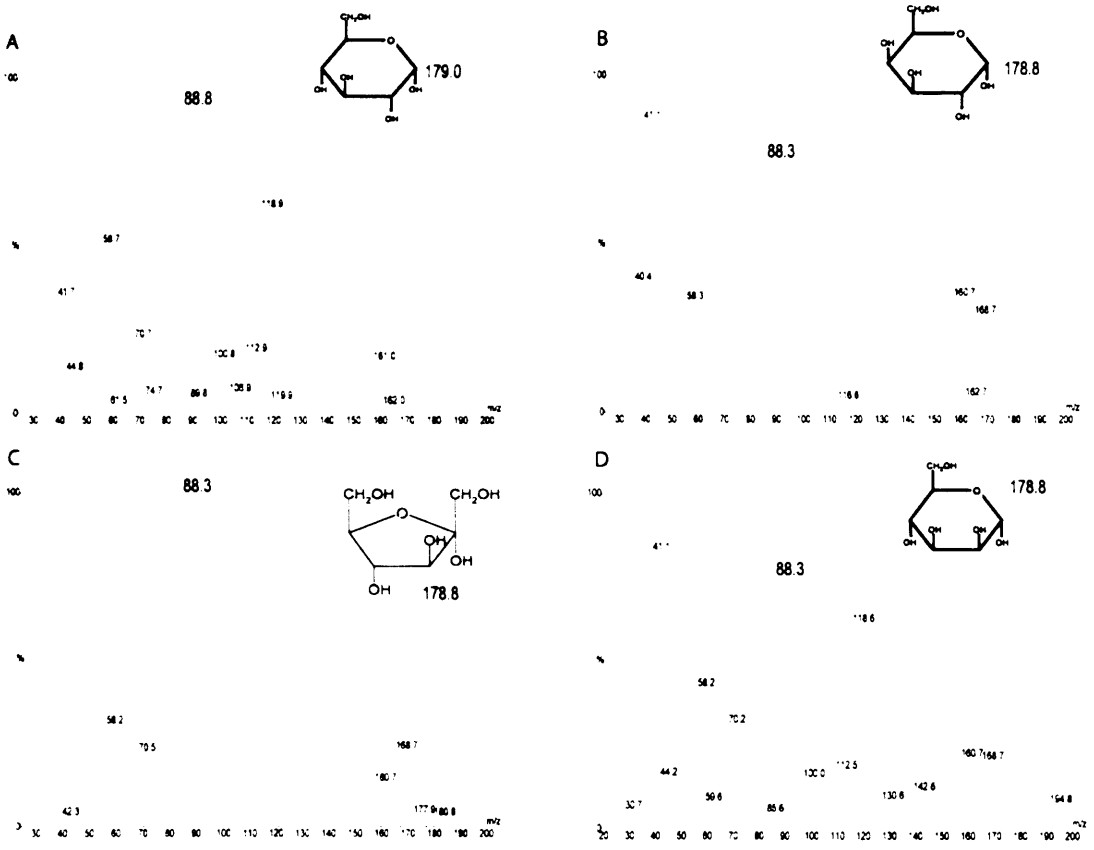

Figure 7.3. Negative ion spectra of $[M-H]^-$ used to analyse potentially interfering hexose monosaccharides. Precursor ions were at m/z 179.0 for glucose (A), 178.8 for galactose (B), 178.8 for fructose (C) and 178.8 for mannose (D). The collision energy was optimised to favour the transition to major product ions at m/z 88.8 (A), 88.3 (B), 88.3 (C) and 88.3 (D).

In addition to the *myo*- form, various other endogenous and synthetic epimers of inositol are known. The mass spectrometer was unable to selectively determine epimers owing to the identical molecular ions and fragmentation ions (Figure 7.4). Thus, in order to quantify each inositol epimer individually an HPLC method would be required to resolve these metabolites based on their unique physical and chemical properties.

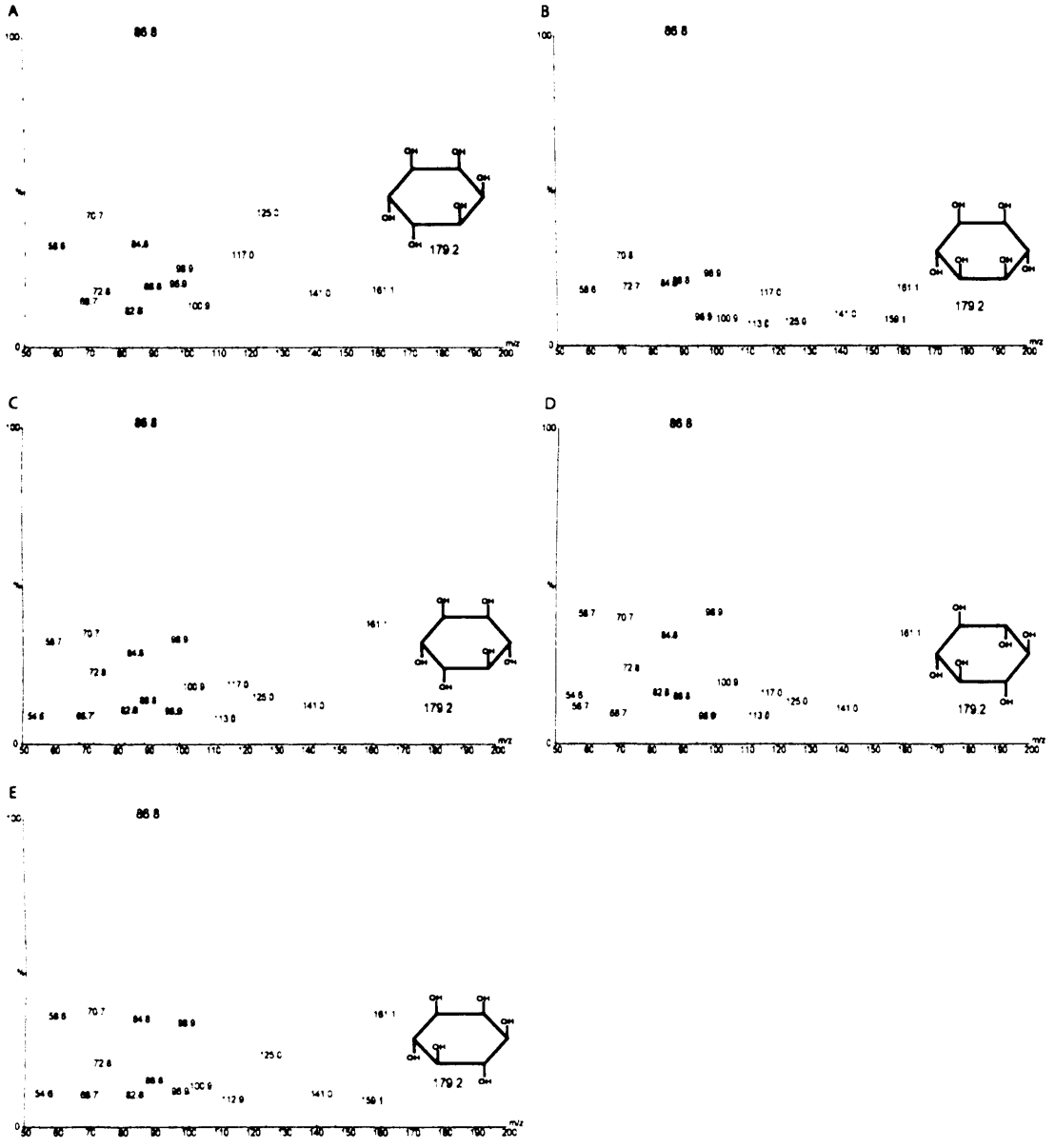

Figure 7.4. Negative ion spectra of [M-H]$^-$ of inositol epimers. Precursor ions were at m/z 179.2 for *allo*-inositol (A), 179.2 for *muco*-inositol (B), 179.2 for L-*chiro*-inositol (C) and 179.2 for *scyllo*-inositol (D) and 179.2 for MI (E). For all inositol epimers, the major product ion was at m/z 86.8 (A, B, C, D). The MS/MS conditions were the same as those selected for *myo*-inositol (see section 7.2.6).

7.3.2 Chromatography

Initially, the HPLC separation method recommended by Kindt et al. was tested using a Metachem (Varian) Polaris Amide (2.0 x 10 mm, 5 µm) column fitted with a MetaGuard Polaris guard column (Metaguard Amide 5 µm, Varian) (Kindt et al., 2004). The mobile phase consisted of 5 mM ammonium acetate/acetonitrile (50:50, v/v) delivered at a flow rate of 0.2 ml/min. Final chromatographic retention times for MI and [$^2H_6$]-MI were between 1.8 and 2 min. Using an aqueous standard, no significant interference was observed from glucose at the selected SRM for MI (178.8 > 86.4) presumably due to differences in m/z of precursor and product ions.

Although glucose did not interfere with the method for normal urine, glucose is present at high concentrations in many other biological fluids and is often found in urine of diabetics. Therefore to assess the general applicability of the method, the effect of co-elution of glucose on the intensity of the MI signal was investigated. Co-elution of glucose (at concentrations typically found in serum) significantly suppressed the intensity of the MI signal by approximately seven orders of magnitude (Figure 7.5). Thus, in order to ensure this method could later be adapted for other biological fluids and tissues besides urine, further work was undertaken to identify a column capable of separating hexose monosaccharides, to avoid signal suppression by co-elution.

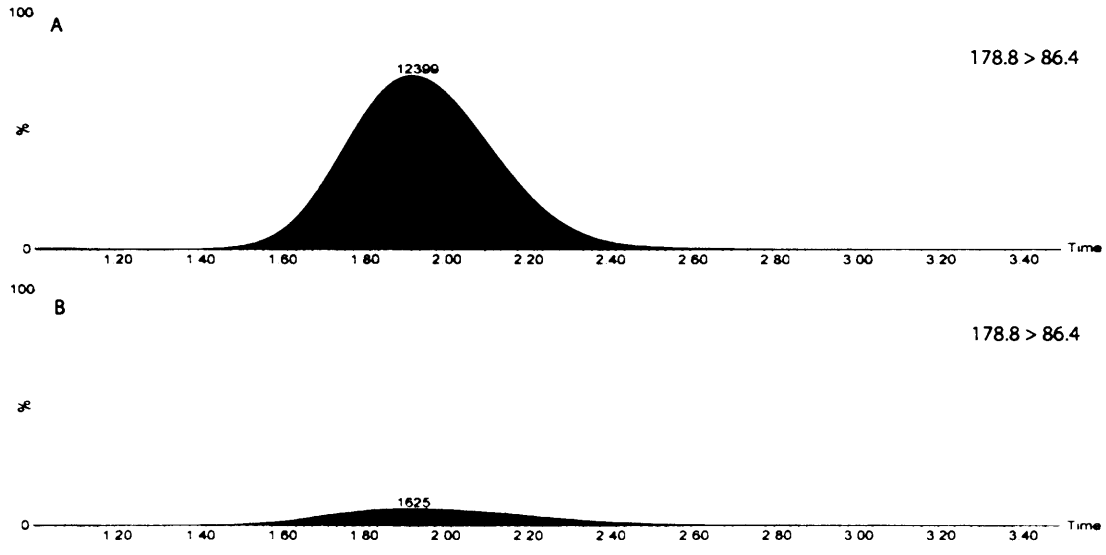

Figure 7.5. Suppression of *myo*-inositol by co-eluting glucose. (A) 10 µM *myo*-inositol aqueous standard, (B) 10 µM *myo*-inositol aqueous standard plus 5 mM glucose aqueous standard. Vertical axes are linked.

Kindt et al. also developed a chiral separation method that was capable of resolving four inositol epimers (*chiro-, muco-, scyllo-* and *myo-*) using 40 minute runs (Kindt et al., 2004). Since this column was able to resolve inositol isomers, it was tested for its ability to resolve glucose and MI to attempt to overcome signal suppression by co-elution. To minimise costs, a guard column was purchased (Chiral-AGP Guard 4.0 x 10 mm; 5 µm, Chromtech). Retention times for MI and glucose were identical (0.87 min) using a mobile phase consisting of 5 mM ammonium acetate and acetonitrile (50:50, v/v; flow rate 0.2 ml/min). Subsequently, aqueous standards of MI and glucose were sent to Chromtech and it was confirmed by the manufacturers that the Chiral-AGP 150 x 4 mm (5 µm) column was not capable of resolving glucose and MI. Thus, the Chiral-AGP column cannot be used to accurately quantify MI in samples with a high concentration of glucose.

Several alternative columns suitable for carbohydrate analysis were then considered. The SUPELCOGEL Pb (300 x 7.8 mm; 5 µm) column was selected as this column was reported to separate glucose and MI (Bulletin 887B, Supelco Literature, Sigma-Aldrich). It was also reported that this column was able to resolve galactose, fructose and mannose from MI, all of which have the same molecular mass. Analysis of aqueous standards confirmed that this column was capable of resolving MI, glucose, galactose, fructose and mannose over a 40 minute run with acceptable chromatographic peak shape (Figure 7.6). Importantly, the elution time of glucose and MI were well separated, by 13 minutes. The ability to resolve these metabolites overcomes potential problems of signal suppression by high concentrations of co-eluting hexose monosaccharides (Figure 7.6).

The specificity of the tandem mass spectrometer for analysis of MI was also confirmed by analysing a mixture of glucose, galactose, fructose, mannose and MI, at a concentration of 20 µM using the SRM channel (*m/z* 178.8 > 86.4) selected for MI. The chromatograms demonstrated that this channel was clear of interference from the other hexoses (Figure 7.7). Thus, interference is minimised because the product ions are different between the pyranoside structure of glucose, galactose, fructose and mannose and the hexahydrocyclohexane structure of MI (Figure 7.7).

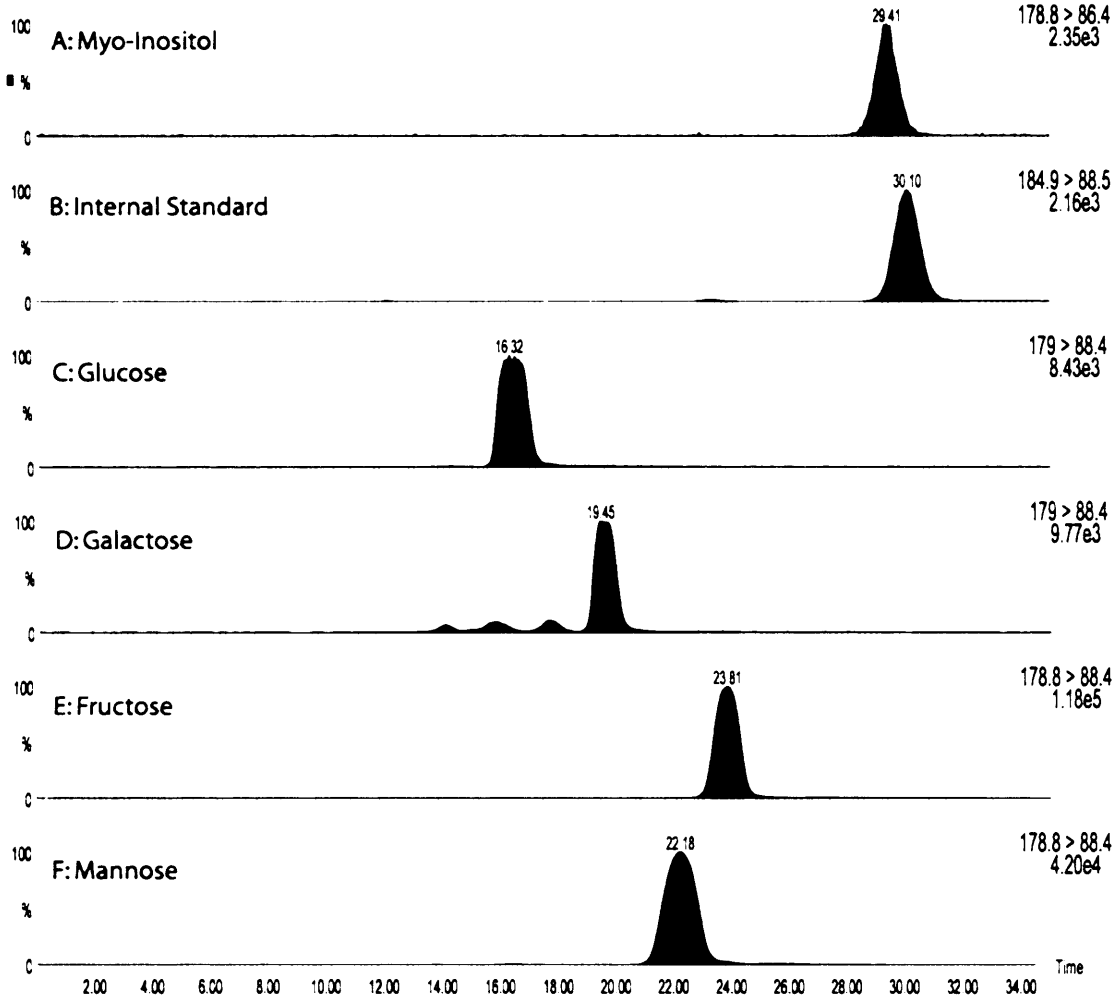

Figure 7.6. Comparison of retention times (min) of four potentially interfering monosaccharides with myo-inositol and the internal standard, using the optimal SRM channel for each molecule. LC-MS/MS chromatograms obtained in SRM mode (channel shown in top right hand corner of each chromatogram) using the SUPELCOGEL Pb (300 x 7.8 mm; 5 µm) column. Representative chromatograms are shown for 20 µM aqueous standards. Vertical axes are linked.

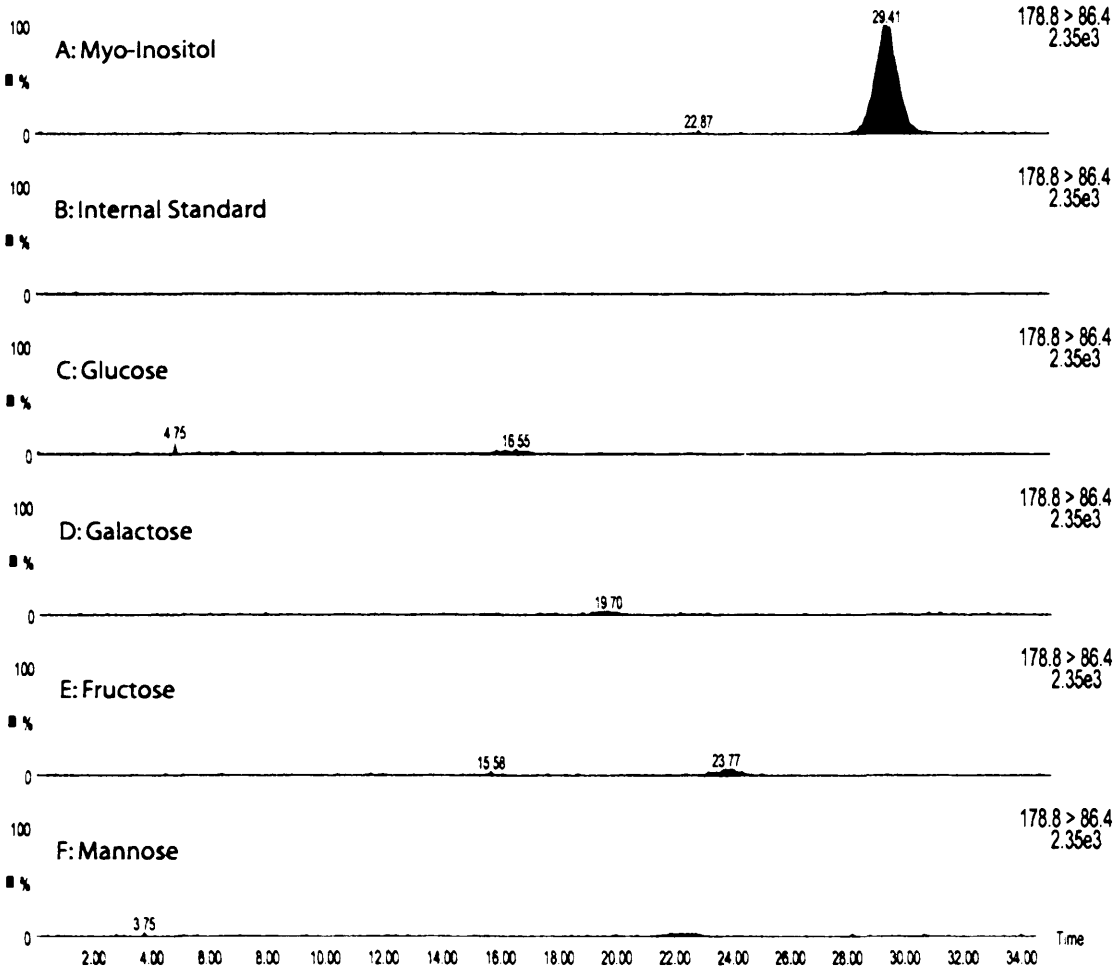

Figure 7.7. Evaluation of potential interference of MS signals for MI by four monosaccharides, using the SRM channel selected for MI (178.8 → 86.4). LC-MS/MS chromatograms obtained using the SUPELCOGEL Pb (300 x 7.8 mm; 5 µm) column. Representative chromatograms are shown for 20 µM aqueous standards. Vertical axes are linked.

As demonstrated, tandem mass spectrometry alone, without chromatographic resolution, could not distinguish the various inositol epimers (Figure 7.3). To determine if the HPLC method was capable of resolving inositol epimers, a mixture of *myo*- and D-*chiro*-inositol was analysed by LC-MS/MS. As indicated on the selected-ion chromatogram, this HPLC column is able to resolve these two epimers by approximately two minutes (Figure 7.8.).

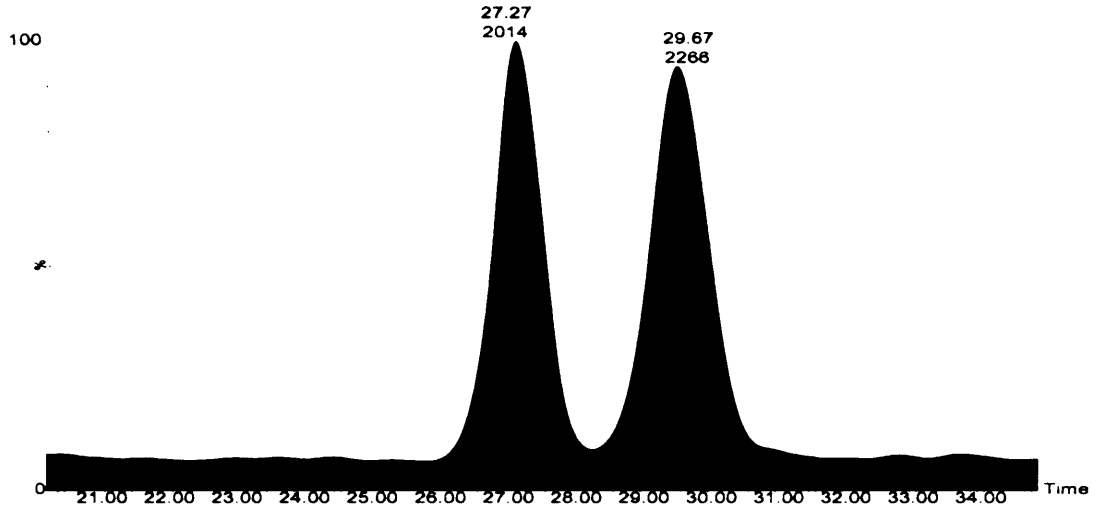

Figure 7.8. Elution profiles of *myo*- and D-*chiro*-inositol on the SUPECLOGEL Pb (300 x 7.8 mm; 5 µm) column. The retention time of 10 µm D-*chiro*- inositol was 27.27 and the retention time of 10 µM *myo*-inositol aqueous standard was 29.67 min. SRM transition m/z 179.2 → 86.8.

Elution profiles of L-*chiro, allo*-, *muco*- and *scyllo*-inositol were subsequently verified (Figure 7.9). Two ions were apparent for *scyllo*-inositol; a narrow chromatographic peak eluting at 26 min had the highest intensity and a second broad chromatographic peak was apparent at 41 min. For *allo*-inositol, a broad chromatographic peak eluted at 46 min and there was a small chromatographic peak at 26 min. A single ion was apparent for L-*chiro*- and *muco*- inositol at 33 and 34 min, respectively. Thus all epimers tested, apart from *muco*-, could be resolved from MI by HPLC. Of note, both L-*chiro*- and D-*chiro*-inositol co-eluted at 27-28 min (Figure 7.8 and 7.9), indicating that the HPLC column was not able to resolve chiral epimers.

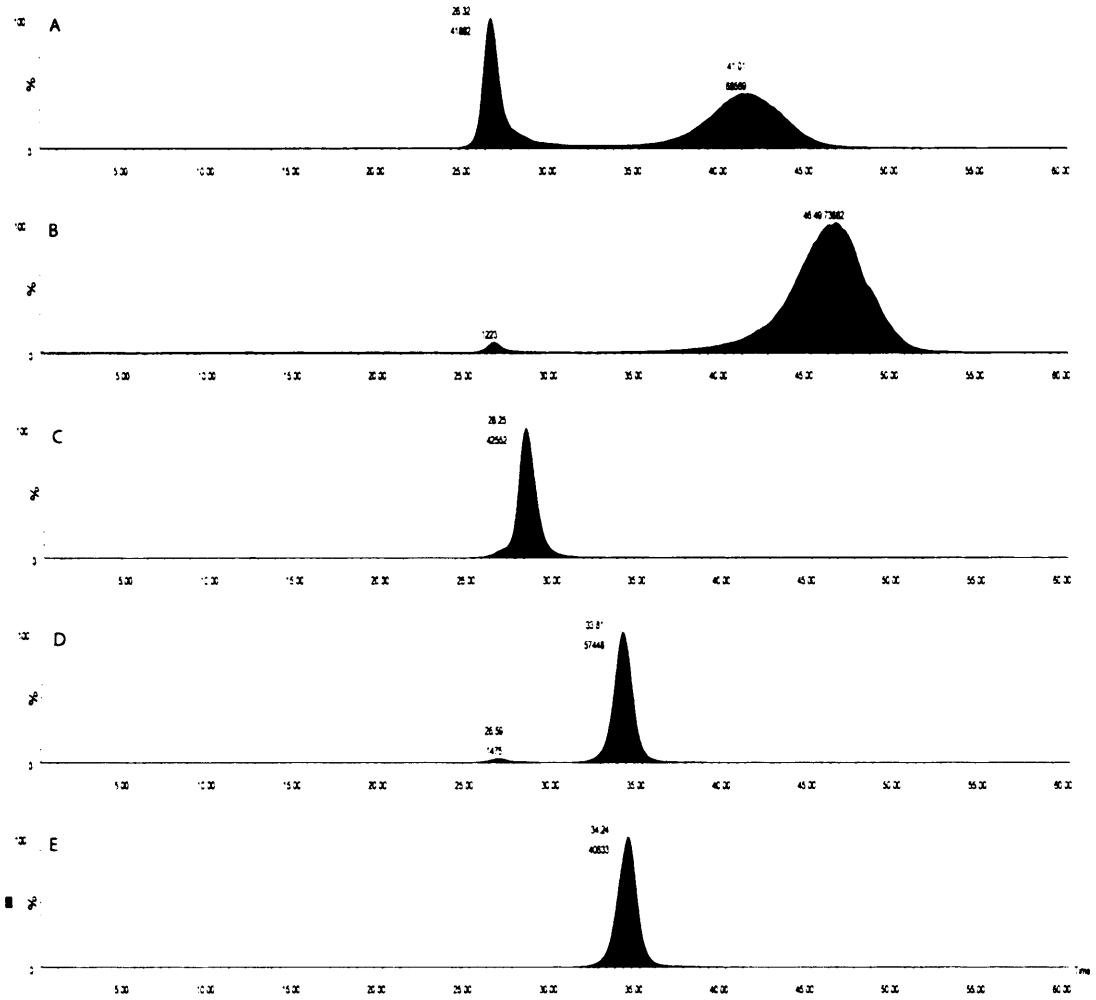

Figure 7.9. Elution profiles of inositol epimers. (A) *Scyllo*-Inositol, (B) *Allo*-Inositol, (C) L-*chiro*-inositol, (D) *Muco*-Inositol, (E) *Myo*-Inositol. In each case, 10 µM aqueous standards were used. SRM transition m/z 179.2 → 86.8. Vertical axes are linked.

7.3.3 Sample Preparation

Samples were prepared using the method reported by Perelló and colleagues (Perello et al., 2004) whereby the urine was passed through an anion-exchange resin which retains ionic compounds and elutes neutral metabolites such as *myo*-inositol. In extracted urine, a prominent ion was apparent eluting at 29 min which matched the retention time of the aqueous MI standard (Figure 7.10). Several other earlier eluting ions were apparent in the extracted urine sample at low intensity using the SRM transitions for MI. The retention times do not match the retention times of the inositol epimers tested. Perhaps these ions correspond to other inositol epimers that were not

tested. Alternatively, MI may be bound to other molecules which could alter the chromatography, yet the bond between these molecules may break in the ion source such that it appears as free MI. Indeed inositol forms many derivatives with phosphates and sugars. Of note, when MI is added to the urine prior to extraction the intensity of the ion at 29 min increased, whilst the intensity of the smaller ions did not change, thus confirming that the ion at 29 min corresponds to free MI in urine.

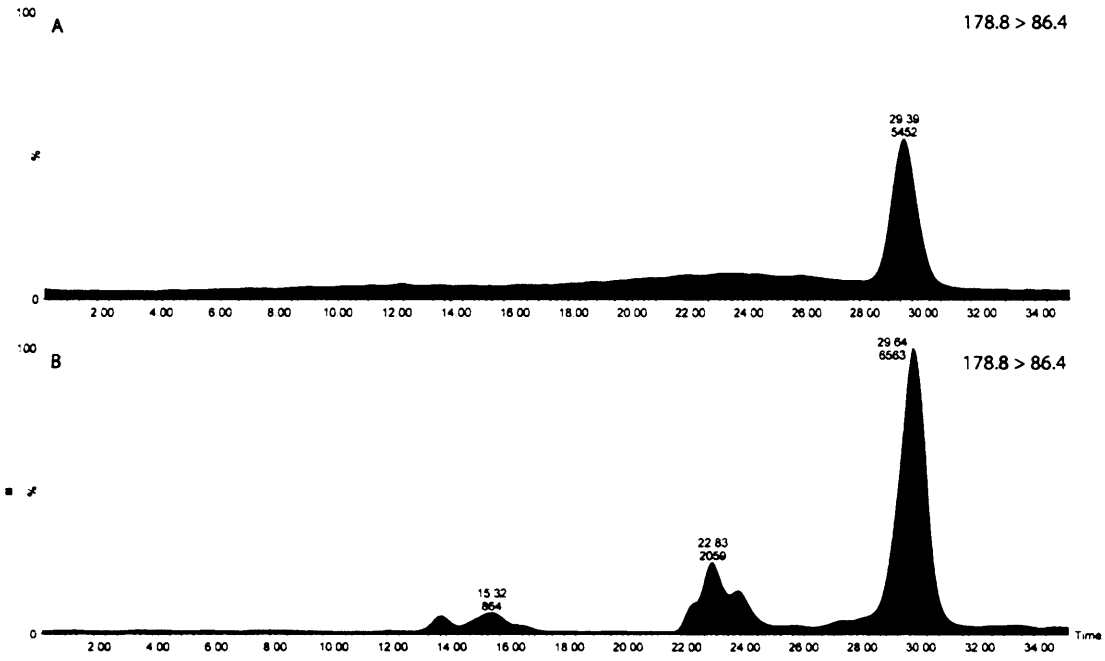

Figure 7.10. Analysis of *myo*-inositol in a urine sample. (A) 20 µM MI, (B) prepared urine sample comprising 1 ml of urine passed through an anion-exchange column (AG 1-X8) with an injection volume of 40 µl. Vertical axes are linked.

7.3.4 Linearity and Precision

The internal standard, [$^2H_6$]-MI, was used for the quantification of MI. Calibration curves made up in dH_2O and urine, were linear throughout a concentration range of 2.5-50 µM (Figure 7.11). The coefficient of linear correlation (r^2) was 0.999 and 0.999 for myo-inositol in aqueous and urine samples, respectively, thus demonstrating that the method developed was suitably linear for quantification purposes.

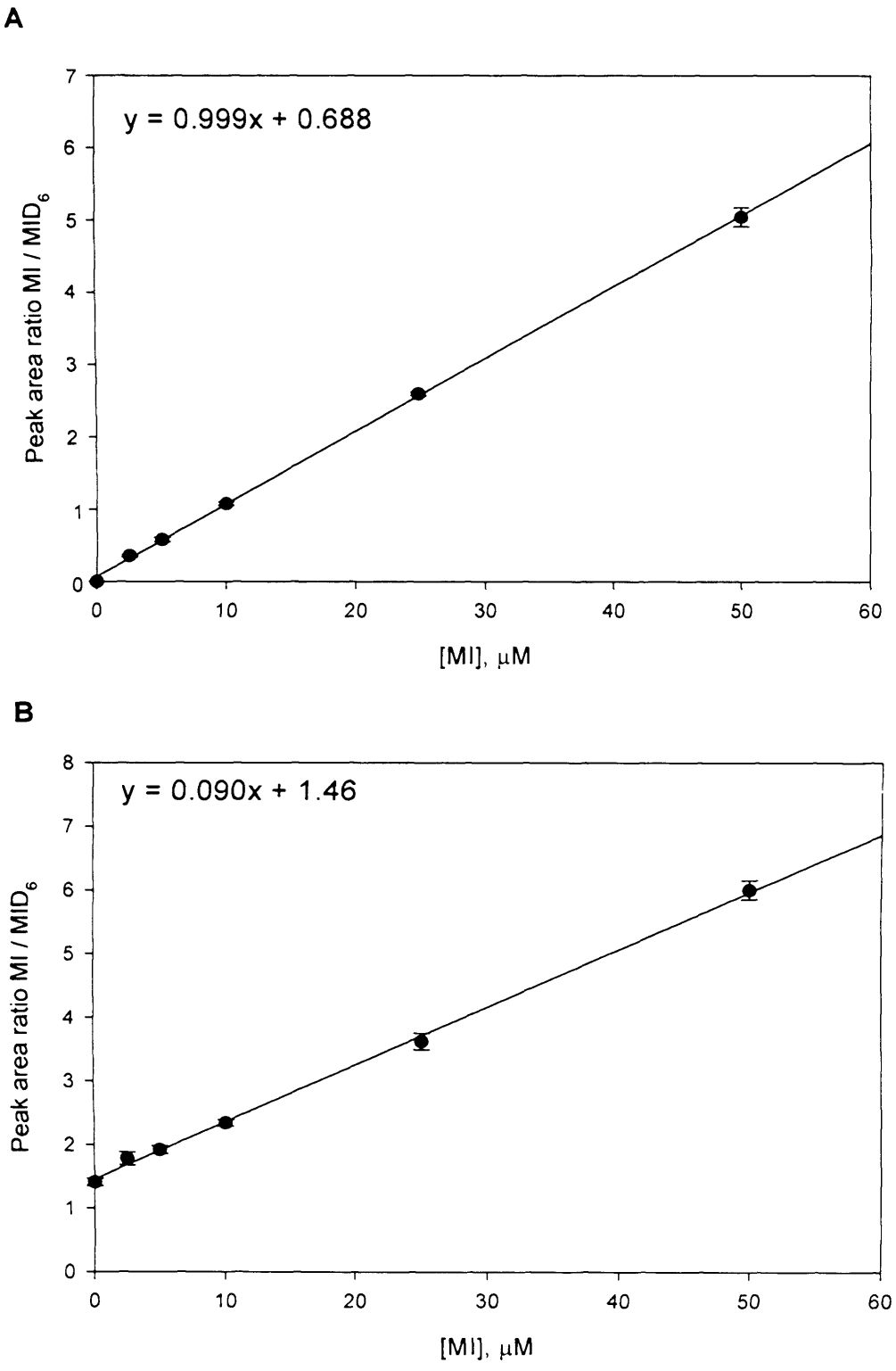

Figure 7.11. Calibration curves of peak-area ratios plotted against myo-inositol concentration. Calibrators were made up in (A) dH_2O and, (B) urine with 10 μmol/L of MID_6 (internal standard) added to each sample. MI data points correspond to 0, 2.5, 5, 10, 25 and 50 μM. Each sample was run in triplicate (n=3).

Preliminary experiments to determine the precision of the proposed LC-MS/MS method were performed with 2.5, 10 and 25 μM of MI made up in dH_2O and urine. All samples contained 10 μM of the internal standard, [$^6H_3$]-MI. Overall, intra-assay coefficients of variation (CVs) ranged from 1.33 to 4.92 % and inter-assay CVs ranged from 5.49 to 13.4 % for the analysis of MI aqueous standards (Table 7.1). Intra-assay coefficients of variation (CVs) ranged from 6.95 to 14.1 % and inter-assay CVs ranged from 4.39 to 10.3 % for the analysis of MI in urine.

Sample	Spiked concentration added (μM)	Precision	**MI**	
			Mean concentration (μM ±SD)	CV (%)
Aqueous	2.5	Intra-assay (n=8)	2.83 ± 0.13	4.51
Aqueous	10	Intra-assay (n=8)	10.97 ± 0.54	4.92
Aqueous	25	Intra-assay (n=8)	27.04 ± 0.36	1.33
Urine	2.5	Intra-assay (n=8)	2.81 ± 0.40	14.14
Urine	10	Intra-assay (n=8)	9.54 ± 0.66	6.95
Aqueous	2.5	Inter-assay (n=7)	2.72 ± 0.36	13.4
Aqueous	10	Inter-assay (n=7)	10.21 ± 0.66	6.42
Aqueous	25	Inter-assay (n=6)	26.12 ± 1.43	5.49
Urine	10	Inter-assay (n=8)	10.21 ± 1.05	10.26
Urine	25	Inter-assay (n=8)	24.49 ± 1.08	4.39

Table 7.1. Inter- and Intra-assay precision of the LC-MS/MS method for aqueous and urine samples. The precision was determined by repeated assay of standard aqueous solutions and urine samples, spiked with 0, 2.5, 10 or 25 μM of myo-inositol. CV, coefficient of variation.

7.4 Conclusion and Discussion

Evidence has accumulated to suggest that inositol, in combination with folic acid, may prevent more cases of NTDs than folic acid alone. Thus, the PONTI study has been set-up to evaluate the benefit of inositol for the prevention of recurrent NTDs. In order to monitor patient compliance the method developed in this chapter will be used to quantify MI in urine. Liquid chromatography tandem mass spectrometry was the method of choice since it combines the specificity of tandem mass spectrometry with the selectivity of liquid chromatography providing enhanced sensitivity, accuracy and high throughput.

In this study, it has been demonstrated how tandem mass spectrometry is able to differentiate between molecules with the same molecular mass such as glucose, fructose, mannose and *myo*-inositol due to variations in product ion masses, which ultimately gives rise to different SRM transitions. Similarly, the LC-MS/MS method reported by Kindt et al. also demonstrated that *myo*-inositol and other hexose monosaccharides have different fragmentation patterns (Kindt et al., 2004). In contrast, Perrello et al. used LC-MS to quantify MI by monitoring m/z = 198, which corresponds to the MI adduct with ammonium cation, an abundant pseudo molecular ion (Perello et al., 2004). Unlike tandem mass spectrometry, LC-MS is unable to differentiate between metabolites with the same molecular weight.

Despite the specificity of tandem mass spectrometry, results from this study show that simultaneous elution of glucose with MI considerably suppresses the signal for MI by approximately seven orders of magnitude. Thus, in order to analyse MI in tissue samples such as serum with a high concentration of glucose, an LC column would be required to separate the two metabolites. Monosaccharide analyses are a challenge for chromatography due to the diversity of compounds with chemical and physical properties only differing slightly. Hence, HPLC separations depend on differences in conformation, configuration and bonding. In resin-based SUPELCOGEL columns, carbohydrates elute in descending order of molecular size with monosaccharides last (Bulletin 887B, Supelco Literature, Sigma-Aldrich). The pores in the resins exclude polysaccharides and larger oligosaccharides, which elute first. Smaller di- and monosaccharides enter the pores, interact with the counter-ions and are more strongly retained. The lead-form resin in SUPELCOGEL Pb columns provides the highest resolution and best selectivity for monosaccharides. It was confirmed in this study that the SUPELCOGEL Pb column is capable of resolving glucose, galactose, fructose, mannose and MI over a 40 min run time. Therefore these metabolites will enter the

mass spectrometer at different times thereby overcoming signal suppression by co-eluting metabolites.

The LC-MS method reported by Perello et al. also achieved successful resolution of MI and glucose using an Aminex HPX-87C column (Perello et al., 2004). In contrast, the LC-MS/MS method developed by Kindt et al. to quantify MI in rat brain tissue using LC-MS/MS did not resolve *myo*-inositol and glucose, although this may not be a problem in tissues were the concentration of glucose is minimal (Kindt et al., 2004). In healthy persons, urine glucose concentration is minimal, however, it can be present at high concentration in diabetics. Participants involved in the PONTI study may have undiagnosed diabetes which could interfere with the quantification of *myo*-inositol. More importantly, it is hoped that in the future this method could be adapted for other tissues such as serum and whole mouse embryos to aid other research projects.

Kindt et al. reported the use of a novel chiral LC-MS/MS method, using the Chiral-AGP column (ChromTech), to resolve *myo*-inositol from other endogenous inositol epimers including *chiro-, muco-* and *scyllo*-inositol (Kindt et al., 2004). Their analysis of rat brain homogenate revealed that *myo*-inositol was the only major inositol component present in this tissue. In the present study, the SUPELCOGEL Pb column used was able to resolve *scyllo-, allo-* and *chiro*-inositol from *myo*-inositol, but *muco*-inositol had the same retention time as *myo*-inositol. Furthermore the SUPELCOGEL Pb column used in this study is considerably cheaper than the Chiral-AGP column used by Kindt et al (Kindt et al., 2004). Published data on inositol epimers in urine concluded that the two major components are *myo-* and *chiro*-inositol (Kennington et al., 1990). However, the urine sample analysed in this study appeared to contain only *myo*-inositol although analysis of more urine samples is required.

In order to monitor MI levels in urine, it will be necessary to determine creatinine concentration. Creatinine is a waste product of creatine and creatine phosphate, which are important energy stores in muscle. Creatinine is produced at a fairly constant rate by the body and is excreted from the body entirely by the kidneys. Thus, the measurement of creatinine in urine acts as an index of urinary excretion rate (Jackson, 1966). This provides a means to normalise the concentration of metabolites in urine irrespective of how dilute or concentrated the urine sample is. Thus, MI concentration will be expressed per mmol of creatinine. Creatinine will be quantified by LC-MS/MS using an established laboratory protocol (Dr. Kevin Mills, personal communication, 2007).

Further work is required to establish normal reference levels of MI in urine and to determine how these levels change when single and repeated doses of MI are administered. To monitor patient compliance in the PONTI study, it will be particularly important to assess how the 1g MI tablets taken each day affect MI concentrations in the urine of women before and during the first trimester of pregnancy. One study showed that the blood inositol concentration was not significantly different between non-pregnant and pregnant women in the first, second and third trimesters (Quirk and Bleadale, 1983). However, a more recent study involving a larger number of women demonstrated that concentrations of inositol do vary during pregnancy (Groenen et al., 2005). Concentrations of inositol determined pre-conceptually were comparable to those determined at 6 weeks after last menstrual period. Later in the first trimester, the serum inositol concentration decreased, and then concentrations gradually increased after 21 weeks. Notably, inositol concentrations at 30 and 37 weeks of pregnancy were found to be significantly associated with birth weight.

In summary, the proposed LC-MS/MS method has been developed to specifically quantify MI in urine. Initial analyses of intra- and inter-run precision demonstrated that the method was robust and reproducible, whilst water- and urine-based calibration curves were linear between 2.5 and 50 µM. With further work, this method will be used for monitoring patient compliance in the PONTI study and it could also potentially be used as a tool for investigating the prevention of NTDs in mouse models.

CHAPTER 8

Final discussion

The overall aim of this thesis was to investigate metabolic effects in the cause and prevention of NTDs. In particular, the role of embryonic metabolism has been focussed upon as little is known about it, presumably due to the constraints of analytical methods. Thus, initially a method was developed to quantify S-adenosylmethionine (SAM) and S-adenosylhomocysteine (SAH) in neurulation-stage mouse (chapter 3). This method was then used to investigate the effect of methylation cycle intermediates and inhibitors, which are known to cause cranial NTDs, on the abundance of SAM and SAH (chapter 4). Exposure of non-mutant mouse embryos to methionine or the MAT inhibitors, cycloleucine and ethionine, resulted in increased SAH levels associated with a decreased SAM/SAH ratio. This could affect methylation of a wide range of biomolecules including DNA, proteins and lipids. Further studies are needed to investigate whether changes in SAM/SAH ratio are sufficient to induce changes in methylation.

Experiments carried out using whole embryo culture confirmed that the DNA methylation inhibitor, azacytidine, is a teratogen capable of causing cranial NTDs in non-mutant embryos (chapter 4). Subsequent analysis of these embryos revealed that azacytidine did not affect the abundance of SAM and SAH indicating that this inhibitor is acting downstream of the methylation and folate cycle. Thus, DNA methylation is of critical importance for neural tube closure and folic acid may prevent NTDs through the provision of methyl groups for DNA methylation patterns. Further experiments could investigate the effect of azacytidine on global and specific DNA methylation in cultured embryos. To investigate whether folic acid prevents NTDs through the provision of methyl groups, future studies could be undertaken to analyse the effects of supplementary folic acid on DNA methylation in folate-preventable NTD mouse models. Another approach would be to test whether folic acid is capable of preventing NTDs caused by exposure to azacytidine.

In order to establish whether intrinsic defects in methylation cycle metabolism in the embryo could be involved in determining susceptibility to NTDs, the abundance of SAM and SAH was quantified in human cell lines (chapter 4). The LC-MS/MS method was adapted for use with cell pellets and subsequently two different types of cell lines from NTD and control patients were analysed. The results showed that there was very little variation in the concentration of SAM and SAH between samples. To fully understand the role of one-carbon metabolism in the etiology of human NTDs, a large study is required linking changes in folate and methylation cycle metabolites with genotype.

The role of folate deficiency in the cause of NTDs is not conclusive and experiments in this thesis have attempted to elucidate possible answers. Effective folate deficiency in three mouse models (*splotch, curly tail* and $+/+^{ct}$) has been shown to increase the incidence of exencephaly (chapter 5 and 6, Figure 8.1). Previous dietary studies using non-mutant mouse models have shown that folate deficiency alone is not sufficient to cause NTD (Burgoon et al., 2002). Whereas, my study demonstrated that folate deficiency can increase the incidence of NTD in combination with a genetic disturbance. In *splotch* embryos, the combined effects of the *Pax3* mutation and folate deficiency increases the incidence of NTDs. Whilst in *curly tail* and $+/+^{ct}$ embryos, modifier genes in the genetic background appear to summate with the folate deficiency to increase the incidence of NTDs. Of note, the expression of these modifier genes alone is not sufficient to cause NTDs.

One important finding from the folate deficiency studies (chapter 5 and 6, Figure 8.1) was that folate deficiency affects the growth and development of neurulation-stage embryos. Retardation of embryonic growth and development may therefore render an embryo more susceptible to the NTD phenotype caused by the underlying genetic mutation. The neuroepithelium and supporting mesenchymal cells that facilitate neural tube closure are rapidly proliferating cells that require high levels of folate to produce the required high levels of nucleotides in order to facilitate DNA replication. If neuroepithelial cells exhaust their internal supply of nucleotides, cellular replication will be slowed and the development of the neural folds retarded. Indeed previous studies have implicated a delay in the development of the neural folds with the formation of NTDs (Van Allen et al., 1993). Thus, prevention of NTDs by folic acid may involve stimulation of cell proliferation to overcome reduced cell proliferation or to counteract the increased cell death. To investigate whether folate deficiency increases the incidence of NTDs by retarding growth and development, analysis of cell proliferation and apoptosis in the neural tube is required.

Studies of maternal folate in human NTD cases have demonstrated that sub-optimal folate status is linked to NTD risk (reviewed in chapter 1). The data presented in this thesis shows how maternal folate is reduced and homocysteine is increased under folate deficient conditions (chapter 5 and 6, Figure 8.1). Maternal status does not predict that all embryos will develop NTDs, moreover, the risk of having a NTD affected pregnancy depends on the genotype of the embryo and the risk increases when folate is limiting. Studies combining polymorphic data with dietary intake in the first-trimester would be an interesting area in which to investigate how genetic and environmental factors interact to affect NTD risk in humans.

In order to understand the role of folic acid in preventing NTDs, it is useful to initially understand folate metabolism during neurulation. Analysis of intra- and extracellular folate levels was carried out in order to investigate how embryonic folate status changes as the neural tube is closing (chapter 5 and 6). Analysis of monoglutamylfolate (extracellular folate) in all mouse models suggests that the demand for monoglutamylfolate during neurulation exceeds placental uptake such that monoglutamylfolate concentration decreases with development. Thus, monoglutamylfolate is being gradually taken up into cells where a polyglutamate chain is added to aid cellular retention. Under normal dietary conditions, in *splotch* embryos the polyglutamylfolate concentration (intracellular folate) decreased with development whilst it remained constant in *ct/ct* and $+/+^{ct}$. Under folate deficient conditions, the polyglutamylfolate concentration in *splotch* embryos was comparable to that in *splotch* embryos from the normal diet at all stages of development. High polyglutamylfolate concentrations were observed in *ct/ct* and $+/+^{ct}$ embryos which decreased with development to the same level as that observed under normal dietary conditions. The high polyglutamylfolate concentrations may indicate that the fetus can parasitize maternal folate stores for its own requirements even in the face of maternal folate deficiency. Indeed several studies have reported that folate deficiency leads to up-regulation of folate receptors (Antony, 2007).

To test how folate deficiency affects the methylation cycle, the abundance of SAM and SAH was analysed (chapter 5 and 6, Figure 8.1). In *splotch* and $+/+^{ct}$ embryos, folate deficiency resulted in increased concentrations of SAH and a decreased SAM/SAH ratio. It is not clear however whether this change in the abundance of SAH affected methylation reactions which in turn prevented closure of the neural tube. Elevated SAH itself may simply be a biomarker of a disturbed methylation cycle. The concentration of SAM was markedly high in *ct/ct* and was further increased under folate deficient conditions. It is unclear why the metabolic response differed in *ct/ct* embryos, perhaps it suggests that the *ct* mutation directly affects one-carbon metabolism.

	ct/ct	*+/+ct*	*splotch*
Maternal Folate	↓	↓	↓
Maternal Homocysteine	↑	↑	↑
No. of implants per litter	↓	↓	No change
No. of resorptions per litter	↑	↑	No change
Incidence of exencephaly	↑	↑	↑
Prevention of exencephaly	FA	FA, MI	FA
Embryonic Size (Crown-rump length)	↓	↓	↓
Embryonic Development (no. of somites)	↓	↓	↓
Embryonic Folate Content	↓	↓	↓
Embryonic Folate Concentration	No change	No change	↓
SAM	↑	↑	No change
SAH	No change	↑	↑
Ratio SAM/SAH	↑	↓	↓

Figure 8.1 A summary of findings investigating folate deficiency in *splotch*, *curly tail* and +/+^{ct} mouse models (chapters 5 and 6).

Further studies are required to investigate how folate deficiency affects methylation reactions. There are many possible methylation targets and it would be difficult to investigate each one individually. However, candidates could be suggested from previous evidence of a role in the process of neurulation. For example, as

demonstrated in this thesis, exposure to the DNA methylation inhibitor, azacytidine, causes cranial neural tube defects thus DNA methylation poses an important area for further investigation. Whole embryo culture would be a useful tool in investigating how inhibitors of other methylation reactions affect neural tube closure, for example inhibition of protein methylation. Apart from changes in methylation, folate deficiency may also affect polyamine synthesis, as SAM is the precursor of this process. The effect of misregulation of polyamine synthesis on neural tube closure is currently unknown and is therefore an area of interest for further studies.

Treatment of folate deficient embryos with folic acid demonstrated how supplementation rescues maternal folate deficiency, arising from insufficient folate in the diet (chapter 5 and 6). This adds weight to the original hypothesis proposed by Smithells et al. to explain the prevention of neural tube defects by folic acid (Smithells et al., 1976). Nowadays an important area of research is the investigation of whether other agents besides folic acid, can help prevent neural tube defects in humans. Studies in the *curly tail* mouse have highlighted the role of inositol in the prevention of NTDs (Greene and Copp, 1997) and inositol deficiency has been shown to cause NTDs in non-mutant mice (Cockroft et al., 1992). Remarkably, the experiments carried out in this thesis show how inositol can prevent NTDs in folate deficient $+/+^{ct}$ embryos. This is the first time inositol has been shown to prevent NTDs in a wild-type mouse and provides further evidence for the need to test whether inositol is capable of preventing human NTDs.

The final chapter of this thesis describes the implementation of a clinical trial to test the efficacy of inositol for the prevention of recurrent NTDs, in combination with folic acid. In order to monitor compliance I developed a LC-MS/MS method to quantify myo-inositol in urine. The specificity of the method was tested and the column chosen is shown to be capable of separating myo-inositol from other potentially interfering monosaccharides. Further work is required to establish normal reference levels in urine collected from healthy adults. Furthermore, experiments need to be undertaken to determine how the urinary myo-inositol concentration changes after single and repeated doses of 1 g/day of myo-inositol before and during pregnancy. Adapting this method for the analysis of myo-inositol in neurulation stage embryos will provide a useful tool in investigating the metabolic effects of inositol treatment in the cause and prevention of NTDs

BIBLIOGRAPHY

Adinolfi, M., Beck, S.E., Embury, S., Polani, P.E., and Seller, M.J., 1976. Levels of alpha-fetoprotein in amniotic fluids of mice (curly tail) with neural tube defects. J. Med. Genet. 13, 511-513.

Afman, L.A., Blom, H.J., Drittij, M.J., Brouns, M.R., and Van Straaten, H.W.M., 2006. Inhibition of transmethylation disturbs neurulation in chick embryos. Brain Res.Dev.Brain Res. 158, 59-65.

Agulnik, A.I., Longepied, G., Ty, M.T., Bishop, C.E., and Mitchell, M., 1999. Mouse H-Y encoding Smcy gene and its X chromosomal homolog Smcx. Mamm. Genome 10, 926-929.

Alessi, D.R. and Downes, C.P., 1998. The role of PI 3-kinase in inositolulin action. Biochimica et Biophysica Acta 1436, 151-164.

Allan, S.J., Kavanagh, G.M., Herd, R.M., and Savin, J.A., 2004. The effect of inositol supplements on the psoriasis of patients taking lithium: a randomized, placebo-controlled trial. Br.J.Dermatol. 150[5], 966-969.

Anderson, R.G.W., Kamen, B.A., Rothberg, K.G., and Lacey, S.W., 1992. Potocytosis: Sequestration and transport of small molecules by caveolae. Science 255, 410-411.

Antony, A.C., 2007. In utero physiology: role of folic acid in nutriet delivery and fetal development. Am J Clin.Nutr. 85 (Suppl), 598S-603S.

Ashizawa, N., Yoshida, M., and Aotsuka, T., 2000. An enzymatic assay for myo-inositol in tissue samples. J. Biochem. Biophys. Methods 44, 89-94.

Asrar, F.M. and O'Connor, D.L., 2005. Bacterially synthesised folate and supplemental folic acid are absorbed across the large intestine of piglets. Journal of Nutritional Biochemistry 16, 587-593.

Auerbach, R., 1954. Analysis of the developmental effects of a lethal mutation in the house mouse. J. Exp. Zool. 127, 305-329.

Barber, R.C., Bennett, G.D., Greer, K.A., and Finnell, R.H., 1999. Expression patterns of folate binding proteins one and two in the developing mouse embryo. Mol. Genet. Metab. 66, 31-39.

Barlow, D.P., 1995. Gametic imprinting in mammals. Science 270, 1610-1613.

Beechey, C.V. and Searle, A.G., 1986. Mutations at the Sp locus. MNL 75, 28.

Bennett, G.D., An, J., Craig, J.C., Gefrides, L.A., Calvin, J.A., and Finnell, R.H., 1998. Neurulation abnormalities secondary to altered gene expression in neural tube defect susceptible splotch embryos. Teratology. 57, 17-29.

Bennett, G.D., VanWaes, J., Moser, K., Chaudoin, T., Starr, L., and Rosenquist, T.H., 2006. Failure of homocysteine to induce neural tube defects in a mouse model. Birth Defects Research Part B, 77(2), 89-94.

Bergo, M.O., Leung, G.K., Ambroziak, P., Otto, J.C., Casey, P.J , and Young, S.G., 2000. Targeted inactivation of the isoprenylcysteine carboxyl methyltransferase gene causes mislocalization of K-Ras in mammalian cells. J. Biol. Chem. 275, 17605-17610.

Berry, R.J., Li, Z., Erickson, J.D., Li, S., Moore, C.A., Wang, H., Mulinare, J., Zhao, P., Wong, L.Y.C., Gindler, J., Hong, S.X., Correa, A., and China-US Collaborative Project Neu, 1999. Prevention of neural-tube defects with folic acid in China. N. Engl. J. Med. 341, 1485-1490.

Blom, H.J., Shaw, G.M., Den Heijer, M., and Finnell, R.H., 2006. Neural tube defects and folate: case far from closed. Nature Reviews Neuroscience 7, 724-731.

Bolon, B., Welsch, F., and Morgan, K.T., 1994. Methanol-induced neural tube defects in mice: Pathogenesis during neurulation. Teratology. 49, 497-517.

Borman, G.B., Smith, A.H., and Howard, J.K., 1986. Risk factors in the prevalence of anencephalus and spina bifida in New Zealand. Teratology 33, 221-230.

Botto, L.D. and Yang, Q.H., 2000. 5,10-Methylenetetrahydrofolate reductase gene variants and congenital anomalies: A HuGE review. Am. J. Epidemiol. 151, 862-877.

Boyles, A.L., Hammock, P., and Speer, M.C., 2005. Candidate gene analysis in human neural tube defects. Am.J Med.Genet. 135(1), 9-23.

Brender, J.D., Suarez, L., Felkner, M., Gilani, Z., Stinchomb, D., Moody, K., Henry, J., and Hendricks, K., 2006. Maternal exposure to arsenic, cadmium, lead and mercury and neural tube defects in offspring. Environmental Research 101, 132-139.

Brigle, K.E., Westin, E.H., Houghton, M.T., and Goldman, I.D., 1991. Characterisation of two cDNAs encoding folate-binding proteins from L1210 murine leukemia cells. Increased expression associated with a genomic rearrangement. Journal of Biological Chemistry 266[26], 17243-17249.

Brook, F.A., Estibeiro, J.P., and Copp, A.J., 1994. Female predisposition to cranial neural tube defects is not because of a difference between the sexes in rate of embryonic growth or development during neurulation. J. Med. Genet. 31, 383-387.

Brook, F.A., Shum, A.S.W., Van Straaten, H.W.M., and Copp, A.J., 1991. Curvature of the caudal region is responsible for failure of neural tube closure in the curly tail (ct) mouse embryo. Development. 113, 671-678.

Brouns, M.R., Matheson, S.F., Hu, K.Q., Delalle, I., Caviness, V.S., Jr., Silver, J., Bronson, R.T., and Settleman, J., 2000. The adhesion signaling molecule p190 RhoGAP is required for morphogenetic processes in neural development. Development. 127, 4891-4903.

Brown, D. and Waneck, G.L., 1992. Glycosyl-phsphatidylinositol-anchored membrane proteins. Journal of American Society Nephrology 3, 895-906.

Bry, K. and Hallman, M., 1991. Perinatal development of inositol synthesis and catabolism in rabbit kidney. Biology of the Neonate 60, 249-257.

Burgoon, J.M., Selhub, J., Nadeau, M., and Sadler, T.W., 2002. Investigation of the effects of folate deficiency on embryonic development through the establishment of a folate deficient mouse model. Teratology. 65, 219-227.

Burren, K.A., Mills, K., Copp, A.J., and Greene, N.D.E., 2006. Quantitative analysis of s-adenosylmethionine and s-adenosylhomocysteine in neurulation-stage mouse embryos by liquid chromatography. Journal of Chromatography B: Biomedical Sciences and Applications, 844(1), 112-8.

Campbell, L.R., Dayton, D.H., and Sohal, G.S., 1986. Neural tube defects: A review of human and animal studies on the etiology of neural tube defects. Teratology. 34, 171-187.

Capdevila, A. and Wagner, C., 1998. Measurement of plasma S-adenosylmethionine and S-adenosylhomocysteine as their fluorescent isoindoles. Anal. Biochem. 264, 180-184.

Carmel, R. and Jacobsen, W., 2001. Homocysteine in health and disease. Cambridge University Press, Cambridge.

Carroll, E., Gerrelli, D., Gasca, S., Berg, E., Beier, D., Copp, A., and Klingensmith, J., 2003. Cordon-bleu is a conserved gene involved in neural tube formation. Dev. Biol. 262, 16-31.

Carter, C.O., 1974. Clues to the aetiology of neural tube malformations. Dev. Med. Child Neurol. 16 (Suppl.32), 3-15.

Carter, M., Chen, X., Slowinska, B., Minnerath, S., Glichstein, S., Shi, L., Campagne, F., Weinstein, H., and Ross, M.E., 2005. Crooked tail (Cd) model of human folate-responsive neural tube defects is mutated in Wnt coreceptor lipoprotein receptor-related protein 6. Proceedings of the National Academy of Sciences USA 102[36], 12843-12848.

Carter, M., Ulrich, S., Oofuji, Y., Williams, D.A., and Ross, M.E., 1999. Crooked tail (Cd) models human folate-responsive neural tube defects. Hum. Mol. Genet. 8, 2199-2204.

Caspary, W.F. and Crane, R.K., 1970. Active transport of myo-inositol and its relation to the sugar transport system in hamster small intestine. Biochimica et Biophysica Acta 203, 308-316.

Castro, R., Rivera, I., Ravasco, P., Camilo, M.E., Jakobs, C., Blom, H.J., and De Almeida, I.T., 2004. 5,10-methylenetetrahydrofolate reductase (MTHFR) 677C-->T and 1298A-->C mutations are associated with DNA hypomethylation. J Med.Genet. 41[6], 454-458.

Caudill, M.A., Wang, J.C., and Melnyk, S., 2001. Intracellular s-adenosylhomocysteine concentrations predict global DNA hypomethylation in tissues of methyl-deficient cystathionine beta-synthase heterozygous mice. Journal of Nutrition 131(11), 2811-2818.

Cavalli, P. and Copp, A.J., 2002. Inositol and folate-resistant neural tube defects. J. Med. Genet. 39, e5.

Centers for Disease Control and Prevention., 1999. Knowledge and use of folic acid by women of childbearing age - United States, 1995 and 1998. Morb.Mortal.Wkly.Rep. 48, 325-327.

Centers for Disease Control and Prevention., 2002. Folate status in women of childbearing age, by race/ethnicity -- United States, 1997-2000. MMWR 51[36], 808-810.

Centers for Disease Control and Prevention., 2004. Spina bifida and anencephaly before and after folic acid mandate -- United States, 1995-1996 and 1999-2000. MMWR 53[17], 362-365.

Chatkupt, S., Hol, F.A., Shugart, Y.Y., Geurds, M.P.A., Stenroos, E.S., Koenigsberger, M.R., Hamel, B.C.J., Johnson, W.G., and Mariman, E.C.M., 1995. Absence of linkage between familial neural tube defects and PAX3 gene. J. Med. Genet. 32, 200-204.

Chen, W.-H., Morriss-Kay, G.M., and Copp, A.J., 1995. Genesis and prevention of spinal neural tube defects in the curly tail mutant mouse: involvement of retinoic acid and its nuclear receptors RAR-beta and RAR-gamma. Development. 121, 681-691.

Chen, W.-H., Morriss-Kay, G.M., and Copp, A.J., 1994. Prevention of spinal neural tube defects in the curly tail mouse mutant by a specific effect of retinoic acid. Dev. Dyn. 199, 93-102.

Chen, Z., Karaplis, A.C., Ackerman, S.L., Pogribny, I.P., Melnyk, S., Lussier-Cacan, S., Chen, M.F., Pai, A., John, S.W., Smith, R.S., Bottiglieri, T., Bagley, P., Selhub, J., Rudnicki, M.A., James, S.J., and Rozen, R., 2001a. Mice deficient in methylenetetrahydrofolate reductase exhibit hyperhomocysteinemia and decreased methylation capacity, with neuropathology and aortic lipid deposition. Hum. Mol. Genet. 10, 433-443.

Chi, N. and Epstein, J.A., 2002. Getting your Pax straight: Pax proteins in development and disease. Trends Genet. 18, 41-47.

Chiao, J.H., Roy, K., Tolner, B., Yang, C.-H., and Sirotnak, F.M., 1997. RFC-1 gene expression regulates folate absorption in mouse small intestine. Journal of Biological Chemistry 272[17], 11165-11170.

Choumenkovitch, S.F., Selhub, J., Bagley, P.J., Maeda, N., Nadeau, M.R., Smith, D.E., and Choi, S.W., 2002. In the cystathionine beta-synthase knockout mouse, elevations in total plasma homocysteine increase tissue S-adenosylhomocysteine, but responses of S-adenosylmethionine and DNA methylation are tissue specific. J. Nutr. 132, 2157-2160.

Christensen, B., Arbour, L., Tran, P., Leclerc, D., Sabbaghian, N., Platt, R., Gilfix, B.M., Rosenblatt, D.S., Gravel, R.A., Forbes, P., and Rozen, R., 1999. Genetic polymorphisms in

methylenetetrahydrofolate reductase and methionine synthase, folate levels in red blood cells, and risk of neural tube defects. Am. J. Med. Genet. 84, 151-157.

Clements, R.S. and Diethelm, A.G., 1979. The metabolism of myo-Inositol by the human kidney. Journal of Laboratory Clinical Medicine 93[2], 210-219.
Cockroft, D.L., 1988. Changes with gestational age in the nutritional requirements of postimplantation rat embryos in culture. Teratology. 38, 281-290.

Cockroft, D.L., Brook, F.A., and Copp, A.J., 1992. Inositol deficiency increases the susceptibility to neural tube defects of genetically predisposed (curly tail) mouse embryos in vitro. Teratology. 45, 223-232.

Coelho, C.N.D., Weber, J.A., Klein, N.W., Daniels, W.G., and Hoagland, T.A., 1989. Whole rat embryos require methionine for neural tube closure when cultured on cow serum. J. Nutr. 119, 1716-1725.

Cogram, P., Hynes, A., Dunlevy, L.P.E., Greene, N.D.E., and Copp, A.J., 2004. Specific isoforms of protein kinase C are essential for prevention of folate-resistant neural tube defects by inositol. Hum. Mol. Genet. 13, 7-14.

Cogram, P., Tesh, S., Tesh, J., Wade, A., Allan, G., Greene, N.D.E., and Copp, A.J., 2002. D-chiro-inositol is more effective than myo-inositol in preventing folate-resistant mouse neural tube defects. Hum. Reprod. 17, 2451-2458.

Copp, A., Cogram, P., Fleming, A., Gerrelli, D., Henderson, D., Hynes, A., Kolatsi-Joannou, M., Murdoch, J., and Ybot-Gonzalez, P., Neurulation and neural tube closure defects. In: Tuan, R.S. and Lo, C.W. (Eds.), Developmental Biology Protocols, Volume 1, Vol. 2. Humana Press Inc, Totowa, New Jersey, 1999, pp. 135-160.

Copp, A.J., 2005. Neurulation in the cranial region - normal and abnormal. Journal of Anatomy, 207(5): 623-635.

Copp, A.J., Genetic models of mammalian neural tube defects. In: Bock, G. and Marsh, J. (Eds.), Neural Tube Defects (Ciba Foundation Symposium 181), John Wiley & Sons, Chichester, 1994, pp. 118-134.

Copp, A.J. and Brook, F.A., 1989. Does lumbosacral spina bifida arise by failure of neural folding or by defective canalisation? J. Med. Genet. 26, 160-166.

Copp, A.J., Brook, F.A., Estibeiro, J.P., Shum, A.S.W., and Cockroft, D.L., 1990. The embryonic development of mammalian neural tube defects. Prog. Neurobiol. 35, 363-403.

Copp, A.J., Brook, F.A., and Roberts, H.J., 1988a. A cell-type-specific abnormality of cell proliferation in mutant (curly tail) mouse embryos developing spinal neural tube defects. Development. 104, 285-295.

Copp, A.J., Crolla, J.A., and Brook, F.A., 1988b. Prevention of spinal neural tube defects in the mouse embryo by growth retardation during neurulation. Development. 104, 297-303.

Copp, A.J. and Greene, N.D.E., 2000. Neural tube defects: prevention by folic acid and other vitamins. Indian J. Pediatr. 67, 915-921.

Copp, A.J., Greene, N.D.E., and Murdoch, J.N., 2006. Mouse mutants as models of neural tube defects. Neural Tube Defects: from origin to treatment. Edited by Diego F.Wyszynski. 198-213.

Copp, A.J., Greene, N.D.E., and Murdoch, J.N., 2003. The genetic basis of mammalian neurulation. Nat. Rev. Genet. 4, 784-793.

Copp, A.J., Shum, A.S.W., and Brook, F.A., 1993. Analysis of neural tube defects in a mouse mutant using whole embryo culture. Toxic. in Vitro 7, 679-684.

Cowchock, S., Ainbender, E., Prescott, G., Crandell, B., Lau, L., Heller, R., Muir, W.A., Kloza, E., Feigelson, M., Mennuti, M., and Cederquist, L., 1980. The recurrence risk for neural tube defects in the United State: a collaborative study.

Cox, R. and Irving, C.C., 1977. Inhibition of DNA methylation by S-adenosylethionine with the production of methyl-deficient DNA in regenerating rat liver. Cancer Res. 37, 222-225.

Curtin, J.A., Quint, E., Tsipouri, V., Arkell, R.M., Cattanach, B., Copp, A.J., Fisher, E.M., Nolan, P.M., Steel, K.P., Brown, S.D.M., Gray, I.C., and Murdoch, J.N., 2003. Mutation of Celsr1 disrupts planar polarity of inner ear hair cells and causes severe neural tube defects in the mouse. Curr. Biol. 13, 1-20.

Czeizel, A.E. and Dudás, I., 1992. Prevention of the first occurrence of neural-tube defects by periconceptional vitamin supplementation. N. Engl. J. Med. 327, 1832-1835.

Czeizel, A. and Metneki, J., 1984. Recurrence risk after neural tube defects in a genetic counselling clinic. J. Med. Genet. 21, 413-416.

Daly, S., Mills, J.L., Molloy, A.M., Conley, M., McPartlin, J., Lee, Y.J., Young, P.B., Kirke, P.N., Weir, D.G., and Scott, J.M., 2002. Low-dose folic acid lowers plasma homocysteine levels in women of child-bearing age. Q. J. Med. 95, 733-740.

Dansky, L.V. and Finnell, R.H., 1991. Parental epilepsy, anticonvulsant drugs, and reproductive outcome: epidmiologic and experimental findings spanning three decades. 2: Human studies. Reprod.Toxicol. 5, 301-355.

De Cabo, S.F., Santos, J., and Fernandez-Piqueras, J., 1995. Molecular and cytological evidence of S-adenosyl-L-homocysteine as an innocuous undermethylating agent in vivo. Cytogenetics and Cell Genetics 71[2], 187-192.

De Marco, P., Calevo, M.G., Moroni, A., Arata, L., Merello, E., Finnell, R.H., Zhu, H., Andreussi, L., Cama, A., and Capra, V., 2002. Study of MTHFR and MS polymorphisms as risk factors for NTD in the Italian population. J. Hum. Genet. 47, 319-324.

De Marco, P., Calevo, M.G., Moroni, A., Merello, E., Raso, A., Finnell, R.H., Zhu, H.P., Andreussi, L., Cama, A., and Capra, V., 2003. Reduced folate carrier polymorphism (80A --> G) and neural tube defects. Eur. J. Hum. Genet. 11, 245-252.

De Marco, P., Merello, E., Mascelli, S., and Capra, V., 2006. Current perspectives on the genetic causes of neural tube defects. Neurogenetics 7(4), 201-21,

Dove, S.K. and Michell, R.H., 2000. Inositol lipids and phosphates in cell control. Neurotransmissions 16, 3-17.

Dunlevy, L.P., Chitty, L.S., Burren, K.A., Doudney, K., Stojilkovic-Mikic, T., Stanier, P., Scott, R., Copp, A.J., and Greene, N.D., 2007. Abnormal folate metabolism in foetuses affected by neural tube defects. Brain 130[4], 1043-1049.

Dunlevy, L.P.E., Burren, K.A., Chitty, L.S., Copp, A.J., and Greene, N.D.E., 2006. Excess methionine supresses the methylation cycle and inhibits neural tube closure in mouse embryos. FEBS Letters 580, 2803-2807.

Dunlevy, L.P.E., Burren, K.A., Mills, K., Chitty, L.S., Copp, A.J., and Greene, N.D.E., 2006. Integrity of the methylation cycle is essential for mammalian neural tube closure. Birth Defects Res.Part A Clin Mol.Teratol. 76, 544-552.

Ebino, K.Y., Suwa, T., Kuwabara, Y., Saito, T.R., and Takahashi, K.W., 1998. Coprophagy in female mice during pregnancy and lactation. Jikken Dobutsu 37[1], 101-104.

Economides, D.I., Ferguson, J., MacKenzie, I.Z., Darley, J., Ware, H., and Holmes-Siedle, M., 1992. Folate and vitamin B12 concentrations in maternal and fetal blood, and amniotic fluid in second trimester pregnancies complicated by neural tube defects. Br. J. Obstet. Gynaecol. 99, 23-25.

Edwards, M.J., Shiota, K., Smith, M.S., and Walsh, D.A., 1995. Hyperthermia and birth defects. Reprod.Toxicol. 9, 411-425.

Ehlers, K., Stürje, H., Merker, H.-J., and Nau, H., 1992. Valproic acid-induced spina bifida: A mouse model. Teratology. 45, 145-154.

Elwood, J.M. and Elwood, J.H., 1980. Epidemiology of anencephalus and spina bifida. Oxford University Press, Oxford.

Elwood, J.M., Little, J., and Elwood, J.H. Epidemiology and control of neural tube defects. Oxford: Oxford University Press . 1992.

Elwood, P.C., 1989. Molecular cloning and characterisation of the human folate-binding protein cDNA from placenta and malignant tissue culture (KB) cells. Journal of Biological Chemistry 264[25], 14893-14901.

Embury, S., Seller, M.J., Adinolfi, M., and Polani, P.E., 1979. Neural tube defects in curly-tail mice. I. Incidence and expression. Proc. R. Soc. Lond. B 206, 85-94.

Emery, A.E., Timson, J., and Watson Williams, E.J., 1969. Pathogenesis of spina bifida. Lancet 2, 909-910.

Epstein, D.J., Vekemans, M., and Gros, P., 1991. splotch (Sp2H), a mutation affecting development of the mouse neural tube, shows a deletion within the paired homeodomain of Pax-3. Cell 67, 767-774.

Erbe, R.W. and Wang, J.C., 1984. Folate metabolism in humans. American Journal of Medical Genetics 17, 277-287.

Ernest, S., Carter, M., Shao, H., Hosack, A., Lerner, N., Colmenares, C., Rosenblatt, D.S., Pao, Y.-H., Ross, M.E., and Nadeau, J.H., 2006. Parallel changes in metabolite and expression profiles in crooked-tail mutant and folate-reduced wild-type mice. Human Molecular Genetics 15[23], 3387-3393.

Eskes, T.K.A.B., 1998. Neural tube defects, vitamins and homocysteine. Eur. J. Pediatr. 157 Suppl. 2, S139-S141.

Essien, F.B., 1992. Maternal methionine supplementation promotes the remediation of axial defects in Axd mouse neural tube mutants. Teratology. 45, 205-212.

Essien, F.B. and Wannberg, S.L., 1993. Methionine but not folinic acid or vitamin B-12 alters the frequency of neural tube defects in Axd mutant mice. J. Nutr. 123, 27-34.

Estibeiro, J.P., Brook, F.A., and Copp, A.J., 1993. Interaction between splotch (Sp) and curly tail (ct) mouse mutants in the embryonic development of neural tube defects. Development. 119, 113-121.

Finkelstein, J.D., 1998b. The metabolism of homocysteine: pathways and regulation. Eur. J Pediatr. 157 Suppl 2, S40-S44.

Finkelstein, J.D., 1998a. The metabolism of homocysteine: pathways and regulation. Eur. J. Pediatr. 157 Suppl. 2, S40-S44.

Fisher, E. and Scambler, P., 1994. Human haploinsufficiency--One for sorrow, two for joy. Nature Genet. 7, 5-7.

Fisher, M.C., Zeisel, S.H., Mar, M.H., and Sadler, T.W., 2002. Perturbations in choline metabolism cause neural tube defects in mouse embryos in vitro. FASEB J. 16, NIL4-NIL30.

Fisher, M.C., Zeisel, S.H., Mar, M.H., and Sadler, T.W., 2001. Inhibitors of choline uptake and metabolism cause developmental abnormalities in neurulating mouse embryos. Teratology. 64, 114-122.

Fleming, A. and Copp, A.J., 1998. Embryonic folate metabolism and mouse neural tube defects. Science 280, 2107-2109.

Fleming, A. and Copp, A.J., 2000. A genetic risk factor for mouse neural tube defects: defining the embryonic basis. Hum. Mol. Genet. 9, 575-581.

Food and Drug Administration, 1996. Food Standards: Amendment of standards of indentity for enriched grain products to require addition of folic acid. Federal Register 61[44], 8781-8797.

Friso, S. and Choi, S.W., 2002. Gene-nutrient interactions and DNA methylation. J. Nutr. 132, 2382S-2387S.
Friso, S., Choi, S.W., Dolnikowski, G.G., and Selhub, J., 2002a. A method to assess genomic DNA methylation using high-performance liquid chromatography/electrospray ionization mass spectrometry. Anal. Chem. 74, 4526-4531.

Friso, S., Choi, S.W., Girelli, D., Mason, J.B., Dolnikowski, G.G., Bagley, P.J., Olivieri, O., Jacques, P.F., Rosenberg, I.H., Corrocher, R., and Selhub, J., 2002b. A common mutation in the 5,10-methylenetetrahydrofolate reductase gene affects genomic DNA methylation through an interaction with folate status. Proc.Natl.Acad.Sci.U.S.A 99[8], 5606-5611.

Frosst, P., Blom, H.J., Milos, R., Goyette, P., Sheppard, C.A., Matthews, R.G., Boers, G.J.H., Den Heijer, M., Kluijtmans, L.A.J., Van den Heuvel, L.P., and Rozen, R., 1995. A candidate genetic risk factor for vascular disease: A common mutation in methylenetetrahydrofolate reductase. Nature Genet. 10, 111-113.

Gefrides, L.A., Bennett, G.D., and Finnell, R.H., 2002. Effects of folate supplementation on the risk of spontaneous and induced neural tube defects in splotch mice. Teratology. 65, 63-69.

Gelderblom, W.C.A., Jaskiewicz, K., Marasas, W.F.O., Thiel, P.G., Horak, M.J., Vleggaar, R., and Kriek, N.P.J., 1988. Fumonisins - novel mycotoxins with cancer promoting activity produced by Fusarium moniliforme. Appl.Environ.Microbiol. 54, 1806-1811.

Gellekink, H., Oppenraaij-Emmerzaal, A., van Rooij, E.A., Struys, M., Den Heijer, H.J., and Blom, H.J., 2005. Stable-isotope dilution liquid chromatography-electrospray injection tandem mass spectrometry method for fast, selective measurement of S-Adenosylmethionine and S-Adenosylhomocysteine in plasma. Clinical Chemistry 51[8], 1487-1492.

Goetsch, C., 1962. An evaluation of aminopterin as an abortifacient. American Journal of Obstetrics and Gynecology , 1474-1477.

Goldman, I.D., 1971. The characteristics of the membrane transport of amethopterin and the naturally occurring folates. Ann.N.Y.Acad.Sci. 186, 400-422.

Goulding, M.D., Chalepakis, G., Deutsch, U., Erselius, J.R., and Gruss, P., 1991. Pax-3, a novel murine DNA binding protein expressed during early neurogenesis. EMBO J. 10, 1135-1147.

Goyette, P., Sumner, J.S., Milos, R., Duncan, A.M., Rosenblatt, D.S., Matthews, R.G., and Rozen, R., 1994. Human methylenetetrahydrofolate reductase: isolation of cDNA, mapping and mutation identification. Nature Genet. 7, 195-200.

Greene, N.D. and Copp, A.J., 2005. Mouse models of neural tube defects: investigating preventive mechanisms. Am. J. Med. Genet. C. Semin. Med. Genet. 135, 31-41.

Greene, N.D.E. and Copp, A.J., 1997. Inositol prevents folate-resistant neural tube defects in the mouse . Nature Med. 3, 60-66.

Greene, N.D.E. and Copp, A.J., 2006. The embryonic basis of neural tube defects. Neural Tube Defects: from origin to treatment.Edited by Diego F.Wyszynski. 15-28.

Greene, N.D.E., Dunlevy, L.E., and Copp, A.J., 2003. Homocysteine is embryotoxic but does not cause neural tube defects in mouse embryos. Anat. Embryol. 206, 185-191.

Greene, N.D.E., Gerrelli, D., Van Straaten, H.W.M., and Copp, A.J., 1998. Abnormalities of floor plate, notochord and somite differentiation in the loop-tail (Lp) mouse: a model of severe neural tube defects. Mech. Dev. 73, 59-72.

Grillo, M.A. and Colombatto, S., 2005. S-adenosylmethionine and protein methylation. Amino Acids 28[4], 357-362.

Groenen, P.M., Peer, P.G., Wevers, R.A., Swinkels, D.W., Franke, B., Mariman, E.C., and Steegers-Theunissen, R.P., 2003. Maternal myo-inositol, glucose, and zinc status is associated with the risk of offspring with spina bifida. Am. J Obstet. Gynecol. 189, 1713-1719.

Groenen, P.M.W., Roes, E.M., Peer, P.G.M., Merkus, H.M.W.M., Steegers, E.A.P., and Steegers-Theunissen, R.P.M., 2005. Myo-inositol, glucose and zinc ocnentrations determined in the periconceptual period, during and after pregnancy. European Jounal of Obstetrics & Gynecology and Reproductive Biology, 127(1), 50-55.

Gruneberg, H., 1954. Genetical studies on the skeleton of the mouse. VIII. Curly tail. J. Genet. 52, 52-67.

Guenther, B.D., Sheppard, C.A., Tran, P., Rozen, R., Matthews, R.G., and Ludwig, M.L., 1999. The structure and properties of methylenetetrahydrofolate reductase from Escherichia coli suggest how folate ameliorates human hyperhomocysteinemia. Nat. Struct. Biol. 6, 359-365.

Guerra-Shinohara, E.M., Morita, O.E., Peres, S., Pagliusi, R.A., Sampaio Neto, L.F., D'Almeida, V., Irazusta, S.P., Allen, R.H., and Stabler, S.P., 2004. Low ratio of S-adenosylmethionine to S-adenosylhomocysteine is associated with vitamin deficiency in Brazilian pregnant women and newborns. Am J Clin.Nutr. 80, 1312-1321.

Gunn, T.M., Juriloff, D.M., and Harris, M.J., 1995. Genetically determined absence of an initiation site of cranial neural tube closure is causally related to exencephaly in SELH/Bc mouse embryos. Teratology. 52, 101-108.

Hall, M.H., 1972. Folic acid deficiency and congenital malformation. J. Obstet. Gynaecol. Br. Commonw. 79, 159-161.

Hallman, M., Bry, K., and Hoppu, K., 1992. Inositol supplementation in premature infants with respiratory distress syndrome. New England Journal of Medicine 326, 1233-1239.

Hamblet, N.S., Lijam, N., Ruiz-Lozano, P., Wang, J., Yang, Y., Luo, Z., Mei, L., Chien, K.R., Sussman, D.J., and Wynshaw-Boris, A., 2002. Dishevelled 2 is essential for cardiac outflow tract development, somite segmentation and neural tube closure. Development. 129, 5827-5838.

Handel, J., Dam, M., Gram, L., Winkel, P., and Jorgensen, I., 1984. The effect of carbamazepine and valproate on folate metabolism in man. Acta Neurol Scand 69, 226-231.

Hansen, D.K. and Billings, R.E., 1985. Phenytoin teratogenicity and effects on embryonic and maternal folate metabolism. Teratology 31, 363-371.

Hansen, D.K., Dial, S.L., and Grafton, T.F., 1995. Lack of attenuation of valproic acid-induced embryotoxicity by compounds involved in one-carbon transfer reactions. Toxic. in Vitro 9, 615-621.

Hansen, D.K. and Grafton, T.F., 1991. Lack of attenuation of valproic acid-induced effects by folinic acid in rat embryos in vitro. Teratology. 43, 575-582.

Hansen, D.K., Streck, R.D., and Antony, A.C., 2003. Antisense modulation of the coding or regulatory sequence of the folate receptor (Folate binding protein-1) in mouse embryos leads to neural tube defects. Birth Defects Research (Part A) 67, 475-487.

Hantusch, B., Kalt, R., Krieger, S., Puri, C., and Kerjaschki, D., 2007. Sp1/Sp3 and DNA-methylation contribute to basal transcriptional activation of human podoplanin in MG63 versus Saos-2 osteoblastic cells. BMC Molecular Biology 8, 1-24.

Harris, M.J., 2001. Why are the genes that cause risk of human neural tube defects so hard to find? Teratology. 63, 165-166.

Harris, M.J. and Juriloff, D.M., 2005. Maternal diet alters exencephaly frequency in SELH/Bc strain mouse embryos. Birth Defects Res.Part A Clin.Mol.Teratol. 73, 532-540.

Harris, M.J. and Juriloff, D.M., 2007. Mouse mutants with neural tube closure defects and their role in understanding human neural tube defects. Birth Defects Res.Part A Clin Mol.Teratol., 79(3): 187-210.

Hartz, C.S. and Schalinske, K.L., 2006. Phosphatidylethanolamine N-methyltransferase and regulation of homocysteine. Nutrition Reviews 64[10 Pt 1], 465-467.

Heid, M.K., Bills, N.D., Hinrichs, S.H., and Clifford, A.J., 1992. Folate deficiency alone does not produce neural tube defects in mice. J. Nutr. 122, 888-894.

Hemberger, M., 2002. The role of the X chromosome in mammalian extra embryonic development. Cytogenetic and Genome Research 99, 210-217.

Hildebrand, J.D. and Soriano, P., 1999. Shroom, a PDZ domain-containing actin-binding protein, is required for neural tube morphogenesis in mice. Cell 99, 485-497.

Hishida, R. and Nau, H., 1998. VPA-induced neural tube defects in mice. I. Altered metabolism of sulfur amino acids and glutathione. Teratogenesis Carcinog. Mutagen. 18, 49-61.

Hoffbrand, A.V., Newcombe, B.F., and Mollin, D.L., 1966. Method of assay of red cell folate activity and the assay as a test for folate deficiency. J.Clin.Pathol. 19, 17-28.

Holmberg, J., Clarke, D.L., and Frisén, J., 2000. Regulation of repulsion versus adhesion by different splice forms of an Eph receptor. Nature 408, 203-206.

Holub, B.J., 1986. Metabolism and function of myo-inositol and inositolphospholipids. Annual Review of Nutrition 6, 563-597.

Hooper, N.M., 1997. Glycosyl-phosphatidylinositol anchored membrane enzymes. Clin. Chim. Acta 266, 3-12.

Horne, D.W., 1997. Microbiological assay of folates in 96-well microtiter plates. Methods Enzymol. 281, 38-43.

Ishibashi, M., Ang, S.-L., Shiota, K., Nakanishi, S., Kageyama, R., and Guillemot, F., 1995. Targeted disruption of mammalian hairy and Enhancer of split homolog-1 (HES-1) leads to up-regulation of neural helix-loop-helix factors, premature neurogenesis, and severe neural tube defects. Genes Dev. 9, 3136-3148.

Jackson, S., 1966. Creatinine in urine as an index of urinary excretion rate. Health Phys. 12[6], 843-850.

Jacob, R.A., Gretz, D.M., Taylor, P.C., James, J., Pogribny, I.P., Miller, B.J., Henning, S.M., and Swendseid, M.E., 1998. Moderate folate depletion increases plasma homocysteine and decreases lymphocyte DNA methylation in post-menopausal women. Journal of Nutrition 128, 1204-1212.

Jacques, P.F., Bostom, A.G., Williams, R.R., Ellison, R.C., Eckfeldt, J.H., Rosenberg, I.H., Selhub, J., and Rozen, R., 1996. Relation between folate status, a common mutation in methylenetetrahydrofolate reductase, and plasma homocysteine concentrations. Circulation 93, 7-9.

James, S.J., Melnyk, S., Pogribna, M., Pogribny, I.P., and Caudill, M.A., 2002. Elevation in S-adenosylhomocysteine and DNA hypomethylation: potential epigenetic mechanism for homocysteine-related pathology. J. Nutr. 132, 2361S-2366S.

Janerich, D.T. and Piper, J., 1978. Shifting genetic patterns in anencephaly and spina bifida. J. Med. Genet. 15, 101-105.

Jensen, H.E., Andersen, L.L.I., and Hau, J., 1991. Fetal malformations and maternal alpha-fetoprotein levels in curly tail (ct) mice. Int. J. Feto-Maternal Med. 4, 205-209.

Jones, P.A., 1999. The DNA methylation paradox. TIG 15, 34-37

Jones, P.A., Taylor, S.M., and Wilson, V.L., 1983. Inhibition of DNA methylation by 5-azacytidine. Recent.Results.Cancer Res. 84, 202-211.

Juriloff, D.M., Gunn, T.M., Harris, M.J., Mah, D.G., Wu, M.K., and Dewell, S.L., 2001. Multifactorial genetics of exencephaly in SELH/Bc mice. Teratology. 64, 189-200.

Juriloff, D.M. and Harris, M.J., 2000. Mouse models for neural tube closure defects. Hum. Mol. Genet. 9, 993-1000.
Kalter, H., 2000. Folic acid and human malformations: a summary and evaluation. Reprod. Toxicol. 14, 463-476.

Kamen, B.A., Wang, M.T., Streckfuss, A.J., Peryea, X., and Anderson, R.G., 1988. Delivery of folates to the cytoplasm of MA104 cells is mediated by a surface membrane receptor that recycles. Journal of Biological Chemistry 263[27], 13602-13609.

Kane, M.T., Norris, M., and Harrison, R.A.P., 1992. Uptake and incorporation of inositol by preimplantation mouse embryos. J. Reprod. Fertil. 96, 617-625.

Kang, S.-S., Wong, P.W.K., Zhou, J., Sora, J., Lessick, M., Ruggie, N., and Greevich, G., 1988. Thermolabile methylenetetrahydrofolate reductase in patients with coronary artery disease. Metabolism: Clinical and Experimental 37, 611-613.

Karfunkel, P., 1974. The mechanisms of neural tube formation. Int. Rev. Cytol. 38, 245-271.

Keller, R., Davidson, L., Edlund, A., Elul, T., Ezin, M., Shook, D., and Skoglund, P., 2000. Mechanisms of convergence and extension by cell intercalation. Philosophical Transactions of the Royal Society of London. B:Biological Sciences 355, 897-922.

Kennington, A.S., Hill, C.R., Craig, J., Bogardus, C., Raz, I., Ortmeyer, H.K., Hansen, B.C., Romero, G., and Larner, J., 1990. Low urinary chiro-inositol excretion in non-insulin-dependent diabetes mellitus. N. Engl. J. Med. 323, 373-378.

Kim, E., Lowenson, J.D., MacLaren, D.C., Clarke, S., and Young, S.G., 1997. Deficiency of a protein-repair enzyme results in the accumulation of altered proteins, retardation of growth, and fatal seizures in mice. Proceedings of the National Academy of Sciences USA 94, 6132-6137.

Kindt, E., Shum, Y., Badura, L., Snyder, P.J., Brant, A., Fountain, S., and Szekely-Klepser, G., 2004. Development and validation of an LC/MS/MS procedure for the quantification of endogenous myo-inositol concentrations in rat brain tissue homogenates. Anal. Chem. 76, 4901-4908.

Kirke, P.N., Daly, L.E., and Elwood, J.H., 1992. A randomised trial of low dose folic acid to prevent neural tube defects. Arch. Dis. Child. 67, 1442-1446.

Kirke, P.N., Daly, L.E., Molloy, A., Weir, D.G., and Scott, J.M., 1996. Maternal folate status and risk of neural tube defects. Lancet 348, 67-68.

Kirke, P.N., Molloy, A.M., Daly, L.E., Burke, H., Weir, D.G., and Scott, J.M., 1993. Maternal plasma folate and vitamin B12 are independent risk factors for neural tube defects. Q. J. Med. 86, 703-708.

Kok, R.D., Steegers-Theunissen, R.P.M., Eskes, T.K.A.B., Heerschap, A., and Van der Burg, P.P., 2003. Decreased relative brain tissue levels of inositol infetal hydrocephalus. American Journal of Obstetrics and Gynecology 188, 978-980.

Koleske, A.J., Gifford, A.M., Scott, M.L., Nee, M., Bronson, R.T., Miczek, K.A., and Baltimore, D., 1998. Essential roles for the Abl and Arg tyrosine kinases in neurulation. Neuron 21, 1259-1272.

Kouzuma, T., Takahashi, M., Endoh, T.U., Kaneko, R., Ura, N., Shimamoto, K., and Watanabe, N., 2001. An enzymatic cycling method for the measurement of myo-inositol in biological samples. Clin. Chim. Acta 312, 143-151.

Kutzbach, C. and Stokstad, E.L.R., 1971. Mammalian methylenetetrahydrofolate reductase: partial purification, properties and inhibition by s-adenosylmethionine. Biochimica et Biophysica Acta 250, 459-477.

Lakkis, M.M., Golden, J.A., O'Shea, K.S., and Epstein, J.A., 1999. Neurofibromin deficiency in mice causes exencephaly and is a modifier for Splotch neural tube defects. Dev. Biol. 212, 80-92.

Lanier, L.M., Gates, M.A., Witke, W., Menzies, A.S., Wehman, A.M., Macklis, J.D., Kwiatkowski, D., Soriano, P., and Gertler, F.B., 1999. Mena is required for neurulation and commissure formation. Neuron 22, 313-325.

Lardelli, M., Williams, R., Mitsiadis, T., and Lendahl, U., 1996. Expression of the Notch 3 intracellular domain in mouse central nervous system progenitor cells is lethal and leads to disturbed neural tube development. Mech. Dev. 59, 177-190.

Laurence, K.M., James, N., Miller, M.H., Tennant, G.B., and Campbell, H., 1981. Double-blind randomised controlled trial of folate treatment before conception to prevent recurrence of neural-tube defects. Br. Med. J. 282, 1509-1511.

Laurence, K.M., James, N., Miller, M., and Campbell, H., 1980. Increased risk of recurrence of pregnancies complicated by fetal neural tube defects in mothers receiving poor diets, and possible benefit of dietary counselling. Br. Med. J. 281, 1592-1594.

Lee, J. and Chung, B.C., 2006. Simultaneous measurement of urinary polyols using gas chromatography/mass spectrometry. Journal of Chromatography B 831[1-2], 126-131.

Letts, V.A., Schork, N.J., Copp, A.J., Bernfield, M., and Frankel, W.N., 1995. A curly-tail modifier locus, mct1, on mouse chromosome 17. Genomics 29, 719-724.

Levine, J., Aviram, A., Holan, A., Ring, A., Barak, Y., and Belmaker, R.H., 1997. Inositol treatment of autism. Journal of Neural Transmission 104[2-3], 307-310.

Levine, J., Barak, Y., Gonzalves, M., Szor, H., Elizur, A., Kofman, O., and Belmaker, R.H., 1995. Double-blind, controlled trial of inositol treatment of depression. Am. J. Psychiatry 152, 792-794.

Levine, J., Rapaport, A., Lev, L., Bersudsky, Y., Kofman, O., Belmaker, R.H., Shapiro, J., and Agam, G., 1993. Inositol treatment raises CSF inositol levels. Brain Research 627[1], 168-170.

Lewis, D.P., Van Dyke, D.C., Stumba, P.J., and Berg, M.J., 1998. Drug and environmental factors associated with adverse pregnancy outcomes. Part I: Antiepileptic drugs, contraceptives, smoking and folate. Ann Pharmacother 32, 802-817.

Li, D., Pickell, L., Liu, Y., and Rozen, R., 2006. Impact of Methylenetetrahydrofolate Reductase Deficiency and Low Dietary Folate on the Development of Neural Tueb Defects in Splotch Mice. Birth Defects Res.Part A Clin.Mol.Teratol. 76, 55-59.

Liang, G., Salem, C.E., Yu, M.C., Nguyen, H.D., Gonzales, F.A., Nguyen, T.T., Nicholas, P.W. and Jones, P.A., 1998. DNA Methylation differences associated with tumour tissues identified by genome scanning analysis. Genomics 53, 260-268.

Limpach, A., Dalton, M., Miles, R., and Gadson, P., 2000. Homocysteine inhibits retinoic acid synthesis: A mechanism for homocysteine-induced congenital defects. Exp. Cell Res. 260, 166-174.

Locksmith, G.J. and Duff, P., 1998. Preventing neural tube defects: The importance of periconceptional folic acid supplements. Obstet. Gynecol. 91, 1027-1034.

Loenen, W.A.M., 2006. S-Adenosylmethionine: jack of all trades and master of everything? Biochemical Society Transactions 34[2], 330-333.

Lombardini, J.B. and Talalay, P., 1971. Formation, functions and regulatory importance of S-Adenosylmethionine. Adv.Enzyme Regulation 9, 349-384.

Low, M.G., 1989. The gycosyl-phosphatidylinositol anchor of membrane proteins. Biochimica et Biophysica Acta 988, 427-454.

Lucock, M., 2000. Folic acid: nutritional biochemistry, molecular biology, and role in disease processes. Mol. Genet. Metab 71, 121-138.

Lucock, M.D., Wild, J., Smithells, R., and Hartley, R., 1989. In vivo characterisation of the absorption and biotransformation of pteroylglutamic acid in man: A model for future studies. Biochem.Med.Metabol.Biol. 42, 30-42.

Luippold, G., Delabar, U., Kloor, D., and Muhlbauer, B., 1999. Simultaneous determination of adenosine, S-adenosylhomocysteine and S-adenosylmethionine in biological samples using solid-phase extraction and high-performance liquid chromatography. J. Chromatogr. B Biomed. Sci. Appl. 724, 231-238.
MacDonald, K.B., Juriloff, D.M., and Harris, M.J., 1989. Developmental study of neural tube closure in a mouse stock with a high incidence of exencephaly. Teratology. 39, 195-213.

Maddox, D.M., Manlapat, A., Roon, P., Prasad, P., Ganapathy, V., and Smith, S.B., 2003. Reduced-folate carrier (RFC) is expressed in placenta and yolk sac, as well as in cells of the developing forebrain, hindbrain, neural tube, craniofacial region, eye, limb buds and heart. BMC. Dev. Biol 3, 6.

Malinow, M.R., Nieto, F.J., Kruger, W.D., Duell, P.B., Hess, D.L., Gluckman, R.A., and Block, P.C., 1997. The effects of folic acid supplementation on plasma total homocysteine are modulated by multivitamin use and methylenetetrahydrofolate reductase genotypes. Arteriosclerosis, Thrombosis, and Vascular Biology 17, 1157-1162.

Marasas, W.F.O., Riley, R.T., Hendricks, K.A., Stevens, V.L., Sadler, T.W., Gelineau-van Waes, J., Missmer, S.A., Cabrera, J., Torres, O., Gelderblom, W.C.A., Allegood, J., Martinez, C., Maddox, J., Miller, J.D., Starr, L., Sullards, M.C., Roman, A.V., Voss, K.A., Wang, E., and Merrill, A.H., 2004. Fumonisins disrupt sphingolipid metabolism, folate transport, and neural tube development in embryo culture and in vivo: a potential risk factor for human neural tube defects among populations consuming fumonisin-contaminated maize. J. Nutr. 134, 711-716.

Martin, C. and Zhang, Y., 2005. The diverse functions of histone lysine methylation. Nat Rev.Mol.Cell Biol 6[11], 838-849.

Martin, C.C., Laforest, L., Akimenko, M.A., and Ekker, M., 1999. A role for DNA methylation in gastrulation and somite patterning. Dev. Biol. 206, 189-205.

Martinez-Barbera, J.P., Rodriguez, T.A., Greene, N.D.E., Weninger, W.J., Simeone, A., Copp, A.J., Beddington, R., and Dunwoodie, S., 2002. Folic acid prevents exencephaly in Cited2 deficient mice. Hum. Mol. Genet. 11, 283-293.

Mason, J.B., 2003. Biomarkers of nutrient exposure and status in one-carbon (methyl) metabolism. J. Nutr. 133 Suppl 3, 941S-947S.

Matsuda, M., 1990. Comparison of the incidence of 5-azacytidine-induced exencephaly between MT/Hokldr and Slc:ICR mice. Teratology. 41, 147-154.

Matsuda, M. and Keino, H., 1994. An open cephalic neural tube reproducibly induced by cytochalasin D in rat embryos in vitro. Zool. Sci. 11, 547-553.

Matsuda, M. and Yasutomi, M., 1992. Inhibition of cephalic neural tube closure by 5-azacytidine in neurulating rat embryos in vitro. Anat. Embryol. 185, 217-223.

Matsumoto, A., Hatta, T., Moriyama, K., and Otani, H., 2002. Sequential observations of exencephaly and subsequent morphological changes by mouse exo utero development system: analysis of the mechanism of transformation from exencephaly to anencephaly. Anat. Embryol. 205, 7-18.

Mattson, M.P., 2003. Methylation and acetylation in nervous system development and neurodegenerative disorders. Ageing Res. Rev. 2, 329-342.

Matuszewski, B.K., Constanzer, M.L., and Chavez-Eng, C.M., 2003. Startegies for the assessment of matrix effectin quantitative bioanalytical methods based on HPLC-MS/MS. Anal.Chem. 75[13], 3019-3030.

McKay, J.A., Williams, E.A., and Mathers, J.C., 2004. Folate and DNA methylation during in utero development and aging. Biochemical Society Transactions 32[6], 1006-1007.

McKeever, M.P., Weir, D.G., Molloy, A., and Scott, J.M., 1991. Betaine-homocysteine methyltransferase: organ distribution in man, pig and rat and subcellular distribution in the rat. Clinical Science 81, 551-556.

McKillop, D.J., Pentieva, K., Daly, D., McPartlin, J.M., Hughes, J., Strain, J.J., Scott, J.M., and McNulty, H., 2002. The effect of different cooking methods on folate retention in various foods that are amongst the major contributors to folate intake in the UK diet. British Journal of Nutrition 88, 681-688.

Melnyk, S., Pogribna, M., Pogribny, I.P., Yi, P., and James, S.J., 2000. Measurement of plasma and intracellular S-adenosylmethionine and S-adenosylhomocysteine utilizing coulometric electrochemical detection: alterations with plasma homocysteine and pyridoxal 5'-phosphate concentrations. Clin. Chem. 46, 265-272.

Menzies, A.S., Aszodi, A., Williams, S.E., Pfeifer, A., Wehman, A.M., Goh, K.L., Mason, C.A., Fässler, R., and Gertler, F.B., 2004. Mena and vasodilator-stimulated phosphoprotein are required for multiple actin-dependent processes that shape the vertebrate nervous system. J. Neurosci. 24, 8029-8038.

Miller, J.W., Nadeau, M.R., Smith, J., Smith, D., and Selhub, J., 1994. Folate-deficiency-induced homocysteinaemia in rats: disruption of S-adenosylmethionine's co-ordinate regulation of homocysteine metabolism. Biochem. J 298 (Pt 2), 415-419.

Mills, J.L., McPartlin, J.M., Kirke, P.N., Lee, Y.J., Conley, M.R., Weir, D.G., and Scott, J.M., 1995. Homocysteine metabolism in pregnancies complicated by neural- tube defects. Lancet 345, 149-151.

Mills, J.L., Tuomilehto, J., Yu, K.F., Colman, N., Blaner, W.S., Koskela, P., Rundle, W.E., Forman, M., Toivanen, L., and Rhoads, G.G., 1992. Maternal vitamin levels during pregnancies producing infants with neural tube defects. J. Pediatr. 120, 863-871.

Moephuli, S.R., Klein, N.W., Baldwin, M.T., and Krider, H.M., 1997. Effects of methionine on the cytoplasmic distribution of actin and tubulin during neural tube closure in rat embryos. Proc. Natl. Acad. Sci. USA 94, 543-548.

Molloy, A.M., Kirke, P., Hillary, I., Weir, D.G., and Scott, J.M., 1985. Maternal serum folate and vitamin B12 concentrations in pregnancies associated with neural tube defects. Arch. Dis. Child. 60, 660-665.

Molloy, A.M. and Scott, J.M., 1997. Microbiological assay for serum, plasma, and red cell folate using cryopreserved, microtiter plate method. Methods Enzymol. 281, 43-53.

Morin, I., Devlin, A.M., Leclerc, D., Sabbaghian, N., Halsted, C.H., Finnell, R.H., and Rozen, R., 2003. Evaluation of genetic variants in the reduced folate carrier and in glutamate carboxypeptidase II for spina bifida risk. Mol.Genet.Metab. 79, 197-200.

Morriss-Kay, G.M. and Tuckett, F., 1985. The role of microfilaments in cranial neurulation in rat embryos: effects of short-term exposure to cytochalasin D. J. Embryol. Exp. Morphol. 88, 333-348.

Murdoch, J.N., Doudney, K., Paternotte, C., Copp, A.J., and Stanier, P., 2001a. Severe neural tube defects in the loop-tail mouse result from mutation of Lpp1, a novel gene involved in floor plate specification. Hum. Mol. Genet. 10, 2593-2601.

Murdoch, J.N., Henderson, D.J., Doudney, K., Gaston-Massuet, C., Phillips, H.M., Paternotte, C., Arkell, R., Stanier, P., and Copp, A.J., 2003. Disruption of scribble (Scrb1) causes severe neural tube defects in the circletail mouse. Hum. Mol. Genet. 12, 87-98.

Murdoch, J.N., Rachel, R.A., Shah, S., Beermann, F., Stanier, P., Mason, C.A., and Copp, A.J., 2001b. Circletail, a new mouse mutant with severe neural tube defects: Chromosomal localisation and interaction with the loop-tail mutation. Genomics 78, 55-63.

Murrell, A., Heeson, S., Bowden, L., Constancia, M., Dean, W., Kelsey, G. and Reik, W., 2001. An intragenic methylated region in the imprinted *Igf2* gene augments transcription. EMBO reports, 2, 1101-1106.

Nau, H., Hauck, R.S., and Ehlers, K., 1991. Valproic acid-induced neural tube defects in mouse and human: aspects of chirality, alternative drug development, pharmacokinetics and possible mechanisms. Pharmacol. Toxicol. 69, 310-321.

Needham, S.R., Jeanville, P.M., Brown, P.R., and Estape, E.S., 2000. Performance of a pentafluorophenylpropyl stationary phase for the electrospray ionisation high-performance liquid chromatography-mass spectrometry-mass spectrometry assay of cocaine and its metabolites ecgonine methyl ester in human urine. Journal of Chromatography B: Biomedical Sciences and Applications 748[1], 77-87.

Nestler, J.E., Jakubowicz, D.J., Reamer, P., Gunn, R.D., and Allan, G., 1999. Ovulatory and metabolic effects of D-chiro-inositol in the polycystic ovary syndrome. N. Engl. J. Med. 340, 1314-1320.

Netzloff, M.L., Streiff, R.R., Frias, J.L., and Rennert, O.M., 1979. Folate antagonism following teratogenic exposure to diphenylhydantoin. Teratology 19, 45-50.

Neumann, P.E., Frankel, W.N., Letts, V.A., Coffin, J.M., Copp, A.J., and Bernfield, M., 1994. Multifactorial inheritance of neural tube defects: Localization of the major gene and recognition of modifiers in ct mutant mice. Nature Genet. 6, 357-362.

Newell-Price, J., Clark, A.J., and King, P., 2000. DNA methylation and silencing of gene expression. Trends Endocrinol. Metab 11, 142-148.

Ogawa, Y., Kaneko, S., Otani, K., and Fukushima, Y., 1991. Serum folic acid levels in epileptic mothers and their relationship to congenital malformations. Epilepsy Research 8, 75-78.

Oka, C., Nakano, T., Wakeham, A., De la Pompa, J.L., Mori, C., Sakai, T., Okazaki, S., Kawaichi, M., Shiota, K., Mak, T.W., and Honjo, T., 1995. Disruption of the mouse RBP-Jkappa gene results in early embryonic death. Development. 121, 3291-3301.

Okano, M., Bell, D.W., Haber, D.A., and Li, E., 1999. DNA methyltransferases Dnmt3a and Dnmt3b are essential for de novo methylation and mammalian development. Cell 99, 247-257.

Oommen, A.M., Griffin, J.B., Sarath, G., and Zempleni, J., 2005. Roles of nutrients in epigenetic events. Journal of Nutritional Biochemistry 16, 74-77.

Padmanabhan, R., 1997. Effect of cotreatment of valproic acid (VPA) and folinic acid (FA) on axial skeletalmorphogenesis in the TO mouse. Congenital Anomalies 34, 314A.

Padmanabhan, R. and Shafiullah, M.M., 2003. Amelioration of sodium valproate-induced neural tube defects in mouse fetuses by maternal folic acid supplementation during gestation. Congenit. Anom. (Kyoto) 43, 29-40.

Pani, L., Horal, M., and Loeken, M.R., 2002. Rescue of neural tube defects in Pax-3-deficient embryos by p53 loss of function: implications for Pax-3-dependent development and tumorigenesis. Genes Dev. 16, 676-680.

Peeters, M.C.E., Shum, A.S.W., Hekking, J.W.M., Copp, A.J., and Van Straaten, H.W.M., 1996. Relationship between altered axial curvature and neural tube closure in normal and mutant (curly tail) mouse embryos. Anat. Embryol. 193, 123-130.

Perello, J., Isern, B., Costa-Bauza, A., and Grases, F., 2004. Determination of myo-inositol in biological samples by liquid chromatography-mass spectrometry. J. Chromatogr. B Analyt. Technol. Biomed. Life Sci. 802, 367-370.

Pfeiffer, C.M. and Gregory, J.F., 1996. Enzymatic deconjugation of erythrocyte polyglutamyl folates during preparation for folate assay: investigation with reverse-phase liquid chromatography. Clinical Chemistry 42, 1847-1854.

Phelan, S.A., Ito, M., and Loeken, M.R., 1997. Neural tube defects in embryos of diabetic mice - Role of the Pax-3 gene and apoptosis. Diabetes 46, 1189-1197.

Piedrahita, J.A., Oetama, B., Bennett, G.D., Van Waes, J., Kamen, B.A., Richardson, J., Lacey, S.W., Anderson, R.G.W., and Finnell, R.H., 1999. Mice lacking the folic acid-binding protein Folbp1 are defective in early embryonic development. Nature Genet. 23, 228-232.

Pogribny, I.P., Miller, B.J., and James, S.J., 1997. Alterations in hepatic p53 gene methylation patterns during tumor progression with folate/methyl deficiency in the rat. Cancer Lett. 115, 31-38.

Poirier, L.A., 2002. The effects of diet, genetics and chemicals on toxicity and aberrant DNA methylation: an introduction. J. Nutr. 132, 2336S-2339S.

Prasad, P.D., Ramamoorthy, S., Leibach, F.H., and Ganapathy, V., 1995. Molecular Cloning of the human placental folate transporter. Biochemistry and Biophysics Research Communications 206[2], 681-687.

Qiu, A., Jansen, M., Sakaris, A., Hee Min, S., Chattopadhyay, S., Tsai, E., Sandoval, C., Zhao, R., Akabas, M.H., and Goldman, I.D., 2006. Identification of an intestinal folate transporter and the molecular basis for hereditary folate malabsorption. Cell 127, 917-928.

Quirk, J.G. and Bleadale, J.E., 1983. myo-Inositol homeostasis in the human fetus. Obstetrics and Gynecology 62, 41-44.

Rasmussen, S.A. and Frias, J.L., 2006. Genetics of syndromic neural tube defects. Neural Tube Defects: from origin to treatment.Edited by Diego F.Wyszynski. 185-197.

Ratnam, M., Marquardt, H., Duhring, J.L., and Freisheim, J.H., 1989. Homologous membrane folate binding proteins in human placenta: Cloning and sequence of a cDNA. Biochemistry 28, 8249-8254.

Read, A.P. and Newton, V.E., 1997. Waardenburg syndrome. J. Med. Genet. 34, 656-665.

Richter, B., Stegmann, K., Roper, B., Bodddeker, I., Ngo, E.T., and Koch, M.C., 2001. Interaction of folate and homocysteine pathway genotypes evaluated in susceptibility to neural tube defects (NTD) in a German population. J.Hum.Genet. 46, 105-109.

Robert, E. and Guidbaud, P., 1982. Maternal valproic acid and congenital neural tube defects. Lancet 2, 937.

Rosales, O.R., Isales, C.M., and Bhargava, J., 1998. Overexpression of protein kinase C alpha and beta1 has distinct effects on bovine aortic endothelial cell growth. Cell Signal. 10, 589-597.

Rosenquist, T.H., Ratashak, S.A., and Selhub, J., 1996. Homocysteine induces congenital defects of the heart and neural tube: Effect of folic acid. Proc. Natl. Acad. Sci. USA 93, 15227-15232.

Rothenberg, S.P., Da Costa, M.P., Sequeira, J.M., Cracco, J., Roberts, J.L., Weedon, J., and Quadros, E.V., 2004. Autoantibodies against folate receptors in women with a pregnancy complicated by a neural-tube defect. N.Engl.J Med 350[2], 134-142.

Rozen, R., 2006. Genetic risk factors for neural tube defects. Neural Tube Defects: from origin to treatment. Edited by Diego F.Wyszynski. 176-184.

Russell, W.L., 1947. Splotch: a new mutation in the house mouse. Genetics 32, 350-358.

Sadler, T.W., 1980. Effects of maternal diabetes on early embryogenesis: II. Hyperglycemia-induced exencephaly. Teratology. 21, 349-356.

Sadler, T.W., 1978. Distribution of surface coat material on fusing neural folds of mouse embryos during neurulation. Anat. Rec. 191, 345-350.

Sadler, T.W., 2005. Embryology of neural tube development. American Journal of Medical Genetics 135C, 2-8.

Sadler, T.W., Greenberg, D., Coughlin, P., and Lessard, J.L., 1982. Actin distribution patterns in the mouse neural tube during neurulation. Science 215, 172-174.

Sadler, T.W., Merrill, A.H., Stevens, V.L., Sullards, M.C., Wang, E., and Wang, P., 2002. Prevention of fumonisin B1-induced neural tube defects by folic acid. Teratology. 66, 169-176.

Saitsu, H., Ishibashi, M., Nakano, H., and Shiota, K., 2003. Spatial and temporal expression of folate-binding protein 1 (Fbp 1) is closely associated with anterior neural tube closure in mice. Dev. Dyn. 226, 112-117.

Sakai, Y., 1989. Neurulation in the mouse: manner and timing of neural tube closure. Anat. Rec. 223, 194-203.

Sausedo, R.A., Smith, J.L., and Schoenwolf, G.C., 1997. Role of nonrandomly oriented cell division in shaping and bending of the neural plate. J. Comp. Neurol. 381, 473-488.

Scalera, V., Natuzzi, D., and Prezioso, G., 1991. Myo-inositol transport in rat intestinal brush border membrane vesicles, and its inhibition by D-glucose. Biochimica et Biophysica Acta 1062, 187-192.

Schoenwolf, G.C., 1979. Observations on closure of the neuropores in the chick embryo. Am. J. Anat. 155, 445-466.

Schorah, C.J., Wild, J., Hartley, R., Sheppard, S., and Smithells, R.W., 1983. The effect of periconceptional supplementation on blood vitamin concentrations in women at recurrence risk for neural tube defect. Br. J. Nutr. 49, 203-211.

Scott, J.M., 1999. Folate and vitamin B12. Proc. Nutr. Soc. 58, 441-448.

Scott, J.M., Weir, D.G., and Kirke, P.N., 1995. Folate and Neural Tube Defects. Folate in Health and Disease. 329-360.

Seller, M.J., 1981. An essay on research into the causation and prevention of spina bifida. Z. Kinderchir. 34, 306-314.

Seller, M.J., 1983. The cause of neural tube defects: some experiments and a hypothesis. J. Med. Genet. 20, 164-168.

Seller, M.J., 1987. Neural tube defects and sex ratios. Am. J. Med. Genet. 26, 699-707.

Seller, M.J., 1994a. Risks in spina bifida. Dev. Med. Child Neurol. 36, 1021-1025.

Seller, M.J., 1994b. Vitamins, folic acid and the cause and prevention of neural tube defects. In: Bock, G. and Marsh, J. (Eds.), Neural Tube Defects (Ciba Foundation Symposium 181), John Wiley & Sons, Chichester, pp. 161-173.

Seller, M.J., Embury, S., Polani, P.E., and Adinolfi, M., 1979. Neural tube defects in curly-tail mice. II. Effect of maternal administration of vitamin A. Proc. R. Soc. Lond. B 206, 95-107.

Seller, M.J. and Perkins, K.J., 1983. Effect of hydroxyurea on neural tube defects in the curly-tail mouse. J. Craniofac. Genet. Dev. Biol. 3, 11-17.

Seller, M.J. and Perkins, K.J., 1986. Effect of mitomycin C on the neural tube defects of the curly-tail mouse. Teratology. 33, 305-309.

Seshadri, S., Beiser, A., Selhub, J., Jacques, P.F., Rosenberg, I.H., D'Agostino, R.B., Wilson, P.W., and Wolf, P.A., 2002. Plasma homocysteine as a risk factor for dementia and Alzheimer's disease. N. Engl. J. Med. 346, 476-483.

Shane, B., 1989. Folylpolyglutamylsynthase synthesis and role in the regulation of one-carbon metabolism. Vitamins and Hormones 45, 263-335.

Shane, B., Tamura, T., and Stokstad, R.E.L., 1980. Folate Assay: A comparison of radioassay and microbiological methods. Clinica Chimica Acta 100, 13-19.

Shaw, G.M., Carmichael, S.L., Yang, W., Selvin, S., and Schaffer, D.M., 2004. Periconceptional dietary intake of choline and betaine and neural tube defects in offspring. Am. J. Epidemiol. 160, 102-109.
Shaw, G.M., Lammer, E.J., Zhu, H.P., Baker, M.W., Neri, E., and Finnell, R.H., 2002. Maternal periconceptional vitamin use, genetic variation of infant reduced folate carrier (A80G), and risk of spina bifida. Am. J. Med. Genet. 108, 1-6.

She, Q.B., Nagao, I., Hayakawa, T., and Tsuge, H., 1994. A simple HPLC method for the determination of S-adenosylmethionine and S-adenosylhomocysteine in rat tissues: the effect of vitamin B6 deficiency on these concentrations in rat liver. Biochem. Biophys. Res. Commun. 205, 1748-1754.

Shears, S.B., 1998. The versatility of inositol phosphates as cellular signals. Biochimica et Biophysica Acta 1436, 49-67.

Shen, F., Wu, M., Ross, J.F., Miller, D., and Ratnam, M., 1995. Folate receptor type gamma is primarily a secretory protein due to lack of an efficient signal for glycosylphosphatidylinositol modification:protein characterisation and cell type specificity. Biochemistry 34[16], 5660-5665.

Shin, J.H. and Shiota, K., 1999. Folic acid supplementation of pregnant mice suppresses heat-induced neural tube defects in the offspring. J. Nutr. 129, 2070-2073.

Shiota, K., 1988. Induction of neural tube defects and skeletal malformations in mice following brief hyperthermia in utero. Biol. Neonate 53, 86-97.

Shiota, K., Shionoya, Y., Ide, M., Venobe, F., Kuwahara, C., and Fukui, Y., 1988. Teratogenic interaction of ethanol and hyperthermia in mice. Proc. Soc. Exp. Biol. Med. 187, 142-148.

Shoob, H.D., Sargent, R.G., Thompson, S.J., Best, R.G., Drane, J.W., and Tocharoen, A., 2001. Dietary methionine is involved in the etiology of neural tube defect-affected pregnancies in humans. J. Nutr. 131, 2653-2658.

Shum, L. and Sadler, T.W., 1988. Embryonic catch-up growth after exposure to the ketone body D,L-beta-hydroxybutyrate in vitro. Teratology. 38, 369-379.

Sierra, E.E. and Goldman, I.D., 1999. Recent advances in the understanding of the mechanism of membrane transport of folates and antifolates. Semin.Oncol. 26[2 Suppl 6], 11-23.

Sirotnak, F.M. and Tolner, B., 1999. Carrier-mediated membrane transport of folates in mammalian cells. Annual Review of Nutrition 19, 91-122.

Smedley, M.J. and Stanisstreet, M., 1986. Calcium and neurulation in mammalian embryos. II. Effects of cytoskeletal inhibitors and calcium antagonists on the neural folds of rat embryos. J. Embryol. Exp. Morphol. 93, 167-178.

Smithells, R.W., Nevin, N.C., Seller, M.J., Sheppard, S., Harris, R., Read, A.P., Fielding, D.W., Walker, S., Schorah, C.J., and Wild, J., 1983. Further experience of vitamin supplementation for prevention of neural tube defect recurrences. Lancet 1, 1027-1031.

Smithells, R.W. and Sheppard, S., 1980. Possible prevention of neural-tube defects by periconceptional vitamin supplementation (letter). Lancet 1, 647.

Smithells, R.W., Sheppard, S., and Schorah, C.J., 1976. Vitamin deficiencies and neural tube defects. Arch. Dis. Child. 51, 944-950.

Smithells, R.W., Sheppard, S., Schorah, C.J., Seller, M.J., Nevin, N.C., Harris, R., Read, A.P., and Fielding, D.W., 1981a. Apparent prevention of neural tube defects by periconceptional vitamin supplementation. Arch. Dis. Child. 56, 911-918.

Smithells, R.W., Sheppard, S., Schorah, C.J., Seller, M.J., Nevin, N.C., Harris, R., Read, A.P., Fielding, D.W., and Walker, S., 1981b. Vitamin supplementation and neural tube defects (letter). Lancet 2, 1425.

Sohn, K.J., Stempak, J.M., Reid, S., Shirwadkar, S., Mason, J.B., and Kim, Y.I., 2003. The effect of dietary folate on genomic and p53-specific DNA methylation in rat colon. Carcinogenesis 24, 81-90.
Spector, R., 1988. Myo-inositol transport through the blood-brain barrier. Neurochemical Research 13[8], 785-787.

Spector, R. and Lorenzo, A.V., 1975. Myo-inositol transport in the central nervous system. American Journal of Physiology 228[5], 1510-1518.

Spiegelstein, O., Cabrera, R.M., Bozinov, D., Wlodarczyk, B., and Finnell, R.H., 2004. Folate-regulated changes in gene expression in the anterior neural tube of folate binding protein-1 (Folbp1)-deficient murine embryos. Neurochem. Res. 29, 1105-1112.

Spiegelstein, O., Eudy, J.D., and Finnell, R.H., 2000. Identification of two putative novel folate receptor genes in humans and mouse. Gene 258, 117-125.

Srinivasan, R., Vigneron, D., Sailasuta, N., Hurd, R., and Nelson, S., 2004. A comparative study of myo-inositol quantification using LCmodel at 1.5 T and 3.0 T with 3 D 1H proton spectroscopic imaging of the human brain. Magn.Reson.Imaging 22[4], 523-528.

Stabler, S.P. and Allen, R.H., 2004. Quantification of serum and urinary S-adenosylmethionine and S-adenosylhomocysteine by stable-isotope-dilution liquid chromatography-mass spectrometry. Clin. Chem. 50, 365-372.

Steegers-Theunissen, R.P.M., Boers, G.H.J., Trijbels, F.J.M., Finkelstein, J.D., Blom, H.J., Thomas, C.M.G., Borm, G.F., Wouters, M.G.A.J., and Eskes, T.K.A.B., 1994. Maternal hyperhomocysteinemia: A risk factor for neural tube defects. Metabolism 43, 1475-1480.

Stevens, V.L. and Tang, J., 1997. Fumonisin B1-induced sphingolipid depletion inhibits vitamin uptake via the glycosylphosphatidylinositol-anchored folate receptor. J. Biol. Chem. 272, 18020-18025.

Struys, E.A., Jansen, E.E., De Meer, K., and Jakobs, C., 2000. Determination of S-adenosylmethionine and S-adenosylhomocysteine in plasma and cerebrospinal fluid by stable-isotope dilution tandem mass spectrometry. Clin. Chem. 46, 1650-1656.

Stuart, J.A., Anderson, K.L., Kirk, C.J., and Michell, R.H., 1993. The intracellular distribution of inositol phosphates. Biochemical Society Transactions 21, 361S.

Stumpo, D.J., Bock, C.B., Tuttle, J.S., and Blackshear, P.J., 1995. MARCKS deficiency in mice leads to abnormal brain development and perinatal death. Proc. Natl. Acad. Sci. USA 92, 944-948.

Swanson, D.A., Liu, M.L., Baker, P.J., Garrett, L., Stitzel, M., Wu, J.M., Harris, M., Banerjee, R., Shane, B., and Brody, L.C., 2001. Targeted disruption of the methionine synthase gene in mice. Mol. Cell. Biol. 21, 1058-1065.

Takeuchi, I.K. and Takeuchi, Y.K., 1985. 5-Azacytidine-induced exencephaly in mice. J. Anat. 140, 403-412.

Tetsuo, M., Zhang, C., Matsumoto, H., and Matsumoto, I., 1999. Gas chromatographic-mass spectrometric analysis of urinary sugar and sugar alcohols during pregnancy. Journal of Chromatography B 731[1], 111-120.

Thiersch, J.B. and Wash, S., 1952. Therapeutic abortions with a folic acid antagonist, 4-aminopteroylglutamic acid (4-Amino P.G.A) administered by the oral route. Am.J Obstet.Gynecol. 1298-1304.

Ting, S.B., Wilanowski, T., Auden, A., Hall, M., Voss, A.K., Thomas, T., Parekh, V., Cunningham, J.M., and Jane, S.M., 2003. Inositol- and folate-resistant neural tube defects in mice lacking the epithelial-specific factor Grhl-3. Nature Med. 9, 1513-1519.

Toriello, H.V. and Higgins, J.V., 1983. Occurrence of neural tube defects among first-, second-, and third-degree relatives of probands: results of a United States study. American Journal of Medical Genetics 15[4], 601-606.
Tran, P., Hiou-Tim, F., Frosst, P., Lussier-Cacan, S., Bagley, P., Selhub, J., Bottiglieri, T., and Rozen, R., 2002. The curly-tail (ct) mouse, an animal model of neural tube defects, displays altered homocysteine metabolism without folate responsiveness or a defect in Mthfr. Mol. Genet. Metab 76, 297-304.

Trembath, D., Sherbondy, A.L., Vandyke, D.C., Shaw, G.M., Todoroff, K., Lammer, E.J., Finnell, R.H., Marker, S., Lerner, G., and Murray, J.C., 1999. Analysis of select folate pathway genes, PAX3, and human T in a Midwestern neural tube defect population. Teratology. 59, 331-341.

Trotz, M., Wegner, C., and Nau, H., 1987. Valproic acid-induced neural tube defects: reduction by folinic acid in the mouse. Life Sci. 41, 103-110.

Turner, L.A., Morrison, H., and Prabhakaran, V.M., 2001. Do we need another randomized controlled trial of folic acid alone? Epidemiology 12, 262-265.

Uthus, E.O., 2003. Simultaneous detection of S-adenosylmethionine and S-adenosylhomocysteine in mouse and rat tissues by capillary electrophoresis. Electrophoresis 24, 1221-1226.

Vafai, S.B. and Stock, J.B., 2002. Protein phosphatase 2A methylation: a link between elevated plasma homocysteine and Alzheimer's Disease. FEBS Lett. 518, 1-4.

Van Allen, M.I., Kalousek, D.K., Chernoff, G.F., Juriloff, D., Harris, M., McGillivray, B.C., Yong, S.-L., Langlois, S., MacLeod, P.M., Chitayat, D., Friedman, J.M., Wilson, R.D., McFadden, D., Pantzar, J., Ritchie, S., and Hall, J.G., 1993. Evidence for multi-site closure of the neural tube in humans. Am. J. Med. Genet. 47, 723-743.

Van den Veyver, I.B., 2002. Genetic effects of methylation diets. Annu. Rev. Nutr. 22, 255-282.

Van der Put, N.M.J., Gabreëls, F., Stevens, E.M.B., Smeitink, J.A.M., Trijbels, F.J.M., Eskes, T.K.A.B., Van den Heuvel, L.P., and Blom, H.J., 1998. A second common mutation in the methylenetetrahydrofolate reductase gene: An additional risk factor for neural-tube defects. Am. J. Hum. Genet. 62, 1044-1051.

Van der Put, N.M.J., Steegers-Theunissen, R.P.M., Frosst, P., Trijbels, F.J.M., Eskes, T.K.A.B., Van den Heuvel, L.P., Mariman, E.C.M., Den Heyer, M., Rozen, R., and Blom, H.J., 1995.

Mutated methylenetetrahydrofolate reductase as a risk factor for spina bifida. Lancet 346, 1070-1071.

Van der Put, N.M.J., Eskes, T.K.A.B., and Blom, H.J., 1997a. Is the common 677C-->T mutation in the methylenetetrahydrofolate reductase gene a risk factor for neural tube defects? A meta-analysis. Q. J. Med. 90, 111-115.

Van der Put, N.M.J., Thomas, C.M.G., Eskes, T.K.A.B., Trijbels, F.J.M., Steegers-Theunissen, R.P.M., Mariman, E.C.M., De Graaf-Hess, A., Smeitink, J.A.M., and Blom, H.J., 1997b. Altered folate and vitamin B12 metabolism in families with spina bifida offspring. Q. J. Med. 90, 505-510.

Van der Put, N.M.J., Van Straaten, H.W.M., Trijbels, F.J.M., and Blom, H.J., 2001. Folate, homocysteine and neural tube defects: An overview. Proceedings of the Society for Experimental Biology and Medicine 226, 243-270.

Van Straaten, H.W.M., Blom, H., Peeters, M.C.E., Rousseau, A.M.J., Cole, K.J., and Seller, M.J., 1995. Dietary methionine does not reduce penetrance in curly tail mice but causes a phenotype-specific decrease in embryonic growth. J. Nutr. 125, 2733-2740.

Van Straaten, H.W.M. and Copp, A.J., 2001. Curly tail: a 50-year history of the mouse spina bifida model. Anat. Embryol. 203, 225-237.

VanAerts, L.A.G.J.M., Blom, H.J., Deabreu, R.A., Trijbels, F.J.M., Eskes, T.K.A.B., Peereboom-Stegeman, J.H.J.C., and Noordhoek, J., 1994. Prevention of neural tube defects by and toxicity of L-homocysteine in cultured postimplantation rat embryos. Teratology. 50, 348-360.

VanAerts, L.A.G.J.M., Poirot, C.M., Herberts, C.A., Blom, H.J., De Abreu, R.A., Trijbels, J.M.F., Eskes, T.K.A.B., Peereboom-Stegeman, J.H.J.C., and Noordhoek, J., 1995. Development of methionine synthase, cystathionine-b-synthase and S-adenosyl-homocysteine hydrolase during gestation in rats. J. Reprod. Fertil. 103, 227-232.

Wagner, C., Briggs, W.T., and Cook, R.J., 1985. Inhibition of glycine N-methyltransferase by folate derivatives: implications for regulation of methyl group metabolism. Biochemistry and Biophysics Research Communications 127, 746-752.

Wald, D.S., Bishop, L., Wald, N.J., Law, M., Hennessy, E., Weir, D., McPartlin, J., and Scott, J., 2001. Randomized trial of folic acid supplementation and serum homocysteine levels. Arch. Intern. Med. 161, 695-700.

Wald, N., Sneddon, J., Densem, J., Frost, C., Stone, R., and MRC Vitamin Study Res Group, 1991. Prevention of neural tube defects: Results of the Medical Research Council Vitamin Study. Lancet 338, 131-137.

Wald, N.J., Hackshaw, A.K., Stone, R., and Sourial, N.A., 1996. Blood folic acid and vitamin B12 in relation to neural tube defects. Br. J. Obstet. Gynaecol. 103, 319-324.

Wallace, H.M., Fraser, A.V., and Hughes, A., 2003. A perspective of polyamine metabolism. Biochem. J. 376, 1-14.

Wallingford, J.B. and Harland, R.M., 2002. Neural tube closure requires Dishevelled-dependent convergent extension of the midline. Development. 129, 5815-5825.

Wang, X., Shen, F., Freisheim, J.H., Gentry, L.E., and Ratnam, M., 1992. Differential stereospecificities and affinities of folate receptor isoforms for folate compounds and antifolates. Biochemical Pharmacology 44[9], 1898-1901.

Warkany, J., Beaudry, P.H., and Hornstein, S., 1959. Attempted abortion with aminopterin (4-amino-pteroylglutamic acid). Am.J.Dis.Child. 97, 36-42.

Watanabe, M., Osada, J., Aratani, Y., Kluckman, K., Reddick, R., Malinow, M.R., and Maeda, N., 1995. Mice deficient in cystathionine b-synthase: Animal models for mild and severe homocyst(e)inemia. Proc. Natl. Acad. Sci. USA 92, 1585-1589.

Waterland, R.A., 2006. Assessing the effects of high methionine intake on DNA Methylation. Journal of Nutrition 136, 1706S-1710S.

Waterland, R.A. and Jirtle, R.L., 2003. Transposable elements: targets for early nutritional effects on epigenetic gene regulation. Mol. Cell Biol. 23, 5293-5300.

Weil, M., Jacobson, M.D., and Raff, M.C., 1997. Is programmed cell death required for neural tube closure. Curr. Biol. 7, 281-284.

Weir, D.G., Molloy, A.M., Keating, J.N., Young, P.B., Kennedy, S., Kennedy, D.G., and Scott, J.M., 1992. Correlation of the ratio of S-adenosyl-L-methionine to S-adenosyl-L-homocysteine in the brain and cerebrospinal fluid of the pig: implications for the determination of this methylation ratio in human brain. Clin. Sci. (Lond) 82, 93-97.

Weitman, S.D., Lark, R.H., Coney, L.R., Fort, D.W., Frasca, V., Zurawski, J., and Kamen, B.A., 1992. Distribution of the folate receptor GP38 in normal and malignant cell lines and tissues. Cancer Research 52, 3396-3401.

Whitehead, R. and Bates, C., 1997. Recommendations on folate intake. Lancet 350, 1642-1643.

Wild, J., Schorah, C.J., Sheldon, T.A., and Smithells, R.W., 1993. Investigation of factors influencing folate status in women who have had a neural tube defect-affected infant. Br. J. Obstet. Gynaecol. 100, 546-549.

Wilson, D.B. and Wyatt, D.P., 1988. Closure of the posterior neuropore in the vl mutant mouse. Anat. Embryol. 178, 559-563.

Wolff, G.L., Kodell, R.L., Moore, S.R., and Cooney, C.A., 1998. Maternal epigenetics and methyl supplements affect agouti gene expression in Avy/a mice. FASEB J. 12, 949-957.

Xu, W., Baribault, H., and Adamson, E.D., 1998. Vinculin knockout results in heart and brain defects during embryonic development. Development. 125, 327-337.

Yamada, K., Chen, Z., Rozen, R., and Matthews, R., 2001. Effects of common polymorphisms on the properties of recombinant human methylenetetrahydrofolate reductase. Proc.Natl.Acad.Sci.U.S.A 98, 14853-14858.

Yamamoto, M., Acevedo-Duncan, M., Chalfant, C.E., Patel, N.A., Watson, J.E., and Cooper, D.R., 1998. The roles of protein kinase C beta I and beta II in vascular smooth muscle cell proliferation. Exp Cell Res. 240, 349-358.

Yates, J.R., Ferguson Smith, M.A., Shenkin, A., Guzman Rodriguez, R., White, M., and Clark, B.J., 1987. Is disordered folate metabolism the basis for the genetic predisposition to neural tube defects? Clin. Genet. 31, 279-287.

Ybot-Gonzalez, P. and Copp, A.J., 1999. Bending of the neural plate during mouse spinal neurulation is independent of actin microfilaments. Dev. Dyn. 215, 273-283.

Ybot-Gonzalez, P., Savery, D., Gerrelli, D., Signore, M., Mitchell, C.E., Faux, C.H., Greene, N.D., and Copp, A.J., 2007. Convergent extension, planar-cell-polarity signalling and initiation of mouse neural tube closure. Development 134[4], 789-799.

Yen, I.H., Khoury, M.J., Erickson, J.D., James, L.M., Waters, G.D., and Berry, R.J., 1992. The changing epidemiology of neural tube defects: United States, 1968-1989. Am. J. Dis. Child. 146, 857-861.

Yi, P., Melnyk, S., Pogribna, M., Pogribny, I.P., Hine, R.J., and James, S.J., 2000. Increase in plasma homocysteine associated with parallel increases in plasma S-adenosylhomocysteine and lymphocyte DNA hypomethylation. J. Biol. Chem. 275, 29318-29323.

tube defects and maternal biomarkers of folate, homocysteine and glutathione m
Defects Res.Part A Clin Mol.Teratol. 76[4], 230-236.

Zhong, W.M., Jiang, M.M., Schonemann, M.D., Meneses, J.J., Pedersen, R.A.
Jan, Y.N., 2000. Mouse numb is an essential gene involved in cortical neurogen
Acad. Sci. USA 97, 6844-6849.

Zhu, H., Yang, W., Lu, W., Zhang, J., Shaw, G.M., Lammer, E.J., and Finnell,
known functional polymorphism (Ile120Val) of the human PCMT1 gene and risk
Molecular Genetics and Metabolism 87[1], 66-70.